University of Edinburgh

College of Science and Engineering

School of Chemistry

Polymer Microarrays - Development and Applications

By

Guilhem Tourniaire

Doctor of philosophy

December 2006

University of Edinburgh

College of Science and Engineering
School of Chemistry

Abstract

Polymer Microarrays - Development and Applications

By

Guilhem Tourniaire

The global aims of this PhD were to investigate and develop high throughput methods for screening libraries of biocompatible polymers.

Initial studies involved the development of a novel polymer microarray platform which would provide unsurpassed miniaturisation for polymer screening. This required substantial development and optimisation of several parameters and the best results were achieved by printing polymers dissolved in 1-methyl-2-pyrrolidinone and patterned using a contact microarrayer with solid pins. In order to obtain minimal background interference while studying the adsorption of proteins and the adhesion of living cells on the polymers, microarray platforms were developed that used different substrates. The first one used a gold-coated substrate that quenched non-specifically bound fluorescently-labelled proteins, whereas the second utilised a hydrogel coating that prevented non-specific cellular adhesion. Additionally, it was shown that the platform using the gold coated substrate was ideally suited to the high throughput study of the physico-chemical properties of the arrayed polymer libraries, via scanning electron microscopy, FT-IR and TOF-SIMS. These polymer microarray platforms provided high throughput while minimising the amount of both polymers and expensive reagents used.

To demonstrate the range of properties displayed by the polymer libraries and their versatility the polymer microarrays were used with both adherent and non-adherent immortalised cell lines. In both cases, it was demonstrated that polymers could be selected that provided selective cellular immobilisation. Such methodologies were subsequently utilised to identify novel materials that allowed gentle immobilisation of human primary renal tubular epithelial cells and mouse bone marrow dendritic cells.

This platform was applied to the identification of polymers with potential applications in the field of stem cell biology. In one project, polymers were screened for the selective immobilisation of multipotent mesenchymal stromal cell populations from human bone marrow. Initial results showed that several poly(urethanes) with large soft segments provided unexpectedly high selective adhesion of the stromal population. The second project investigated the use of novel substrates that maintained mouse embryonic stem cell cultures in their undifferentiated phenotypic state.

Finally, the polymer microarray platform was optimised for the study of protein adhesion. Initial experiments showed that this platform could be applied to a range of plasma and glyco-proteins. It was demonstrated that different proteins showed very different patterns of adsorption over the printed polymers. As a result, it was hypothesised that such platforms may have the potential to be used as diagnostic tool for the identification of proteins in biological samples and serum profiling applications.

Contents

CHAPTER 2: DEVELOPMENT OF POLYMER MICROARRAYS

CHAPTER 3: SCREENING OF BIOCOMPATIBLE POLYMERS FOR CELLULAR ADHESION

CHAPTER 4: POLYMER MICROARRAYS APPLIED TO STEM CELLS

CHAPTER 5: DEVELOPMENT OF POLYMER MICROARRAYS FOR PROTEIN ADSORPTION STUDIES

CHAPTER 6: EXPERIMENTAL

Figures

Tables

Declaration of Authorship

The research described in this thesis was carried out by the author under the supervision of Prof. Mark Bradley at the University of Southampton between October 2002 and December 2004 and at the University of Edinburgh between January 2005 and April 2006. No part of this thesis has been previously submitted at this or any other university for any other degree or a professional qualification. Part of this work has been published in the scientific literature and part of it is protected under patent:

Patent:

Arrays for screening polymeric materials (GB 2408331).

Articles:

Tourniaire, G.; Collins, J.; Campbell, S.; Mizomoto, H.; Ogawa, S.; Thaburet, J. F.; Bradley, M. *Chem. Commun.(Camb.)* **2006**, 2118-2120.

Mant, A.; Tourniaire, G.; Diaz-Mochon J.J.; Elliott, T.J.; Williams, A.P.; Bradley, M.; *Biomaterials*, **2006**, 5299-5306.

Diaz-Mochon, J.J.; Tourniaire, G.; Bradley, M.; *Chem. Soc. Rev.*, **2007**, 449-457.

Acknowledgements

Firstly, I would like to thank Professor Mark Bradley for his invaluable advice and the trust he placed in me throughout my research project. I would also like to thank Asahi Kasei who sponsored my research, and all of the members of the ASL laboratory in Southampton (Jasmine, Hitoshi, Jeff and Yucheng), without whom my research would not have been possible, since they synthesised all of the polymers that I have used.

Also, I would like to thank our collaborators who have allowed us to develop practical applications for our method; in Southampton, Dr. Jane Collins and Sara Campbell who carried out the renal epithelial cell experiments, Professor Richard Oreffo and Dr. Rahul Tare who worked with me on the STRO-1 cell enrichment, Dr. Salim Khakoo and Dr. Alexandra Mant who did most of the work on the phagocytosis, and finally Therese Nestor and Professor David O'Connor. In Edinburgh, I would particularly like to thank Dr Josh Brickman who personally trained me in the culture of embryonic stem cells and allowed me to use his facilities, and Dr. Korinna Henseleit and Fella Hammachi who were always there to answer my silly questions.

I would like to thank everybody in the Bradley group, and in particular Juan Jo and Rosario who have always been there when needed; whether to answer complicated technical questions, to train me or just to share a coffee or a beer! And Albert, Rong and Ferdous for taking over the polymer microarray work, good luck guys!

I would like to thank all my friends from back home, from Kingston, Southampton and Edinburgh to help me stay sane and remind me that science isn't everything in life…

Finally, I would like to thank my family (Mum and Dad, and Mamie and Papi) for their support (on all levels) throughout my education, as they know it wasn't always easy! And obviously I would like to thank my love, Deborah, for her support and help until the very end of this thesis.

Abbreviations

a.u.	arbitrary units
CGH	comparative genomic hybridization
CV	coefficient of variance
DAPI	4',6-diamidino-2-phenylindole
DMF	dimethylformamide
DNA	deoxyribonucleic acid
ECM	extracellular matrix
ELISA	enzyme-linked immunosorbent assay
em	emission
ESC	embryonic stem cell
ex	excitation
FCS	fetal calf serum
FITC	fluorescein isothiocyanate
GFP	green fluorescent protein
HSA	human serum albumin
HS	whole human serum
IgG	Immunoglobulin-G
IR	infrared
LIF	leukaemia inhibitory factor
MALDI	matrix assisted laser desorption/ionisation-mass spectrometry
MEM	modified Eagle's medium
ms	millisecond
MS	mass spectrometry
NMP	*N*-methyl-pyrrolidinone
Oct4	octamer-4
PBS	phosphate-buffered saline
PA	poly(acrylate)
PAA	poly(allylamine)
PNA	peptide nucleic acid
PU	poly(urethane)
PVDF	poly(vinyldiene fluoride)
RNA	ribonucleic acid
RT	room temperature
SAMs	self-assembled monolayers
SEM	scanning electron microscopy
SIMS	secondary ion mass spectrometry
SNP	single nucleotide polymorphisms
SPR	surface plasmon resonance
THF	tetrahydrofuran
TOF	time-of-flight
XPS	x-ray photoelectron spectroscopy

Chapter 1: Introduction

1.1 Microarray

1.1.1 Introduction

The Encarta dictionary defines an array as: "a group of things arranged in an impressive or structured way" hence literally, a microarray is a microscopic group of things arranged in an impressive or structured way. In molecular biology, a microarray can be described as a collection of distinct capture molecules attached or deposited onto a substrate at defined locations.

One of the first application of microarrays was described over ten years ago by Mark Schena *et al.*[1], who developed an array of cDNA probes to monitor the expression of 45 *Arabidopsis* genes in parallel. Since then, many different types of capture molecules (including antibodies, proteins, carbohydrates, small molecules and biomaterials) have been immobilised, allowing the study of a wide range of biological, chemical and medicinal systems. In all cases the key facet of microarrays is that they allow multiple tests to be performed in a single experiment. Over the past ten years, developments in the field of microarrays have required contributions from many areas of basic science, engineering and computing. Today, microarrays continue to evolve and provide essential tools in many areas of research. Their applications generally fall into one of the three following categories[2]:

- **Survey arrays** are used to identify patterns within a very large number of samples.
- **Scan arrays** have been developed for diagnostics. They contain fewer probes that have been carefully selected resulting in more robust and easily interpreted results.
- **Efficient arrays** refer to techniques that do not require assays to be run in parallel but take advantage of the high multiplexing capability of arrays resulting in reduced time, cost and material.

The quality of the data generated depends upon the physical quality of the arrays and control of the variables used for manufacturing such arrays. When developing new applications, researchers are faced with an ever increasing choice of parameters such as the type of surfaces and capture molecules used, the methods of immobilisation, detection and analysis employed.

1.1.2 Surfaces and immobilisation

The surfaces used to create an array must be optimised for the immobilisation of the biomolecule of interest, as well as preventing the non-specific binding of the target molecules. The choice of a given surface will have major influences on the method of immobilisation, the concentration and retained bioactivity of the probes immobilised, and finally, the ease of interaction/binding between probes and targets. When developing an array containing multiple probes, homogeneity in concentration and activity of the different probes is critical to the success of any assay.

1.1.2.1 Type of immobilisation

The immobilisation of a given biomolecule will be affected by a combination of the nature of the surface, the properties of the biomolecule and the liquid medium in which it is delivered. The mechanism of immobilisation of biomolecules on a surface can be divided into two main categories[3]:

- Adsorption, which relies on non-covalent interactions between the biomolecules and the surface. These interactions can be classified according to their relative strength: Electrostatic interactions (10-20 Kcal/mol) arise from the presence of charge on the substrate and biomolecule. Hydrogen bond interactions (3-7 Kcal/mol) originate from the interaction of an electronegative atom and a hydrogen atom, which is bonded to another electronegative atom. Van der Waals (1-2 Kcal/mol) forces arise from the polarisation of molecules into dipoles, and hydrophobic forces (1-2 Kcal/mol) are generated from nonpolar molecules that tend to self-associate in the presence of aqueous solution.

- Covalent immobilisation, which relies on the formation of an irreversible chemical bond between the biomolecules and the functionalised surface. The formation of such bonds is generally achieved through the reaction of functional groups such as an amine or a thiol on the biomolecule and aldehyde or epoxide of active ester on the substrate[4]. Recently, versatile strategies based on the reactions of photoactivated carbene[5] have allowed the covalent immobilisation of a variety of proteins[6] and small molecules[7]. This approach benefits from the high reactivity of the carbene which readily undertakes an insertion reaction with a variety of chemical bonds: C-H, O-H, C-Cl, N-H, Si-H and C=C.

1.1.2.2 Type of surface

Depending on the intended application, the surface may need specific properties such as thermal and chemical stability, flatness and homogeneity. Additionally the substrate must be compatible with the detection method used in order to achieve high sensitivity. For example, if fluorescence is used as a detection method then the surface should have a low fluorescent background.

In the light of the commercialisation of microarrayers and detection systems, surface formats have been standardised, with a compact microscope slide format, with a printing area of up to 75 mm x 25 mm allowing over 20,000 thousands spots (50 µm diameter) to be printed on a single slide. Currently, this format has become a standard, however, it should be noted that many other formats are still being used, such as the bottom of multiwell plates, which allowing smaller arrays to be interrogated with different analytes in each well[8].

Regarding the chemical nature of the surfaces, there is a huge range on offer depending on the desired application and the biomolecules to immobilise. The most widely used substrates are based on glass slides. Glass substrates are reasonably flat, transparent, resistant to high temperature and easy to handle, but more importantly, there is a wide range of well established protocols for the modification of their surface properties[4].

Silicon substrates are also suitable for functionalisation[9]. Gold substrates have been employed for several applications as they can easily be functionalised by self-assembled

monolayers (SAMs) of alkane thiolates[10]. SAMs consists of a single layer of molecules on a substrate. These SAMs allow patterning via photolithographic techniques[11]. SAMs of alkyl thiolates on gold are photosensitive; as a result, they can be selectively patterned by exposure to ultraviolet light (UV) through a Photomask (**Figure 1.5**). Finally, gels and membranes have also been used as substrates since they provide a three dimensional architecture with greater capacities of immobilisation and thus enhanced detection sensitivities[12].

The choice of substrate and surface chemistry has a major impact on the performance of any type of microarray assay and should be carefully selected for any given application.

1.1.3 Printing technologies

One of the cornerstones of microarray technologies is the ability to deliver nano- and picoliter volumes of materials onto a substrate in a defined pattern with speed, reproducibility and at high density. This capability has been aided by the emergence of several new companies that have focussed on developing robotic instrumentation to achieve these goals. Currently, there are a huge range of different technologies available, however, none is perfect and they should be carefully selected depending on the intended application. In order to give an overview of the subject, these printing systems will be divided into two main technologies: contact-printing (sometimes referred to as pin-printing) and reagent jetting (also called ink-jet based deposition) technologies.

1.1.3.1 Contact printing[13]

The term "contact printing" found its definition in the fact that at a given point in the process there is continuity between the transfer device (pin), the solution delivered and the substrate onto which the solution is deposited. This technology is based around a high precision X-Y-Z robot that holds one or more pins that are dipped into the solution contained in the source plate (usually a 384 well plate), and then deposited by contact onto the substrate. The main factors affecting this printing are a combination of the physical and chemical properties of the pin(s), the solution(s), the substrate and the printing parameters of the robot (speed and number of deposition). Among the most important properties are the viscosity and surface tension of the liquids, the wetting

characteristics of both the substrate and pins and finally parameters controlling the robot such as speed of deposition. Additionally, external factors like humidity and temperature can affect the quality of the printing.

Initial experiments were carried out with a simple solid pin but over recent years many different pin designs have been developed allowing a wide range of feature sizes, each of which have some advantages and some drawbacks (**Figure 1.1**).

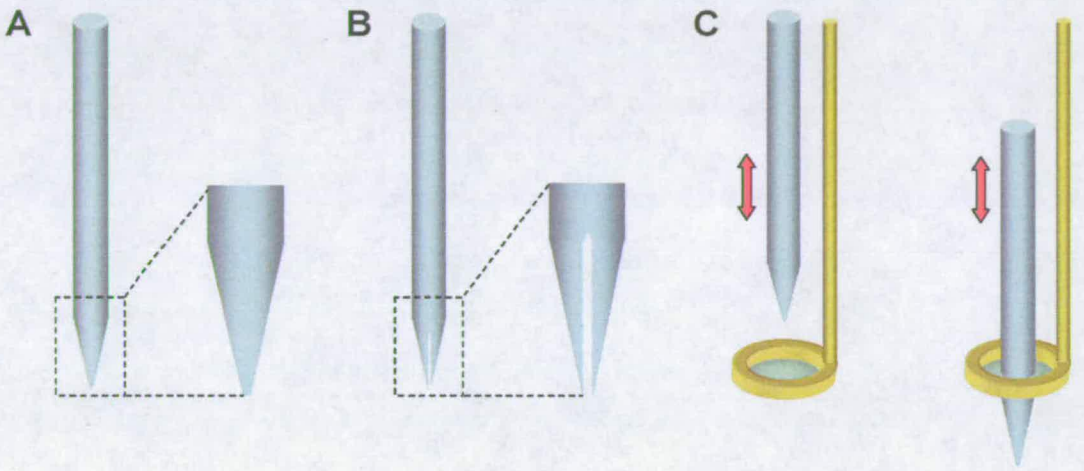

Figure 1.1 *Contact printing pins, (A) & (B) solid pin and spilt pins, respectively, with a magnification of their head, (C) ring and pin system with an illustration of its motion through the film of liquid within the ring.*

Solid pins:

Solid pins are plain needles that must be washed and re-loaded after every deposition. As a result only a single spot is created by inking. The size of the feature created (which is related to the amount of liquid transferred) can be modified by changing the diameter of the pin used. The main advantages of these devices are their low sample wastage, excellent spot-size reproducibility and robustness.

Split and Stealth[14] pins:

Split and Stealth pins were inspired by the design of traditional ink pens, in which a slit is used to draw up ink. The Stealth pins are amongst the most widely used pins. Their main advantage is that they allow the deposition of hundreds of spots without having to

reload. On the down side, these pins can easily become damaged resulting in non-uniform depositions. They also waste a lot of sample (>70%),as they require a pre-blotting step in order to obtain uniform spot size, and are sensitive to sample evaporation[15].

Ring and pin[16]:

This system captures a film of liquid within a ring by dipping it into the sample solution. The deposition is performed by a solid pin travelling through the liquid film, which subsequently transfers a drop of solution onto the substrate without disrupting the liquid film in the ring. In this design the ring acts as a reservoir allowing multiple printing of the same solution. The main drawbacks of this technique are the large dead volume used to generate the ring, and the stability of the film, which can be affected by factors such as humidity and temperature.

Many other pin based technologies (including Hitachi X-cut pin[17], capillary pins, dip-pen nanolithography[18]) have been recently developed, but it is too early to evaluate the impact that these devices will have in the field of array production.

1.1.3.2 Non-contact printing[19]

Inkjet systems are the more advanced of the printing systems, and rely on technology commonly used in desktop printers, where extremely small volumes of solution are deposited without contact between the dispensing tip and substrate. The main advantages of this system compared with the contact printing are gentle deposition, enabling printing on fragile substrates, and better control of the quantities of liquid delivered, allowing a wider range of spot sizes to be printed. These systems can be divided into three competing technologies: thermal, piezo and solenoid jets (**Figure 1.2**).

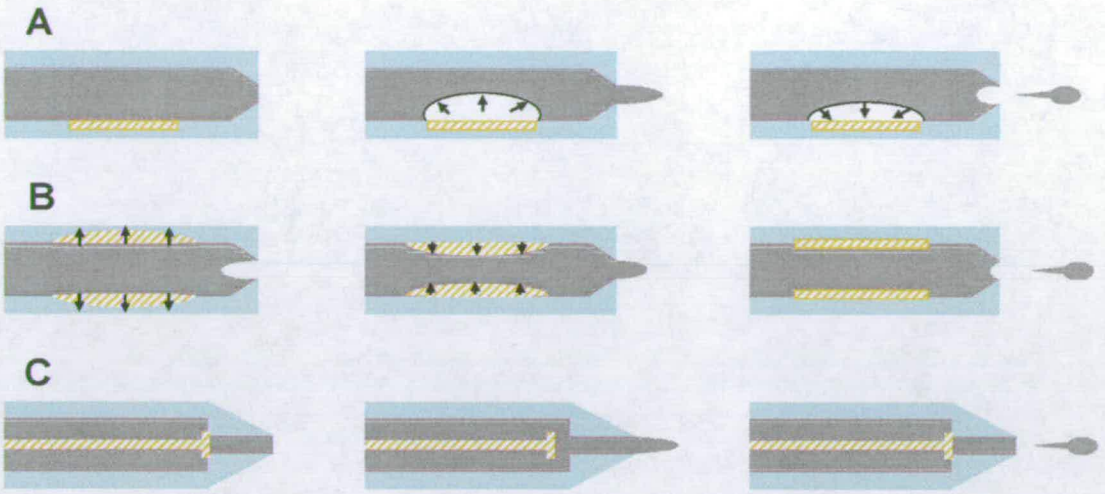

Figure 1.2 *Inkjet printing systems, cross sectional view of inkjet nozzles illustrating the generation of droplets, (A) thermal jet, (B) piezo jet, (C) solenoid jet.*

Thermal jet:

The thermal jet, also called a bubble jet, is based on the rapid heating of the solution (using resistance), which generates a vapour bubble that forces the liquid out of the nozzle. One of the main limitations of these printers arises from the fact that they were optimised for specific ink composition, printing densities and substrates. These limitations probably explain why no microarrayer manufacturer has actually commercialised such a design. Nevertheless, due to very affordable costs, several researchers have published work that used modified desktop printers for the delivery and patterning of biomolecules[20].

Piezo jet:

The piezo jet is probably the most popular non-contact system; it uses a pressure wave generated by a rapid dimensional change of a piezoelectric material to eject a droplet from the nozzle. Commercial desktop printers use dozens to hundreds of such nozzles, however, most piezo-based microarrayers use a single channel. In this system, the liquid delivery is controlled by the duration and amplitude of the voltage applied to the piezo material allowing up to several hundred spots to be delivered per second. The size of the spot generated is usually closely related to the diameter of the nozzle, however, it can

easily be increased by delivering several spots in the same position. Microdrop GmbH uses piezo technology in combination with a heated nozzle[21] allowing the printing of highly viscous liquids such as waxes.

Solenoid jet:

The solenoid jets use electrically controlled high speed valves that prevent the pressurised reagent from leaking out of the nozzle. These allow unsurpassed control of delivered solutions varying from a few nanoliters to several microliters[22]. Unlike the previous systems, the volume dispensed is directly proportional to the pulse width which controls the valve opening. The main limitation of this system comes from the lower limit of volume delivery (~1 nl), which is too large to produce high density microarrays.

1.1.4 Detection methods

The adaptation of diverse assays to microarray formats has led researchers to investigate the use of various detection methods, some of which were previously used in other assays, and some that were specially designed for microarray applications. The most important parameters dictating the quality of a detection technique are described below[23]:

- The **sensitivity** is related to the lowest detectable amount of a given analyte (also referred to as the limit of detection).
- The **resolution** is the smallest change in quantity that can be detected. In a multiplex assay, it can also be used to describe the ease by which two different analytes can be analysed.
- **Signal-to-noise ratio (S/N)** is the ratio of the measured value (signal) to the background value (noise). In a microarray, S/N is often given by the intensity of the analyte over the intensity level given by the non-specific binding on the substrate or the intrinsic background value of the substrate.
- The **specificity** of a binder is the ability of its binding site to distinguish between the ligand to which the binder is specific, and other compounds. It is particularly important when using multiplexed detection, such as mixture of antibodies where cross-reactivity can reduce both the sensitivity and S/N of an assay.

- The **dynamic range** represents the range of concentrations (usually expressed as a log value) over which a given detection system is able to measure an analyte. In fluorescence, this range is between the lowest detectable amount (taking into account the background), and the amount giving rise to signal saturation.

When assessing a detection method many others factors will also come into play including cost, reproducibility, ease of development and safety. An ideal detection method would have high sensitivity, resolution, signal-to-noise ratio, specificity and reproducibility, a large dynamic range and a low cost. None of the detection methods currently available are perfect, and it is the duty of the assay developer to assess which parameters should dictate the selection of any specific method.

The detection methods used in the field of microarrays can be divided into two main categories:

- Label-based detection using a chemical that can be readily visualised (such as a dye) attached to the molecule to be detected.
- Label-free detection, which "directly" detects the molecule of interest.

1.1.4.1 Label-based detection

A wide range of labels have been adapted for use in a microarray format, which are classified by the different physico-chemical properties they encompass. The most popular labels are based on fluorescence, chemiluminescence, and radioactivity. Label-based detection can be divided into two sub-categories. Firstly, when the label is directly attached to the molecule of interest (direct labelling) or, secondly, when the label is bound to another molecule that specifically recognises the molecule of interest (indirect labelling) to provide a mean of detection (for example, using a fluorescently labelled antibody to detect an immobilised antigen). Direct labelling is usually less labour-intensive, however, the presence of a label can alter the conformation and reactivity of the molecule to which it is attached. The use of an indirect method allows signal amplification, which can significantly increase the sensitivity and resolution of an assay.

Fluorescence:

Fluorescence detection is based on the use of dyes that absorb photons when illuminated at a specific wavelength, and which are subsequently re-emitted at a lower frequency (higher wavelength). Fluorescence dyes are easy to manipulate, are widely available, and they provide high sensitivity, quantitative measurements over large dynamic ranges and also allow multiplexing[24]. As a result, the majority of the research published in the area of microarrays uses fluorescent-based detection.

Several approaches have been developed to further enhance the stability and sensitivity of fluorescent assays, such as the use of fluorescent dendrimers to amplify the detection of oligonucleotides[25], or the use of semiconductor nanocrystals (1-10nm), commonly referred to as Quantum-dots[26,27]. These are usually brighter and more stable than organic fluorophores, and their fluorescent properties can easily be tuned by modifying their size and composition, furthermore, they display very narrow bandwidth emissions allowing for highly multiplexed applications. The main limitations in fluorescence detection come from detector sensitivity and the auto-fluorescence of the background.

Detectors used in fluorescence assays are based on charge coupled devices (CCD's) that convert light into electrical current to allow quantification of the light emitted. The light sources used to illuminate the fluorophores are based on two different technologies; firstly, laser-based systems that provide high excitation intensity and narrow bandwidth but are relatively expensive. Secondly, white light source systems that use large excitation bandwidth gas discharge lamps (e.g. mercury vapour lamps) in conjunction with sets of optical filters to select specific excitation and emission wavelengths. The main advantages of these platforms are their reduced cost (*vs.* the laser-based scanner) and versatility, since filters are commercially available and can be easily changed.

Chemiluminescence:

Chemiluminescence is the production of photons by a chemical or electrochemical reaction. Chemiluminescence has been extensively used as a means of detection and quantification in traditional immunoassays[28] and has been used on a number of microarray platforms. An example of such a reaction involves the catalytic oxidation of

luminol by hydrogen peroxide in the presence of horseradish peroxidase attached to an antibody[29]. The detection and quantification is subsequently carried out using a simple CCD camera, the main advantages being the high sensitivity and low cost.

Radioisotopes:

Radioisotopes (^{33}P, ^{125}I) have been used extensively in the area of biochemistry and genetics to label molecules and follow their fate in various physiological processes. The use of radioisotopes as labels in microarray formats has been successfully investigated[30,31] and these labels provide high sensitivity, however, their use is likely to stay limited as radioactivity raises safety concerns regarding its manipulation and disposal and competing technologies such as fluorescence offer much greater advantages such as multiplexing.

1.1.4.2 Label-free detection

Label-free detection methods have the advantage that they do not rely on the use of a label that can modify the physico-chemical properties of the analyte. Many different label-free detection systems have been investigated, however, their use remains quite limited as they rely on expensive instruments with fairly limited throughputs.

Surface Plasmon Resonance (SPR):

Surface plasmon resonance spectroscopy measures the changes in the index of refraction following the deposition of organic or biomolecular thin film onto noble metal surfaces (Au, Ag, Cu). This technology is widely used in the study of many types of interactions such as protein-protein, antibody-antigen and receptor-ligand. Most microarray applications use an immobilised capture agent (e.g. an antibody) on a gold surface, followed by the addition of analyte (e.g. antigen). As the analyte interacts with the capture agent, the system records in real-time the changes in the reflection angle of light, which is proportional to the amount of immobilised analyte. The main advantage of such a system is its versatility, since it can follow the kinetics of immobilisation of many analytes, however, due to fairly low sensitivity this system requires a relatively large amount of analyte, and its throughput remains quite limited[32].

Mass spectrometry:

Mass spectrometry (MS) is based upon the analysis of matter according to atomic mass. With the advances in the field of proteomics, several platforms have been adapted to the parallel analysis of large numbers of sample. Matrix assisted laser desorption/ionisation time-of-flight (MALDI-TOF) mass spectrometry has been used extensively in the field of proteomics for the identification of novel biomarkers[33,34]. Recently, the development of surface-enhanced laser desorption/ionisation (SELDI) has allowed partial on-chip separation of protein mixtures (before analysis) using a combination of spots showing different physico-chemical protein affinities[35,36].

Time-of-flight secondary ion mass spectroscopy (TOF-SIMS) has also been used in the detection of unlabelled DNA fragments hybridised to complementary PNA strands on a microarray[37]. Mass spectrometry applied to microarray platforms is a powerful detection method, however, limitations arise from limited throughput and difficult quantification.

1.1.4.3 Conclusions

As for any other platform, none of the available detection methods are perfect. Today, most research in the field of microarrays uses fluorescent based detection since it is affordable, sensitive and allows a certain degree of multiplexing. Direct fluorescent-based detection usually requires either specific labelling of the analyte(s) of interest, or unspecific labelling of several analytes in a mixture; these are subsequently identified by their coupling partner on the array (e.g. a DNA microarray). Indirect fluorescent-based detection involving specific labelling requires the operator to know which analyte they wants to measure. However, certain areas of research would greatly benefit from a platform that allows the multiplexed analysis of an unknown mixture of samples. This can be partially implemented by detection systems that rely on mass spectrometry, however, these platforms are usually expensive and their throughput is limited to the analysis of one sample at a time. Tomorrow's detection system is likely to combine a quick detection method such as fluorescence to identify and quantify the microarray spot(s) of interest, together with rapid mass spectrometry for the characterisation of unknown bound analytes.

1.1.5 Applications

1.1.5.1 DNA microarrays

The mapping and sequencing of the human genome highlighted the need for novel methods allowing the rapid deciphering of genetic information. DNA microarrays appeared in the middle of the nineties[1,38] and soon became an essential tool for the characterisation and identification of genes of interest. DNA microarrays rely on the ability of a given DNA molecule to bind specifically to, or hybridise with its complementary DNA (cDNA) sequence. These microarrays are prepared by immobilisation of thousands of oligonucleotides, or cDNA fragments. Following hybridisation with a complex mixture of genetic materials, it is possible to decipher the composition and relative amounts of each of the fragments present in the mixture. Gene expression is a highly complex and tightly regulated process that allows a cell to respond dynamically both to environmental stimuli and to its own changing needs. This regulatory mechanism acts as both an "on/off" switch to control which genes are expressed in a cell as well as a "volume control" that increases or decreases the level of expression of particular proteins as necessary. As a result of extensive developments, DNA microarrays are now the tool behind many genomic discoveries; they are used to profile the expression levels of genes[39,40], to study genomic gain and loss[41], to identify mutation or polymorphism in gene sequences[42] and to re-sequence portions of the genome[43].

The main application of DNA arrays has been in the study of gene expression levels. This approach allows the comparison of the level of gene expression of a control sample with that of a sample subjected to specific conditions such as disease[44,45], cell cycle[46] or a drug treatment[47] by monitoring the nature and quantities of messenger RNA (mRNA) present in the nuclei. Such comparisons can be carried out on a single array by mixing the control and sample probes (prepared by reverse transcription of mRNA into cDNA) labelled with two different fluorophores (e.g. Cy3 and Cy5) (**Figure 1.3**). Following hybridisation, washing and scanning, the identity and relative amounts of each immobilised probe can be obtained directly from the integrated fluorescent intensities

arising from each spot. This approach allows rapid identification of the specific gene sets that are modified under given conditions, and therefore holds great potential for the development of focussed diagnostic arrays[48] for the screening of disease[49] or drug-induced effects[50].

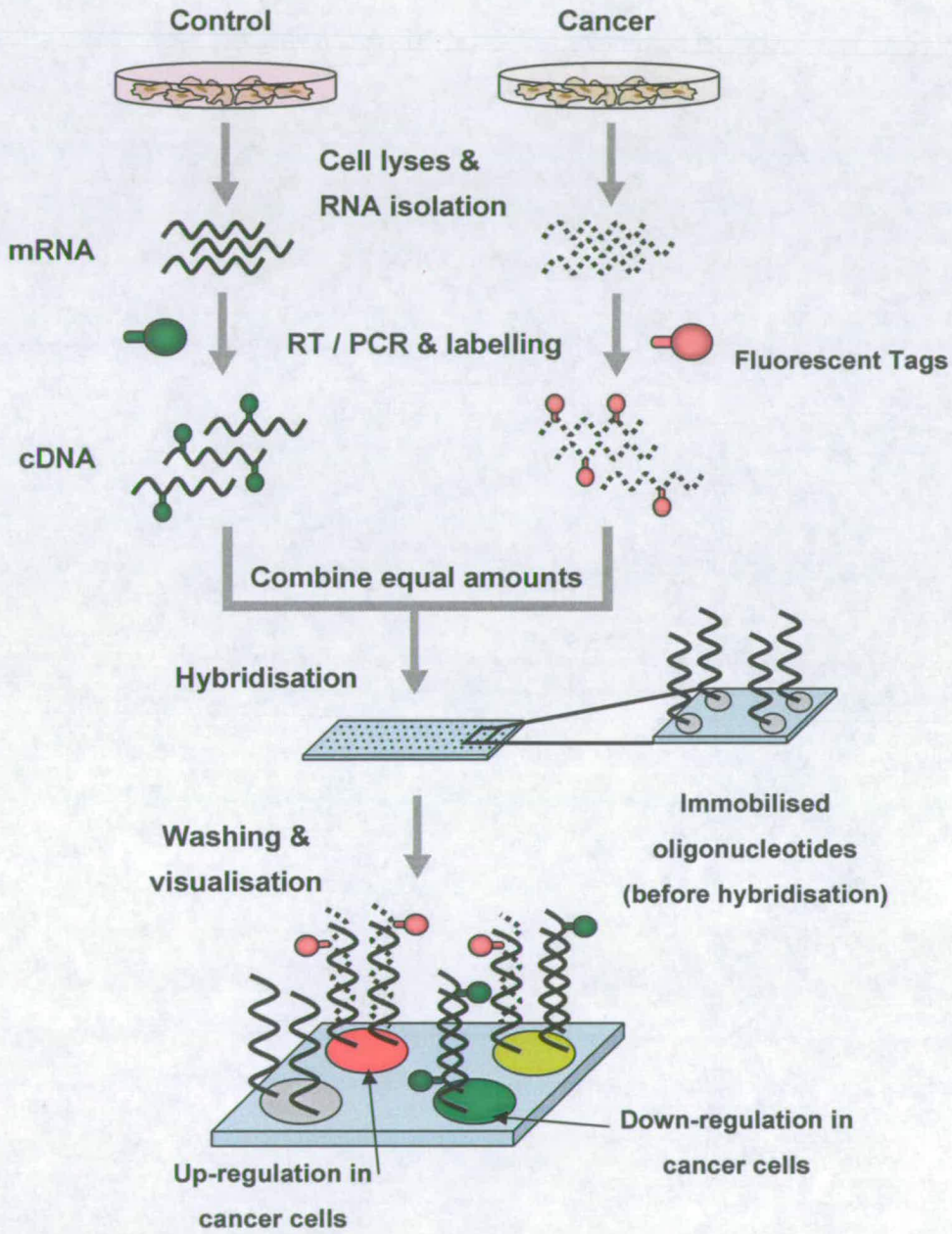

Figure 1.3 *Illustration of a DNA microarray for gene expression studies. General protocol to monitor changes in gene regulation in a cancer patient (cancer vs. control) using a dual-channel microarray.*

Another area in which DNA microarrays hold great potential is in the study of gene gain and loss. It is believed that DNA repair genes are one of the body's frontline defences against mutations. Mutations within these genes often manifest themselves as lost or broken chromosomes. It has been hypothesised that certain chromosomal gains and losses are related to cancer progression[51] and that the patterns of these changes are relevant to clinical prognosis. In one approach, large pieces of DNA from known chromosomal locations are immobilised on a microarray surface and hybridised with a mixture of fluorescently labelled genomic DNA harvested from both normal (control) and diseased (sample) tissue. This technique is sometime referred to as array-based "Comparative Genomic Hybridization" (or array-CGH), it allows for highly multiplexed study of genomic gains and losses and the monitoring of changes in the number of copies of particular genes which may be involved in a disease state, hence providing an insight into the progression of given diseases[52].

DNA microarrays can also be used to study mutations or single nucleotide polymorphisms (SNP). These microarrays can be used to identify sets of mutations common in specific populations (family, cancer, disease[53]). Subsequently, the identified SNP can be used to determine whether a patient is at risk of developing a given disease[54]. Unlike previous applications, these arrays are used with genomic DNA from a single sample.

Finally, DNA microarrays allow the rapid sequencing of whole genome or specific gene sets. Indeed DNA microarrays have been used to sequence the genome of closely related species such as pathogens and allowed the discrimination of different species and sub-species[55]. The results of such studies and the selection of specific probes allow the development of DNA microarrays that can detect the presence of many different pathogens which is of particular interest in environmental and biodefense applications[56].

In the light of the development of new methodologies, DNA microarrays have provided many answers in the field of genomics. However, every method has its limitations and DNA microarrays are no exception. Indeed, the expression of messenger RNA does not always correlate with the quantity of the corresponding protein due to variable translation rates and protein lifetimes. Additionally, mRNA transcripts do not account

for post-translational modifications such as proteolysis, phosphorylation, glycosylation and acetylation[57]. As a result there is a need for both DNA arrays and a highly paralleled and miniaturised approach for the large scale analysis of proteins.

1.1.5.2 Protein and antibody microarrays

Traditional methods for the analysis of proteins made use of gel electrophoresis coupled with mass spectrometry (MS). However, such methods have several limitations, such as the difficulties in detection of low abundance proteins, low reproducibility, time-consuming protocols and difficulties in the separation of hydrophobic membrane proteins and basic or high molecular weight proteins. These methods are also difficult to automate; however, recent developments in multiplexed capillary electrophoresis coupled to MS have allowed the rapid separation and analysis of complex protein mixtures[58].

In an attempt to overcome some of these limitations, so-called protein microarrays have been developed. These are based on the selective binding of proteins with a large variety of capture molecules such as antibodies, proteins, carbohydrates, peptides and small molecules. These arrays have been used to perform two main types of analysis:

- the determination of the abundance of proteins of interest in complex protein samples with highly specific and carefully selected capture agents (usually via antibody-antigen interactions).
- the elucidation of the function and reactivity of given proteins, for example by the study of protein-protein interactions, receptor-ligand interactions and enzymatic activities.

Oligonucleotide/cDNA microarrays are prepared from capture agents and analytes that are relatively stable, and have highly characterised structures and reactivites. On the other hand, proteins present much more complex structures and require a carefully designed environment in order to prevent denaturation. Such difficulties significantly increase the complexity of the array designs, since it becomes essential to have highly engineered surfaces and capture agents. Huge amounts of research have gone into these areas and they are the subject of extensive reviews[59,60].However, only a few examples

of some of the most important applications of such protein microarrays will be presented here.

Antigen/antibody microarrays:

The high affinity and specificity of the antibody/antigen interactions has allowed the development of several platforms that permit the analysis of changes in the abundance/existence of proteins over a large dynamic range (factors of 10^6-10^{10}) in biological samples such as biopsies, body fluids and cell lysates. Such platforms have already demonstrated great potential in the area of serum-protein profiling, allowing the identification of new biomarkers[61]. These discoveries will facilitate the development of diagnostic tools for the rapid identification of disease states[62] and cancers. These arrays can also be used for studying the physiological responses to certain treatments[63]. The immobilisation of large libraries of antibodies and/or antigens can provide a high throughput means of examining the levels of specificity and cross-reactivity of antigen/antibody interactions under specific conditions, using various buffers and surfaces, which can subsequently help in the development and validation of efficient and sensitive assays.

Protein-protein microarrays:

The study of protein-protein interactions usually involves the immobilisation of proteins onto a surface. Immobilisation using fused-proteins is currently one of the most popular methods of protein patterning, as it allows site-specific/non-covalent immobilisation of proteins while maintaining their conformation and activity[64,65]. Following immobilisation, one or more protein(s) of interest is incubated on the array and protein-protein interactions are studied. Such arrays hold great potential in a number of applications such as the identification of enzymatic substrates (see 1.1.5.3 Microarrays for enzymatic assays) and the profiling of signalling pathways[66,67].

Small molecule and peptide microarrays:

Small molecule microarrays consist of peptides, drug-like molecules or natural products immobilised onto a surface and probed for interactions with a protein of interest[68]. They are very stable and can be easily prepared through a variety of immobilisation reactions. They hold promise in the development of drugs as they have the potential to accelerate target-protein identification and also offer a new insight into the study of specific signalling pathways.

Carbohydrate microarrays:

Carbohydrates (glycoproteins, glycolipids, proteoglycans) play major roles in biological pathways, such as cell adhesion, migration and signalling. Several examples of arrays have been developed that allow the detection of carbohydrate-protein interactions. Such arrays present several advantages in that they are highly stable, sensitive and reproducible. A wide range of applications have been developed in such formats[69]. Wang *et al.*[70] probed microbial polysaccharides against human sera, in order to identify human serum antibodies with anti-carbohydrate binding activities against a wide range of microbial infections. Carbohydrate arrays allow the analysis and discovery of known and/or new carbohydrate-mediated molecular recognition in a highly multiplexed manner.

Many other capture molecules have been successfully developed and used to study proteins. Bock *et al.*[71] reported photoaptamer arrays applied to multiplexed proteomic analysis, where proteins bound specifically to aptamers were photo cross-linked for improved signal to noise ratio. Shi *et al.*[72] used molecularly imprinted polymers to generate poly(saccharide)-like cavities that exhibited highly selective recognition for several proteins.

1.1.5.3 Microarrays for enzymatic assays

An enzyme is a protein or RNA produced by living organisms that is able to catalyse or facilitate a specific chemical reaction involving other substances without itself being destroyed or changed. Each enzyme has a specific structure (native conformation), function, distribution of electrical charges, surface geometry, and specificity which depends on its tertiary structure (three-dimensional (3D) shape). Enzymes are responsible for the control of reactions and responsible for the control of cellular metabolism. As a result, they represent an essential class of targets for the development of new therapeutic agents. The early phase of the drug discovery process comprises the identification and validation of biological targets, the development of assays to identify compounds with activity against the target function (hits), and finally the optimisation of these hits. With advances in the field of combinatorial chemistry, researchers are now able to generate large numbers of peptides in a highly multiplexed manner; these peptides are subsequently used to decipher the substrate specificities of a variety of enzymes. However, the rate limiting step in such approaches remains the development of efficient high throughput assays for hit identification and activity assessment. Three main approaches have been investigated in order to interface enzyme research with microarray technologies.

In the first approach, the enzyme's substrates (peptides or proteins[73]) are arrayed onto the surfaces either through covalent attachment[74] or entrapped within a 3D matrix[75]. Following the array fabrication, enzymes are applied on top of the arrayed molecules, and modifications of the arrayed molecules can be recorded using a variety of methodologies including fluorescence[74], radioisotope[76] and MS[77]. The main limitation of this approach arises from the close vicinity of the arrayed molecules to the surface, which can reduce the access and subsequent specificity of the enzymes. This limitation is partially overcome by the use of 3D matrices (hydrogel or glycerol) which allows better accessibility of the substrate while maintaining them in a semi-wet environment.

The second approach involves arraying libraries of enzymes[78]. As in the case of the first approach, this can be undertaken through covalent linkage to the surface[66] or by deposition into 3D matrixes[78], followed by reaction with substrates. The main challenge faced during covalent attachment to a surface is the maintenance of the tertiary structure of the enzyme, which is essential for its specificity and activity.

The last approach consists of arraying the products of enzymatic reactions. In order to achieve the patterning of the enzymatic products, the substrates need to be encoded using a tag that allows controlled immobilisation onto a surface. This can be addressed by generating peptides with unique code tags that are complementary to tags on the surface. This was successfully carried out by Diaz-Mochon *et al.*[79], who generated a library of 10,000 peptides, each encoded with a specific PNA tag (using solid-phase split and mix methodology[80]). Following enzymatic reaction in solution in the presence of the whole peptide library, each enzymatic product (containing a specific PNA tag) can be addressed and studied on a tailor made array of complementary DNA. Unlike the previous methodologies, in this approach the enzymatic reactions do not take place in the vicinity of a surface but in solution which overcomes the limitations of accessibility and specificity.

1.1.6 Conclusions

Over the last 10 years, microarray technology has seen an incredible growth and has now established itself as an industry in its own right. The number of publications in the field of microarray has seen a truly remarkable increase that even other promising fields of science such as nanotechnology and microfluidics are far from matching (**Figure 1.4**).

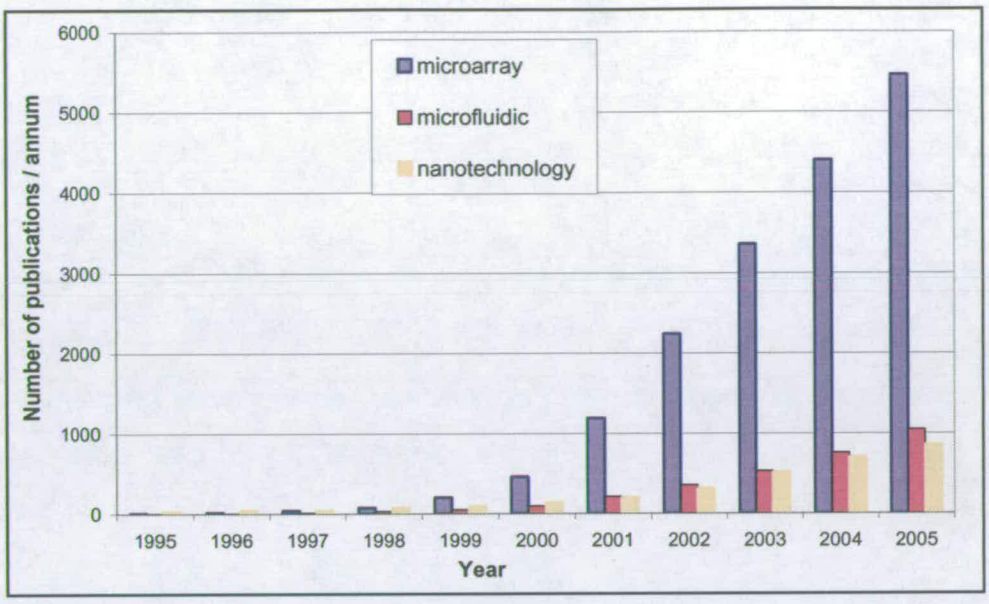

Figure 1.4 *Annual trend in number of publications since 1995, obtained from a search using ISI Web of Science with the term microarray (blue), microfluidic (orange) or nanotechnology (Red).*

The emergence of such an outstanding field would not have been feasible without the collaboration of scientists from many different disciplines. Indeed the microarray area is probably one of the best examples of multidisciplinary approaches with the integration of knowledge from engineers, chemists, biologists, physicists, medical and computer scientists. Traditionally developed to study the expression of genes, the use of microarray platforms that allow faster discovery is now spreading over a range of biological sciences, including the study of proteins (referred to as proteomics), carbohydrates (referred to as glycomics) and enzymes. Tomorrow's challenge is likely to be the integration of huge amounts of data generated using these different platforms[81] in order to further our understanding of oncology, biological pathways and their complex interactions[82,83]. As improvements in robustness and quality of the data are produced, microarray applications are now also emerging in diagnostics[84], where many researchers predict that they will play an essential role in the years to come with the development of pharmacogenomics[85], which correlates drug efficiency and toxicity with the genetic information of a given patient to provide personalised medicine.

1.2 Whole cell microarrays

1.2.1 Introduction

Cell-based assays represent a major part of the screening activities in the biopharmaceutical industry, where they serve as early biological filters in various stages of the drug discovery process[86]. Following the mapping of the human genome, they provide an essential tool for the validation of gene targets.

Like other screening platforms, cell-based assays have been driven toward miniaturisation and automation from traditional Petri dishes to the use of 96 and 384 well plates. Even though higher density plates (1536 and 3456 well plates) are now available, only a few cell-based assays have been successfully adapted to such formats, as their design prevents homogeneous cell distribution due to surface tension. In a search for a smaller format allowing higher parallelisation, reduced cost and lower cell consumption, several researchers have investigated the use of cell-based microarray technology. Like other microarray platforms, the success of cell-based microarrays relies on the development of stable and reproducible assays, which require careful selection and optimisation of various parameters such as the choice of surfaces, immobilisation methods and the means of detection and analysis. However, it should not be forgotten that unlike most biomolecules, cells represent a very complex and is yet not fully characterised biological system, which is extremely sensitive to many environmental factors such as pH, temperature, nutrients and contaminants.

1.2.2 Principles of cellular immobilisation

The surface of the cell is composed of many different molecules including a lipid bilayer, membrane proteins, glycoproteins and small molecules. As a result, the principles underlying the immobilisation of cells onto a surface are far more complex than the immobilisation of single biomolecules. Such complexity suggests that the interactions of the different components of the cell membrane with a given surface should not be considered as independent events, but rather as the result of cooperative and dynamic non-covalent interactions.

The immobilisation of cells onto surfaces has been the subject of extensive research for nearly a century[87]. Several different approaches have been developed, from electrostatic interactions to the use of cell specific antibodies or specific receptors.

One of the most popular means of cellular immobilisation uses the principle of electrostatic interactions, where a highly positively charged surface such as immobilised poly-L-lysine promotes non-specific immobilisation of cells. However, one of the major drawbacks of this approach is the risk that cell health and cycles may be modified by such strong interactions[88,89]. A gentler and more selective cellular immobilisation method is based on biomolecular recognition. This immobilisation route is based on interactions of proteins present on the outer surface of the cells with complementary biomolecules on the substrate. This type of interaction is the cornerstone of several cell-based microarray formats with highly cell-specific interactions, which may be for example between, antibody and antigen [90], or integrins and adsorbed extracellular matrix proteins [91,92].

Two main types of approach have been used for the design of surfaces in cell-based microarray assays. The simplest uses surfaces that promote cell adhesion, whereby a monolayer of cells is grown on both the substrate and the arrayed biomolecules. This approach has been very popular in the development of reverse transfection arrays where cell modification (transfection) occurs only on the deposited feature, while the monolayer of cells surrounding the spot is unchanged[93]. The other approach uses surfaces that are designed to prevent the binding of cells outside the deposited spots, resulting in a patterned array of cells. This can be achieved by a variety of methods, such as coating with hydrophilic gels (polyacrylamide[92] or agarose[94]) or with proteins that block cellular adsorption such as albumin[95]. The main advantage of the latter design is that it facilitates detection and subsequent analysis, since cells are only present on the spotted features, whereas in the monolayer approach, the analysis can be biased by the subjective positioning and size of the analysed spots.

1.2.3 Array fabrication and printing technologies

Unlike DNA arrays where very high density arrays of microscopic spots (usually 5-50 μm in diameter) is desirable, cell microarrays are limited by the minimum size of the arrayed features. Indeed it as been demonstrated that the use of very small features can have an immediate impact on cell fate, as it can mediate cell apoptosis (programmed cell death)[96]. Additionally, even though the use of a single cell screen can, in theory, be achieved, it is usually desirable to study a minimum number of cells (50 to 100) in order to provide statistically relevant and meaningful results. As a result, cell-based microarrays generally use features ranging from 200 μm up to a few millimetres in diameter.

Cell microarrays can be divided into two main categories, depending on whether cells are bound to an array of biomolecules (substrate-based cell microarray), or the cells themselves are microarrayed (genuine cell microarray). The latter approach, which can be used to generate arrays of different cell types, is technically more demanding especially when the arrayed cells need to remain viable.

1.2.3.1 Substrate-based cell microarrays

A wide range of methods and equipment has been used to generate arrays of biomolecules or cells. The simplest consist of directly printing the molecules or cells of interest onto the surface using contact or inkjet printing robots. In another approach, several researchers have used self-assembled monolayers (SAM's) followed by mask and photolithographic methods[95,97], in order to pattern different functionalities on a surface (**Figure 1.5**). These functionalities are subsequently used to immobilise biomolecules that promote or inhibit cellular adhesion. In the case of functionalised SAM arrays, several groups used manual pipetting of the biomolecules or cells of interest to generate the array[97,98].

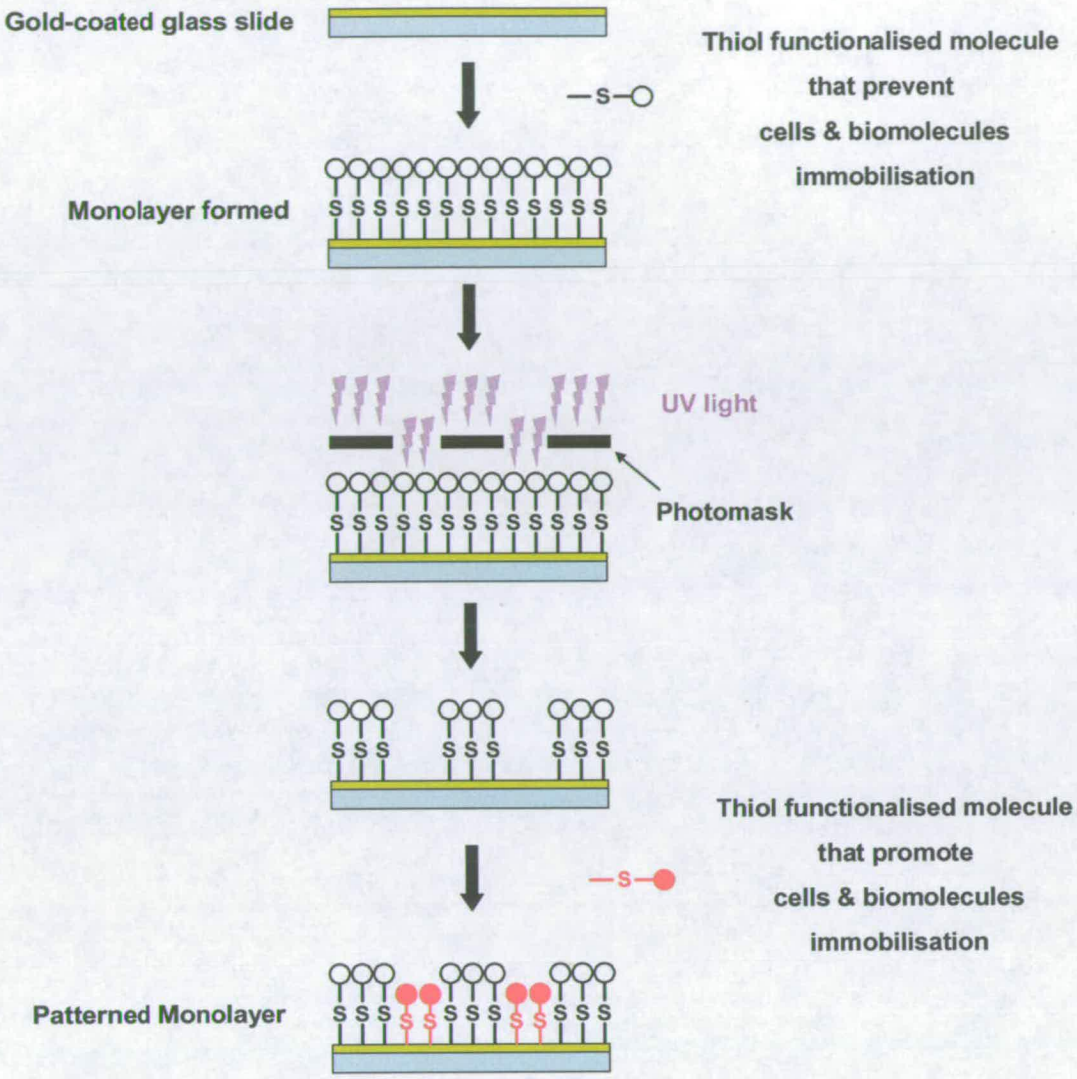

Figure 1.5 *Substrate patterning using SAM and photolithography.*

1.2.3.2 Genuine cell microarrays

The deposition and immobilisation of cells on an array can be particularly challenging if the cells are to remain viable throughout the process. As a result, initial examples of genuine cell microarrays have been developed using frozen[99] or fixed[100,101] cells that were immobilised manually[99-101]. However, a few examples of live cell printing have been published[102-104], and interestingly, all of these experiments were carried out using modified commercial ink-jet printers. Due to their design, the printing of viable cells using these modified systems was limited, and only a few cell lineages were patterned.

1.2.4 Detection methods, imaging and analysis

Most of the detection and imaging systems used in the field of cell-based microarrays rely on fluorescence detection systems. With the drive towards increasing throughput, these systems have required automation for both detection and image analysis. Two main technologies are used for the imaging of such arrays, depending on the level of resolution necessary.

Low resolution systems (2–10 μm), where individual cells do not need to be observed, are based on standard DNA microarray scanners. These systems are compatible with a range of fluorophores and generate single images of a whole microarray. Subsequent analysis is generally carried out with commercial software allowing quantification of fluorescence for each spot[105].

In contrast, high resolution systems (down to 0.2 μm) are based on conventional microscopes fitted with a motorised component allowing the automatic capture of single high resolution image for each spot. The use of these systems, initially developed for microplate assays, is essential when each cell needs to be visualised or subcellular localisation is necessary. The main inconvenience of these systems comes from the handling and analysis of the very large amount of data generated. However, with the development in the field of high content screening, several software packages[106-108] have been developed to carry out automated image analysis. These software packages allow rapid analysis of multiple parameters (including cell number, shape and size and, fluorescent intensities) from hundreds of images in order to provide accurate and meaningful interpretation of various assays.

1.2.5 Main Applications

The field of cell-based microarrays is still in its infancy with most of the research published over the last five years. Nevertheless, cell-based microarray technologies are now emerging for a variety of applications: transfection microarrays are used in gene function studies, microarrays of antibodies, glycans, proteins and peptides are used to study the nature and function of cell membrane components, and microarrays of biomaterials and small molecules, respectively, are used for tissue engineering and cytotoxicity studies.

1.2.5.1 Transfection microarrays

One of the first demonstrations of cell-based microarrays was carried out by Ziauddin and Sabatini[93] where cells were transfected with expression vectors. Transfection microarrays allow a large number of different genes to be screened in parallel for induction or repression of a given function in the cells. In this approach, expression vectors are mixed with a matrix such as gelatine and printed onto a glass microscope slide. Transfection reagents can be added to the matrix or directly added on top of the slide surface. A layer of cells is then grown onto the array and after an incubation of 40 hours, the cells growing on top of the expression vector become transfected giving rise to clusters of 30-80 cells expressing the encoded protein which in turn results in a change in cellular physiology or phenotype. This methodology was successfully used to identify proteins with specific functional characteristics, to localise proteins at the subcellular level and to study the effect of protein on cellular phenotype. Another application was developed by How and co-workers[109] where a similar methodology was used to screen the transfection efficiency of libraries of synthetically prepared polyplexes and lipoplexes. All these modifications can be detected by methods that are used in traditional multiwell plate approaches. Specific proteins can be identified and localised by immunostaining or by co-transfection of a reporter gene such as green fluorescent protein (GFP).

Initial experiments were carried out with expression constructs of cDNAs, but more recently several groups have reported the use of short interfering RNA (siRNA) and short hairpin RNA (shRNA) to knockdown the expression of selected genes [110].

A wide range of transfection reagents have already been successfully used in microarrays, from liposomes and dendrimers[109] to cationic polymers[111] and viral carriers[112]. Transfection microarrays have several advantages, they are compact, easy to handle, they use small quantities of reagents and cell, and provide a highly multiplexed assay. Moreover, as the proteins are translated within the environment of living mammalian cells, they fold correctly.

The transfection arrays have shown great promise, however, a number of issues still have to be addressed for this technology to be widely accepted or recognised. The main limitation comes from the fact that the method is only applicable to cells that transfect easily such as HEK293. Over recent years, several strategies have been investigated to overcome such limitations. Yamauchi *et al.*[111] reported the use of an electroporation type transfection microarray, suitable for use with certain primary cells whereas Bailey *et al.* [112] made use of a viral vector to improve the scope of the method. Another limitation of transfection microarrays is that they are only suitable for cells that adhere to the spot containing the expression vector. In order to solve this problem Kato *et al.*[113] have developed a methodology allowing the immobilisation of a non-adherent cell line by use of a biocompatible anchor for membrane (BAM). This system consists of an oleyl group that inserts into the lipid bilayer of cell membrane resulting in immobilisation of the non-adherent cells. In a later study, Kato *et al.* demonstrated that these immobilised non-adherent cells could be transfected for expression of GFP or knockdown of genes by RNAi[114].

1.2.5.2 Cell-based microarrays for study of cell membrane composition and properties

Another area in which cell-based microarrays have flourished is in the identification and profiling of cell membrane composition and properties.

Antibody Arrays:

Antibody arrays provide a means of high throughput profiling of blood cell populations and are now being developed as diagnostic tools for applications ranging from blood typing to the identification of leukaemias and drug-induced changes in cell surface antigens. The first application of antibody arrays was first developed over two decades ago by Chang who immobilised antibodies for the identification of allotypes of human leukocyte antigens[115]. Several groups have reported the development of antibody arrays to screen antibody-protein interactions[60]. This approach was used by Liu [90] who spotted antibody onto a polystyrene surface to identify clusters of differentiation (CD) antigens present on the surface of whole prostate cancer cells. These CD antigens are used to classify the different leukocyte subpopulations. Another application of antibody arrays is to identify cell surface markers that can be subsequently used for the isolation of given cell populations[95]. These arrays can also provide a means of studying cellular processes induced by antibody recognition, such as increased intracellular calcium following CD3 immunocomplex formation on the surface of human Jurkat T-cell lymphoma cells[116]. More recently, Campbell *et al.*[117] have developed an antibody array for blood typing applications. These arrays comprise of antibodies immobilised on a gold surface and allow the identification of red blood cell surface antigens using whole blood in a label-free detection mode.

One of the main challenges of such applications is to maintain the antibodies' antigen-binding activity. Indeed, activity can be greatly affected by denaturation or steric hindrance following spotting onto surfaces. Significant research into improving such limitations has been undertaken, and this has been extensively documented in a series of reviews[59,60].

Glycan:

Glycans are polysaccharides that are present both within the cells (where they play an important role in intrinsic signalling), and on the outer surface of the cell membrane. Surface glycans can be recognised by specific binding proteins (lectins) which play an important role in cellular adhesion, glycoprotein synthesis, and protein regulation, but also in immune function where they recognise carbohydrates present on pathogen surfaces. The interaction between glycans and lectins was shown to be of low monovalent affinity and high polyvalent affinity, which indicates multi-site binding[118]. As a result, arrays that study the interactions of isolated lectins with immobilised glycans represent only partially the *in vivo* situation. However, it was recently demonstrated that glycan microarrays could be utilised with whole cells to identify and quantify carbohydrate-mediated cellular adhesion. Indeed, Nimrichter *et al.* demonstrated[114] selective adhesion of CD4+ T-cells to an array of 45 different glycan that were covalently attached to a glass surface.

Peptide-MHC:

The major histocompatibility complex (MHC) is a set of molecules present on cell surfaces that are responsible for lymphocytes recognition and antigen presentation. Following the presentation of an antigen on the surface of a macrophage, a specific immune response is triggered by the proliferation of T-cells. It has been shown by Soen *et al.*[119] that immobilisation of a series of peptide-MHC complexes allows the detection of specific T-cells that recognise disease-related antigens in a mixed cell population. Peptide-MHC complex microarrays should allow the identification and characterisation of multiple epitope-specific T-cell populations. As a result, this approach holds great potential as a diagnostic tool for the presence of viral and bacterial infections, cancer, autoimmunity, and successful vaccination.

Double-layer lipid membrane:

Synthetic membranes composed of phospholipid bilayers are designed to mimic the behaviour of plasma membranes present on the surface of cells. Biologically active molecules of interest can be embedded within these membranes to allow the study of

biological processes ranging from simple ligand/receptor interactions to complex cell-cell signalling. The major advantage of this model compared to traditional immobilisation of molecules of interest directly onto a substrate (as presented above in the case of antibodies, glycans and peptide-MHC) is the lateral fluidity of such synthetic membranes. Indeed, the ability of bioactive molecules to freely move and distribute within such an environment allows the study of complex interactions in which dimerisation or oligomerisation of the analytes of interest is necessary for a given biological signalling event. Given the growing interest of such technology, several groups have investigated the multiplexing of lipid bilayer-supported assays by creating patterned arrays of lipid bilayer membranes. Yamazaki *et al.*[120] have, for example, developed arrays of membrane on fused silica through a lithographic procedure, and successfully utilised these membrane arrays for the study of mammalian membrane proteins responsible for adhesion, antigen presentation and subsequent activation of intact T-cells.

1.2.5.3 Cell-based microarrays for tissue engineering

Another area in which cell based microarray technology is flourishing is in the discovery of new materials for cell biology and tissue engineering. Indeed one of the major challenges in these fields is to develop methods for the restoration, maintenance and enhancement of tissue and organ function. In order to accomplish these goals it is essential to control the fate of the engineered tissues. One of the major obstacles to this is the limited availability of materials that can support the growth, proliferation and/or differentiation of specific cells. Due to the immense diversity of cells present in our bodies, there is no universal material for this purpose. As a result, a large amount of research is invested in the discovery of new synthetic or naturally derived materials that can support specific tissues.

The use of high throughput approaches for the generation and analysis of new cell supports offers an important tool in finding correlations between the design and performance of materials suited to this purpose. Consequently, Anderson *et al.* developed a microarray platform that allowed the synthesis and screening of a library of

poly(acrylates)[121]. Following the generation of the polymer library, embryonic stem cells (ESC) were incubated and were shown to differentiate on certain polymer spots. Cell compatibility was then measured in terms of the cellular coverage of each polymer spot. These polymer microarrays allow the rapid identification of several polymers of interest. Moreover, the high multiplexing ability of such screens should permit the study of structure-activity relationships, which will ultimately bring a better understanding of the factors affecting cellular adhesion and proliferation.

Another approach used to mediate cellular adhesion and differentiation is to coat a substrate directly with extracellular matrix proteins. This methodology was applied in a study of the adhesion of three common cell lines (HEK, PC12 and NIH 3T3) to 14 different extracellular matrix (ECM) proteins[91]. Additionally, the adhesion of primary and immortalised chondrocytes to certain ECM proteins was investigated, and it was shown that these closely related cells had different adhesion profiles. Flaim and co-workers[92] printed 5 different ECM proteins, but this time in 32 different combinations, to study which of these protein mixtures could maintain the function of primary rat hepathocytes, and also drive the differentiation of mouse ESC toward an early hepatic fate. These studies demonstrated that microarray technology could be interfaced with the study of cell-ECM protein interactions, which could provide important insights into how to direct the *in vitro* differentiation of stem cells. Traditionally, ESC differentiation is carried out by supplementing the culture media with cytokines (small secreted proteins which mediate and regulate a number of cellular systems), or by the use of co-culture which involves the growing of ESC on a layer of feeder cells. Yamazoe and Iwata[98] used the latter approach and developed a model microarray experiment based on an array of 3 different feeder cells used as a support to direct the differentiation of ESC towards a neuronal fate. After 8 days of ESC culture onto the 3 different feeder cells, differentiation towards the neuronal cell type was assessed by immunocytochemical staining, and reverse transcription polymerase chain reaction analysis. Both methods showed that only the ESC's grew onto stromal PA6 cells presenting neural markers.

1.2.5.4 Cell-based microarrays for drug discovery

The generation of new chemical entities has increased dramatically over recent years with advances in combinatorial chemistry, genomics and proteomics. Cell-based screening represents about 50 % of all screening activities within the biopharmaceutical industries, thus there is huge pressure for the development of highly paralleled, miniaturised and reliable assays to evaluate the efficiency and toxicity of new drug candidates. However, the number of approved new drugs has not followed the development of new compounds, in part due to a large proportion of these new entities failing at various stages of their toxicity evaluations. In view of these problems, Bailey and co-workers developed a microarray format using small molecules embedded within a biodegradable polymer matrix[122]. This microarray was successfully utilised to screen the cytotoxicity of the immobilised compounds on different cell lines. Additionally, they demonstrated how this type of small molecule microarray could be used in conjunction with genetically engineered cells to find correlations between the down-regulation of some genes and the subsequent cell fate induced by a specific compound.

When a chemical enters the human body, a variety of enzymes are involved in its break down (metabolism) and clearance. These brackdown mechanisms involve the formation of metabolites which are sometimes biologically active. Indeed, this process forms the basis of the so-called "prodrugs", where the breakdown products of the administered substance are effectively the active compounds. However, in some cases, the generated metabolites of exogenous chemicals can lead to unwanted effects and harmful biological responses. As a result, metabolite screens are particularly useful in the early phases of any drug development. Lee *et al.* have developed a cell based microarray platform for metabolising enzyme toxicology assays (MetaChip)[123]. In this approach, different isoforms of the cytochrome P450 were encapsulated in sol-gel spots and then printed a gradient of concentrations of 3 anti-cancer prodrugs onto these spots. The slide containing the P450 sol-gels and prodrug solutions was subsequently stamped onto a monolayer of human breast cancer cells (MCF7). After 6 hours of incubations, the cytotoxicity of the metabolites was evaluated by measuring the percentage of dead cells

in contact with each spot and calculating the LD_{50}. Finally, the cytotoxicity results were confirmed by traditional solution phase reactions.

1.2.5.5 Conclusion and Perspectives

The field of cell-based microarrays is still very much in its genesis and many technical issues still have to be addressed in order to produce reproducible and meaningful results using these methodologies. However, the economic pressure to generate higher throughput methods, while minimising expensive reagents and the consumption of rare cell lines, has promoted development of many original solutions. The majority of advances in the field of cell-based microarrays have occurred with multidisciplinary approaches that integrate the latest advances from the fields of chemical and cellular biology, surface sciences, robotics and bioinformatics.

Until recently, most successful cell microarray platforms were based on the immobilisation of cells through interactions with biomolecules arrayed on the substrate (substrate-based cell microarray). Advances in microfluidics[124-126] and electrode-based cellular manipulation[127-129] are likely to bring unsurpassed control of cellular patterning of both adherent and non-adherent viable cells. These advances will allow a wider range of applications, and should facilitate the transfer of cell microarray technologies from academic-based laboratories toward more widespread use within industrial research laboratories.

1.3 Biomaterials and biocompatibility

1.3.1 Biomaterials

1.3.1.1 Introduction to biomaterials

The European Society of Biomaterials has defined a bio-material as a "material intended to interface with biological systems to evaluate, treat, augment or replace any tissue, organ or function of the body"[130].

The use of biomaterials can been traced back to over 2,000 years ago, when metals such as gold were used in dentistry[131]. Most early implants were doomed to failure due to poor understanding of the complex events involved in the interactions of a material with its biological environment. Over the last century, advances in the fields of chemistry, biology and physics have helped to further the understanding of some of these critical mechanisms that occur at a biomaterial surface. This understanding has provided the basis for the development of biomaterials with properties tailored to their specific application. In modern times, biomaterials have become an integral part of medicine, with applications in the implantation of medical devices, artificial organs and prostheses, as well as in the controlled delivery of drugs, and as scaffold for tissue engineering. Millions of devices and implants are used every year in applications as diverse as blood vessel replacement, catheters, contact lenses, joint prostheses, dental filling material and blood bags. The safety and efficiency of drug delivery can be enhanced by the use of biomaterials (mainly polymers), which allow a better control over the duration and localisation of drug release. In tissue engineering, scientists use biomaterials as scaffolds, to provide structure and a suitable environment for the growth of living cells to create viable skin, bone, cartilage, tissues as well as blood vessels.

Biomaterials can be made of various synthetic or natural materials such as pure metals, metal alloys, ceramics and polymers. Before the 20th century, wood, ivory and common metals (iron, gold, silver, copper) were used to make simple prosthetic devices to fix teeth, noses or bones. Most of these materials lacked the desired mechanical properties; however, the development of several metal alloys and coatings at the beginning of the 20th century led to materials with enhanced corrosion resistance, strength and stiffness, allowing the development of several skeletal prostheses and orthopaedic implants.

Bioceramics, which include glasses, have been used in medical applications throughout history. These were traditionally used outside the body as containers for tissue-culture, eyeglasses or porcelain crowns in dentistry. The applications of bioceramics and bioactive glasses as implants were only developed in the late 1960s. At that time, researchers were searching for chemically inert materials for long-term survival of implants. The use of hydroxyapatite (a naturally occurring ceramic material) which is the mineral component of bone was investigated for this purpose. Following implantation of this material into bone tissues, it was noticed that these ceramics resisted rejection and were actually bonding to bone. Since then, many different classes of bioceramics have been developed, and they are now routinely used as coating materials in orthopaedic devices and as bone fillers. When compared to metallic or polymeric materials, bioceramic materials successfully reduce implant rejection and inflammatory reactions; however, their main limitations come from low fracture toughness, low mechanical strength and the relative difficulties in processing them.

1.3.1.2 Polymers as biomaterials

Polymers can encompass a wide range of physical and chemical properties; they can be used either directly or coated onto other materials, they are readily functionalised and they can be degraded by the body after a desired period. Additionally, they are easily processed and come in many different forms including solids, fibres, films and gels. As a result, biopolymers are currently the materials of choice for thousands of medical applications (**Table 1.1**).

Initially utilised for their mechanical properties and high chemical resistance, biocompatible polymers are used as components of prosthetic devices including hip implants, artificial lenses, vascular graft and catheters. More recently, new drugs (protein or peptide-based) have been developed that require novel formulations for efficient delivery. This discovery has led to the widespread use of biodegradable polymers for the controlled release of drugs and gene therapy. Additionally, in tissue engineering, polymers provide structures onto which three-dimensional tissues and organs can theoretically be generated.

Polymers	Applications
Cellulose and derivatives	Membrane for dialysis
Poly(alkyl cyanoacrylates)	Wound closure, drug delivery
Poly(amides)	Sutures
Poly(carbonates)	Device housings
Poly(ethylene oxides)	Coatings for tissue engineering
Poly(ethylene terephthalate)	Surgical mesh, vascular prostheses
Poly(lactic acid)	Tendon repair, sutures, drug delivery
Poly(lactic/glycolic acid)	Drug delivery, sutures
Poly(methyl methacrylate)	Intraocular lenses, contact lenses, bone cement
Poly(urethanes)	Catheters, vascular prostheses, coatings, heart valves
Poly(vinyl chlorides)	Tubing, blood bags
Silicones	Catheters, artificial hearts
Ultra high molecular weight poly(ethylene)	Hip & knee bearing surfaces

Table 1.1 *Some of the most widely used polymers and their biomedical applications.*

1.3.2 Biocompatibility

All biomaterials are by definition biocompatible, but each individual application requires a material that complies with specific mechanical, chemical and biological parameters, hence the meaning of the term 'biocompatibility' depends on its specific application. A definition of biocompatibility has been given by D.F. Williams: "Biocompatibility is the ability of a material to perform with an appropriate host response in a specific application"[130].

Since then, several definitions of biocompatibility have been published which refer to specific applications of the biomaterials, such as the biocompatibility of short-term implantable devices[132]. However, most recent definitions usually describe two main principles, the 'biofunctionality', which refers to the ability of the material/device to perform with an appropriate host response in a specific application (as in the first definition), and the 'biosafety' which relates to the exclusion of any harmful effect of the material/device on the organism. For a material to be deemed biocompatible, it must encompass specific properties such as:

- Lack of cytotoxicity
- Inhibition or promotion of cell-material interactions as required
- Minimal immune response and inflammation
- Optimal chemical, physical and mechanical properties

In order to study the complexity of the factors involved in biocompatibility testing, it is essential to understand some of the steps involved in the mechanisms induced when a biomaterial is implanted into a body, commonly referred to as the 'foreign body response' (**Figure 1.6**).

The first event following implantation is the non-specific adsorption of proteins onto the surface of the implanted material. These adsorbed proteins then mediate adhesion of a number of different cells (monocytes, leukocytes and platelets) which may result in the upregulation of certain cytokines and instigate a subsequent proinflammatory process.

Inflammatory processes usually involve the differentiation of monocytes into macrophages, whose role is to clean wound sites by phagocytosing foreign materials, dead cells and bacteria. In the presence of an implant that is much larger than the macrophages, such phagocytosis is impossible. As a result, a chronic inflammatory process is initiated by fusion of adhered macrophages into multinucleated foreign body giant cells. These cells secrete cytokines and degradative agents such as superoxides and free radicals that can damage the implant. The final stage of the foreign body reaction involves the formation of an avascular collagen shell deposited around the foreign body in order to isolate it from the host tissues. The encapsulation of the foreign material can result in several undesirable reactions such as chronic pain, device rejection and failure (e.g. sensor function may be prevented by its encapsulation).

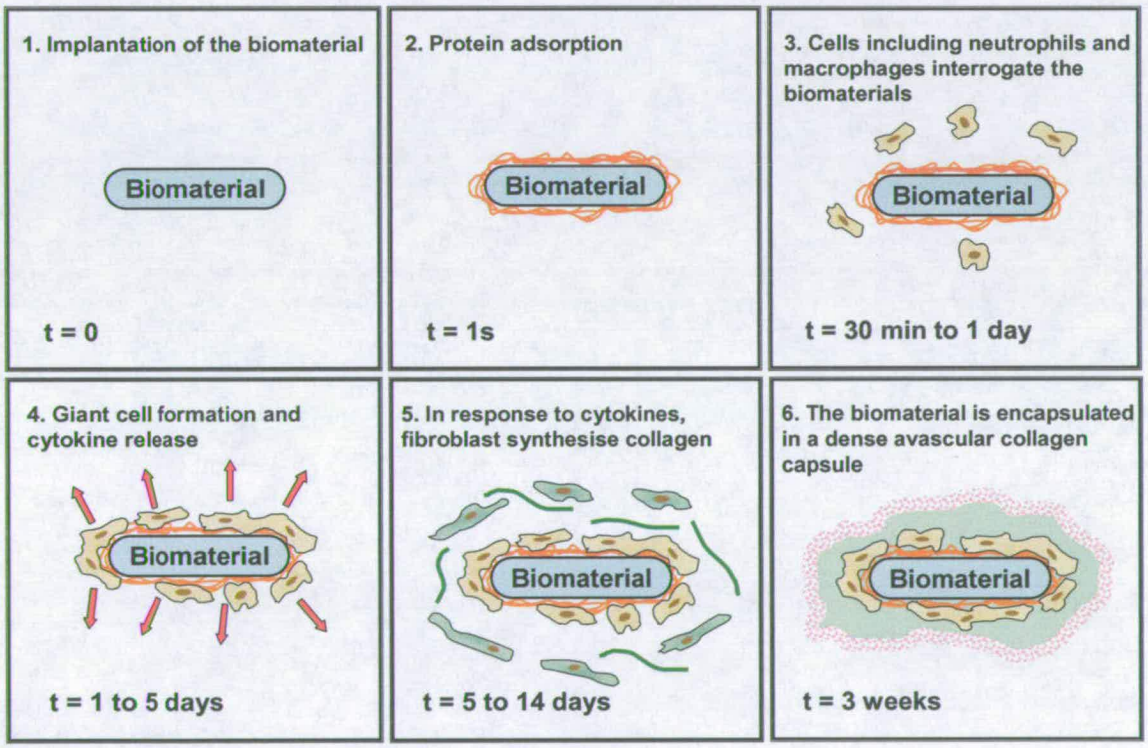

Figure 1.6 *Illustration of the foreign body response.*

1.3.3 Blood compatibility

Another essential aspect of biocompatibility is the compatibility of a material that comes into contact with flowing blood, usually referred to as haemocompatibility. In order to understand the intricacies involved in haemocompatibility, it is essential to study some of the bodies regulation mechanisms involved in wound healing and protection against intrusion by foreign organisms. In short, when a foreign material comes into contact with blood, there is a rapid adsorption onto its surface of plasma proteins such as albumin, fibrinogen, immunoglobulin G and fibronectin. A proportion of these proteins are then displaced by less abundant proteins like factor XII (Hageman factor) and high molecular weight kininogen (HMWK)[133]. Upon activation of factor XII (XIIa), several regulatory systems are initiated, namely the coagulation cascade, fibrinolytic system, kinin system and complement system[134] (**Figure 1.7**).

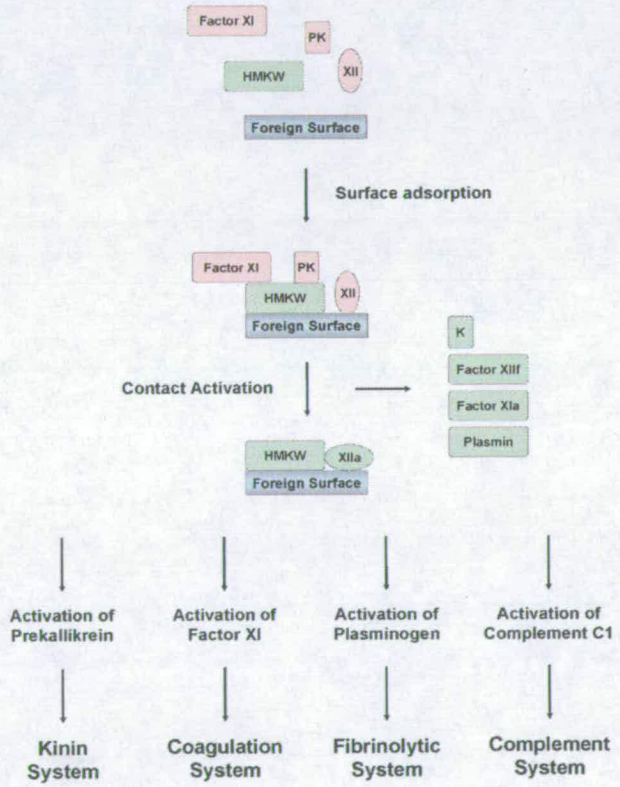

***Figure 1.7** A simplified representation of activation of regulatory systems following contact with a foreign surface.*

The coagulation cascade (Figure 1.8) involves the activation of soluble plasma proteins, and leads to the formation of a fibrin clot that stops blood from flowing. This cascade process can be triggered by either exposure to factors derived from damaged tissue (extrinsic pathway), or by surface-mediated reactions (intrinsic pathway). Both pathways lead to the formation of thrombin which in turn induces the formation of fibrin monomers from fibrinogen, and subsequent adhesion, activation and aggregation of platelets.

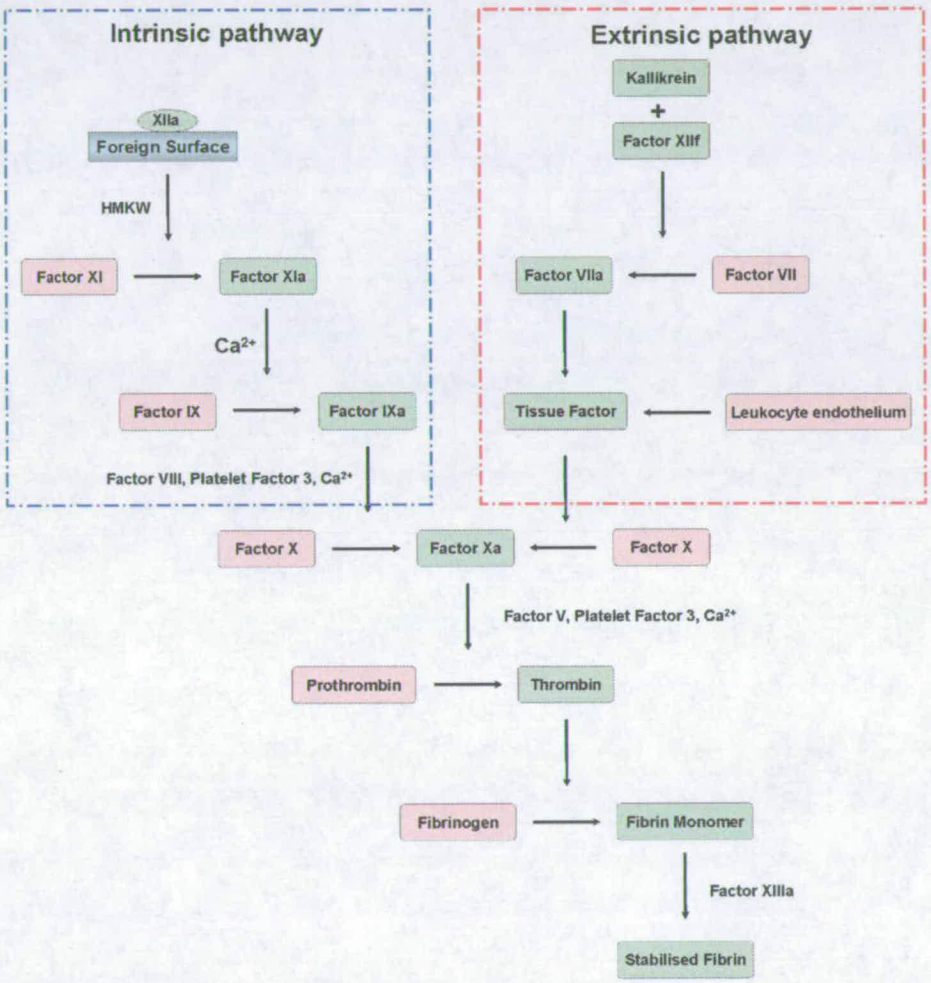

Figure 1.8 *Simplified schematic representing the coagulation cascade, by activation of Factor XII (due to the presence of a foreign surface that initiates the intrinsic pathway), or by activation of Factor VII (due to a trauma (tissue damage) that initiates the extrinsic pathway).*

The fibrinolytic system uses plasmin (a serine protease) to cleave the fibrin network and ultimately degrade unneeded blot clots.

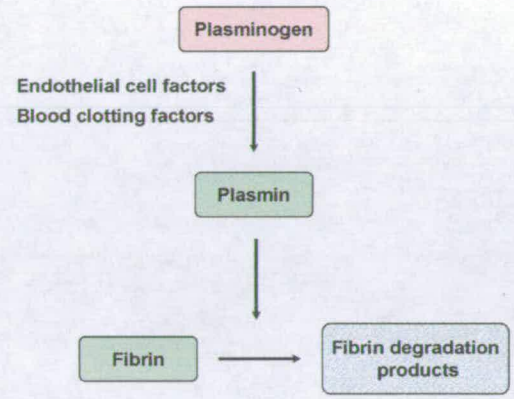

Figure 1.9 *Simplified schematic representing the fibrinolytic system*

The kinin system activates the formation of kallikrein which amplifies the activation of the coagulation and fibrinolytic system. Additionally, kallikrein cleaves HMWK to produce bradykinin, which is a potent inflammatory mediator that induces vasodilation to help the recruitment of leukocytes.

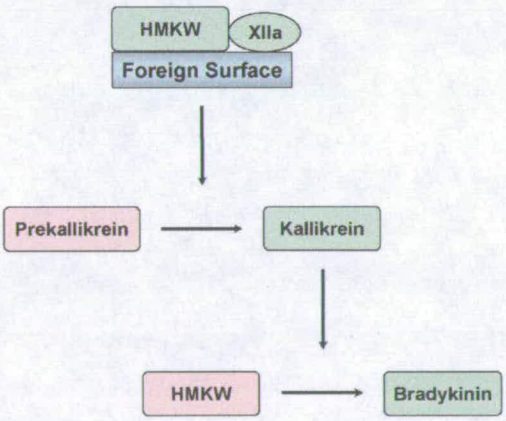

Figure 1.10 *Simplified schematic representing the kinin system*

The complement system is an essential part of the immune response which recognises and clears pathogens from the body. The classical pathway of the complement system can be activated by the action of factor XII fragment (XIIf) on Complement 1 (C1). However, it has also been shown that in presence of foreign material, activation of the complement system acts primarily via an alternative pathway, by the activation of adsorbed protein Complement 3 (C3)[135].

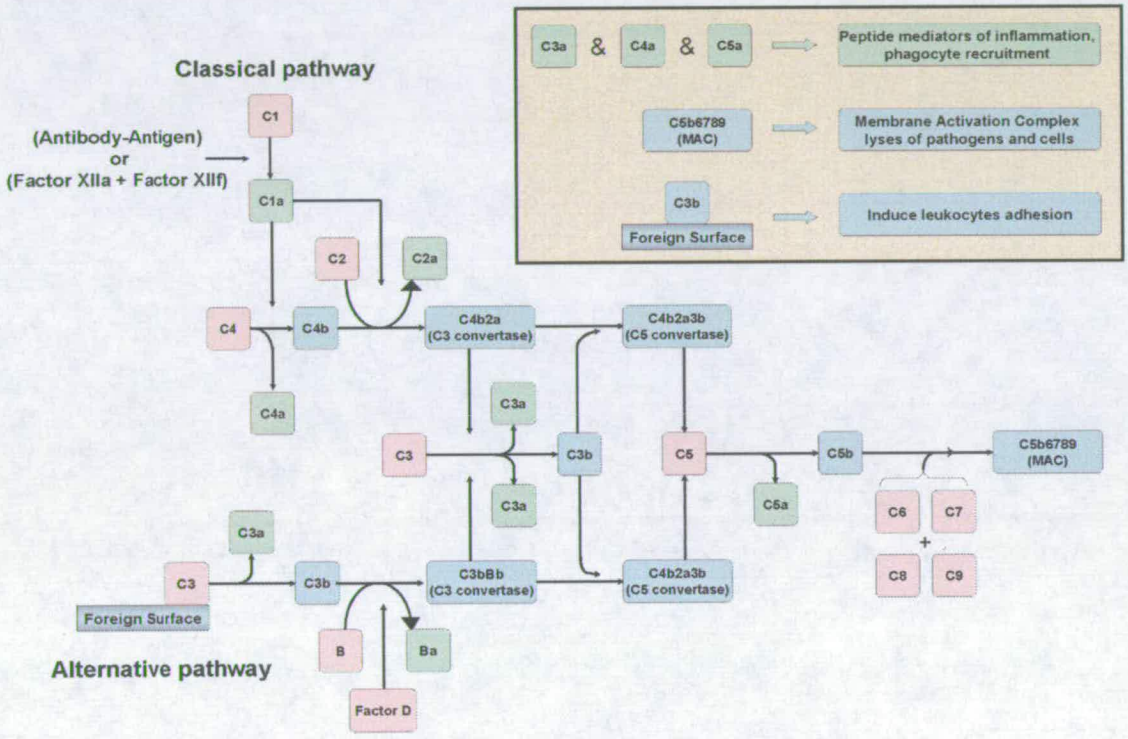

Figure 1.11 *Simplified schematic representing the complement system.*

The interaction of a foreign material with the complement system is sometimes referred to as "immunocompatibility". It must be emphasised that the complement system plays a major part in the inflammatory response, and hence influences both the haemocompatibility and biocompatibility of biomaterials[136].

The four regulatory systems described above are intricately related, with common factors at different levels. These regulatory systems will control the extent of clot formation and the inflammatory response to a foreign material, which is ultimately linked to the haemocompatibility of a biomaterial.

The two major risks associated with poorly haemocompatible materials are:

- the formation of a large clot or thrombus[137] which can block the flow of blood through the circulatory system. Additionally, such thrombi can be carried through the vascular system and lead to blockage in other parts of the body leading to embolisation and possible fatal injury[138].

- the development of a chronic wound through continuous inflammation may lead to prolonged suffering for the patient, and may also lead to complications such as infections[139], sepsis and possible malignancy[140].

From these considerations, Labarre defined a haemocompatible surface as "a surface able to keep under control coagulation and inflammation processes at its interface with normal blood, in given haemodynamic conditions"[141].

Both biocompatibility and haemocompatibility of biomaterials are dependent on initial protein adsorption steps, and as a result, the performance of these materials is highly dependent on surface features such as surface area, crystallinity, hydrophobicity, surface roughness, and surface chemistry. In recent years, many researchers have investigated the modification of the surface properties as a strategy to control the host response at the interface with the biomaterial.

1.3.4 Strategies to enhance the biocompatibility

Biomaterial scientists have developed several strategies to enhance the blood and biocompatibility of foreign surfaces. One of the most popular strategies uses the hydrophilicity or hydrophobicity of the material surface to alter the adsorption of proteins. Alternative approaches have been developed to improve the biocompatibility by enhancing the cellular recognition of the materials. Additionally, haemocompatibility has been drastically improved by the use of small molecules that interact with the coagulation cascade or inflammatory host response.

1.3.4.1 Modifying protein adsorption

Proteins irreversibly bind onto hydrophobic surfaces, whereas adsorption of proteins onto hydrophilic surfaces is usually limited and reversible. A popular method of reducing protein adsorption involves increasing the hydrophilicity of the surface by functionalisation of the surface with hydrophilic polymers such as poly(hydroxyethyl methacrylates) (PHEMA), poly(ethylene glycol) (PEG or PEO) and their derivatives. These polymeric chains can be immobilised onto a material surface through both covalent and non-covalent interactions using a variety of methodologies including grafting [142], coating, and self-assembly[143].

The opposite approach consists of generating highly hydrophobic surfaces. These surfaces irreversibly bind proteins and facilitate the formation of passivating layers that lower platelet adhesion and activation, subsequently enhancing the haemocompatibility[144,145].

Instead of functionalising the surface of materials, another approach aimed at improving biocompatibility consists of producing bulk polymers that can control protein adsorption:

- **Hydrogels** are water-swollen polymeric networks prepared from hydrophilic monomers; they are insoluble due to the presence of chemical or physical cross-links. They have been widely used as biomaterials as they present tissue-like properties and good biocompatibility[146,147]. These hydrogels can be synthesised from cross-linked acrylate and methacrylate monomers, or from co-polymerisation of polyethylene glycol with another monomer such as poly(α-hydroxy acid)[148] or poly(lactic acid) (PLA)[149]. Modification of synthetic procedures, such as the polymerisation conditions and the amount of cross-linker, can afford easy control of a wide range of properties.

- **Microdomain containing polymers** are co-polymers composed of both hydrophilic and hydrophobic moieties. The presence of these microdomains confers upon these polymeric materials a unique organisation of proteins adsorption. These materials have been shown to provide reversible platelet attachment whilst preventing platelet activation[150]. The most popular of these polymers are poly(urethanes), which contain both hard (hydrophobic) and soft (hydrophilic) segments. Alternative examples are co-polymers of hydroxyethyl methacrylate (HEMA) and styrene[151]. Unlike hydrogels, these materials have many desirable properties such as high elasticity, tensile strength and durability[152]. As a result, these materials have found widespread use in blood-contacting applications where prolonged non-thrombogenicity is desired.

1.3.4.2 Increasing cellular recognition

Cellular adhesion is controlled via the interaction of extracellular matrix proteins with cell-surface receptors such as integrins and selectins.

One of the most commonly used strategies for increasing cellular recognition involves mimicking the binding sites of integrins by use of small peptide sequences. The most general peptide sequence used is arginine-glycine-aspartic acid (RGD), which promotes the adhesion of most cells, whereas other sequences have been shown to promote

specific cellular processes, for example, VTXG promotes platelet adhesion[153] and IKVAV promotes neurite extension of neurons [154].

Oligosaccharides are the primary ligands for selectin cell-receptors[155]. Scientists have successfully functionalised PEO hydrogels with different densities of oligosaccharides in order to promote hepatocyte adhesion, and subsequent culture[156].

1.3.4.3 Strategies to enhance haemocompatibility

Researchers have developed various methodologies to interfere directly with the coagulation cascade and inflammatory responses in order to improve the haemocompatibility of biomaterials. A widely used methodology for this purpose consists of immobilising heparin onto the surface of implanted materials. Heparin is a well-known anti-coagulant that regulate the activity of inhibitors of the coagulation system, resulting in the neutralisation of thrombin[157].

Finally, haemocompatibility has been improved by loading biodegradable materials with drugs that act on the inflammatory response. Nguyen *et al.* observed reduced platelet and leukocyte activation and deposition on poly(L-lactic acid) (PLLA) stents loaded with two different anti-inflammatory drugs, curcumin and paclitaxel[158].

1.3.4.4 Future directions in biomaterial design

Biomaterials were traditionally designed and selected for their inertness. A better understanding of the body response to foreign materials has allowed the development of several strategies to synthesise or functionalise materials with enhanced biocompatibility. Recent advances in tissue engineering and drug delivery has driven researchers to develop a new range of biomaterials with additional characteristics such as stealth properties, responsiveness and specificity[159]. The so-called "smart materials" are capable of undergoing modifications triggered by changes in their biological environment. For example, a drug encapsulated within a biocompatible polymer matrix can be released within the patient at a specific site in response to a local change in pH[160], and sheets of cells can be released from their substrate in response to a change in temperature[161]. The design of the biomaterials of tomorrow will rely more than ever on the exchange and integration of knowledge from researchers in various areas of science.

1.3.5 High throughput technologies and biocompatible polymers

1.3.5.1 High throughput synthesis

The generation of new materials represents an area where a large parameter space can be investigated including composition, synthetic parameters, purification, and processing, thus it is particularly suited to the application of combinatorial and high throughput methodologies. Major advances in the field of material synthesis were achieved with the development of automated synthesis platforms[162] allowing a series of discrete materials to be synthesised in parallel under very controlled conditions. Additionally, the synthesis of materials presenting gradients of compositions or properties is unique to the material field. Indeed, instead of synthesising a series of single compounds with slightly different properties, it is sometimes possible to generate a material showing a gradient of properties across its surface. For example, Washburn *et al.* generated thin-films of polymers showing gradients of crystallinity [163] using a custom built flow-coater[164], while vapour deposition of inorganic compounds has been used for the generation of new luminescent materials[165].

1.3.5.2 High throughput screening

The rapid synthesis of hundreds of new materials is useless if the analysis and screening of these materials' properties does not achieve a similar throughput. As a result, many analytical apparatus have been automated to allow the analysis of a variety of parameters with minimal operator intervention. For materials synthesised as single compounds, the screening apparatus can be coupled with autosamplers (e.g. gas chromatography and differential scanning calorimetry (DSC)), or the materials can be placed into multiwell plates or arrayed onto surfaces (e.g. Fourier transform infra red spectrophotometer (FT-IR), matrix-assisted laser desorption/ionization time-of-flight mass spectrometer (MALDI TOF-MS)). Many physico-chemical properties can thus be analysed in a high throughput manner with commercial apparatus.

However, due to the wide range of tests necessary to evaluate biomaterials, there is no single apparatus capable of biocompatibility assessment. Most biocompatibility evaluations involve the study of several biological responses at the interface with the biomaterial. To reduce the cost of analysis and the amount of material required, most methodologies begin with the formation of biomaterial films. Traditional methods for the generation of such films used spin-coating[166] which is time-consuming and difficult to automate. High throughput approaches in many areas of biology have led to the development and widespread use of multiwell plate systems. These have subsequently been adopted in biomaterial research where, for example, a series of polymer solutions can easily be transferred into the wells of a microplate using an automated liquid handling station, followed by simple solvent casting to form a thin polymer film.

1.3.5.3 High throughput analysis

As more and more data are generated, it has become essential to develop computer programs that facilitate interpretation of the results. Traditionally, developed as stand-alone, these software use a variety of visualisation options to enhance the understanding of the results and accelerate the identification of hits. However, recent advances in chem-informatics and molecular modelling have led a few companies to develop integrated solutions for material research. These complex software programs are sometimes integrated with several apparatus and can perform a range of applications from the modelling and design of experiments (DoE), to the control of synthetic parameters, and the collection of data and final analysis and interpretation.

1.3.5.4 Conclusions

The field of combinatorial and high throughput material research is still very much in its infancy. Many developments that originated from the pharmaceutical research have now been adapted to the field of material research. However, due to the complexity and diversity of biocompatibility testing of biomaterials, it has been difficult to standardise platforms allowing high throughput determination of *in vitro* properties of biocompatible materials. Over the coming years, it will be essential for this field to undertake some kind of standardisation in order to allow researchers to share their results and hopefully develop a better understanding of the factors affecting the biocompatibility. Ultimately, the generation of scientific consensus should allow bio- and chem-informatic researchers to development new molecular modelling platforms able to predict the biocompatibility of materials prior to their synthesis. Together with advances in cellular biology, the biomaterial sciences of tomorrow will address several issues in medicine from the generation of artificial organs via tissue engineering to the development of new therapies aided by the controlled release of drugs and genetic materials.

1.4 Aim for the thesis

The aim of this thesis was to development high throughput methodologies to test the biocompatibility of libraries of polymers.

The first step of this approach was to investigate the use of a contact microarrayer to pattern libraries of polymers. Following optimisation of the printing parameters, it was shown that this platform could be used to carry out high throughput physico-chemical characterisations of the arrayed polymers.

The polymer microarray platform was subsequently adapted for the study of cellular adhesion. It was shown that this assay could be multiplexed with more than one cell line.

The polymer microarray for cellular adhesion was applied to the identification of polymers that support:

- the immobilisation of adherent immortalised cell lines.
- the immobilisation and growth of human primary renal tubular epithelial cells.
- the immobilisation of non-adherent immortalised cell lines.
- the immobilisation of mouse bone marrow dendritic cells and the subsequent study of cellular phagocytic activity on the identified polymers.

The polymer microarray for cellular adhesion was applied to the identification of polymers with potential applications in the field of stem cell biology:

- for the selective enrichment of multipotent mesenchymal stromal cell population from human bone marrow.
- for the maintenance of the undifferentiated phenotype of mouse embryonic stem cells cultured *in vitro*.

Finally, the scope of the polymer microarray was widened by adapting it to the adhesion of proteins onto polymer libraries.

EX BIBL. UNIV. EDINBURGH

Chapter 2: Development of polymer microarrays

2.1 Development of polymer microarrays

In order to develop a high throughput method for the study of protein adsorption and cellular adhesion onto polymers, while minimising the quantities of polymers, reagents and cells used, it was decided to develop a highly miniaturised and parallel platform. To this end, a microarray platform where each polymer could be immobilised as a microscopic spot was investigated. It was decided that both protein adsorption and cellular adhesion onto the different polymers would be evaluated by fluorescence measurements, which provided a common and versatile tool. The first three parameters investigated during the development of this method were: the surface onto which the polymers were printed, the solvent used to prepare the polymer solutions, and the printing conditions used by the microarrayer. It is important to note that these three parameters are not independent of each other and will influence the quality and reproducibility of the final polymer microarray.

2.1.1 Surfaces

The first step in the development of the polymer microarrays was to identify two substrates, one giving low protein adhesion, and the other preventing cellular binding in order to achieve a low fluorescent background and easy spot localisation. Initially the polymer microarray was developed for the study of protein adsorption, and it was later adapted for the study of cellular adhesion.

2.1.1.1 Surfaces for the study of protein adsorption

The first step in the development of this method was to identify a substrate with low protein adhesion in order to achieve a low fluorescent background. Protein adhesion to different substrates was measured by assessment of the fluorescent background resulting from incubation with fibrinogen (25 $\mu g.mL^{-1}$) labelled with AlexaFluor® 647 in PBS at pH 7.40. A large number of surfaces were investigated including functionalised glass, metal, and polymeric surfaces (**Table 2.1**).

Material	Nature of surface	Intensity of the background (a.u.)
Glass	Aminoalkylsilane	1 400 000
	Superfrost Plus	800 000
	Polysine	110 000
Metal	Aluminium	28 000
	Solid steel	20 000
Polymeric film	PVDF	300 000
	Poly(ethersulfone)	NA
Coated Glass	Blocking buffer-coated	20 000
	Gold-coated	6 000

Table 2.1 *Background intensity (arbitrary units) determined using [Fg]=25 $\mu g.mL^{-1}$; incubation 3 Hr @ 37°C; fluorescence determined using Cy5 filter and area: ø 250 µm. (The details of the materials can be found in Chapter 6)*

The results of these incubations (**Table 2.1**) showed that many of the different functionalised glass substrates gave very high background intensities. Both metal surfaces gave reasonably low background intensities, but the roughness of the surfaces resulted in poorly reproducible printing. Two polymeric films made of materials used in disposable syringe filters for low protein binding were also investigated. The results obtained with these films were poor as poly(vinyldifluoride) (PVDF) gave a high

background, and the poly(ethersulfone) was inadequate for this method as it was auto-fluorescent at the studied wavelength. Finally, standard glass slides were coated with gold and a blocking buffer[167]. The latter was efficient for reducing protein binding but the blocking buffer layer dissolved locally upon polymer printing. Gold coated slides produced very promising results since the intensity of the background was by far the lowest achieved (**Table 2.1**). However, these low fluorescent intensities do not result from low protein adsorption but from well studied phenomenon of quenching of the fluorescent dye when in close contact with a noble metal surface (Förster Quenching)[168-172]. As a result it was decided that further method development and optimisation would be carried out on gold coated glass slides for protein adhesion studies.

2.1.1.2 Surfaces for cellular adhesion

In order to develop a cell-based microarray format, the substrate had to comply with several requirements. Firstly, the substrate had to be unaltered by the contact printing of the polymer solution in organic solvent, which ruled out the use of polymer coatings such as poly(hydroxyethyl methacrylate) p(HEMA)[173] which could be dissolved locally and give rise to polymer mixtures. Secondly, a substrate with low levels of background cell binding had to be developed to facilitate data analysis and thirdly, the substrate had to be stable under UV-irradiation to allow sterilisation prior to the plating of the cells.

Several functionalised and gold-coated glass slides were investigated for this application, most of which provided a suitable surface for polymer printing, and could be readily sterilised under UV-irradiation, but unfortunately they did not prevent cellular adhesion. As a result, several substrate modifications used in cellular patterning applications were investigated. The following substrates were prepared and tested: C18-functionalised slides, perfluoroalkylthiol monolayers on gold coated slides[11] and Silane-Prep™ slides dip-coated with a layer of agarose gel. The C18-functionalised slides, as expected, were highly hydrophobic and were able to reduce non-specific binding, but not all cell lines could be blocked in this manner. The use of perfluoroalkylthiol-modified slides inhibited cellular adhesion, however it was impossible to use UV-irradiation for sterilisation as this degraded the surface. The best results were obtained by

dip-coating aminoalkylsilane slides (Silane-Prep^{TM}; Sigma) with a thin film of agarose (**Figure 2.1**). Although agarose gels have been used to amplify loading on DNA arrays[12], and are known to inhibit cellular adhesion in a number of different formats[20,174], agarose had not been directly used as a substrate for cell-based microarray assays. Importantly agarose is readily sterilized by UV irradiation and does not dissolve in most organic solvents.

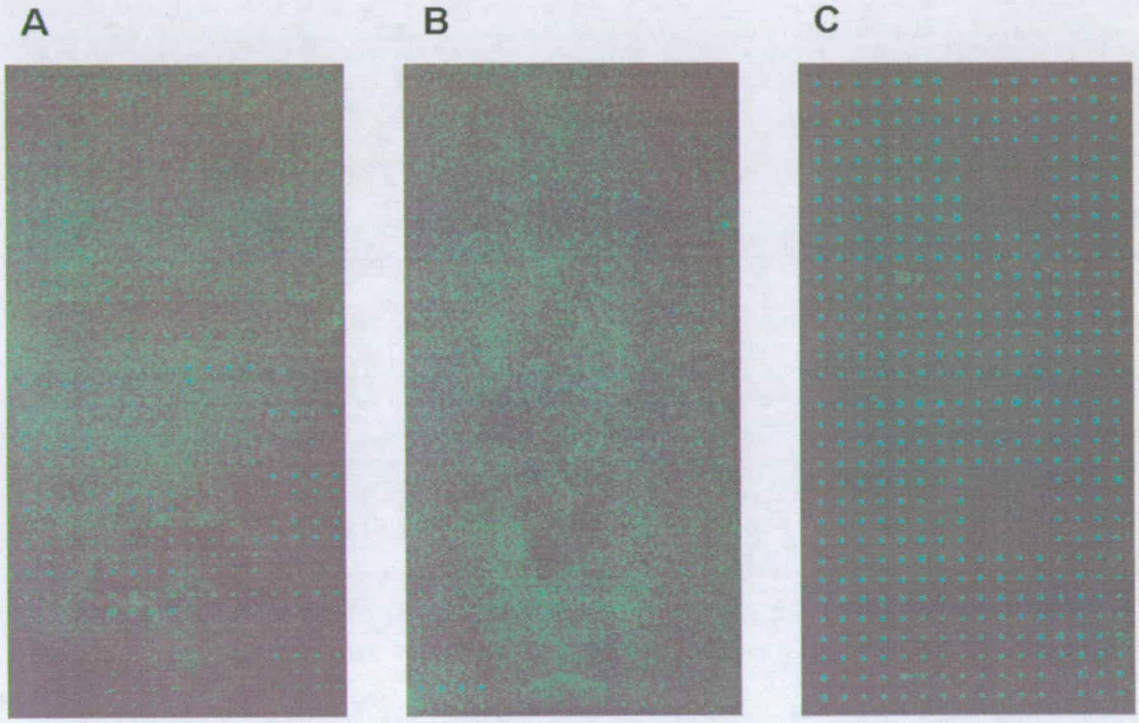

Figure 2.1 *Non-specific cell binding reduction using an agarose-coated substrate. Non-processed images obtained with STRO-1+ cells stained with CellTracker^{TM} Green on different substrates; (A) unmodified glass slide, (B) C18-functionalised and (C) agarose coated.*

2.1.2 Solvents

In order to study the effect of different polymer solvents on the quality of the printing, polymer solutions were prepared at 1.0 % w/v and subsequently printed using 150 μm solid pins (Genetix). The 1.0 % w/v concentration was selected as it was the single highest concentration allowing good solubilisation across the various polymer libraries.

A variety of solvents were investigated. Initially, poly(acrylates) (Appendix II) were printed after dissolution in three different alcohols (methanol (MeOH), ethanol (EtOH) and isopropanol (IPA)) each mixed with 10% water, and poly(urethanes) (Appendix I) were printed in tetrahydrofuran (THF), dichloromethane (DCM) and chloroform ($CHCl_3$). Both methanol and isopropanol-based polymer solutions gave regular spots. However, polymers prepared with the ethanoic mixture tended to spread when spotted onto gold-coated substrates. Printing of poly(urethanes) in THF, DCM and chloroform was shown to be difficult as solvent evaporation prevented uniform printing, especially for large numbers of samples. Additionally, when the printing was satisfactory, it was noticed that upon drying, ring formation[175] could be observed. As a result, the use of a low volatility solvent suitable for both libraries of polymers was investigated. *N*-methyl-pyrrolidinone (NMP) was selected as over 90 % of the polymers from both libraries were soluble in this solvent, and its boiling point (202 °C /1 atm) prevented rapid solvent evaporation which allowed large numbers of polymers and microarrays to be printed in a single run. In order to fully remove the solvent following printing of the polymer, the arrays were dried under vacuum at 45 °C overnight.

2.1.3 Printing and washing of the polymer microarray

Printing was carried out using a Qarray^{mini} (Genetix) contact microarrayer. This arrayer allows the control of a variety of parameters including inking time, stamping time, number of stamps per spot and washing conditions.

Two types of microarraying pins were investigated:

- **Split pins** (75 μm aQu, Genetix, UK) contain a slit that act as reservoir for the solution to print. Using these it is possible to print more than one spot per inking and to control the spot size by changing the stamping time (the time during which the pin needle is in contact with the substrate). Unfortunately, their design was not compatible with the printing of polymer solutions combined with the use of the integrated washing station, since following pin washing with ethanol or water (the only solvents compatible with the washing station), polymers (especially polyurethanes) precipitated inside the slit making any further printing impossible. The only solution to this problem was to sonicate the pins extensively in NMP in order to remove any precipitate. Since this prohibited the development of a high throughput method for the generation of polymer arrays, the use of another pin design was investigated.
- **Solid pins** (150μm aQu, Genetix, UK), whose design is very similar to sewing pins, were investigated. Using solid pins, the main factors affecting the shape and uniformity of the printed spots were the nature of the solvent and substrate used. Since the gold-coated substrate and NMP solvent were selected, it was very difficult to tune the spot size using solid pins (unlike split pins, the stamping time has hardly any effect on the size of spot printed using solid pins). The only parameter investigated was the use of more than one stamp per spot providing more than one deposition of polymer solution in the same position. It was found that best spot uniformity was obtained using 5 stamps per spot.

Finally as mentioned above, the washing station was only compatible with ethanol and water. This represented a major problem especially when washing followed poly(urethane) printing as it caused precipitation and subsequent cross-contamination of the next samples. As a result, it was decided that when printing more polymer samples than the number of pins available at the time (16 pins), manual washing of the pins using a cloth and acetone was necessary following the automatic washing step.

2.1.4 Evaluation of spot size reproducibility

In order to determine the reproducibility of the printing method using the parameters selected above (NMP as solvent and solid pins to deliver the polymer solutions), an array containing 128 different poly(urethanes) (**Table 6.4**) each printed as four replicate spots was generated on gold-coated slides. To allow rapid evaluation of spot size (FIPS software, LaVision Biotech) the array was incubated with fibrinogen labelled with AlexaFluor® 647. Following incubation, the array was washed, dried and scanned (**Figure 2.2**).

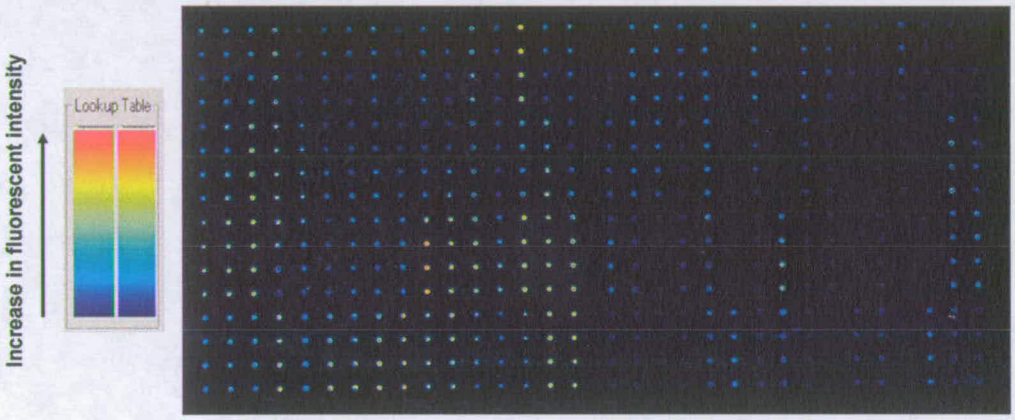

Figure 2.2 *Fluorescent scan of a polymer microarray containing 128 polyurethanes showing the adsorption of AlexaFluor® 647 labelled fibrinogen. Each polymer is printed as 4 identical spot vertically.*

The average diameter for 120 different polymers was evaluated and the overall mean diameter and standard deviation calculated (the diameter of 8 remaining polymers could not be measured as they showed no protein adhesion). Due to the low resolution (10 μm) of the Bioanalyser 4F/4S scanner, the diameters were evaluated to the nearest 10 μm. Each set of four spots prepared from the same polymer were of similar diameter (+/-10 μm) (**Table 6.4**). Mean spot diameter over the whole array (120 polymers) was 306 μm with a standard deviation of 20 μm, which gave a coefficient of variance of about 6 %, which was satisfactory when considering the high throughput with which the array was generated. As a result, all subsequent array printing described in this thesis were generated using the parameters described above.

2.2 Physical characterisation of polymer spots on the microarray

Characterisation of the printed polymer spots on the microarray was explored as a potential means of high throughput physical and chemical characterisation. This included scanning electron microscopy to study the morphology of the printed spots, Fourier transform infrared (FT-IR) microscopy and time-of-flight secondary ion mass spectroscopy (TOF-SIMS) to study the composition of the surface of the printed polymer spots.

2.2.1 Scanning Electron Microscopy

Scanning electron microscopy (SEM) uses finely focused electron beams to scan across a sample to produce high resolution images. Unlike traditional optical microscopes that use light waves to create a magnified image, SEM creates a 3-dimensional image with a resolution of several nanometres. Since the SEM microscope illuminates the samples with electrons, the samples have to be made to conduct electricity in most cases. This is undertaken with a sputter coater which deposits a thin film of conductive material such as gold or carbon black onto the sample.

Prior to scanning, polymer microarrays were covered with a thin film of gold using a sputter coater. The coated array was cut into two pieces in order to fit in the sample holder; finally, the piece of microarray was inserted in the vacuum chamber and subsequently scanned. This allowed the study of spot morphology in the microarray format. Out of 48 different polymer spots recorded, most showed smooth and uniform surfaces, and only 10 spots were non-uniform or with a globular surface. (**Figure 2.3**). When the composition and molecular weight (27 to 170 kDa) of these 10 irregular spots were studied, no clear correlations were found. It was therefore impossible to draw any clear conclusions as to why these polymers failed to produce uniform spots upon microarray printing and drying. However, scanning electron microscopy provided a convenient method to aquire morphological information at the micrometer scale on large number of printed polymer spots in a single experiment.

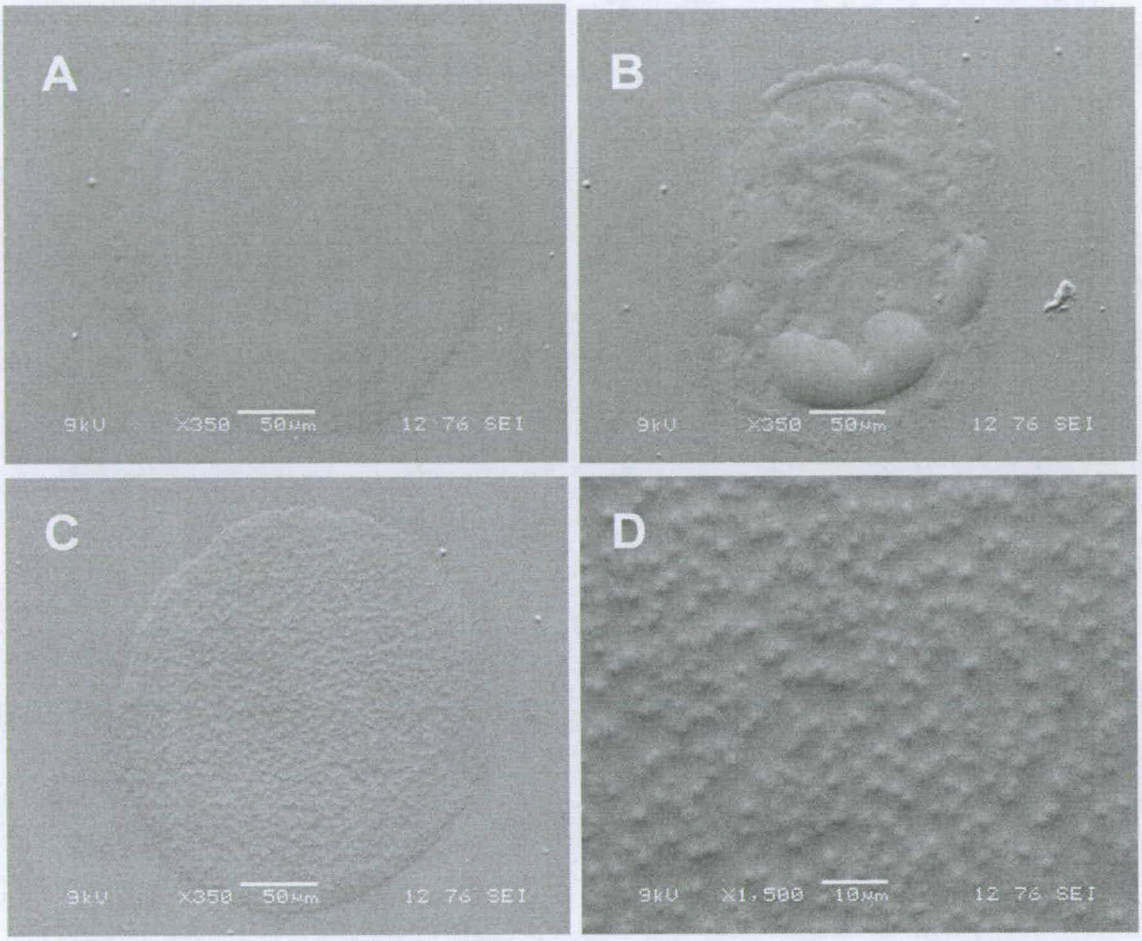

Figure 2.3 *Scanning electron micrographs of polymer spots printed on gold-coated slides. (A) a uniform and smooth spot of PU-12; (B) a non-uniform spot of PU-179; (C) a uniform spot of PU-63 with a globular surface; (D) Higher resolution micrograph showing the globular surface of spot C.*

2.2.2 FTIR microscopy

Fourier transform infrared (FT-IR) spectroscopy is an invaluable tool in organic structure determination, based on the interaction of IR radiation with matter. A molecule absorbs infrared radiation when the vibration of the atoms in the molecule produces an oscillating electric field with the same frequency as the frequency of incident IR radiation. Typical infrared spectroscopy involves recording absorption information across a range of frequencies (4000 to 400 cm^{-1}) in order to obtain a spectrum from which absorption bands (related to specific bond vibration and stretching) can be correlated to chemical bonds within a compound. An FT-IR microscope consists of a FT-IR spectrometer coupled to a light microscope with an integrated CCD camera and automated X-Y-Z stage. This type of platform allows the automated IR spectroscopic analysis of large areas, and subsequent mapping of functional groups. As a result, an FT-IR microscope can be programmed to visualise functional group distribution across an array of polymer spots. As a proof of concept, an entire spot of 2BCg7-1.0 poly(acrylate) was mapped by following the absorption corresponding to the carbonyl functionality (1727 cm^{-1}) of the methacrylate-based monomers and a 3-dimensional projection was obtained (**Figure 2.4**).

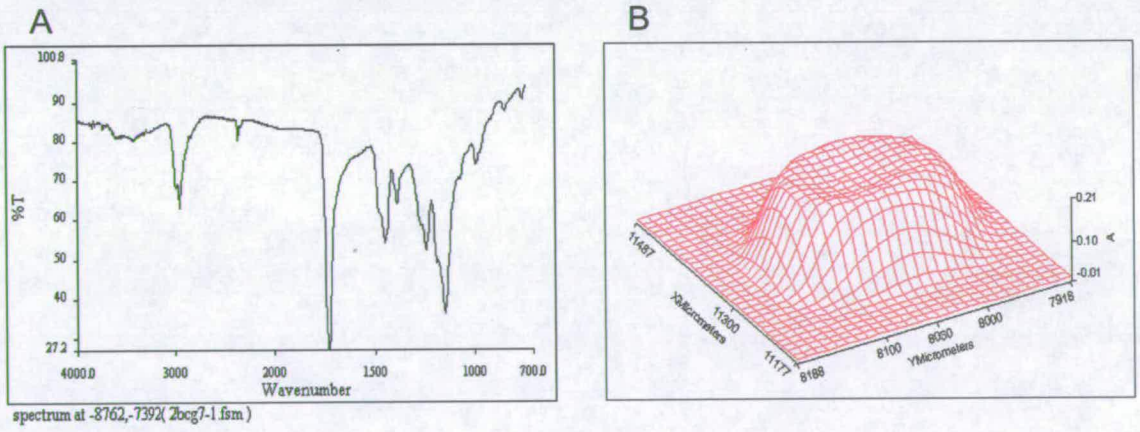

Figure 2.4 *FTIR microscopy of a poly(acrylate) spot of 2BCg7-1.0; (A) FTIR transmittance spectra taken in the middle of the polymer spot; (B) 3-dimentional mapping of the absorption of the carbonyl functionality (1727 cm^{-1}) across the entire polymer spot.*

2.2.3 TOF-SIMS

TOF-SIMS combines two analytical techniques: SIMS involves bombarding a surface with primary ions (such as Gallium, Ga^+), which transfer energy to surface atoms through a collision cascade allowing fragmentation and subsequent emission of clusters of atoms. These clusters are subsequently analysed using TOF mass analysis, which is based on the fact that ions with identical energy and different masses travel with different velocities allowing the generation of a mass spectrum in which each band corresponds to a cluster of different mass/charge (*m/z*). This technique was applied to determine the surface composition of an arrayed series of poly(acrylates) synthesised using different ratios of 2-methoxyethyl methacrylate (MEMA) and diethylaminoethyl methacrylate (DEAEMA) (MEMA/DEAEMA mol. % = 100/0; 95/5; 90/10; 85/15; 80/20; 75/25; 70/30; 65/35).

All of the polymer spots revealed strong mass ions at *m/z* = 59 and 69, respectively, for $^+C_2H_4$-O-CH_3 ions from MEMA and for the main methacrylate chain ions ($^+C_4H_5O$). All of the polymer spots containing DEAEMA presented additional mass ions at *m/z* = 72, 86 and 100 corresponding to the side chain ions $^+N(C_2H_5)_2$, $^+CH_2$-$N(C_2H_5)_2$ and $^+C_2H_4$-$N(C_2H_5)_2$, respectively. As a result, the polymer spot surface composition was calculated from the intensity ratios of the peaks (*m/z* = 100/59). The molecular percentages of DEAEMA obtained experimentally were plotted against molecular percentages of DEAEMA introduced during polymerisation (**Figure 2.5**). The analysis showed that the ratio of DEAEMA calculated from the recorded spectra were higher than the ratio of DEAEMA monomer introduced during polymerisation. These results are likely to be due to the fragment ion (*m/z* = 100) containing diaminoethyl functionality, which was more easily fragmented than the fragment ion containing the methoxy group (*m/z* = 59). Therefore, the results obtained from this technique provided only semi-quantitative information.

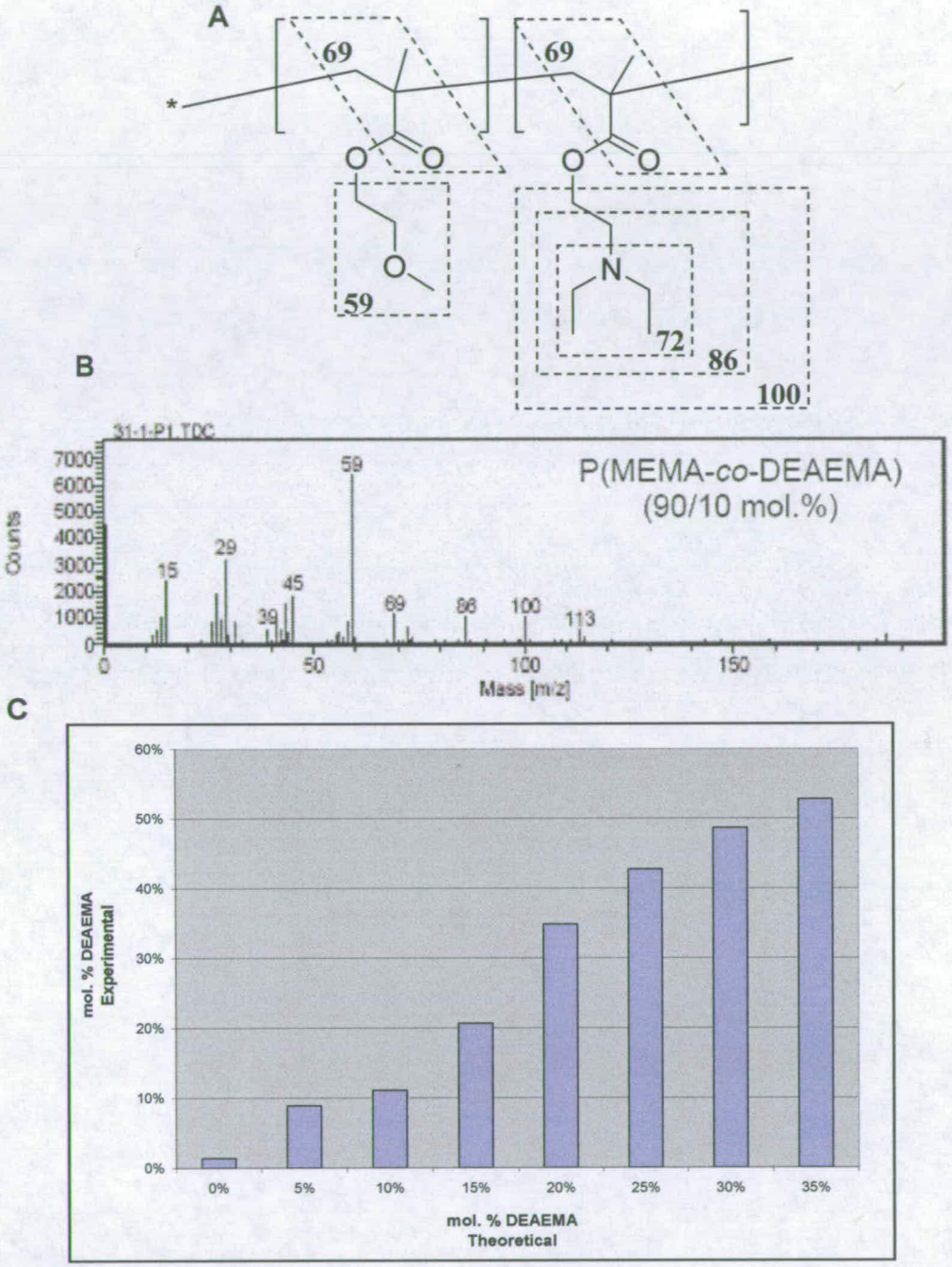

Figure 2.5 *(A) ions assigned by TOF-SIMS, (B) example of TOF-SIMS spectrum for a poly(MEMA-co-DEAEMA) copolymer, (C) compositional analysis of the polymer spots: experimental compositions obtained from the TOF-SIMS analyses versus theoretical compositions obtained from the amount of monomers used in the polymerisation.*

2.3 Conclusions

A high throughput method allowing the patterning of large numbers of polymers on a microscope slide was developed using a contact microarrayer. Several parameters (surface, solvent, pins and printing conditions) were optimised in order to generate polymer microarrays with uniform and reproducible features. The best results were obtained by preparing polymer solutions in NMP as solvent and printing using solid pins. Using different surfaces, these polymer microarrays can be used for different applications; gold coated surfaces can be used for the evaluation of protein adsorption, whereas agarose coated slides can be used to study cellular adhesion. Additionally, it was shown that the polymer microarrays can be used to study the properties of the printed polymers. Scanning electron microscopy allowed the study of the the printed spots morphologies. However, from the chemical composition and molecular weight of the printed polymer, it was impossible to draw any clear conclusions as to why specific polymers failed to produce uniform and smooth spots. Chemical functionality and composition analyses were undertaken using Fourier Transform Infra Red (FT-IR) microscopy and time-of-flight secondary ion mass spectrometry (TOF-SIMS). FT-IR microscopy allowed the characterisation and mapping of chemical functionality across the printed polymer spot whereas TOF-SIMS provided semi-quantitative informations regarding the surface composition of the polymer spots. These experiments emphasise the versatility of the polymer microarray platform which can be utilised for both biological and chemical high throughput experimentations.

Chapter 3: Screening of biocompatible polymers for cellular adhesion

Following the successful patterning of polymer solutions to generate a polymer microarray, this platform was used to identify new polymers that support the adhesion and/or growth of a variety of cells, ranging from immortalised adherent cell lines to the more challenging primary and non-adherent cells.

3.1 Assay development

3.1.1 Introduction

Initial work was carried out on arrays of 120 poly(urethanes) each printed as four identical spots using available immortalised adherent mammalian cell lines (B16F10 and ND7). In order to evaluate cell adhesion on the different polymer spots, fluorescent probes such as CellTracker™ (Molecular Probes, Invitrogen) were used to label the cells. CellTracker™ can freely pass through cell membranes, but once inside, it is transformed into cell impermeant reaction products, preventing leakage and/or contamination of adjacent cells. Additionally, the fluorescently labelled cells can be easily fixed with aldehyde fixatives permitting long-term storage and visualisation.

Most developmental work was carried out using a low resolution scanner (BioAnalyser 4F/4S with FIPS, LaVision) as it was the only available analysis system at the time. Cell binding was evaluated by integrating the fluorescence intensity across the whole area of the spot. The mean fluorescence intensity and coefficient of variation for each set of four identical polymer spots was then calculated. Background corrections were carried out by subtracting the mean fluorescence intensity of 32 "background spots" from the mean fluorescence intensities calculated for each library member.

3.1.2 Assay description

Following preparation of the polymer arrays on the agarose-coated substrate, each polymer microarray slide was covered with a suspension of labelled cells (typically 10^6 cells / slides in 15 mL cell culture medium). After 24 hours of incubation, the microarrays were rinsed in PBS to remove any non-specific binding, and the cells were fixed in 4.0 % w/v *p*-formaldehyde solution for 15 minutes. Excess *p*-formaldehyde was removed with PBS, and water was used to remove traces of salt prior to drying and scanning.

3.1.3 Reproducibility study

Initial experiments were carried out to evaluate the reproducibility of the method, both *intra* and *inter*-slide. The *intra*-slide reproducibility was assessed by calculating the coefficient of variation among the four identical spots of each polymer, whereas the *inter*-slide reproducibility was evaluated by calculating the correlation coefficient when plotting the background corrected fluorescence intensities for each of the 120 polymers (**Table 6.6**) resulting from the same experiment run on two identical arrays.

The initial screening was performed using B16F10 and ND7 mouse cell lines stained with CellTracker™ Green and Orange, respectively. The average *intra*-slide variation was minimal for ND7 cell stained with CellTracker™ Orange (average CV of 14 % and 15 % for slide 1 and 2, respectively), while in the case of B16F10 cells stained with CellTracker™ Green, the average CV were 36 and 32 % (for slide 3 and 4, respectively). The *inter*-slide reproducibility, (**Figure 3.1** and **Table 6.6)** evaluated using two identical slides, gave correlation coefficients of r^2=0.85 and 0.79 with ND7 and B16F10 cells, respectively, showing good chip to chip reproducibility and showing the robustness of the method.

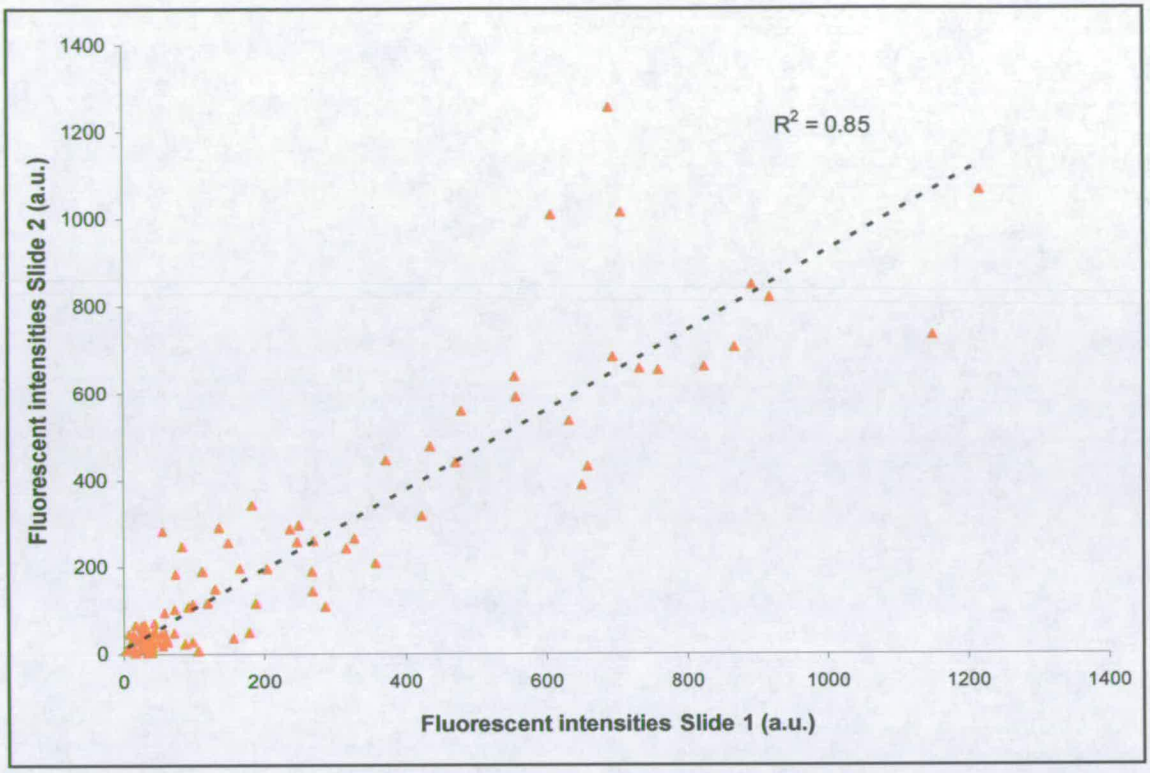

Figure 3.1 *Scatter plot representing inter-slide reproducibility. Each data point represents the background corrected mean fluorescence intensity of each polymer arising from the binding of ND7 cells stained with CellTracker™ Orange, from experiments run on two identical arrays.*

3.1.4 Effect of staining on cellular adhesion

The possible effect of the stain on cellular adhesion was assessed by comparing ND7 adhesion using CellTracker™ Orange to the adhesion of ND7 cells stained with CellTracker™ Green. When comparing the cellular adhesion of these two experiments, the correlation coefficient was r^2=0.73, which showed that the nature of the stain had minimal effect on cellular binding (**Figure 3.2** and **Table 6.7**).

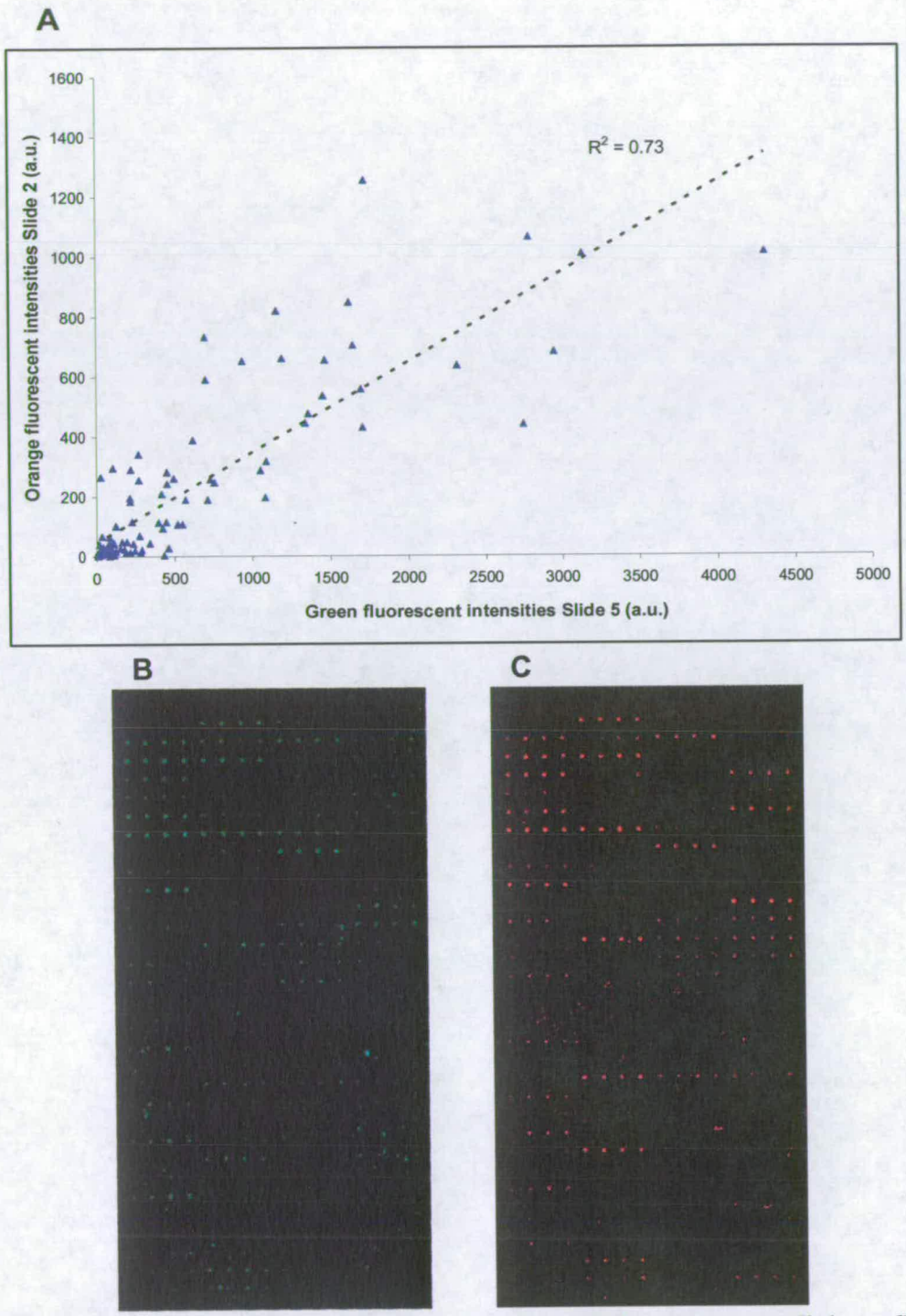

Figure 3.2 *(A) Scatter plot representing the effect of the stain on cellular adhesion. Each data point represents the background corrected mean fluorescence intensity of each polymer arising from the binding of ND7 cells stained with CellTracker™ Green (B) and CellTracker™ Orange (C) from experiments ran on two identical arrays.*

3.1.5 Multiplexing of adhesion

Evaluation of the feasibility of simultaneous screening of two different cell lines was carried out using a mixture of ND7 and B16F10 cells (labelled with CellTracker™ Orange and Green, respectively, and containing $1.5x10^6$ cells of each lineage) plated onto the polymer array. The slide was scanned using both Cy3 and FITC filters and the cellular adhesion for each cell line was evaluated as described previously (see section 3.1.3). In this duplex experiment, the *intra*-slide reproducibility was similar to the single cell experiments (average CV's calculated from the four identical polymer spots were 13 % and 27 % for ND7 and B16F10, respectively). Comparison of the duplex and single cell experiments gave correlation coefficients for ND7 and B16F10 cells of r^2=0.83 and r^2=0.68, respectively (**Figure 3.3** and **Table 6.8**) which were only slightly lower than the *inter*-slide reproducibility observed for a single cell line. These discrepancies are probably related to competitive cellular binding onto certain polymers.

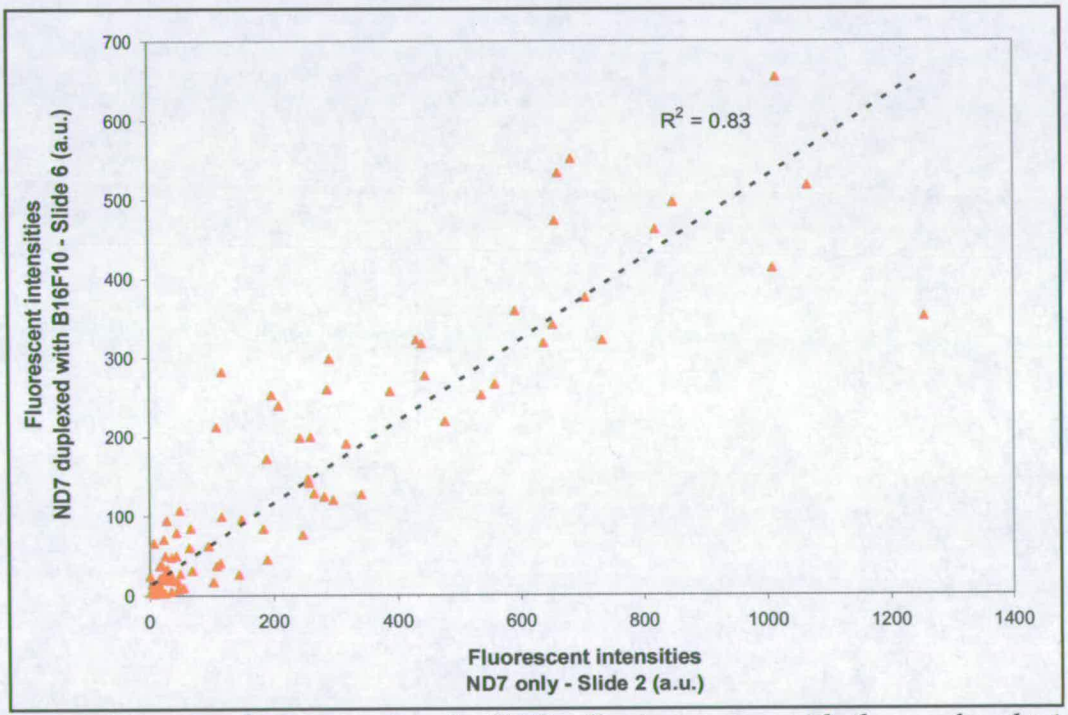

Figure 3.3 *Scatter plot comparing the ND7 adhesion screen with the results obtained from ND7 duplexed with B16F10. Each data point represents the background corrected mean fluorescence intensity of each polymer arising from the binding of ND7 cells stained with CellTracker™ Orange run twice, in the presence of ND7 only (Single) and as a mixture of ND7 and B16F10 cells (Duplex).*

3.2 Applications of cellular adhesion screens

The polymer microarray was used to identify new materials onto which human primary renal tubular epithelial cells could be cultured. A library of 120 poly(urethanes) (**Table 6.9**) was printed onto agarose-coated slides. The cells were plated at 10^5 cells per slide and incubated for 5 days. Following fixation and permeabilisation, the cells were incubated with CAM5-2 an anti-cytokeratin monoclonal antibody and visualised using AlexaFluor® 488 labelled IgG antibody. Finally, Hoechst 33342 was used to stain the nuclei. Analysis was carried out using the high resolution HCS platform and the Pathfinder™ software. This platform is based on a fluorescent microscope with an X-Y-Z stage, and allows the automated capture of single images (0.46 mm^2) for each polymer spot with a resolution of 0.58 μm (**Figure 3.4**).

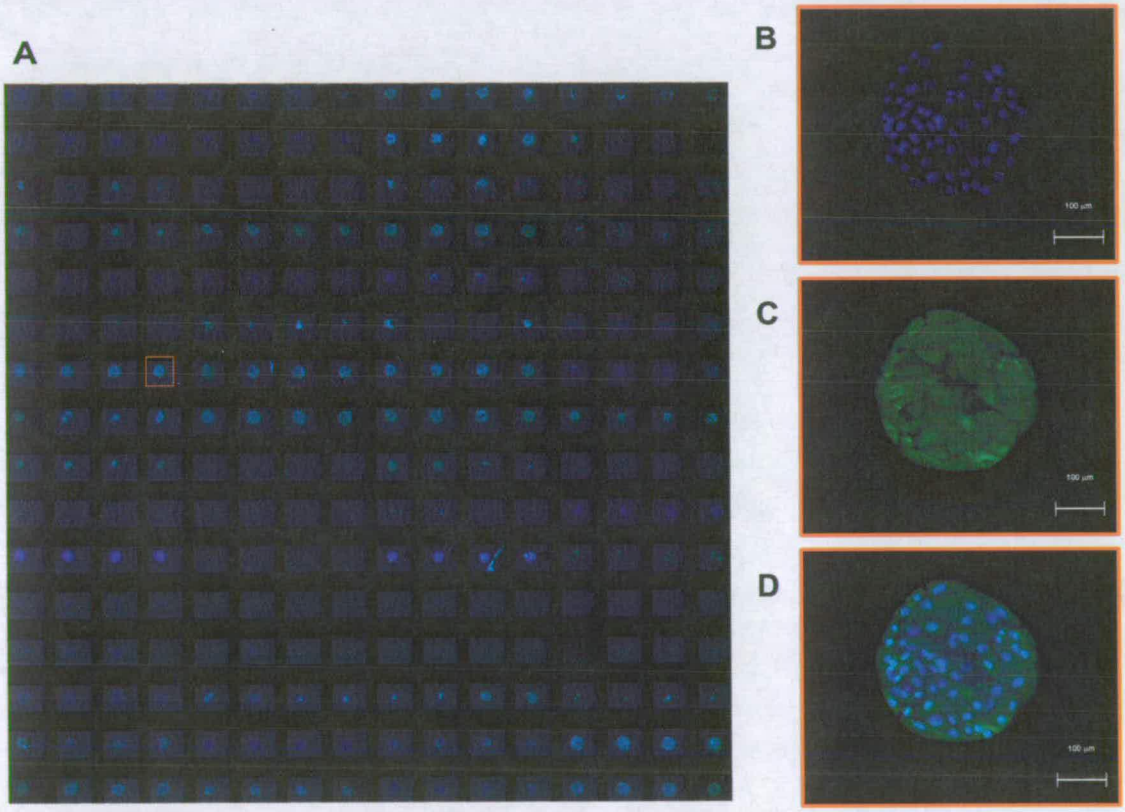

Figure 3.4 *Primary renal tubular epithelial cells on polymer array. (A) Cells on an array containing 60 polymers each printed as 4 replicate spots; one polymer spot with no background subtraction. (B) Nuclei stained with Hoechst 33342. (C) Cam5-2 antibody staining with AlexaFluor®488 secondary antibody. (D) Composite image of (B) and (C) (the bar represents 100 μm).*

Cell compatibility was evaluated as the total number of cells immobilised onto each polymer spot. Several poly(urethanes) were shown to provide significant cell attachment, with a mean over the four identical polymer spots of up to 153 human renal tubular epithelial cells (**Table 6.9**). The 6 poly(urethanes) showing the highest number of bound cells (more than 140 cells per spot) all contained 4,4'-methylenebis(phenylisocyanate) (MDI) (PU-18; 161; 165; 182; 195; 217), while the diol PTMG (650 Da or 1000 Da) was present in four of these top six polymers. It was possible to elucidate the effects of the molecular weight (MW) of the polyol by studying the relationship between cellular adhesion and composition of twelve different polymers all prepared from poly(tetramethylene glycol) (PTMG) and 4,4'-methylene bis(phenylisocyanate) (MDI) using ethylene glycol (EG) or propylene glycol (PG) or no chain extender. When considering each series of four polymers prepared from the same chain extender, the highest binding of renal tubule epithelial cells was observed with PTMG with a MW of 650 Da (**Figure 3.5**). In conclusion, to obtain a polyurethane that provides good cellular adhesion for the culture of human primary renal tubular epithelial cells, it should be synthesised from the aromatic monomer MDI as diisocyanate, and a relatively short polyol such as PTMG 650.

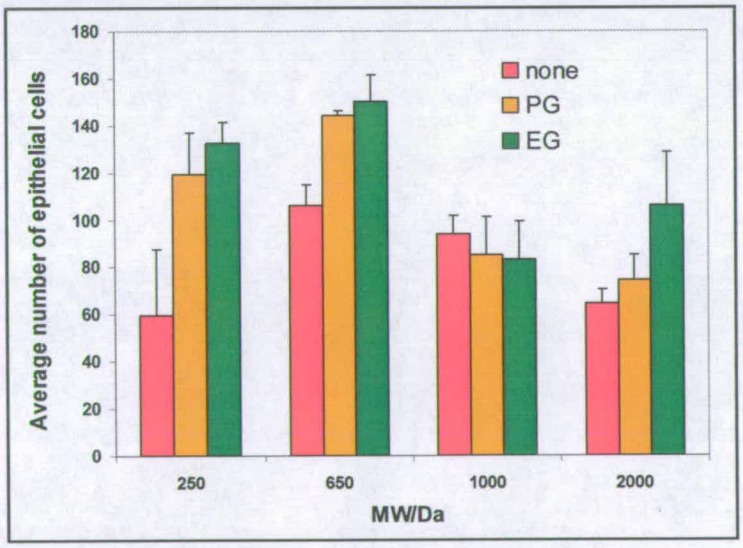

Figure 3.5 *Influence of the polyol molecular weight on the adhesion of human renal tubular epithelial cells. Average number of cells bound to each 4 identical polymers spots plotted against the molecular weight of the PTMG (the error bars represent the standard errors).*

3.3 Immobilisation of non-adherent cells

Non-adherent cells include a large number of therapeutically important cell lineages, such as several cancer cells, blood cells and stem cells. Recent advances in cell-based assays have demonstrated a need for substrates providing immobilisation of these non-adherent lineages[113,176]. Traditional immobilisation of non-adherent cells is based on electrostatic interactions using highly positively charged surfaces such as poly-L-lysine[177] or polyethylenimine (PEI)[178]. One of the major drawbacks of this approach is the risk that cell health and cycles may be modified by such strong interactions. As a result, there is a need for new materials providing mild immobilisation of non-adherent lineages for several applications, including simple phenotypic studies by confocal microscopy, and the development of innovative cell-based assays.

3.3.1 Initial investigation

Preliminary investigations were carried out using three immortalised non-adherent cell lines: JURKAT (human leukaemic T-cell lymphoblast)[179], JY (human B-cell lymphoblast)[180] and RMA-S (murine T-cell lymphoma)[181,182]. Each cell line was stained with CellTracker™ Green and was plated (10^6 cells / slide) onto an array of 120 poly(urethanes), each printed as four identical spots on agarose coated slides. Following 24 hours of incubation, the polymer microarrays and bound cells were washed and fixed prior to scanning with a low resolution scanner. Cell binding was evaluated as described previously (see section 3.1.1). With JURKAT cells, none of the 120 polymers provided cellular adhesion, however both RMA-S and JY cells showed significant polymer-specific immobilisation (Table 6.10). The immobilisation of these non-adherent cells was shown to be highly dependent on both the structure and properties of the polymer and the nature of the cells investigated (Figure 3.6). The selectivity toward RMA-S and JY cell lines was remarkable, PU-198, 199 and 202 bound RMA-S only, whereas PU-194, 195, 207 and 210 bound predominantly JY cells. PU-211 and 214 were the only two polymers to give moderate cellular immobilisation for both cell lines. When analysing the composition of the polymers which showed selectivity for a cell line, it was found that the polymers selective toward RMA-S all contained long PTMG as

polyol (PTMG 1000 or 2000), and diethyl bis(hydroxymethyl)malonate (DHM) as chain extender; whereas three out of four of the polyurethanes selective toward JY contained the highly hydrophobic monomer 2,2,3,3,4,4,5,5-octafluoro-1,6-hexanediol (OFHD) as chain extender.

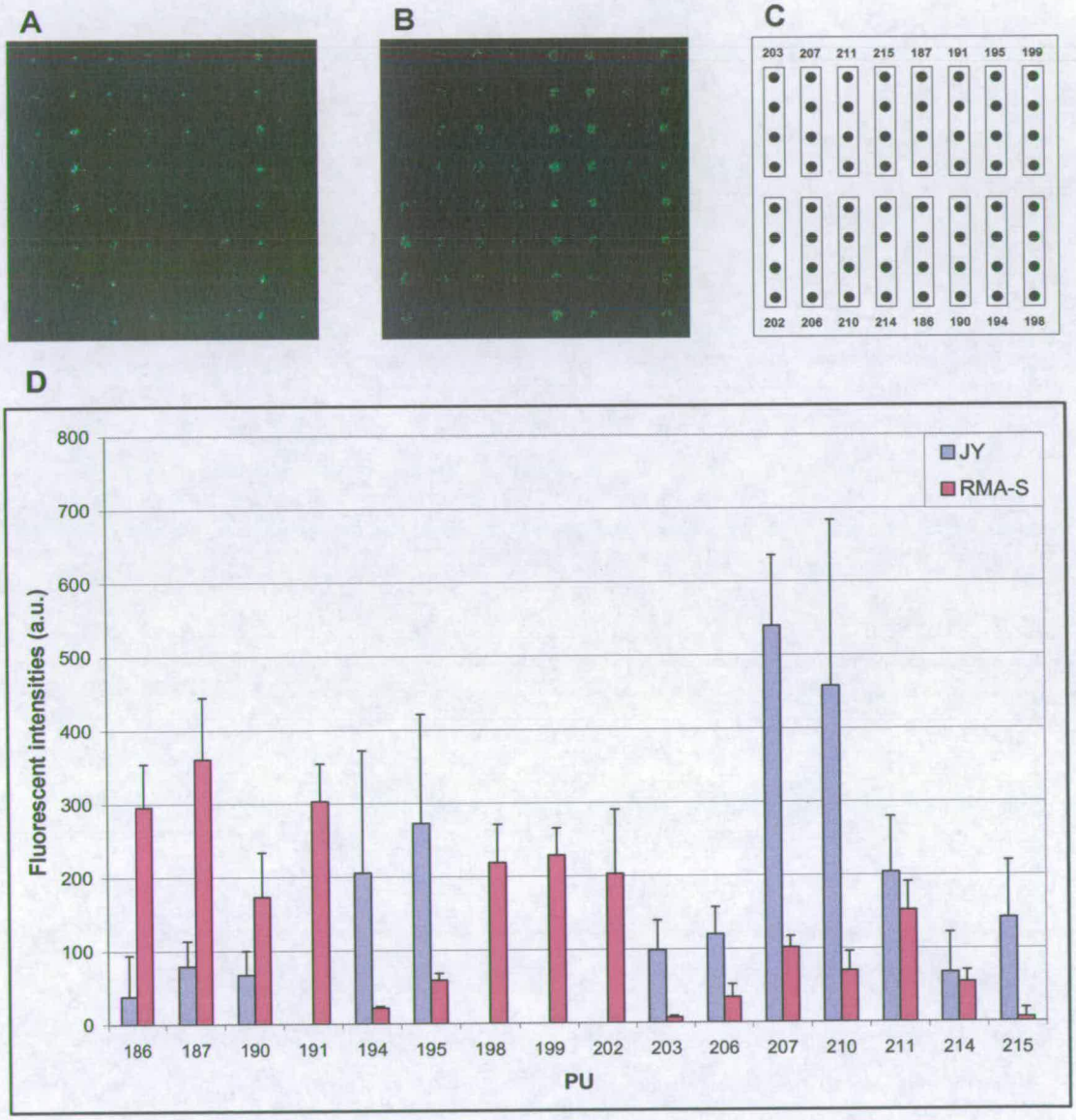

Figure 3.6 *Polymer specificity for 2 non-adherent cell lineages. Scans (non-processed) were obtained for cell lines stained with CellTracker™ Green over an array of 16 polymers each printed as four spots. Microarray screening shown with (A) JY cells, and (B) RMA-S cells, (C) schematic representation of the array, (D) cell binding expressed as background corrected mean fluorescent intensity with error bars representing the standard errors.*

3.3.2 Immobilisation of mouse bone marrow dendritic cells

Dendritic cells (DC) play a central role in the initiation of immune responses and in the maintenance of immune tolerance to "self" [183]. As professional antigen presenting cells, they can engulf particulate matter such as pathogens, necrotic and apoptotic cells by phagocytosis, then process these targets and present them at the cell surface bound to MHC class I or MHC class II molecules[184]. This ability means that DC are intensively studied as targets for vaccine design, particularly for vaccines against tumours. Dendritic cells are a rare constituent of any organ, and one of the most common experimental sources is to purify the immature, highly phagocytic cells from mouse bone marrow. However, immature murine bone marrow dendritic cells (BMDC) are extremely sensitive to stimuli that cause maturation[185], which affects their ability to capture antigens by phagocytosis, while immobilisation is quite generally complicated by the fact that cellular behaviour may be modified by interactions with the materials used to coat the substrates[88,89]. However, the immobilisation of DC would be important for several applications, ranging from simple phenotypic studies by microscopy, to the development of innovative cell-based assays. A library of 120 poly(urethanes) was screened using the microarray platform, in order to identify polymers able to immobilise the BMDC. The validity of the selected polymers was confirmed by studying the phagocytic activity of the BMDC cells while immobilised onto the selected polymer surfaces (**Figure 3.7**).

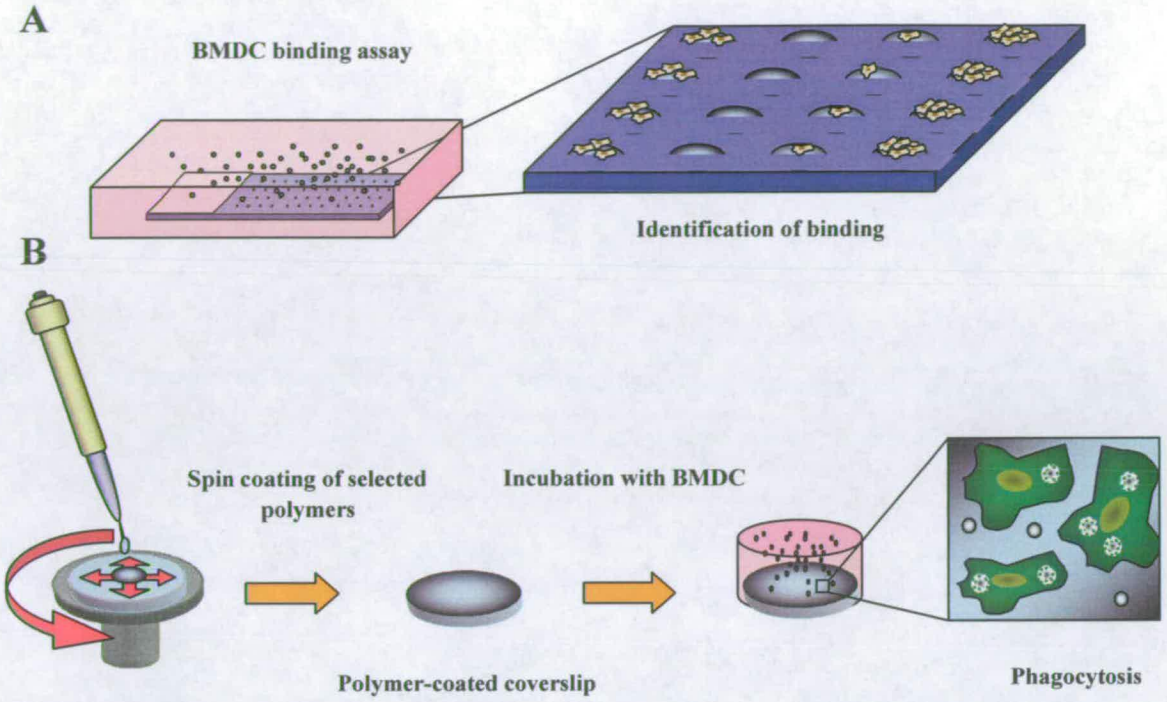

Figure 3.7 *General protocol for the identification of substrates for phagocytosis studies; (A) microarray binding assay allowed for the selection of the best binding polymers; (B) the selected polymers were spin coated on coverslip; following sterilisation, these were incubated with BMDC, prior to be supplied with latex beads for phagocytosis evaluation.*

3.3.2.1 Polymer microarray screening

A polymer microarray containing 120 poly(urethanes) each printed as four identical spots, was incubated with 4.10^6 stained BMDC at 37 °C with 5.0 % CO_2 for two hours. Following washing, the cells were fixed, rinsed and further stained with a 0.5 µg/ml solution of 4',6-diamidino-2-phenylindole (DAPI). Image capture and analyses were carried out using the high resolution HCS platform and the Pathfinder™ software. Cell compatibility was determined by identifying the polymer spots with the most adhered cells using both the DAPI and FITC channels (**Table 6.11**). Three different polyurethanes (PU159, PU166 and PU174) were shown to immobilise more than 10 cells per spot (mean across four identical spots). The cell compatibility of these three polymers was further evaluated by studying the phagocytic activity of immobilised BMDC on different surfaces.

3.3.2.2 Phagocytic study of immobilised BMDC

The selected polymers (PU159, PU166 and PU174) were spin-coated onto glass coverslips (22 mm diameter) to provide a thin film of polymer. Additionally, three types of control coverslips were prepared, one set of non-coated glass coverslips (incubated in PBS alone), and two sets coated with two different grades of commercially available poly-L-lysine (histology and tissue culture grades). BMDC were plated and allowed to adhere to the different coverslips. Cells were then supplied with 3.0 μm diameter latex microspheres and incubated for 30 min at 37 °C. Post-incubation, the cells were fixed and stained for the endoplasmic reticulum protein calnexin, which provides a convenient counterstain revealing the presence of internalised microspheres (**Figure 3.7**). Phagocytic capacity was determined by confocal microscopy and counting of the number of microspheres that had been completely internalised (**Table 3.1**).

Treatment	Adhesion	Number of cells	Number of internalised microspheres	**Microspheres / Cell**
Control 1 (incubated in PBS)	Poor	73	324	**4.4**
Control 2 Poly-L-lysine, (histology)	Good	312	421	**1.3**
Control 3 Poly-L-lysine, (tissue culture)	Excellent	529	684	**1.3**
PU159	Good	297	969	**3.3**
PU166	Excellent	556	1249	**2.2**
PU174	Good	301	1073	**3.6**

Table 3.1 *Phagocytosis of latex microspheres by immobilised BMDC on different substrates. Qualitative evaluation of BMDC adhesion, number of BMDC in the fields of view, number of internalised microspheres and mean number of microspheres per BMDC.*

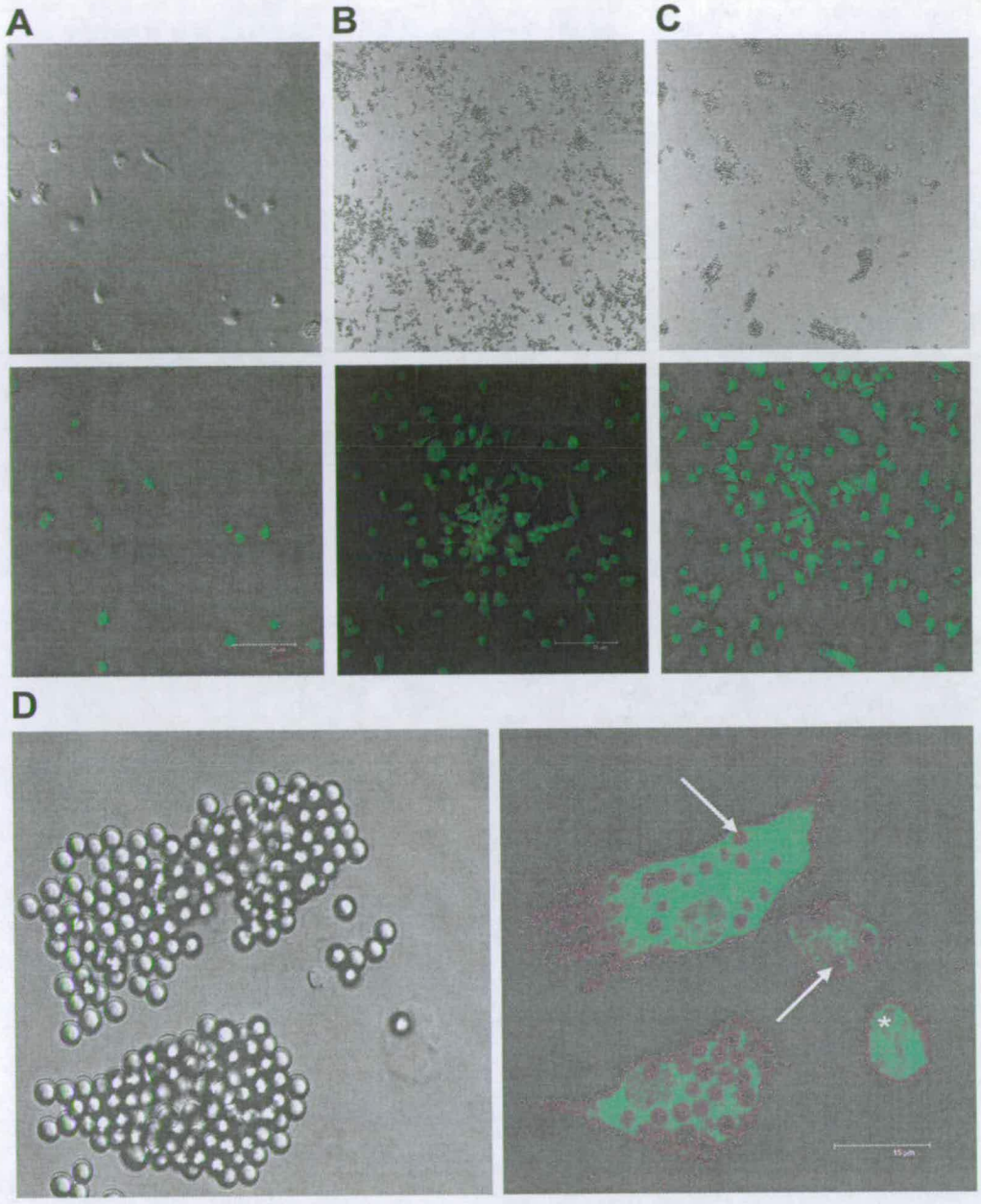

Figure 3.8 *Confocal laser scanning microscopy (bottom), with corresponding phase contrast (top) images of BMDC adhered to coverslips and stained with anti-calnexin antibodies to reveal the presence of internalised microspheres. (A), (B) and (C) images taken with an x40 objective, coverslips treated with PBS alone; with poly L-lysine (tissue culture grade) and PU174, respectively. (D) PU174, images taken with an x100 objective. The fluorescence image shows in more detail two internalised microspheres (arrows). The asterisk denotes the position of a microsphere that has bound to the cell surface (shown in the corresponding phase contrast image), but has not been internalised.*

Interestingly, the greatest phagocytic capacity (an average of 4.4 microspheres per cell) was observed in cells that had adhered to coverslips treated with PBS alone (**Figure 3.7**, A). However, the degree of adhesion of cells to this substrate was very poor, and the cells were liable to be washed away from the coverslip both during the assay, and afterwards during staining. Poly-L-lysine of both grades greatly improved adhesion, but there was a concomitant decrease in the phagocytic capacity to an average of 1.3 microspheres per cell (**Figure 3.7**, B). Although many microspheres were bound to the cell surface, closer examination of optical sections revealed that most had not been internalised. One possible explanation is that the physical restriction of cell movement caused by adhesion to a substrate inhibits the cytoskeletal rearrangements necessary during phagocytosis. In support of this idea, phagocytosis decreased to zero when the concentration of poly-L-lysine was increased ten-fold. Similar signalling pathways are involved in both cell adhesion to a substrate, and adhesion to a particle to be phagocytosed[186]. Whereas cell adhesion can stimulate membrane extension, as for the filopodia and ruffles that engulf a particle, there are also cases where adhesion can inhibit membrane protrusion, such as the inhibition of cell migration in culture caused by cell-cell contacts[187], which may provide an explanation for the observed decrease in phagocytosis by cells adhered to poly-L-lysine. In addition to reducing the phagocytic capacity, poly-L-lysine caused greater background binding of microspheres to the coverslip than was observed for the polymers and PBS control. This is most likely due to charge interactions, since the microspheres carry a net negative charge, and lysine is a positively charged amino acid at physiological pH.

By contrast, phagocytic capacity was much greater for the three polymers, with average values of 3.3 and 3.6 microspheres per cell for PU159 and PU174 (**Figure 3.7**, C and D) respectively, although these values were still less than that observed in the PBS control sample (**Table 3.1**). Adhesion, defined as the number of cells in a field of view, was greater for PU166 than PU159 and PU174, but this was accompanied by a decrease in phagocytic capacity to 2.2 microspheres per cell. Taken together with the results for

poly-L-lysine, it appears that there is a trade-off between the degree of adhesion and phagocytic capacity. However, while adhesion to PU166 was as good as to tissue-culture grade poly-L-lysine, PU166 enabled almost double the phagocytic capacity. These observations suggest that the poly(urethanes) are superior to poly-L-lysine for the adhesion of BMDC, because they mediate good adhesion whilst allowing much greater phagocytic activity. Interestingly, all three selected polymers were synthesised from the same monomers: PTMG as polyol and MDI as diisocyanate.

3.4 Conclusions

The polymer microarray platform was successfully used for the screening of cellular adhesion. It was shown that this very high throughput platform gave good reproducibility and also versatility since it can be used with a large range of fluorescent markers (dyes and antibodies). Additionally, the wide range of properties encompassed by the polymer libraries allowed the identification of several polymers that provided immobilisation of both adherent and non-adherent cell lineages. Finally, the platform was successfully utilised with clinically derived cells to identify new polymeric materials for (a) the growth of primary renal tubular epithelial cells and (b) the gentle immobilisation of BMDC, allowing enhanced phagocytosis and phenotypic studies.

Chapter 4: Polymer microarrays applied to stem cells

4.1 Introduction

Stem cells possess the capability of self-renewal and are also capable of differentiation to produce one or more types of mature cell, and are classified according to both their potency and source[188,189].

Potency describes their ability to differentiate into different cell types. Totipotent stem cells are produced by the first few divisions of the fertilised egg cell arising from the fusion of an egg and a sperm cell. These cells can grow into any type of cell without exception. Pluripotent stem cells are the descendants of totipotent cells, and they can grow into any cell type with the exception of totipotent stem cells. Multipotent stem cells can only produce cells within a closely related cell family. For example, haematopoietic stem cells (HSC), can give rise to all blood cells including red blood cells, white blood cells and platelets. Unipotent stem cells can only produce one cell type. They are distinguished from non-stem cells by their self-renewal properties.

Stem cells can be derived from a number of sources. Adult stem cells are usually multipotent, and they are scarce among differentiated cells in almost all tissues [190]. As well as their complex isolation, one of the main difficulties in the use of such cells is their resistance to culture outside their original environment. Embryonic stem cells (ESC) are isolated from the inner mass cells of an early stage embryo (sometime called a blastocyst). ESC are totipotent, which confers them with much greater developmental potential than that of adult stem cells. Under specific conditions, they can easily be multiplied and maintained in culture. Cord blood stem[191] cells are derived from the blood of the placenta and umbilical cord after birth. They are considered to be multipotent. Compared to adult stem cells, they offer the advantage of being more easily isolated, however, their number is limited. Cancer stem cells are the fourth source of stem cells, and are formed from malignant transformation of adult stem cells. These are suspected to be the source of some or all tumours[192,193].

The therapeutic use of stem cells began in the 1970's with the transplantation of HSC into patients with diseased blood or bone marrow[194]. Following many advances in the field of medical biology, stem cells became the subject of extensive research and is now been investigated in many therapy areas[195-197], from the development of new treatments to the study of development and gene control, and also, potentially, for drug and toxicity studies[198-200]. However, in order to fulfil these expectations, several limitations in stem cell methodologies have to be addressed.

The main limitations in the use of adult stem cells arise from their limited availability, and their complicated isolation. These difficulties are also related to their expansion *ex-vivo,* and thus their potential has to be demonstrated outside diseased blood and bone marrow treatment.

Conversely, embryonic stem cells have far greater potential. They can potentially develop into any cell type, and they are capable of dividing and renewing themselves for long periods of time *in vitro* providing an almost unlimited source of cells. However, human embryonic stem cells have only been isolated recently[201], and many factors including the control of their differentiation have to be investigated before useful applications can be developed.

The aim of the two studies undertaken in this chapter were to apply polymer microarray technology to the identification of novel materials for stem cell research. The first study involved the identification of materials that allowed selective enrichment of stromal stem cells (STRO-1+) from nucleated marrow cells. The second study investigated novel materials that could support the growth of embryonic stem cells and maintain their undifferentiated phenotypes.

4.2 Selective enrichment of multipotent mesenchymal stromal cells (STRO-1)

4.2.1 Introduction

Adult stem cells have been found in organs all over the body[190,202]. One of the most studied sources of adult stem cells is the bone marrow, which is the tissue at the centre of large bones. The bone marrow contains several types of stem cells or progenitor cells. Among the most important of these are the haematopoietic stem cells (HSC) which produce all of the different blood cell types. It has been demonstrated that bone marrow stromal cells provide the environment for HSC differentiation[203]. In addition, these bone marrow stromal cells can generate bone, cartilage and fat cells[204]. Whether stromal cells are best classified as stem cells or progenitor cells for these tissues is still in question. There is also a question as to whether bone marrow stromal cells and so-called mesenchymal stem cells are in fact the same population. Until the stem cell activity of the bone marrow stromal cell population, or any subpopulation, is clearly demonstrated, it has been agreed by the International Society for Cellular Therapy (ISCT) that this heterogeneous population should be defined as multipotent mesenchymal stromal cells (MSC) [205].

In order to study and potentially develop useful applications for MSC, it is essential to isolate this particular population which represents only a small proportion of the cells present in the bone marrow (about 7 % of the unselected human bone marrow mononuclear cell)[206]. Currently, enrichment of human MSC is carried out from unselected human bone marrow mononuclear cell preparations by immunoselection with a STRO-1 monoclonal antibody[207] which recognises a cell surface antigen expressed by MSC [206-208]. This methodology is expensive and time-consuming as it requires the use of flow cytometry to select the STRO-1 positive population (STRO-1+). Additionally the purified population end up labelled which may not be desirable.

In the previous chapter (see section 3.3.1), it was demonstrated that several polymers showed specific adhesion of given cell lines. Thus, in this study, the enrichment of human progenitor cells from unselected human bone marrow mononuclear cell preparations was investigated by means of specific adhesion to polymeric surfaces. The first step of this study was to screen a library of poly(urethanes) printed in a microarray format for binding to both unselected human bone marrow mononuclear cell preparation and the STRO-1+ fraction isolated by magnetically activated cell sorting (MACS). Subsequently, polymers selected in the polymer microarray screen were coated onto coverslips to provide a large surface, and the experiment repeated in order to confirm the initial results.

4.2.2 Microarray screens

The screen with the STRO-1+ cellular fraction was used to identify polymers showing a high affinity for the STRO-1+ cells, whereas the experiment run with unselected human bone marrow mononuclear cell preparations was used to evaluate whether the cellular adhesion to these polymers was specific for the STRO-1+ fraction. Detection of these two cellular preparations was facilitated by selectively immunolabelling STRO-1+ cells using STRO-1 mouse monoclonal primary antibody[207], followed by the (FITC)-conjugated AffiniPure $F(ab')_2$ fragment Goat anti-mouse IgM and the nuclear stain Hoechst 33342. Analysis was carried out using the high resolution HCS platform and the Pathfinder™ software. In the first screen (STRO-1+ cells only) all cells were fluorescent at both wavelengths (FITC and DAPI) whereas in the screen with human bone marrow mononuclear cells, all nuclei were stained with Hoechst 33342 and only STRO-1+ cells showed FITC fluorescence (**Figure 4.1**). Unselected human bone marrow mononuclear cell preparations and STRO-1+ cellular fraction isolated by magnetic activated cell sorting (MACS)[208] were incubated for 17 hours on two identical polymer microarrays containing 120 poly(urethanes) each printed as four identical spots.

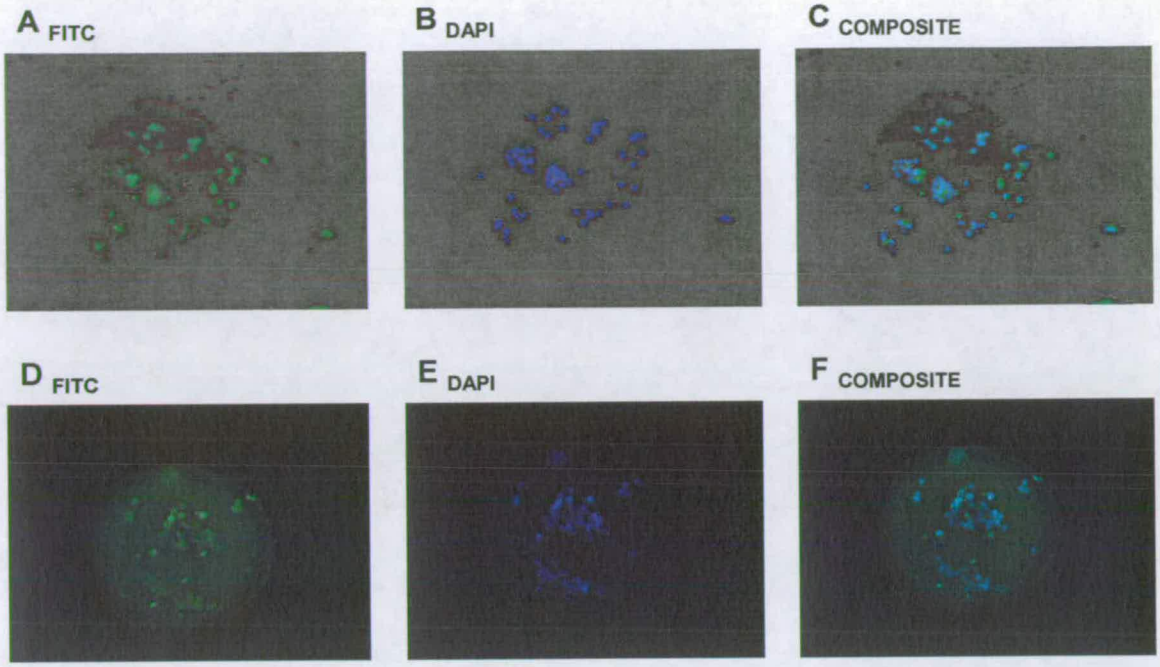

Figure 4.1 *Selective immobilisation of Stro-1+ cells on PU-16. (A), (B) and (C) were performed with Stro-1+ cells isolated by MACS; (D), (E) and (F) were performed using unselected human bone marrow mononuclear cell preparations containing FITC-immunolabelled Stro-1+ cells.*

The first screen (STRO-1+ fraction only) was used to visually identify the polymers showing the highest degree of STRO-1+ adhesion. The second screen (human bone marrow mononuclear cell preparation) was subsequently used to visually evaluate which polymers bound to STRO-1+ selectively. These two screens showed that only a few polymers promoted the adhesion of STRO-1+, within these, PU-16, 17 and 61 exhibited highest selectivity for STRO-1+ and hence were selected for further study.

4.2.3 Coverslip experiments

In order to further confirm the results of these experiments, and study the possible scale-up of the method as a means of cell enrichment, the three selected polymers (PU16, 17 and 61) were spin-coated onto glass coverslips. The polymer-coated coverslips were subsequently incubated with unselected bone marrow mononuclear cell preparations (from 3 individuals) in which the Stro-1+ cells were immunolabelled (as described above in section 4.2.2). Control experiments were carried out by incubating polymer-coated coverslips with non-immunolabelled unselected human bone marrow mononuclear cell preparations, in order to obtain the background cell intensity on each of the poly(urethane) substrates.

Analysis of 5 randomly selected areas (1230 by 940 μm) on each coverslip was carried out using the high resolution HCS platform and the Pathfinder™ software. Quantitative analysis involved measurement of the background corrected FITC intensity of each immobilised STRO-1+ cell. For a cell to be deemed as STRO-1+, its background corrected FITC intensity had to be over the mean plus standard deviation of the control cells. Although the results from patient to patient showed variation in terms of overall immobilised cell density and STRO-1+ proportion, the overall results showed significant level of enrichment of the STRO-1+ population (**Figure 4.2**).

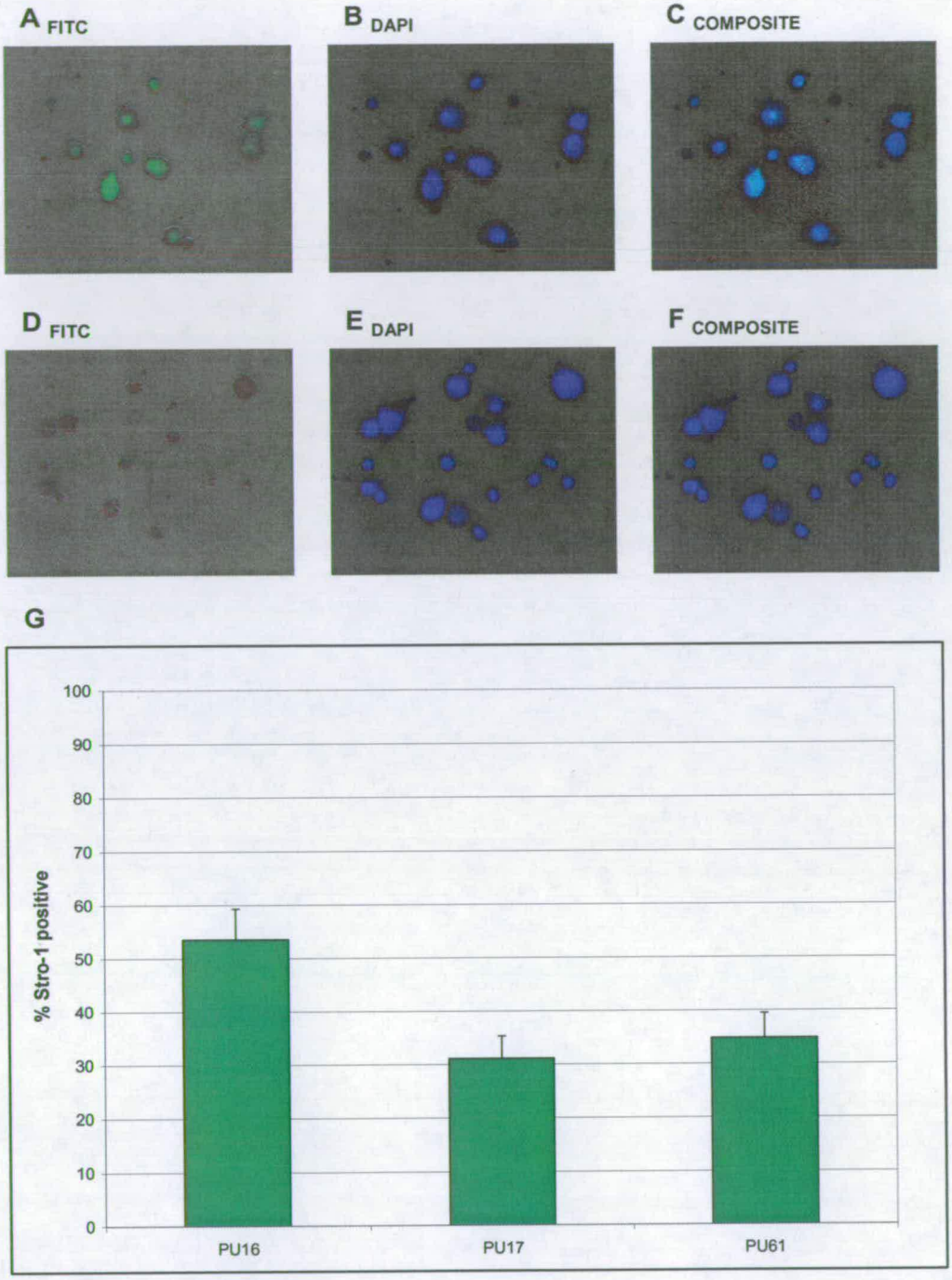

Figure 4.2 *Enrichment of Stro-1+ osteoprogenitor cells on PU-16 coated-coverslip performed using unselected human bone marrow mononuclear cell preparations. (A), (B) and (C) using FITC-immunolabelled and DAPI-stained Stro-1+ cells; (D), (E) and (F) control (non-immunolabelled, DAPI-stained bone marrow mononuclear cells); (G) Overall proportion of Stro-1+ cells immobilized on coated-coverslips.*

4.2.4 Conclusions

Using polymer microarray screening for cellular adhesion, it was possible to identify polymers showing some selectivity toward the STRO-1+ cell fraction. The microarray results were further confirmed by scaling up the experiment on coverslips.

The coverslip experiments showed that up to 50 % of the immobilised cells from human bone marrow mononuclear cell preparation were STRO-1+, which represents a significant enrichment compared with about 7 % in the unselected fraction. Interestingly, when the structures of the three selected polymers were analysed, it was observed that they all contained hydrophilic chains of poly(ethylene glycol) (PEG 2000 or PEG 900) as the polyol and 4,4'-methylene bis(phenylisocyanate) (MDI) as the diisocyanate. The presence of MDI as hard segments within the selected polyurethanes was consistent with previous findings (section 3.2 and 3.3.2), in which the selected polymers providing good cellular immobilisation also contained the MDI monomer. However, the presence of highly hydrophilic long chains of PEG was unexpected, since these polyols are commonly utilised to reduce both protein and cell adhesion in a variety of applications. Despite their relative cellular selectivities, the efficacy of the selected polymers is far that provided by flow cytometry isolation, which achieves nearly pure STRO-1+ population. It is believed that further development in the design of these polymers could enhance their properties. This approach is based on interactions of polymeric materials with specific cellular population and has many advantages compared to expensive and time-consuming enrichment via flow cytometry methods. Additionally, identification of polymers capable of binding and enriching the STRO-1+ population from unselected human bone marrow mononuclear cell preparations has several implications in the fields of tissue engineering and orthopaedics, where the polymer could be utilised as a scaffold or coating for bone regeneration applications[206]. For such an application to be developed many additional experiments are required, including the study of the immobilised progenitor cells' fate and the evaluation of cytotoxicity and blood compatibility of the polymeric materials.

4.3 Novel substrates for embryonic stem cell culture

4.3.1 Introduction

Traditional methods of mouse embryonic stem cell (mESC) culture that maintain the undifferentiated phenotype of the cells involve culture on a layer of feeder cells. However, several reports[209,210] indicate that the feeder layer could be replaced by the addition of leukaemia inhibitory factor (LIF) [211,212] to the growth medium. In the absence of the feeder layer, mESC are usually cultured on protein (gelatine, collagen) coated surfaces.

In this study, the use of polymeric materials as novel substrates for the growth of mESC was investigated. The performance of these materials was evaluated in terms of the conservation of the undifferentiated phenotype in the presence and absence of LIF.

The study was carried out on a library of 124 poly(urethanes) using a modified mESC line (Oct4-GFP). Octamer-4 (Oct4)[213,214] is a transcription factor of the POU family (a group of eukaryotic transcription factors containing a bipartite DNA binding domain referred to as the POU domain)[215]. This protein is critically involved in self-renewal of undifferentiated mESC, thus it is used as a marker of the pluripotent state[216,217]. Oct4-GFP cells have green fluorescent protein (GFP)[218,219] transcription under the control of the Oct4 promoter to give a fluorescent read out of the undifferentiated state of mESC's. Following stem cell differentiation, the level of Oct-4 expression decreases rapidly as does the GFP expression, which reduces the overall fluorescence of the cells[220]. As a result, it is possible to follow the differentiation of these mESC cells by following the intensity of the fluorescence associated with the expression of GFP (**Figure 4.3**).

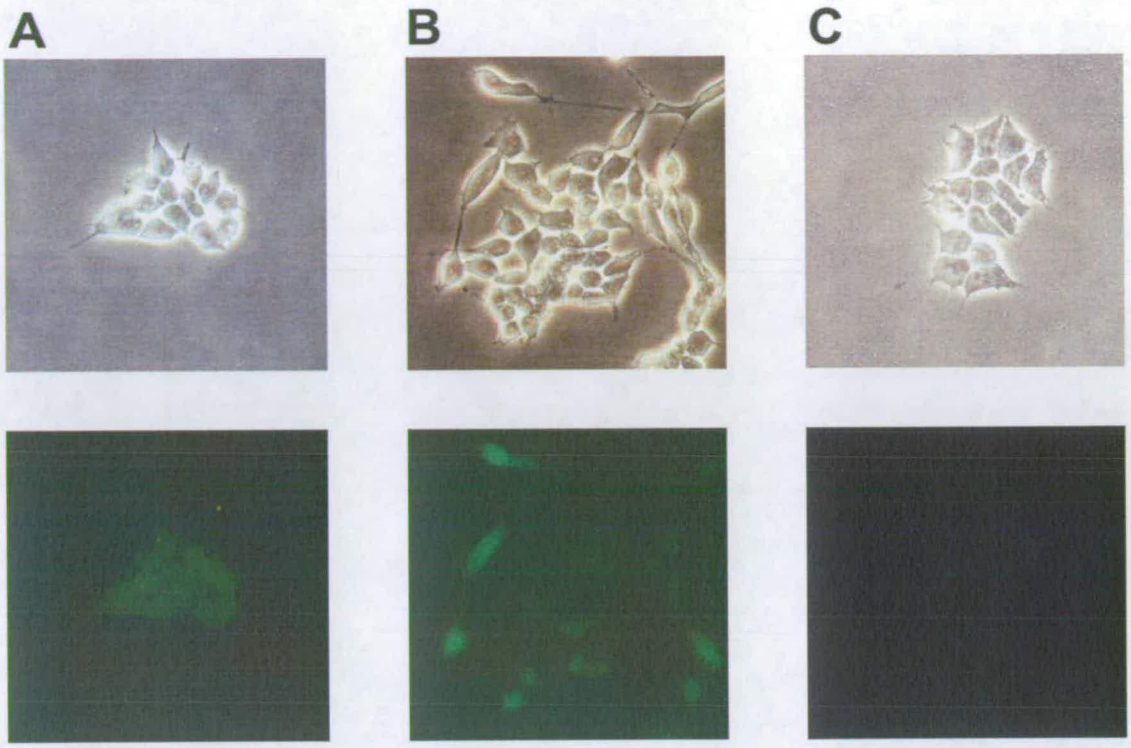

Figure 4.3 *mESC grown on gelatine-coated dishes, at the top, bright field microscopy, at the bottom, fluorescence microscopy using a FITC filter. (A) an undifferentiated colony of Oct4-GFP cells expressing GFP (FITC fluorescence), (B) a colony showing partially differentiated phenotype and (C) a colony showing a fully differentiated phenotype.*

The first step of this study involved a polymer microarray adhesion screen using the Oct4-GFP cells to identify which polymer supported the adhesion and growth of undifferentiated mESC's in presence or absence of LIF in the growth medium. Following the initial screen the best candidates were selected and the experiment was scaled up using polymer-coated coverslips. Following an inconclusive microscopy study, a clonal growth experiment was designed to confirm the initial observations on the microarray.

4.3.2 Polymer microarray adhesion screening

The first screen involved plating 10^5 Oct4-GFP cells per slide on 14 identical polymer microarrays containing 124 poly(urethanes), each printed as 4 identical spots. Each pair of slides was incubated for a different time period, from 24 hours up to 7 days. Seven different time points were assessed with 2 slides per time point. Half the slides were incubated with a medium containing LIF, whereas the other half were incubated for 24 hours only with LIF-containing growth medium, after which the medium was changed to a growth medium without LIF.

At each time point, two slides (one incubated with LIF and one without) were washed and the cells were fixed using 4.0 % p-formaldehyde solution in PBS. Using a fluorescent microscope, the cells on the array were visualised for adhesion and expression of GFP. Out of 124 poly(urethanes), 52 showed immobilisation of mESC on at least one of the 14 polymer microarrays. By monitoring the expression of GFP in the experiment without LIF in the growth medium, 4 poly(urethanes) (PU190; 206; 214; 221) were selected as potential substrates, as they seemed to maintain undifferentiated cellular phenotypes. Following the experiments in presence of LIF, PU161 was selected as a negative control as the cells bound to this polymer differentiated and stopped expressing GFP after a few days of incubation.

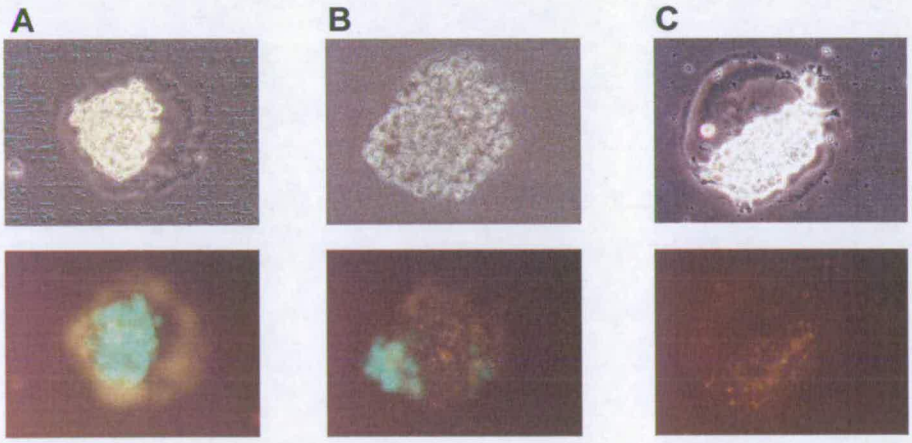

Figure 4.4 *mESC grown on three different polymer microarray spots, at the top, bright field microscopy, at the bottom, fluorescence microscopy using the FITC filter. (A) an undifferentiated colony of Oct4-GFP cells expressing GFP (FITC fluorescence), (B) a partially differentiated colony and (C) a fully differentiated colony of Oct4-GFP cells.*

4.3.3 Coverslip experiments

In order to scale up the experiment, the five selected polymers were spin coated onto glass coverslips (19 mm diameter).

4.3.3.1 Microscopy

The coated coverslips (two for each polymer, 5 polymers selected) were placed in a 12-well plate, and the two remaining wells were coated with 0.2 % gelatine which was used as a control. Following sterilisation under ultraviolet (UV) irradiation, 10^4 cells were plated in each well; half the samples were incubated with LIF-containing growth medium, whereas the other half were incubated without LIF. mESC media were changed every 48 hours. Each plate was incubated for 5, 7 and 9 days respectively, after which each well was rinsed, the cells were fixed and their nuclei stained with Hoechst 33342. After 9 days of incubation, the cells reached confluency and colonies started detaching during the rinsing step on several coverslips, and as a result these coverslips were discarded. Coverslips with attached colonies were mounted on standard microscope slides using the Aquatex mounting medium. Cells growing on top of each coated coverslip were visualised using both DAPI and FITC channels of the high resolution HCS platform and Pathfinder™ software. Coverslips incubated in LIF-containing medium showed a large proportion of GFP expressing colonies. Unfortunately, in the absence of LIF, very large discrepancies in differentiation were observed depending on the area visualised within the same coverslip (**Figure 4.5**).

It was hypothesised that such discrepancies could arise from an autocrine effect. Indeed, mESC produce LIF, and when these cells are cultured at high density, the autocrine effect has been demonstrated to be sufficient to maintain mESC pluripotentiality[221-223]. As a result, it was impossible to draw any clear conclusions from this experiment. It was thus decided to design an experiment using a much lower cell density and a different marker of the undifferentiated phenotype in order to confirm the results obtained on the polymer microarray, that suggested these polymers could adhere mESC while maintaining their undifferentiated phenotype.

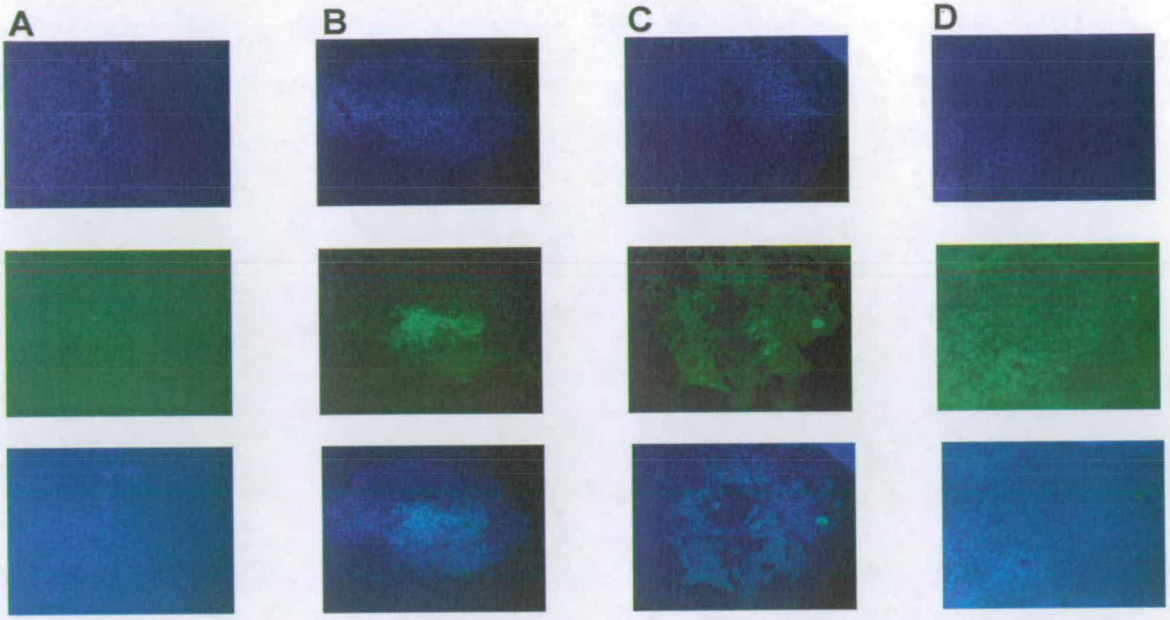

Figure 4.5 *mESC grown for 9 days on the same PU221-coated coverslip in the medium without LIF. Top to bottom show the same areas visualised using DAPI, FITC filters and composite of the two previous images, respectively. (A) Fully differentiated colony, (B) and (C) partially differentiated colony, and (D) fully undifferentiated colony.*

4.3.3.2 Clonal growth experiment

The clonal growth experiment consisted of plating cells onto the coverslips at very low density (50 cells/coverslip) and incubating over 9 days in order to form colonies from single cells. The experiment was run both in the presence or absence of LIF on each of the polymer-coated coverslip. To increase the confidence in the results, a total of 3 replicate experiments were carried out. At the end of each experiment, alkaline phosphatase activity was used to assess the pluripotentiality of the mESC grown in each colony[209]. The alkaline phosphatase detection kit (Sigma, UK) is a histochemical semi-quantitative test to assess the alkaline phosphatase activity of cells. Following fixing, each colony was stained according to manufacturer protocols and their pluripotentiality was assessed by evaluating the proportion of stained cells within each colony (**Figure 4.6**). Colonies showing a fully undifferentiated phenotype (more than 70 % stained cells) were scored as "1", partially differentiated as "2" (between 70 % and 30 % stained cells) and colonies showing a differentiated phenotype were scored as "3" (less than 30 % stained cells).

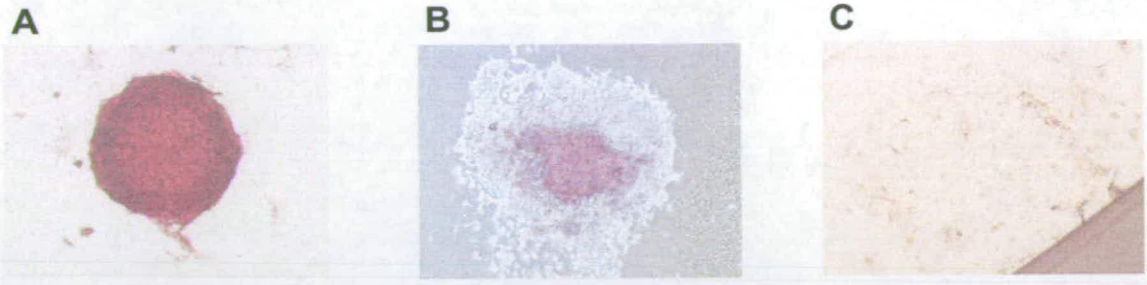

Figure 4.6 *mESC colonies stained with alkaline phosphatase, (A) fully undifferentiated, (B) partially differentiated, and (C) fully differentiated colonies.*

Following scoring for each colony on each set of three identical polymer-coated coverslips, the average scores in presence and in absence of LIF in the growth media were calculated (**Table 4.1**).

PU	Phenotype scoring in presence of LIF	Phenotype scoring in absence of LIF
190	1.37	3.00
206	1.30	2.75
214	1.59	3.00
221	1.93	2.78
161	2.11	3.00
0.2 % gelatine	1.58	3.00

Table 4.1 *Results of alkaline phosphatase phenotype scoring of mESC colonies grown for 9 days in presence and absence of LIF.*

The results obtained in the presence of LIF in the growth medium confirm the results of the polymer microarray screen for 3 out of 4 of the poly(urethanes) selected (i.e. PU190; 206 and 214), as their phenotype scoring is below or equal to the one obtained using traditional mESC culture on 0.2 % gelatine coated wells. Additionally, the negative control (PU161) was, as expected, the worst performing surface in this experiment with most colonies partially differentiated.

In absence of LIF in the growth medium, most colonies were scored as differentiated with a phenotype scoring above 2.75. PU190 and 221 scores were slightly lower than on

0.2 % gelatine, but due to the semi-quantitative analysis, these results are not significant and none of the selected polymer or control was successful at maintaining undifferentiated phenotype in absence of LIF.

Using the polymer microarray approach it was possible to successfully identify novel surfaces suitable to support the growth of mESC in undifferentiated phenotypes in the presence of LIF. Unfortunately, none of the polymeric materials selected were able to support the growth of mESC while maintaining their pluripotentiality in the absence of LIF. When the compositions of these polymers were analysed it was observed that three (PU190, 206 and 221) contained the same diisocyanate and chain extender, namely HDI and OFHD. The presence of OFHD, which is a highly fluorinated diol, was unexpected as many surfaces designed to prevent cellular adhesion uses such fluorinated hydrocarbon chains[11]. With growing interest in the control mESC differentiation, the polymer microarray platform could be utilised to study the fate of cells grown on polymers and potentially identify new materials able to support the differentiation of mESC toward specific cell lineages.

4.4 Conclusions

The area of stem cell research is currently one of the most exciting and controversial fields of science. Indeed, since their first discovery, numerous reports promoted the huge impact that stem cell-derived therapies could have on the wellbeing of humanity. Additionally, stem cells are proving to be essential tools in understanding critical biological pathways, and also have a role to play in the development of improved toxicological tests, which have the potential to reduce animal experimentation. However, this field is still in its infancy, and many limitations will have to be overcome before useful applications are available. The main challenges that scientists are faced with today are the isolation, characterisation and culture of specific stem cell subpopulations, together with the control of their development towards specific cell lineages. To accelerate this research, scientists are using the most advanced technologies available, amongst which microarrays have a crucial part to play. Indeed, DNA microarrays have been extensively used to monitor the expression of genes in various stem cells in order

to develop a database[224], which allows better understanding and characterisation of stem cell populations[225]. Other microarray platforms are also ideally suited to the acceleration of research, such as the MSC transfection array developed by Yoshikawa *et al.*[226]. In our approach, we demonstrated that the polymer microarray for cellular adhesion provided a high throughput platform for the identification of new materials with potential in stem cell research. Indeed, novel biomaterials have an essential role to play, not only as new substrates to control the fate of cultured stem cells *in vitro,* but also as matrices in the burgeoning field of tissue engineering [227]. As was the case in the field of microarrays, to rapidly succeed, stem cell research will have to embrace the latest technological advances and promote the exchange of knowledge between scientists all over the world.

Chapter 5: Development of polymer microarrays for protein adsorption studies

In chapter 3 and 4, it was found that the polymer microarray platform could be used to study the adhesion of a whole range of mammalian cell lineages onto the polymer libraries. In this chapter, several parameters were optimised in order to study the adsorption of proteins onto the polymer microarray. The study of protein adsorption represents an important part of biocompatibility evaluation of polymers; these *in vitro* experiments could therefore be used to study polymers that come in contact with blood and body fluids.

5.1 Coverslip optimisation

In order to minimise consumption of expensive protein solutions, it was decided to apply a coverslip after protein solution application to allow the formation of a uniform thin film of solution above the microarray spots. Three types of coverslip were investigated, a standard glass coverslip, and two plastic coverslips designed for DNA hybridisation, HybriSlips™ and GeneFrame®. Three identical polymer microarrays, containing 15 polyurethanes each printed as 24 identical spots were printed on the slide as three clusters of 4 x 2 spots and incubated with fibrinogen labelled with AlexaFluor® 647. Following washing and drying, the slides were scanned and the standard deviation (Std Dev) and coefficient of variance (CV) calculated from the integrated intensity resulting from the 24 identical spots for each of the 15 polymers (**Table 5.1**). The general scheme and a description of the main steps involved in the polymer microarray for protein adsorption experiment are presented in figure 5.1.

PU-	GeneFrame®			HybriSlip™			Standard Glass		
	Mean	Std Dev	CV	Mean	Std Dev	CV	Mean	Std Dev	CV
8	537381	165912	31	382221	163935	43	562671	380190	68
12	89530	34500	39	78344	35275	45	64491	25830	40
16	34652	18505	53	17422	2310	13	213127	281902	132
23	115161	19549	17	108749	40129	37	473192	612770	129
25	1590214	217379	14	534172	290152	54	1103488	417419	38
28	444867	123920	28	255981	90438	35	709675	921472	130
37	922071	138212	15	406169	55318	14	935809	698411	75
63	95392	65622	69	36110	36530	101	30251	3798	13
65	1154731	155388	13	502970	72223	14	515644	94890	18
73	25204	5020	20	18300	10207	56	15762	1444	9
77	692787	146450	21	221143	29875	14	228222	77643	34
79	1269925	216183	17	499887	122040	24	651485	217280	33
91	1538591	115646	8	592509	59932	10	574226	51639	9
92	1927337	185474	10	683217	127542	19	560693	165643	30
101	1853448	120302	6	806953	285894	35	357522	35089	10
Mean	**819419**	115204	**24**	**342943**	94787	**34**	**466417**	265695	**51**

Table 5.1 *Mean fluorescence intensities (arbitrary units), standard deviations and coefficients of variance resulting from the binding of labelled fibrinogen to 15 poly(urethanes) each printed as 24 identical spots.*

Analysis showed that using a glass coverslip the reproducibility was very poor with a mean CV of 51 %, whereas HybriSlips™ and GeneFrame® gave CV's of 34 % and 24 %, respectively. When analysed in detail, it was observed that the average of all the integrated fluorescence with GeneFrame® was over twice the average intensity recorded with Hybrislips™. In order to investigate this result, the background intensity (as measured in 3.1.1) was measured on the part of the coverslip in contact with the protein solutions. The measured backgrounds were 250,000 and 1,300,000 for GeneFrame® and HybriSlips™, respectively.

The high background intensity measured for the HybriSlips™ was related to the high protein adhesion on the coverslip and subsequent lower adhesion to the polymer spots. As a result it was decided that all subsequent experiments should be carried out using the GeneFrame® coverslips.

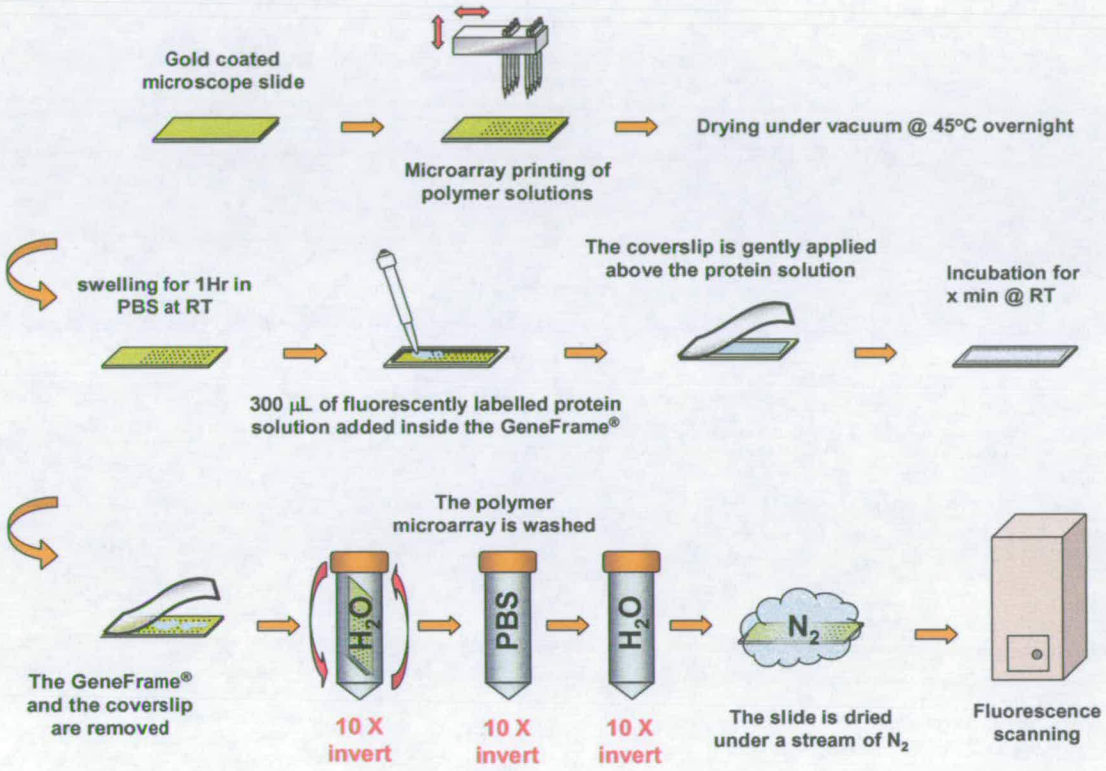

Figure 5.1 *Illustration of the polymer microarray for the protein adsorption study. The polymer microarrays were printed on gold-coated glass slides. Following drying and swelling of the polymer spots, a GeneFrame® was placed on top of the printed slide around the printed arrays. The protein solution was pipetted within the frame prior to the plastic coverslip being gently applied, in order to avoid the entrapment of air bubbles.Following incubation, the GeneFrame® and coverslip were removed and the slide was washed using a standardised 3-baths washing technique (**6.5.2**); finally, the slide was dried under a stream of nitrogen prior to analysis using a fluorescent scanner.*

5.2 Determination of optimal protein concentrations

In order to determine the best concentration of labelled fibrinogen solution to use on the polymer array, a series of solutions of different concentrations were incubated on replicate arrays containing 32 poly(urethanes), each printed as 8 identical spots. The resulting average fluorescence intensities for each set of 8 spots were integrated and plotted against the protein solution concentrations (**Figures 5.2 & 5.3**).

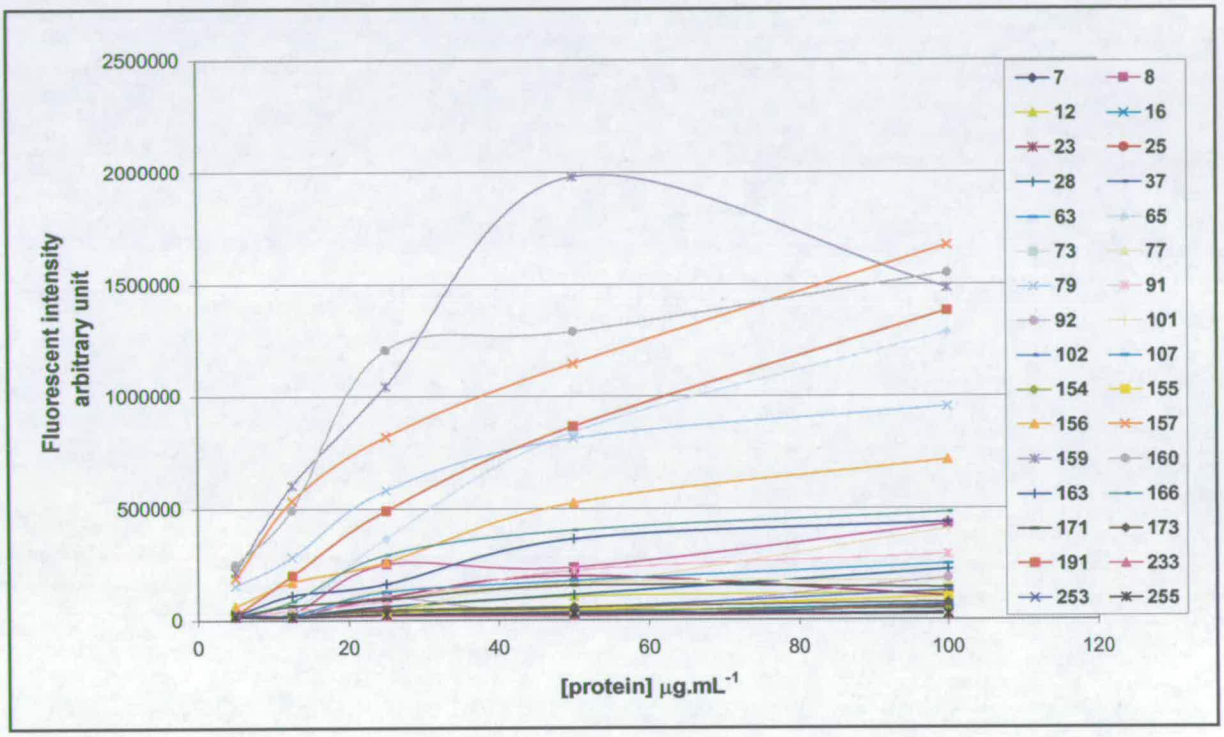

Figure 5.2 *Fluorescence intensity vs. fibrinogen concentration for the 32 printed poly(urethanes), using AlexaFluor® 647 labelled fibrinogen in PBS, incubated for 2 hours at 37 ℃.*

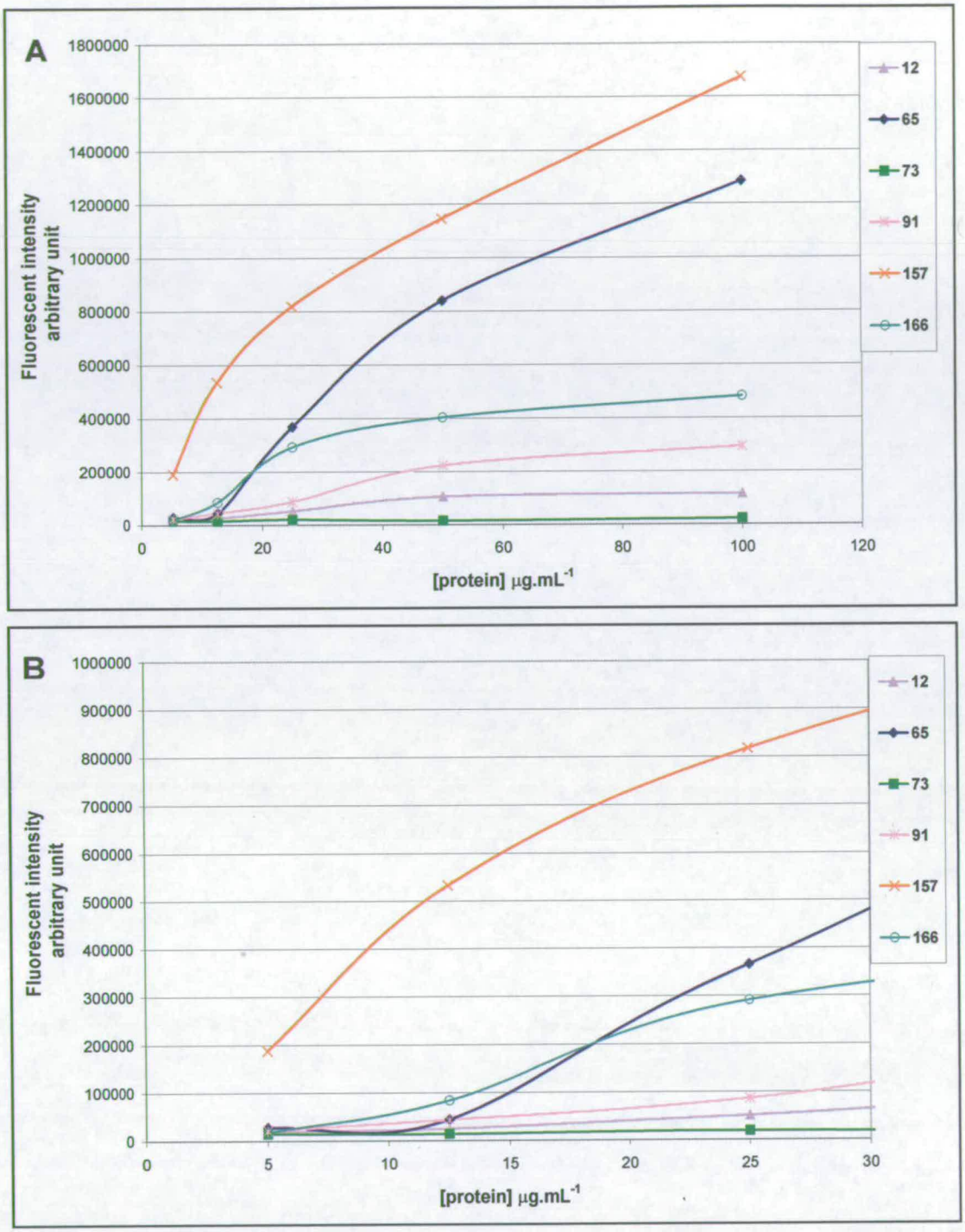

Figure 5.3 *Fluorescence intensity vs. fibrinogen concentration for 6 representative poly(urethanes), using AlexaFluor® 647 labelled fibrinogen in PBS, incubated for 2 hours at 37 °C. (A) Overall results, (B) results obtained for the lower protein concentrations (5 to 25 µg.mL^{-1}).*

It was shown that a concentration of labelled fibrinogen at or below 12.5 $\mu g.mL^{-1}$ was not sufficient, as most low protein binding polymers have a fluorescent intensity close to the background intensity at these concentrations, making it difficult to differentiate their binding properties. However, as the concentration increased, differences in the adhesion properties of the polymers became obvious. In order to minimise protein consumption, it was decided that subsequent protein adhesion studies using labelled fibrinogen would be carried out at 25 $\mu g.mL^{-1}$ as this concentration was the lowest to give good intensity above background (**Figure 5.3**). A similar approach was used for other labelled proteins and a summary of the protein concentration and label used for subsequent studies is given in table 5.2.

Description	Probe	Concentration ($\mu g.mL^{-1}$)	Label
Leukocyte Index	Glycoprotein X	2.50	FITC
	Glycoprotein Y	25.0	FITC
Erythrocyte Index	Glycophorin A	12.5	AlexaFluor® 546
	Glycoprotein Z	2.50	FITC
Plasma proteins	Albumin	25.0	AlexaFluor® 546
	Fibrinogen	25.0	AlexaFluor® 647
	IgG	100	FITC

Table 5.2 *List of proteins used in the adhesion assay together with the concentration and fluorescent label used. Proteins labelled with FITC were commercially available, however protein labelled with AlexaFluor® dyes were labelled according to the manufacturer's instructions (Molecular probes).*

5.3 Reproducibility of the protein adhesion assay

To investigate the reproducibility of the method developed with the parameters described above (both inter- and intra-slide reproducibility), the same experiment was run on two identical slides containing a library of 119 poly(urethanes), each printed as four identical spots, and incubated with Glycoprotein X (2.50 $\mu g.mL^{-1}$ + 0.5 % w/v HSA in PBS for 2 hours at 37 °C). The mean fluorescence intensity and coefficients of variance from the four identical spots were calculated for each polymer array. The intra-slide reproducibility was calculated from the average coefficient of variance for the 128 different poly(urethanes), which was 8.7 and 8.0 % for the slides 1 and 2, respectively. The inter-slide reproducibility was evaluated from the correlation coefficient (R^2) obtained when plotting the average intensity of each polymer obtained from slide 1 and 2 (**Figure 5.4**). Both intra and inter-slide reproducibilities were shown to be satisfactory with an overall coefficient of variance below 10 %, furthermore, the correlation coefficient between the two slides was above 0.96.

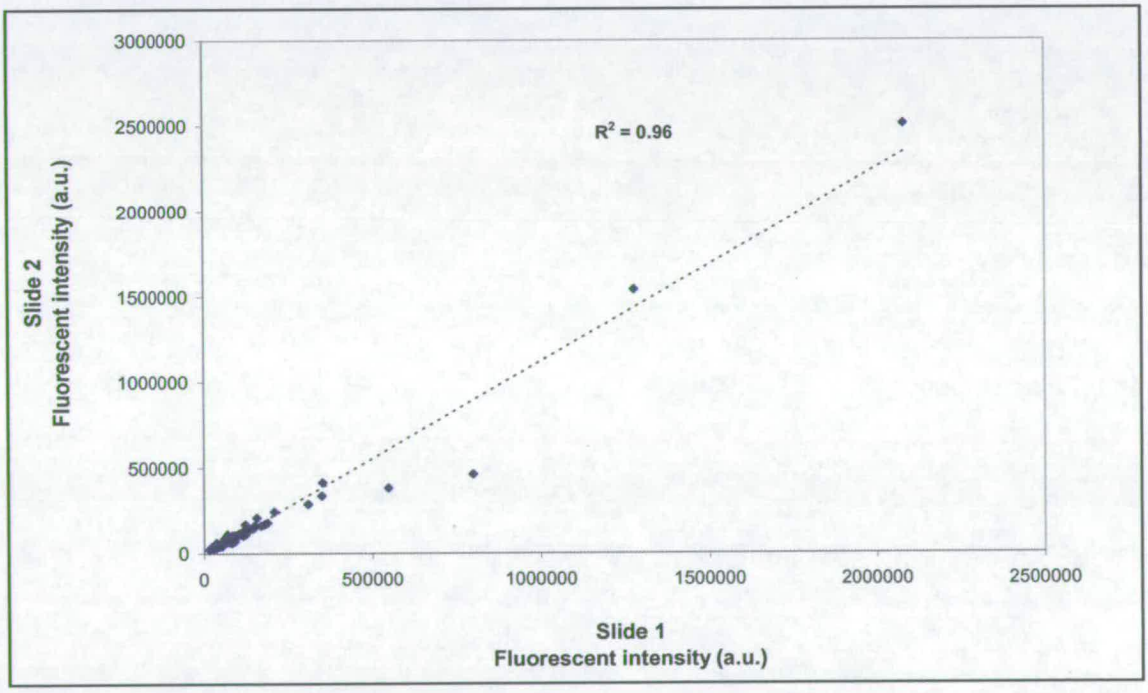

Figure 5.4 *Inter-slide reproducibility, average fluorescence intensities (a.u.) resulting from the binding of Glycoprotein X to two identical microarrays containing 128 poly(urethanes).*

5.4 Duplexing of the protein adhesion assay

In order to investigate the potential for multiplexing of the protein adhesion assay on a polymer microarray (i.e. using more than one labelled protein solution on a single array), a model experiment was carried out using two mixtures of two proteins with different fluorophores:

System 1: on library PA1 (**Table 6.18**)

Slide 1: Glycoprotein X (2.50 $\mu g.mL^{-1}$) + Glycophorin A (12.5 $\mu g.mL^{-1}$)

Slide 2: Glycoprotein X (2.50 $\mu g.mL^{-1}$)

Slide 3: Glycophorin A (12.5 $\mu g.mL^{-1}$)

System 2: on library PA2 (**Table 6.19**)

Slide 4: Glycoprotein Y (25.0 $\mu g.mL^{-1}$) + Glycophorin A (12.5 $\mu g.mL^{-1}$)

Slide 5: Glycoprotein Y (25.0 $\mu g.mL^{-1}$)

Slide 6: Glycophorin A (12.5 $\mu g.mL^{-1}$)

Glycophorin A was labelled with AlexaFluor® 546 and Glycoprotein X and Y were both labelled with FITC.

The first protein mixture (Glycoprotein X + Glycophorin A) was incubated on the polymer microarray "slide 1" containing library PA1. Experiments were also run on the same arrays (PA1) but with a single protein solution (Glycoprotein X only, "slide 2" and Glycophorin A only, "slide 3").

The second protein mixture (Glycoprotein Y + Glycophorin A) was incubated on the polymer microarray "slide 4" containing library PA2. Experiments were also run on the same arrays (PA2) but with a single protein solution (Glycoprotein Y only, "slide 5" and Glycophorin A only, "slide 6").

Following incubation and washing, each slide was scanned, and the fluorescence intensity resulting from protein adhesion on each polymer calculated (Table 6.18 and 6.19). The resulting fluorescence intensities obtained from the dual and single protein solutions were plotted against each other (**Figure 5.5**).

A

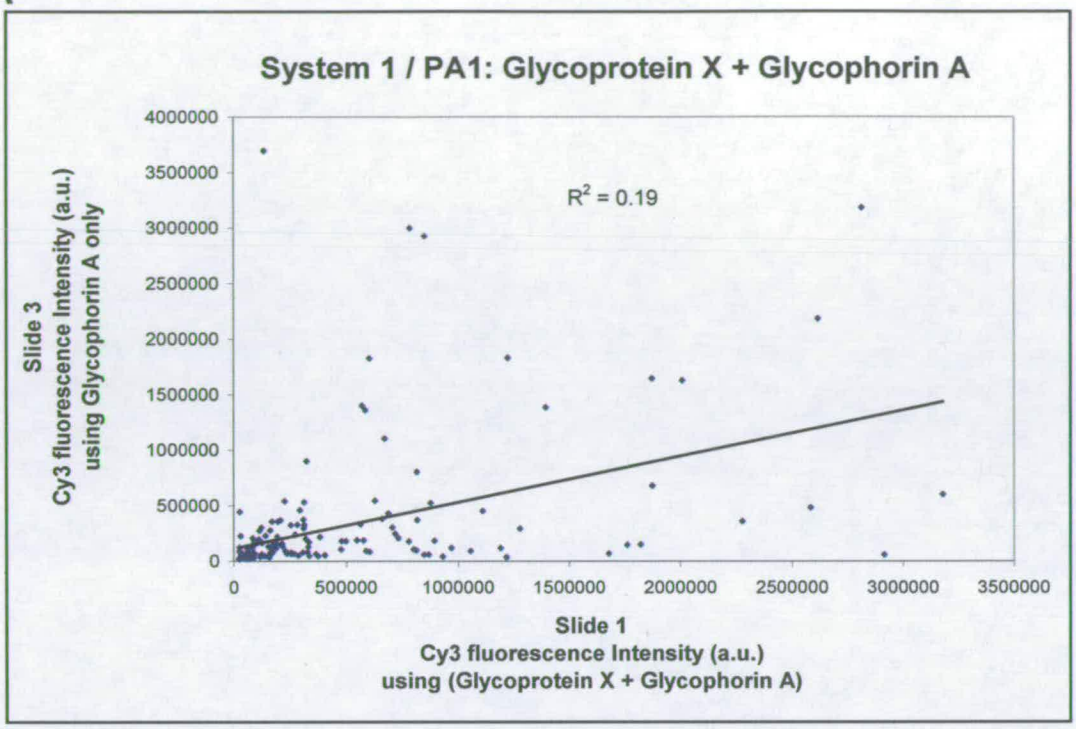
System 1 / PA1: Glycoprotein X + Glycophorin A
Slide 3
Cy3 fluorescence Intensity (a.u.)
using Glycophorin A only
R^2 = 0.19
4000000
3500000
3000000
2500000
2000000
1500000
1000000
500000
0
0
500000
1000000
1500000
2000000
2500000
3000000
3500000
Slide 1
Cy3 fluorescence Intensity (a.u.)
using (Glycoprotein X + Glycophorin A)

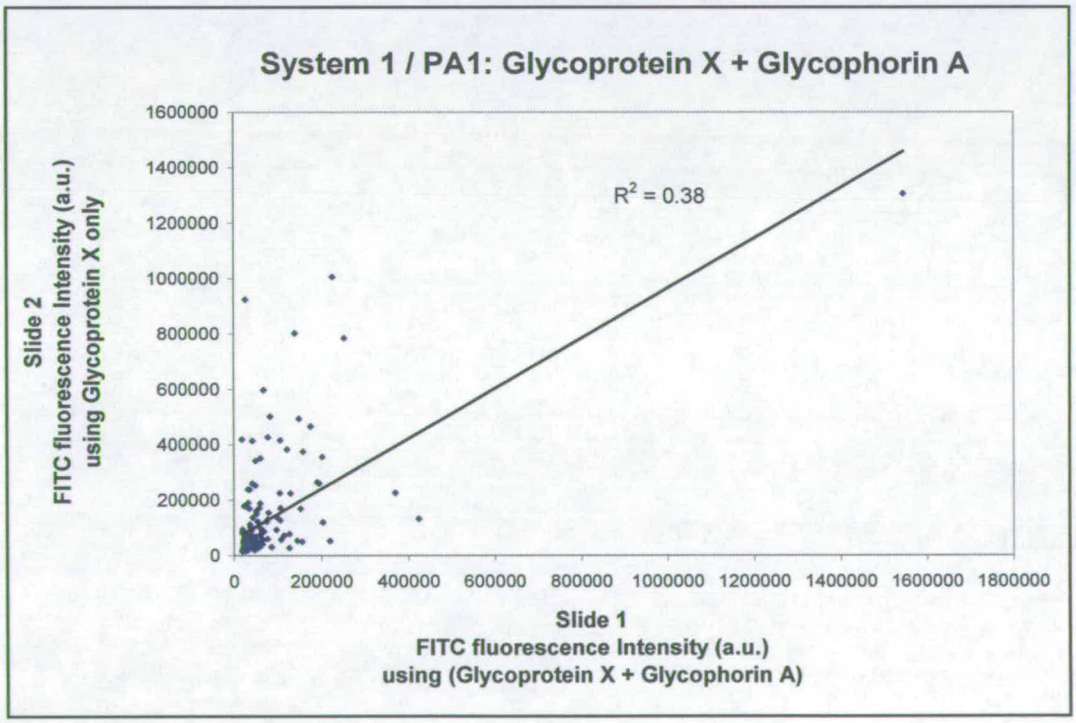
System 1 / PA1: Glycoprotein X + Glycophorin A
Slide 2
FITC fluorescence Intensity (a.u.)
using Glycoprotein X only
R^2 = 0.38
1600000
1400000
1200000
1000000
800000
600000
400000
200000
0
0
200000
400000
600000
800000
1000000
1200000
1400000
1600000
1800000
Slide 1
FITC fluorescence Intensity (a.u.)
using (Glycoprotein X + Glycophorin A)

B

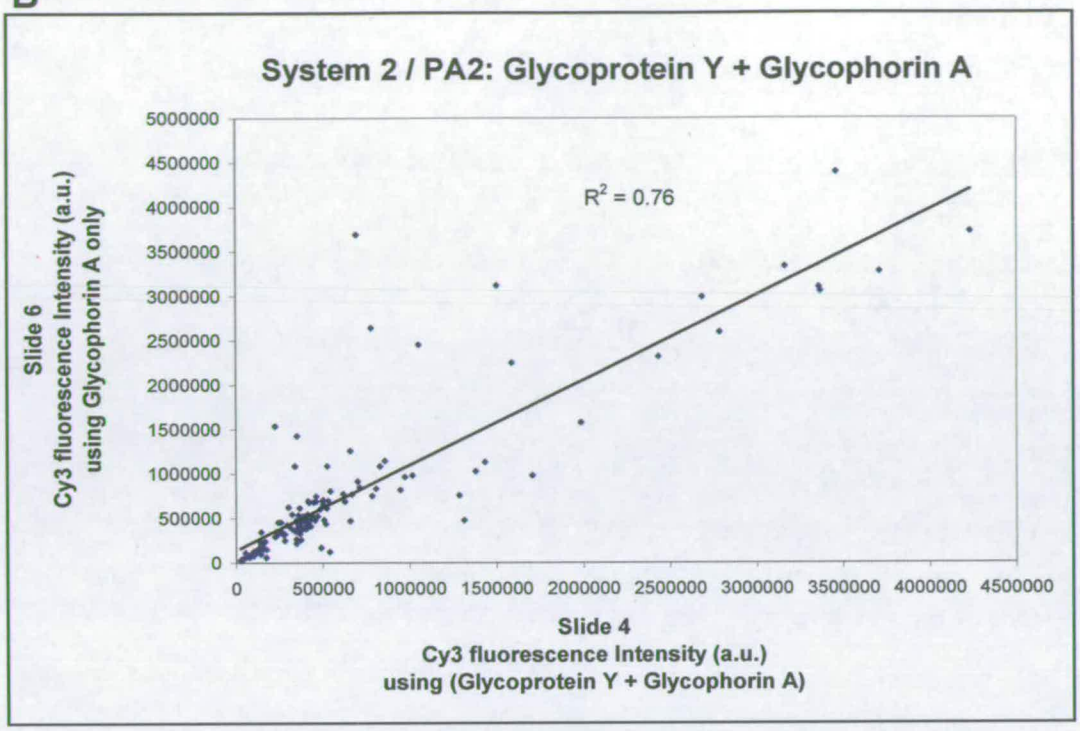

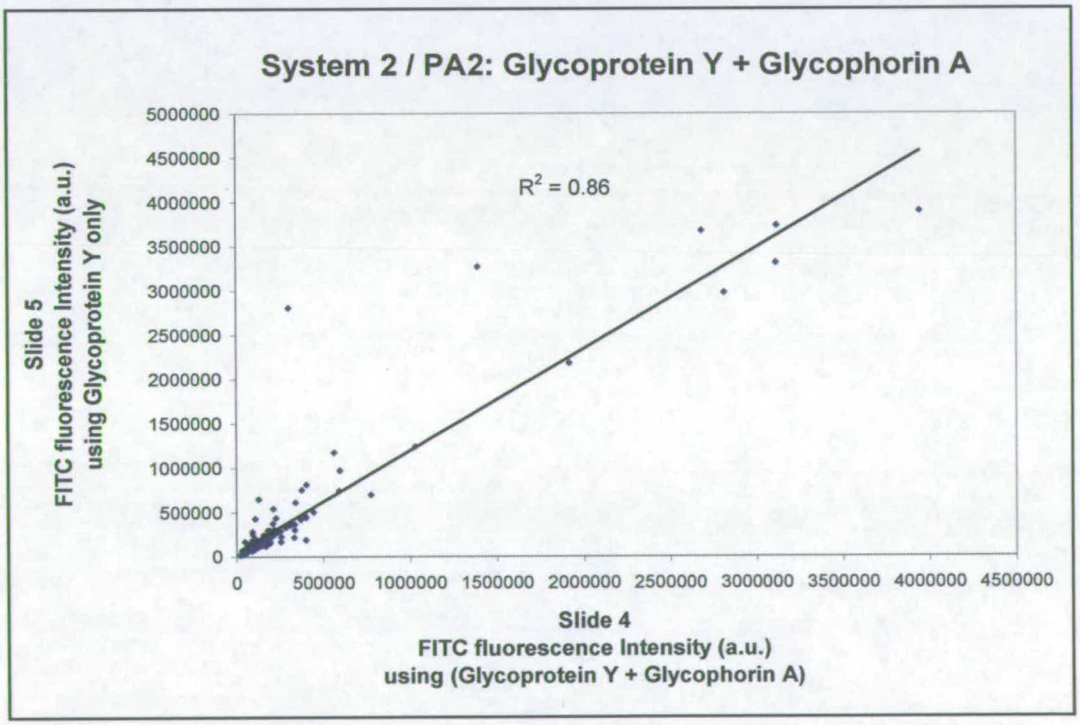

Figure 5.5 *Average fluorescence intensities resulting from the adsorption of a protein, single versus dual protein solutions (A) System 1: Glycophorin A in presence of Glycoprotein X on PA1; (B) System 2: Glycophorin A in presence of Glycoprotein Y on PA2.*

The one probe experiment *versus* the two probe experiment showed very poor correlation of system 1 on PA1 (i.e. Glycophorin A: R^2=0.19; Glycoprotein X: R^2=0.38), whereas system 2 on PA2 gave a good correlation of both labelled proteins (i.e. Glycophorin A: R^2=0.76; Glycoprotein Y: R^2=0.86).

In conclusion, system 1 showed very large discrepancies when comparing results obtained with one and two probes. Such discrepancies could arise from the interaction of the two proteins in solution, or maybe from competitive binding onto the polymers. However, system 2 showed relatively good a correlation between the dual and single probe experiments, and as a result such a system could be utilised in order to increase the throughput of the screening.

5.5 Potential diagnostic applications

A few initial investigations were carried out regarding the potential use of the polymer microarrays developed, as a diagnostic tool for the identification of proteins in complex biological samples. Reddy and Kodadek[228] used arrays of peptoids (oligo-*N*-substituted glycines) as an identification method for proteins via a "fingerprinting" approach. In this study, three different fluorescently labelled proteins were initially bound in the presence of excess unlabelled proteins each on an array of peptoids. When comparing the relative intensities related to each labelled protein across the array, clear differences in protein adsorption were noticed. For each different labelled protein, a set of peptoids bound specifically one protein only (the specificity threshold was set at 10-fold the background fluorescent intensity). From these results, several in-depth investigations were carried out to confirm the potential of this method to detect unlabelled protein in complex biological sample.

In our approach, only the first step of this type of study was carried out. Three identical arrays containing 147 poly(acrylates) were incubated with three different labelled proteins (Fibrinogen, Glycophorin A and Glycoprotein Y) in the presence of 1.0 % v/v human serum to mimic a complex biological sample. The fluorescent intensities arising from the adsorption of labelled protein to each polymer spot were integrated and the

averages for the four identical polymer spots were calculated. These protein adsorptions onto the polymer microarrays were presented as fingerprints/barcodes (DecisionSite, Spotfire, Massachusetts, US) to compare the overall profiles (**Figure 5.6**). To do so, the software used relative fluorescent intensities where each fluorescent intensity value is plotted as a fraction of the most intense sample.

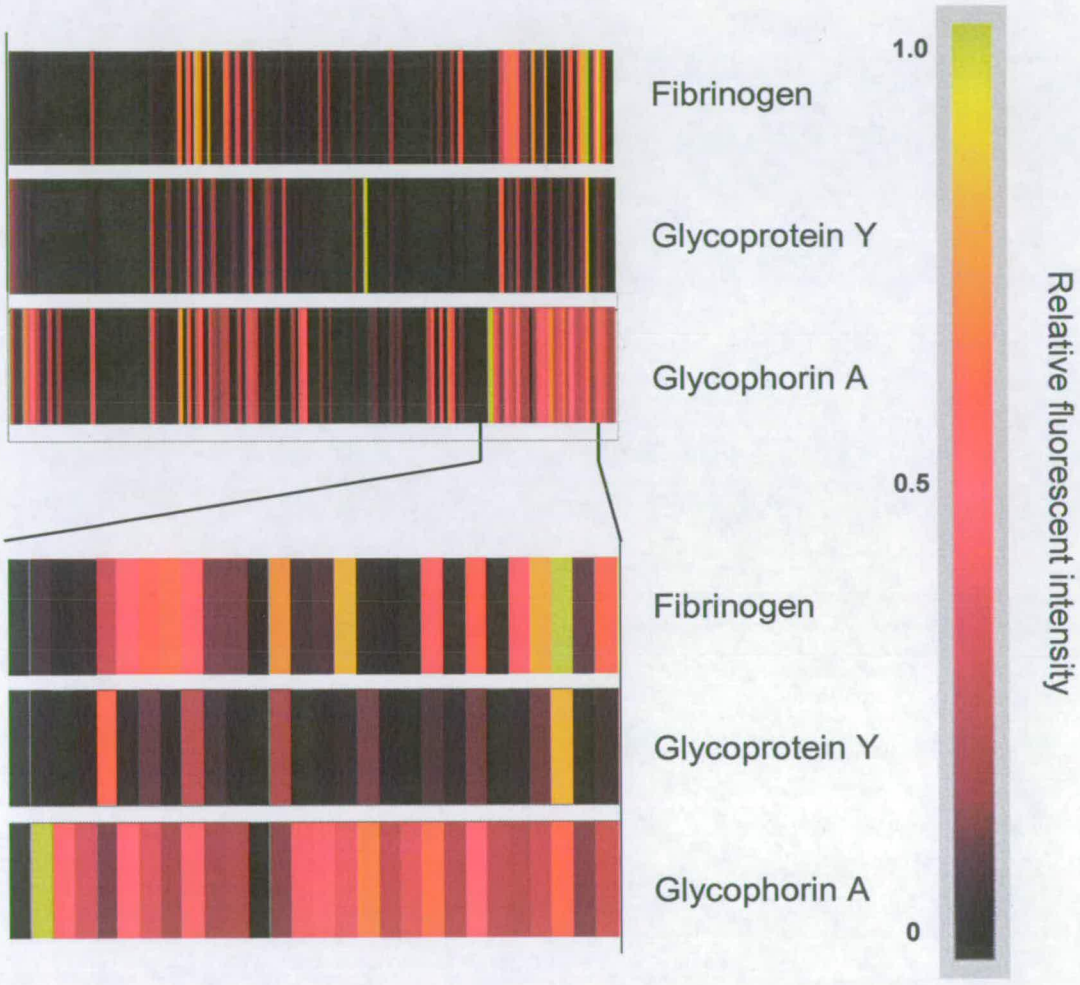

Figure 5.6 *Protein fingerprints showing the relative fluorescent intensity profiles associated with the adsorption of each protein. A part of the barcode was expanded to illustrate the differences in protein adsorption over a few polymer samples. (The colour code is presented on the right; the intensities are expressed as a fraction of the highest binding polymer which is yellow).*

The protein fingerprint for each protein adsorption showed clear differences with the other two proteins fingerprints. To emphasise the specificity of the polymers to the different proteins, a Venn diagram (**Figure 5.7**) was drawn that showed all polymers displaying a fluorescence intensity 10-fold above background intensity for each labelled protein.

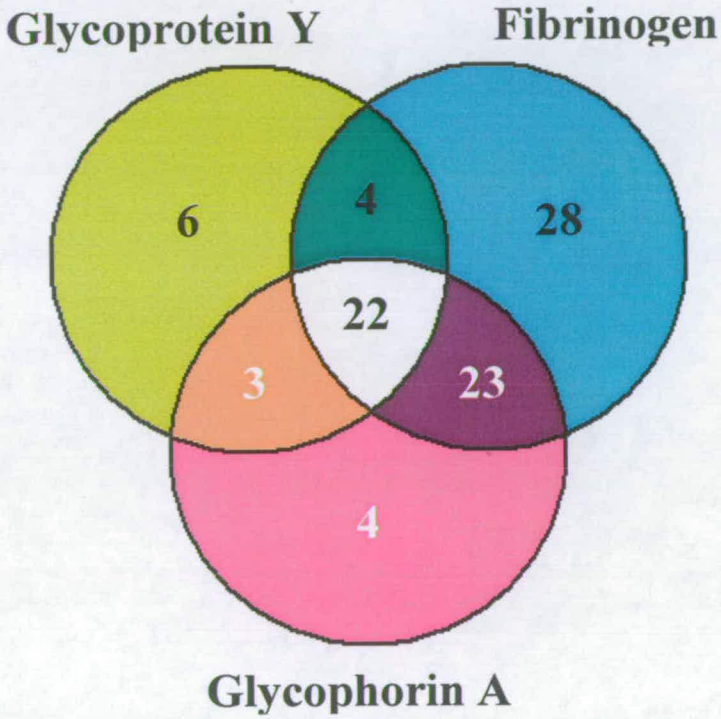

Figure 5.7 *Specific and promiscuous polymers. Venn Diagram presenting the number of specific and promiscuous polymers that adsorbed Glycoprotein X, Glycophorin A and Fibrinogen.*

This Venn diagram showed that 28, 6 and 4 of the polymers were specific for Fibrinogen, Glycophorin Y, and Glycoprotein A, respectively. 22 Polymers non-specifically bound high amounts of the three different proteins and 23, 4 and 3 polymers showed high binding to two different proteins. Although our approach uses over 50-fold less different features than the arrays developed by Reddy and Kodadek, the percentage of probes that provide specific adhesion to a unique protein is proportionally higher with 19, 4.1 and 2.7 % of the probes being specific compared to 2.5, 1.6 and 0.8 %. These

figures suppose that the polymer microarray, even if lacking large number of probes, has the potential to be applied in a similar manner. However, for this platform to be suitable for the analysis of complex biological samples it would be beneficial to increase the number of different polymers, and a range of additional experiments are needed:

The first experiment would be to confirm these adsorptions and specificities using unlabelled protein as it is usually difficult to label a specific protein within a biological sample. Label-free protein could be detected by mean of immunocomplex formation with relevant fluorescently-labelled antibody or set of antibodies ("sandwich"-type with secondary antibody).

The next experiment would involve the determination of the detection limit for the concentration of the proteins of interest. This experiment can be carried out using several microarrays each incubated with the same protein at different concentration in serum, in order to determine the lowest concentration at which this protein is detected. Finally, in order to validate this method it would be essential to study the reproducibility of the methodology over the range of protein concentrations that are detectable.

5.6 Conclusions

A range of investigations was carried out to optimise protein adhesion. GeneFrame® coverslips were selected to minimise protein solution consumption, since these coverslips provided low protein adhesion and high reproducibility and the washing method was standardised for the consistency of the results. The different protein concentrations were optimised to obtain a good signal at minimal protein concentrations. It was shown that by using carefully selected proteins, the assay could be multiplexed with two different labelled proteins. From the results of these investigations and the work of Reddy and Kodadek, it was hypothesised that the polymer microarrays could be utilised as a diagnostic tool for the fingerprint detection of proteins in complex biological samples. Indeed, it was shown that three different labelled proteins gave three very different adhesion fingerprints, and it was therefore possible to identify several polymers with specific adhesion to a single protein. This was only a preliminary study, however, it seems likely that this platform could be utilised for diagnostic applications.

Additionally, since specificity was demonstrated in these experiments, the polymer microarray for protein adsorption could be utilised to identify new substrates for applications in proteomics. Indeed, a series of polymers displaying different protein specificities could be used as a substrate in applications such as surface-enhanced laser desorption ionisation (SELDI) mass spectrometry to facilitate the analysis of protein/peptide mixtures in tissues or plasma. The polymer microarray assay for protein adhesion is a powerful tool allowing parallel screening of hundreds of polymers in a single experiment. Biomaterials, and especially biocompatible polymers, have an essential role to play in tissue engineering applications, in the delivery of new drugs[131], and in stem cell research[227]. The use of polymer microarrays for protein adsorption tailored to the identification of specific polymer properties has potential to accelerate research in many areas of science.

General Conclusions:

A novel method, which allows the patterning of hundreds of polymer spots on a single microscope slide, was developed. Several parameters including the printing conditions, the nature of the substrate and the polymer solvent were optimised in order to obtain uniform and reproducible arrays.

From these experiments, it was concluded that different applications (i.e. cell or protein immobilisation studies) may require different substrates. Protein adsorption studies showed very low levels of background auto-fluorescence when performed using gold-coated slides. In contrast, cell adhesion studies required agarose-coated substrates to achieve minimal non-specific adhesion. Additionally, it was shown that these polymer microarrays were suitable for the high throughput characterisation of the polymer spots, including their morphology, surface composition and functional groups, by SEM, TOF-SIMS and FT-IR, respectively.

The microarray platform was subsequently optimised for cell adhesion screens, where the immobilisation of living cells was evaluated by fluorescent visualisation on each of the printed polymers. The platform was then used to identify novel substrates for the culture of human primary renal tubular epithelial cells *in vitro*, and for the gentle immobilisation of mouse bone marrow dendritic cells. Interestingly, some structure-activity relationships were observed for the polymers selected for the different applications. Indeed, for both cell types, the best results were obtained with polyurethanes containing PTMG as polyol and MDI as diisocyanate. These microarrays may bring further understanding of the factors involved in cellular adhesion of specific cell lines, and could subsequently help in the development of new polymers with enhanced properties.

In order to further demonstrate the versatility of the polymer microarray, this platform was applied to the field of stem cell research. In the first application, the selective immobilisation of a specific adult stem cell population (STRO-1+) from human bone marrow was studied. Using the microarray platform, three polyurethanes were shown to provide selective adhesion, and these results were confirmed on a larger surface using coverslips. These experiments showed that up to 50% of the immobilised cells were part of the STRO-1+ population. Interestingly, the structure-activity investigations yielded some unexpected results, since the three selected polymers were prepared from long hydrophilic chains of poly(ethylene glycol).

The second study involved the identification of novel substrates for the culture of undifferentiated mouse embryonic stem cells (mESC) *in vitro*. mESC are usually cultured on a layer of feeder cells or on gelatine in the presence of the LIF cytokine. The present study involved the culture of mESC on several polymer microarrays over a 9 day period, in order to identify polyurethanes promoting the adhesion and growth of these cells in their undifferentiated phenotypes. Following the selection of the most promising candidates, the experiment was repeated on larger surfaces using polymer-coated glass coverslips. The visualisation of FITC and DAPI to determine the phenotype of the cellular colonies was not sufficient to draw clear conclusions due to very large discrepancies in differentiation within the same coated coverslip. Therefore, in order to confirm the microarray results, a clonal growth experiment was carried out where each colony was grown from single cells to reduce the autocrine effect, and visualisation was carried out using the alkaline phosphatase assay. The clonal growth experiment showed that in the absence of LIF, none of these substrates were able to maintain cellular pluripotentiality. However, in the presence of LIF, 3 out of 4 of the polymers identified using the microarray screen performed at least as well as the gelatine substrate for the culture of mESC.

Finally, the polymer microarray platform was adapted for the high throughput evaluation of protein adsorption. The platform was optimised in order to reduce protein solution consumption, while maintaining a high degree of reproducibility. It was shown that this platform could be easily multiplexed by careful selection of the labelled proteins. To conclude, a proof of concept experiment based on some previously published work was carried out to evaluate the possible use of polymer microarrays in the fingerprint detection of proteins in complex biological fluids for diagnostic applications. The different proteins tested in this preliminary study showed very different adhesion profiles. Therefore, such an approach could be suitable for the fingerprint detection of proteins in complex biological fluids.

The polymer microarray is a very interesting platform for the characterisation of printed polymers. Indeed, it was demonstrated throughout this thesis that the platform provides an ideal format for the parallel screening of large numbers of polymers. The polymer microarray was shown to be suitable for several physico-chemical determinations, including spot morphology and surface composition. Perhaps more importantly, this platform is suitable for the screening of novel cellular substrates. Such a tool could be of particular interest in medical research, when only a very limited number of cells are available and no commercial substrate is suitable. Additionally, the polymer microarray platform has a great flexibility, and these microscopic polymer spots could be used in conjunction with other biomolecules to study a range of microcellular environments. Using the results of structure activity relationship investigations, it may be possible to synthesise novel materials with enhanced properties, and to further our understanding of the complex factors controlling the interactions of biomolecules and living cells with their environments. Advancing knowledge in these areas of science is an essential part of tomorrow's medicine, for which clinicians envision the use of synthetic substrates as scaffolds for the growth of human organs, and the development of a range of therapies based on the careful control of a stem cell's fate.

Chapter 6: Experimental

6.1 General information

6.1.1 Equipment

UV-visible spectrophotometer: Agilent 8453 UV (Agilent Technologies)

QArray^{mini} microarrayer (Genetix)

BioAnalyzer 4F/4S white light scanner and FIPS software (LaVision BioTech)

HCS platform and Pathfinder™ software (IMSTAR)

Biosafety cabinet: HERAsafe KS 18 class II (Heraeus)

Incubator: HERAcell 150 (Heraeus)

Vacuum oven: Vacutherm VT6025 (Heraeus)

6.1.2 Polymers

The polymer libraries (poly(urethane)[229], poly(acrylate)[230] and grafted poly(allylamine)[231] libraries, respectively, Appendix I, II and III) were synthesised by Jean-Francois Thaburet, Hitoshi Mizomoto and Ann Jasmine Jose and were generated as part of a previous project.Most polymer had been previously characterised in terms of molecular weight (by gel permeation chromatography), wettability[229] and glass transition temperature (by differential scanning calorimetry).

6.1.3 Chemicals and solvents

Unless specified, the chemicals, solvents used in all the experiments were obtained from Sigma-Aldrich. Phosphate buffer saline (10 mM phosphate, 27mM KCl, 137 mM NaCl, pH 7.4) is referred to as PBS throughout.

6.1.4 Microscope slides and coverslips

Unless specified, aminoalkylsilane microscope slides were obtained from Sigma-Aldrich, gold-coated slides were obtained from Asahi Kasei and the coverslips from VWR.

6.1.5 Cell culture media and supplements

Unless specified, all cell culture media were from Sigma-Aldrich and all supplements added to the culture medium were supplied by Gibco, Invitrogen.

Unless specified each culture media (Table 6.1) was supplemented with 10 % v/v heat inactivated fetal calf serum, penicillin (100 units.mL^{-1}), streptomycin (100 mg.mL^{-1}) and L-glutamine (4mM).

Cell line	Culture medium
HEK293	DMEM
B16F10	DMEM
ND7	DMEM
HeLa	RPMI 1640
JURKAT	RPMI 1640
RMA-S	RPMI 1640
JY	RPMI 1640
BMDC	R10
STRO-1	α-MEM
ESC (Oct4-GFP)	GMEM

Table 6.1 *Name of the cell lines used and their corresponding culture medium. Dubelcco's modified Eagle's medium (DMEM) and Glasgow's modified Eagle's medium (GMEM).*

6.2 Experimental for Chapter 2

6.2.1 Labelling of fibrinogen

A solution of fibrinogen from human plasma (F3879, Sigma-Aldrich) was prepared (2 $mg.mL^{-1}$ in 0.85 % w/v NaCl). In order to achieve solubilisation, the solution was warmed to 37 °C. Once solubilised, the solution was filtered though a syringe filter (0.45 µm PVDF filter, Whatman). To 750 µL of this solution, 50 µL of sodium bicarbonate solution (1.0 M) was added. This solution was then transferred to a vial containing 0.10 mg of AlexaFluor® 647 succinimidyl ester (A20173, Molecular Probes, Invitrogen) and the reaction mixture was stirred at room temperature for 1 h.

The reaction mixture was loaded onto a column packed with Sephadex G, BioGel P resin (Molecular Probes, Invitrogen). Using an elution buffer (0.01 M K_3PO_4, 0.15 M NaCl, pH 7.2, 0.20 mM NaN_3), the unreacted dye was separated from the labelled protein.

The fraction containing the labelled protein was collected, a small aliquot was diluted 10 fold and analysed using a UV spectrophotometer. Absorbance was measured at 280 and 650 nm (A_{280} and A_{650}). The protein concentration [Fg] and degree of labelling were calculated as follows:

$$[Fg] = (A_{280}-(A_{650}x0.03)) \text{ x dilution factor} / \varepsilon_{Fg}$$

With: $\varepsilon_{Fg} = 513{,}000\ cm^{-1}M^{-1}$ [232]; dilution factor = 10; $A_{280} = 0.240$; $A_{650} = 0.808$

$$\text{Degree of labelling} = (A_{650}x\text{dilution factor}) / (\varepsilon_{Alexa\ 647}x[Fg])$$

With $\varepsilon_{Alexa\ 647} = 239{,}000\ cm^{-1}M^{-1}$ [233]; $MW_{Fg} = 340{,}000\ cm^{-1}M^{-1}$ [232]; $[Fg] = 4.21x10^{-6}$ M.

The labelling gave about 8 moles of AlexaFluor® 647 dye per mole of fibrinogen. The labelled protein solution was divided into small aliquots and frozen at -80 °C.

6.2.2 Surfaces for protein adsorption

The suppliers and references of the different surfaces used in this experiment are summarised below:

Material	Nature of surface	Reference	Supplier
Glass	Aminoalkylsilane	S4651	Sigma-Aldrich,
	Superfrost Plus	631-0108	VWR
	Polysine	631-0107	VWR
Metal	Aluminium	NA	University of Southampton's workshop
	Solid steel	NA	University of Southampton's workshop
Polymeric film	PVDF	FV301490	Goodfellow
	Poly(ethersulfone)	SU303300	Goodfellow
Coated Glass	Blocking buffer (10X)	B6429	Sigma-Aldrich
	Gold	NA	University of Southampton's physical chemistry department

Table 6.2 *Suppliers and references of the different materials used in the protein adsorption study.*

The metallic surfaces (aluminium and steel were cleaned by sonication in a bath of tetrahydrofuran (THF)) were obtained from the workshop of the department of chemistry (University of Southampton, UK).

The commercial blocking buffer[167] (used in immunoassays to prevent the non-specific binding of protein or antibody onto surfaces) was diluted 2 times to obtain x5 blocking buffer. Superfrost Plus slides were incubated in the diluted blocking buffer (30 min @ 37 °C) and rinsed in PBS before use.

Gold-coated slides used for the determination of a suitable surface for protein adsorption microarray were prepared in the department of electrochemistry (University of Southampton), further experiments were carried out using gold-coated slides prepared by Asahi Kasei. First, a layer of chromium was deposited onto the glass; this provided an adhesion layer for the subsequent gold deposition. The slides were rinsed in PBS prior to use.

6.2.2.1 Background protein adhesion

Each cleaned surface was incubated with AlexaFluor 647 labelled fibrinogen (25.0 $\mu g.mL^{-1}$ in PBS, 3 h @ 37°C). Following incubation, each surface was rinsed in PBS and deionised water before drying under a stream of nitrogen. Evaluation of protein adhesion was carried out using the Cy5 filter and the low resolution scanner (BioAnalyzer 4F/4S, LaVision BioTech). Background protein adhesion was evaluated using FIPS (LaVision BioTech), integrating the fluorescence intensity over a circular area of diameter 250 µm.

6.2.2.2 Evaluation of printing quality on low background surfaces

Metallic and glass coated surfaces giving low background fluorescence intensities were re-prepared and printed using the $Qarray^{mini}$ microarrayer with a few poly(acrylates) (3n9, 5c5, 7e7, 5AC9) dissolved in isopropanol/water, (90/10; 10 $mg.mL^{-1}$). Spot uniformity was evaluated visually (Leica LEITZ DM 1L inverted configuration microscope).

6.2.3 Surfaces for cellular adhesion study

6.2.3.1 Substrate preparation

The activation of aminoalkylsilane slides was carried out according to the method of Beier[9]. The slides were activated by disuccinimidylcarbonate in presence of excess diisopropylethylamine (50 and 150 mM, respectively, in DMF, 4 h @ RT). After activation, they were treated immediately with 1-octadecylamine (Clariant) (2.0 mM in 1.0 % v/v diisopropylethylamine in DMF, 4 h @ RT). Finally, the alkylated slides were washed by shaking in a bath of dimethylformamide (DMF), followed by shaking in a bath of acetone, before drying under a stream of nitrogen. These slides were referred to as C18-functionalised slides.

A perfluoroalkylthiol monolayer was formed by immersing the gold coated slide into a solution of 1H,1H,2H,2H-perfluorodecanethiol (Fluorochem, 1.0 mM in methanol, 4 h @ RT), followed by rinsing in methanol and drying under a stream of nitrogen. These slides were referred to as perfluoroalkylthiol-modified slides.

Coating with agarose was achieved by manually dip-coating the slide in agarose Type I-B (1.0 % w/v in deionised water @ 65°C) followed by removal of the coating on the bottom side by wiping with a clean piece of tissue. After drying overnight at room temperature, the coated slides could be stored in microscope slide storage boxes (Simport, VWR) at RT or used immediately for printing. These slides were referred to as agarose-coated slides.

6.2.3.2 Evaluation of background cell binding

The substrates were printed (Qarraymini, Genetix) using solid pins (K2785, Genetix) with 8 polymers (4 poly(acrylates) and 4 poly(urethanes)) (10 mg.mL^{-1} in NMP) (**Table 6.3**) each printed as 4 identical spots using the conditions described in 6.3.1. Following printing and drying, the arrays were incubated with different cell lines (HEK293, HeLa, and ND7) in culture medium (**Table 6.1**) under cell culture conditions (24 h @ 37 °C, 5 % CO2). Following incubation, the cells growing on the surface were washed in PBS and cellular binding to the substrates was assessed visually using a microscope (Leica LEITZ DM 1L inverted configuration microscope).

To illustrate the evaluation of background cell binding (**Figure 2.1**), an experiment was carried out by comparing the adhesion of cells onto 3 identical polymer arrays printed on different substrates. Three arrays of 120 poly(urethanes) were prepared using the conditions described in chapter 6.3.1 on the following substrates: standard glass slide (AA00000102E, Menzel-Gläser), C18-functionalised slide and agarose-coated slide. STRO-1+ cell fraction were isolated and cultivated as described in chapter 6.4.1. STRO-1+ cells (3 x 10^6 cells) were stained with CellTracker™ Green (C2925, Molecular Probes, Invitrogen) according to the manufacturer's protocols. The stained cell suspensions were directly plated onto each polymer arrays (1 x 10^7 cells in 1.5 mL α-MEM / slide) and placed in an incubator (19h @ 37 °C, 5 % CO_2). After washing by dipping in PBS, the cells were fixed in an aqueous solution of p-formaldehyde and sucrose (3.7 % w/v and 4.0 % w/v, respectively) for 15 min, rinsed and stored in PBS at 4 °C. Image capture was carried out with a BioAnalyzer 4F/4S white light scanner using the FITC.

6.2.4 Solvents

The effect of solvent type on the quality of the printing was evaluated using gold coated slides and by the preparation of polymer solution of poly(acrylates) and poly(urethanes) at 10 $mg.mL^{-1}$. The following solutions were prepared:

Polymer	Solvent
Poly(acrylates)	MeOH:H_2O (90:10)
	EtOH:H_2O (90:10)
2c7; 3a7;	IPA:H_2O (90:10)
3n9 and 5c5	NMP
Poly(urethanes)	THF
	DCM
PU155; 157;	$CHCl_3$
166 and 171	NMP

Table 6.3 *Different solvent and solvent mixtures used to dissolve the corresponding polymers.*

For each solvent system, polymer solutions were printed as 4 identical spots using 150 µm aQu solid pins (K2785, Genetix) using the following parameters:

Inking time = 100 ms

Stamping time = 100 ms

1 Stamp / Spot

Following drying under vacuum (12 h @ 45 °C / 200 mbar), the quality of the printed spot was evaluated by microscopy.

6.2.5 Printing and washing

Polymer solutions were prepared at 10 mg.mL^{-1} in NMP. Polymer printing was carried out using the QArray^{mini} microarrayer (Genetix). The pins used were 75 µm aQu split pin (K2800, Genetix) or 150 µm aQu solid pins (K2785, Genetix).

Printing with split pin required a blotting step which involved printing several spots (typically 20 spots) on a "dummy" slide to remove the excess of polymer solution in the slit prior to printing on the target slide in order to obtain reproducible spot sizes. Optimal spot reproducibility was obtained using the following parameters:

Inking time = 200 ms
Stamping time = 1 ms
1 Stamp / Spot

Using the solid pins, optimal spot reproducibility was obtained using the following parameters:

Inking time = 200 ms
Stamping time = 10 ms
5 Stamp / Spot

Washing and drying of the pins using the integrated washing/drying station was carried out using the following parameters:

Ethanol: 5000 ms
Compressed air: 10000 ms

6.2.6 Evaluation of printing reproducibility

126 different poly(urethanes) and 2 poly(acrylates) solutions (10 $mg.mL^{-1}$ in NMP) were prepared and placed in high sample recovery polypropylene 384-well microplates (X7050, Genetix). The polymer arrays were fabricated by contact printing ($QArray^{mini}$, Genetix) with 16 aQu solid pins (K2785, Genetix) using the following printing conditions on gold-coated slide: 5 stamping per spot, 200 ms inking time and 10 ms stamping time. Each solution was printed as four identical spots giving a total of 512 spots. The polymer array was made of two fields of 16 x 16 spots with a spot-to-spot distance of 1120 µm. Once printed, the slides were dried overnight under vacuum (12 h @ 45 °C / 200 mbar).

The study of spot size reproducibility was undertaken by incubating the polymer microarray with a solution of AlexaFluor® 647 labelled fibrinogen ([Fg] = 25 $\mu g.mL^{-1}$ in PBS, 3 h @ 37 °C). Following incubation, the slide was washed, dried and visualised with a BioAnalyzer 4F/4S white light scanner (LaVision BioTech GmbH, D) using the Cy5 filter. Spot size evaluation (measured as diameter with 10 µm increment) was carried out with the FIPS software (LaVision BioTech GmbH, D).

A

Field 1															
61	69	79	87	39	44	48	53	20	24	28	33	4	8	12	16
59	67	77	85	38	43	47	51	19	23	27	31	3	7	3e9	15
57	65	73	83	37	41	46	50	18	22	26	30	2	6	10	14
55	63	71	81	35	40	45	49	17	21	25	29	1	5	9	13

Field 2															
137	141	145	149	121	125	129	133	105	109	113	117	49DM	93	97	101
136	140	144	148	120	124	128	132	104	3e7	112	116	39DM	92	96	100
135	139	143	147	119	123	127	131	103	107	111	115	39DE	91	95	99
134	138	142	146	118	122	126	130	102	106	110	114	89	49DE	94	98

B

Field 1															
320	330	310	330	330	300	310	300	280	340	320	300	340	310	310	300
310	310	310	300	310		260	300	300	320		300	290		320	300
320	320	300	310	330	330	300	320	300	310		320			320	320
320	310	320	300	320	340	330	360	300		290	360		300	310	310

Field 2															
300	290	300	290	280	240	280	260	300	300	280	300	290	320	300	300
280	320	320	280	300	280	300	300	300	310	300	290	280	310	320	320
300	320	320	320	310	240	280	300	300	320	310	290	310	320	310	340
300	290	290	310	340	320	320	330	310	310	300	270	300	270	320	310

Table 6.4 *Spot size evaluation. (A) printed poly(urethane) samples (Appendix I), (B) corresponding spot diameter (μm). The 8 empty cells correspond to the polymer spots that could not be measured.*

6.2.7 Physical characterisation of polymers on the microarray

Physical characterisation of the polymers on the microarray was carried out using polymer microarrays printed using the conditions described above in section 6.2.6.

6.2.7.1 Scanning Electron Microscopy

Polymer microarray slides printed with poly(urethanes) were cut in two using a glass cutter and mounted onto carbon coated specimen tubs prior to sputtering with a thin layer of gold. Scanning electron micrographs were recorded using a JSM 5910 Scanning Electron Microscope (JEOL).

6.2.7.2 FTIR microscopy

FTIR microscopy was carried out using a FT-IR PerkinElmer 2000 Spectrometer combined with an AutoIMAGE FT-IR microscope (PerkinElmer). Spectra were the sum of 16 scans recorded between 4000-650 cm^{-1} with a resolution of 8 cm^{-1}. Spectral processing was carried out using the AutoIMAGE™ Software (PerkinElmer).

6.2.7.3 TOF-SIMS

The array was prepared in our laboratories using the condition described in section 6.2.6 using a series of 8 poly(acrylates) copolymers. The TOF-SIMS analyses were ran in Asahi Kasei, Fuji, Japan. Time of flight secondary ion mass spectrometry (TOF-SIMS) was performed on a TRIFT-III (Physical Electronics) using the following conditions:

Primary ion: Ga+

Primary beam energy: 15 kV

Primary beam current: 600 pA

Secondary ion polarity: positive

Charge neutralisation: 28 eV electron beam

Mass range: 0.5-200 Da

Analysis area: 120 x 120 µm

Beam diameter: ~ 1 µm

Accumulation time: 1 min

% DEAEMA theoretical	0%	5%	10%	15%	20%	25%	30%	35%
$Ratio_1$ (100/59)	0.02	0.10	0.15	0.25	0.32	0.45	0.59	0.73
$Ratio_2$ (100/59)	0.00	0.10	0.10	0.28	0.75	1.04	1.30	1.51
Average	0.01	0.10	0.12	0.26	0.53	0.75	0.95	1.12
% DEAEMA experimental	1.4%	8.9%	11.1%	20.7%	34.8%	42.7%	48.6%	52.8%

Table 6.5 *TOF-SIMS analysis of polymer spots. Ratio calculated from the intensity of peak 100 divided by the intensity of peak 59, and corresponding mol. % DEAEMA determined experimentally.*

6.3 Experimental for Chapter 3

6.3.1 Polymer microarray fabrication

The polymer arrays were fabricated by contact printing (QArray^{mini}, Genetix) with 16 aQu solid pins (K2785, Genetix) using polymer solutions (10 mg.mL^{-1}in NMP) placed in polypropylene 384-well microplates. The following printing conditions were used on agarose-coated slides, 5 stampings per spot, 200 ms inking time and 10 ms stamping time. The typical spot size was 300 μm in diameter with spot-to-spot distances of approximately 1120 μm allowing up to 512 polymers to be printed on a standard 25 x 75 mm slide. 120 poly(urethanes) were printed in quadruplicate within 2 fields of 16 x 16 spots, with two pattern of 4 x 4 spots left empty. Once printed, the slides were dried under vacuum (12 h @ 45 °C / 200 mbar) and sterilised by exposure to UV irradiation for 20 min prior to use.

6.3.2 Cell culture

Immortalised mouse adherent cell lines (ND7 and B16F10, kindly provided by Salim Khakoo, Cancer Research, Southampton, UK) were grown in DMEM growth medium supplemented with heat inactivated fetal calf serum (10 % v/v), penicillin (100 units.mL-^{1}), streptomycin (100 mg.mL^{-1}) and L-glutamine (4 mM) at 37 °C with 5 % CO_2. Cells were stained with CellTracker™ Green or Orange (C2925 or C2927, Molecular Probes, Invitrogen) according to the manufacturer's protocols. Prior to seeding onto the polymer array, cells were suspended in growth medium (1.0 x 10^6 cells/slide 15 mL). The slides were subsequently placed in an incubator (24 h @ 37°C, 5% CO_2). After a controlled washing in PBS (30 mL, 2 min shaking on a microplate shaker at 600 rpm), the cells were fixed in an aqueous solution of *p*-formaldehyde and sucrose (3.7 % w/v and 4.0 % w/v, respectively) for 15 min, rinsed and stored in PBS at 4 °C. Image capture was carried out with a BioAnalyzer 4F/4S white light scanner using the FITC or Cy3 filters.

Slide number	Slide 1			Slide 2			Slide 3			Slide 4		
Slide detail	SI1 ND7 Track 0			SI2 ND7 Track 0			SI1 B16F10 Track G			SI2 B16F10 Track G		
Filter used	Cy3			Cy3			FITC			FITC		
PU	F	CV	F-B	F	CV	F-B	F	CV	F-B	F	CV	F-B
3	315	41	119	313	46	116	245	11	20	227	17	21
4	177	5	-19	199	15	3	224	17	-1	314	24	108
8	182	3	-15	186	4	-10	243	36	18	220	16	14
9	220	3	24	215	24	19	456	40	231	330	42	124
10	232	10	35	233	5	37	320	31	95	299	37	94
12	854	36	658	627	24	430	317	41	91	232	18	27
13	203	3	7	204	7	7	221	26	-5	198	4	-7
14	196	8	0	176	4	-20	215	10	-11	227	24	22
15	225	6	29	214	4	17	257	14	32	236	14	31
16	512	12	315	439	31	242	297	29	72	261	40	55
17	235	11	39	210	7	14	207	15	-18	202	2	-4
18	523	9	327	461	2	265	221	16	-4	217	12	12
19	254	9	58	229	3	33	286	33	61	625	114	419
20	220	9	24	259	35	62	396	40	171	569	55	364
22	259	31	63	223	16	27	200	5	-25	258	24	52
23	284	10	88	219	6	22	375	40	150	275	29	69
24	256	10	60	231	5	35	411	37	186	405	58	199
25	205	4	9	220	12	24	244	18	19	374	54	168
28	303	37	106	203	7	6	265	27	40	208	4	2
29	432	24	235	483	27	287	1006	42	781	1061	50	855
30	251	22	54	215	10	18	222	13	-3	826	89	620
31	221	3	25	212	5	16	223	8	-2	224	6	18
33	211	9	14	225	4	29	351	67	126	206	13	0
35	243	9	46	227	5	30	243	28	17	220	22	14
37	212	19	15	261	40	65	705	39	480	568	62	363
38	212	9	16	199	11	3	245	9	19	347	47	141
40	177	3	-19	186	6	-11	218	8	-8	309	17	104
41	268	17	72	244	16	47	314	61	89	206	7	1
43	344	19	148	451	29	255	217	18	-9	291	19	85
45	295	30	98	223	12	27	306	76	81	191	6	-14
46	231	3	35	232	12	36	272	40	46	191	7	-15
47	194	13	-2	193	16	-3	586	29	360	300	64	94
48	192	4	-4	215	9	19	457	19	231	335	55	129
49	234	11	38	199	2	2	431	55	206	282	25	76
50	228	15	32	212	5	16	625	79	399	456	40	251
53	375	38	178	245	22	49	208	2	-17	201	6	-5
55	846	30	650	584	33	388	293	51	67	219	8	14
57	222	7	26	214	9	18	419	39	194	378	44	172
59	224	4	27	263	25	67	618	22	393	771	63	566
61	253	9	57	244	9	47	223	19	-2	196	2	-10
63	326	6	129	345	6	148	244	31	18	215	9	9
65	1020	16	824	857	10	660	766	64	540	949	32	744
67	206	8	9	221	11	25	282	19	57	326	28	121
69	238	7	42	266	22	69	570	52	345	1001	28	795
71	193	4	-4	200	8	4	292	78	66	191	7	-15
73	202	9	5	206	11	10	184	5	-41	222	27	16
77	195	10	-2	210	8	14	486	43	261	383	35	177
79	253	19	57	291	10	95	1065	76	839	992	16	786
81	280	40	84	443	30	246	235	24	10	217	22	11
83	212	9	15	226	14	30	233	15	8	303	45	97
85	235	8	38	210	11	14	301	40	76	354	35	149
87	180	3	-17	202	16	6	317	31	92	275	29	69
89	199	13	3	205	7	8	239	22	14	522	122	316
91	192	4	-5	237	37	41	247	20	21	242	11	36
92	184	5	-13	195	7	-1	420	57	195	378	28	173
93	203	10	6	241	9	45	384	27	158	398	45	192
94	201	4	5	207	10	10	274	22	48	211	22	5
95	753	14	556	787	17	591	418	17	192	736	67	530
96	331	23	135	486	10	290	1110	83	885	1331	64	1126
97	250	17	54	478	21	281	1279	38	1054	1037	68	832
123	199	9	2	204	17	7	241	11	15	210	5	4

Slide number	Slide 1			Slide 2			Slide 3			Slide 4		
Slide detail	SI1 ND7 Track 0			SI2 ND7 Track 0			SI1 B16F10 Track G			SI2 B16F10 Track G		
Filter used	Cy3			Cy3			FITC			FITC		
PU	F	CV	F-B	F	CV	F-B	F	CV	F-B	F	CV	F-B
159	1088	19	891	1045	16	848	1035	66	810	873	57	667
160	442	15	246	453	19	257	401	52	176	245	19	39
161	569	10	372	641	5	445	1756	58	1530	1356	21	1150
162	482	24	286	304	18	108	698	61	473	475	30	270
163	207	5	11	206	5	9	274	25	48	222	10	16
164	554	28	358	404	13	208	514	51	289	838	63	632
165	619	34	423	513	21	317	629	67	404	317	36	111
166	379	16	183	538	33	341	519	115	293	359	35	153
167	248	9	51	240	11	43	567	54	341	511	34	306
168	361	16	165	393	14	197	422	55	196	1081	43	875
169	192	4	-4	216	17	19	253	15	27	218	14	12
170	227	11	30	221	6	24	238	18	13	260	12	54
171	209	6	13	239	11	42	326	37	100	287	26	81
172	269	24	73	299	28	102	705	47	480	510	33	304
174	444	1	248	491	9	295	606	57	381	511	54	305
175	224	7	27	208	5	12	356	59	131	201	5	-5
176	207	6	10	191	5	-5	275	29	50	242	15	36
177	803	22	607	1205	3	1009	1313	19	1088	1338	18	1132
178	236	13	40	221	6	24	595	96	369	244	12	38
179	243	4	47	224	6	28	338	28	113	432	75	226
180	220	5	24	241	3	44	198	8	-28	211	9	5
181	211	10	15	197	11	0	306	41	81	252	21	46
182	902	20	706	1211	19	1014	2793	33	2567	2794	12	2588
183	466	50	269	456	29	259	1232	19	1006	724	17	519
184	308	15	111	385	29	189	1285	17	1060	995	17	789
185	667	12	471	636	32	439	1156	25	931	1341	20	1135
186	400	32	203	392	26	195	1413	27	1187	723	47	517
187	220	5	24	193	4	-4	216	22	-10	189	9	-17
188	224	2	28	192	8	-5	202	9	-23	196	4	-10
189	289	17	93	304	7	107	1075	71	849	533	34	328
190	828	23	632	732	20	536	844	52	618	1045	21	839
191	352	26	156	232	18	36	488	69	263	577	75	372
192	220	10	24	231	22	34	278	21	53	294	47	89
193	751	10	555	833	18	637	1064	35	838	857	36	651
194	1413	18	1216	1261	19	1065	1495	24	1270	1566	24	1360
195	885	16	689	1451	30	1255	1971	45	1745	1452	12	1246
196	463	29	267	385	8	189	968	13	743	1821	39	1615
197	191	2	-6	201	8	5	234	12	9	260	17	54
198	235	8	39	242	11	46	263	45	37	426	58	220
199	229	11	33	242	16	46	246	26	21	197	5	-9
200	890	16	694	878	10	682	3948	42	3723	2667	37	2461
201	209	8	12	190	8	-7	305	31	80	323	42	117
202	219	3	22	209	4	12	178	3	-47	185	5	-21
203	955	25	759	848	9	652	678	6	453	758	26	552
204	295	7	99	310	5	114	745	71	520	637	73	431
205	220	1	24	251	14	55	232	9	7	438	90	233
206	632	14	435	673	29	476	1220	8	994	926	20	721
207	270	20	74	379	34	183	368	24	143	320	18	114
208	928	22	732	852	18	656	2001	10	1775	1759	20	1554
209	384	10	188	312	24	116	478	52	252	544	44	338
210	1063	15	867	901	24	705	720	60	495	1024	50	818
211	1113	13	917	1016	19	819	740	101	514	410	28	205
212	199	8	2	187	2	-9	310	20	85	238	25	33
213	239	11	42	246	11	49	227	7	2	337	49	132
214	1346	28	1149	929	14	733	1249	54	1023	1189	22	983
215	464	12	268	340	62	143	609	40	384	414	45	208
216	228	16	32	197	5	1	274	36	49	210	6	4
217	675	11	479	754	15	558	901	69	676	1633	42	1428
Mean Background	196			196			225			206		
Mean CV		14			15			36			32	

Table 6.6 *Cell adhesion reproducibility study. F: integrated mean fluorescence intensities, CV: calculated coefficient of variance, F-B: background corrected mean fluorescence intensities.*

Slide number	Slide 2			Slide 5		
Slide detail	SI2 ND7 Track 0			SI2 ND7 Track G		
Filter used	Cy3			FITC		
PU	F	CV	F-B	F	CV	F-B
3	313	46	116	533	60	223
4	199	15	3	265	30	-45
8	186	4	-10	259	21	-51
9	215	24	19	304	64	-7
10	233	5	37	275	29	-36
12	627	24	430	2016	49	1706
13	204	7	7	283	16	-27
14	176	4	-20	208	11	-102
15	214	4	17	225	9	-86
16	439	31	242	762	33	452
17	210	7	14	520	68	210
18	461	2	265	337	19	26
19	229	3	33	231	10	-79
20	259	35	62	251	11	-60
22	223	16	27	371	38	61
23	219	6	22	596	15	285
24	231	5	35	392	28	81
25	220	12	24	371	40	60
28	203	7	6	279	12	-32
29	483	27	287	1363	31	1052
30	215	10	18	405	22	94
31	212	5	16	250	12	-60
33	225	4	29	216	11	-95
35	227	5	30	352	53	42
37	261	40	65	388	79	78
38	199	11	3	218	8	-93
40	186	6	-11	420	61	109
41	244	16	47	413	28	103
43	451	29	255	578	36	267
45	223	12	27	456	18	146
46	232	12	36	304	38	-6
47	193	16	-3	300	41	-11
48	215	9	19	245	21	-66
49	199	2	2	326	25	15
50	212	5	16	328	32	18
53	245	22	49	467	19	156
55	584	33	388	927	50	617
57	214	9	18	429	62	118
59	263	25	67	344	32	33
61	244	9	47	247	25	-64
63	345	6	148	285	9	-25
65	857	10	660	1502	19	1191
67	221	11	25	281	19	-30
69	266	22	69	582	15	271
71	200	8	4	743	72	433
73	206	11	10	368	32	58
77	210	8	14	495	20	184
79	291	10	95	733	32	422
81	443	30	246	1066	52	756
83	226	14	30	339	39	28
85	210	11	14	589	57	278
87	202	16	6	418	33	107
89	205	7	8	311	34	0
91	237	37	41	326	32	16
92	195	7	-1	394	32	83
93	241	9	45	289	13	-22
94	207	10	10	298	23	-13
95	787	17	591	1011	26	700
96	486	10	290	526	32	215
97	478	21	281	762	55	451
123	204	17	7	339	21	28

Slide number	Slide 2			Slide 5		
Slide detail	SI2 ND7 Track 0			SI2 ND7 Track G		
Filter used	Cy3			FITC		
PU	F	CV	F-B	F	CV	F-B
159	1045	16	848	1930	48	1619
160	453	19	257	1041	32	730
161	641	5	445	1650	26	1339
162	304	18	108	857	65	546
163	206	5	9	335	24	24
164	404	13	208	728	12	417
165	513	21	317	1400	16	1089
166	538	33	341	577	39	266
167	240	11	43	540	67	230
168	393	14	197	1392	51	1082
169	216	17	19	552	37	241
170	221	6	24	482	46	171
171	239	11	42	417	33	106
172	299	28	102	429	32	118
174	491	9	295	411	48	100
175	208	5	12	278	39	-32
176	191	5	-5	436	29	125
177	1205	3	1009	3440	52	3129
178	221	6	24	365	7	55
179	224	6	28	770	22	459
180	241	3	44	652	110	341
181	197	11	0	391	65	80
182	1211	19	1014	4612	79	4302
183	456	29	259	803	72	492
184	385	29	189	878	34	567
185	636	32	439	3056	39	2745
186	392	26	195	520	20	209
187	193	4	-4	260	18	-51
188	192	8	-5	271	49	-40
189	304	7	107	826	37	516
190	732	20	536	1762	29	1452
191	232	18	36	390	33	80
192	231	22	34	383	55	72
193	833	18	637	2628	26	2317
194	1261	19	1065	3092	64	2781
195	1451	30	1255	2029	28	1719
196	385	8	189	1024	20	713
197	201	8	5	416	41	105
198	242	11	46	268	14	-43
199	242	16	46	389	39	78
200	878	10	682	3256	43	2945
201	190	8	-7	416	10	105
202	209	4	12	324	22	13
203	848	9	652	1246	7	935
204	310	5	114	708	48	398
205	251	14	55	230	10	-81
206	673	29	476	1671	35	1360
207	379	34	183	522	41	211
208	852	18	656	1777	42	1466
209	312	24	116	756	77	445
210	901	24	705	1956	14	1646
211	1016	19	819	1467	29	1156
212	187	2	-9	238	20	-73
213	246	11	49	499	53	188
214	929	14	733	1007	27	696
215	340	62	143	238	17	-73
216	197	5	1	317	41	6
217	754	15	558	2006	12	1696
Mean Background	196			311		
Mean CV		15			34	

Table 6.7 *Effect of the stain on cellular adhesion. F: integrated mean fluorescence intensities, CV: calculated coefficient of variance, F-B: background corrected mean fluorescence intensities.*

Slide number	Slide 2			Slide 4			Slide 6			Slide 6		
Slide detail	Sl2 ND7 Track 0			Sl2 B16F10 Track G			Sl1 ND7 + B16F10			Sl1 ND7 + B16F10		
Filter used	Cy3			FITC			FITC			Cy3		
PU	F	CV	F-B	F	CV	F-B	F	CV	F-B	F	CV	F-B
3	313	46	116	227	17	21	232	6	10	481	30	282
4	199	15	3	314	24	108	266	29	45	194	10	-5
8	186	4	-10	220	16	14	234	11	13	206	6	7
9	215	24	19	330	42	124	293	21	72	236	22	37
10	233	5	37	299	37	94	212	11	-9	188	6	-10
12	627	24	430	232	18	27	418	20	197	521	10	322
13	204	7	7	198	4	-7	217	10	-4	200	4	1
14	176	4	-20	227	24	22	255	37	34	180	6	-19
15	214	4	17	236	14	31	221	9	0	207	6	8
16	439	31	242	261	40	55	297	9	76	397	10	199
17	210	7	14	202	2	-4	300	38	79	217	6	18
18	461	2	265	217	12	12	308	48	86	327	12	128
19	229	3	33	625	114	419	249	25	28	217	12	18
20	259	35	62	569	55	364	226	9	5	188	5	-11
22	223	16	27	258	24	52	221	4	0	225	8	26
23	219	6	22	275	29	69	228	4	7	269	8	70
24	231	5	35	405	58	199	228	7	7	246	11	47
25	220	12	24	374	54	168	291	25	69	227	7	28
28	203	7	6	208	4	2	219	6	-3	264	25	66
29	483	27	287	1061	50	855	537	64	316	458	30	260
30	215	10	18	826	89	620	273	20	52	220	3	21
31	212	5	16	224	6	18	238	10	17	220	10	21
33	225	4	29	206	13	0	245	38	24	188	4	-10
35	227	5	30	220	22	14	232	17	11	225	10	26
37	261	40	65	568	62	363	330	26	109	258	16	60
38	199	11	3	347	47	141	286	31	65	173	4	-25
40	186	6	-11	309	17	104	247	17	26	187	5	-11
41	244	16	47	206	7	1	250	30	29	198	13	-1
43	451	29	255	291	19	85	259	28	38	345	48	147
45	223	12	27	191	6	-14	246	27	25	293	21	94
46	232	12	36	191	7	-15	196	3	-25	194	3	-5
47	193	16	-3	300	64	94	339	40	118	192	12	-7
48	215	9	19	335	55	129	247	21	26	198	19	-1
49	199	2	2	282	25	76	215	9	-6	193	8	-6
50	212	5	16	456	40	251	309	20	88	235	16	37
53	245	22	49	201	6	-5	263	35	42	306	16	107
55	584	33	388	219	8	14	269	23	47	456	6	257
57	214	9	18	378	44	172	339	33	118	235	10	36
59	263	25	67	771	63	566	408	23	187	283	19	84
61	244	9	47	196	2	-10	225	19	4	206	2	7
63	345	6	148	215	9	9	243	12	22	294	9	95
65	857	10	660	949	32	744	342	28	121	732	20	533
67	221	11	25	326	28	121	342	25	120	248	25	49
69	266	22	69	1001	28	795	401	46	180	229	15	30
71	200	8	4	191	7	-15	199	14	-22	212	11	13
73	206	11	10	222	27	16	215	12	-7	173	4	-26
77	210	8	14	383	35	177	228	13	7	212	16	13
79	291	10	95	992	16	786	346	17	125	260	27	62
81	443	30	246	217	22	11	229	21	8	275	15	76
83	226	14	30	303	45	97	196	2	-25	195	10	-4
85	210	11	14	354	35	149	286	19	65	208	8	9
87	202	16	6	275	29	69	226	21	5	176	8	-22
89	205	7	8	522	122	316	223	22	1	192	7	-6
91	237	37	41	242	11	36	242	33	20	172	9	-26
92	195	7	-1	378	28	173	280	23	59	214	21	15
93	241	9	45	398	45	192	260	7	39	215	9	17
94	207	10	10	211	22	5	194	5	-27	176	8	-22
95	787	17	591	736	67	530	735	43	514	558	17	359
96	486	10	290	1331	64	1126	787	28	565	497	9	298
97	478	21	281	1037	68	832	692	53	471	322	40	124
123	204	17	7	210	5	4	239	17	17	203	4	4

Slide number	Slide 2			Slide 4			Slide 6			Slide 6		
Slide detail	SI2 ND7 Track 0			SI2 B16F10 Track G			SI1 ND7 + B16F10			SI1 ND7 + B16F10		
Filter used	Cy3			FITC			FITC			Cy3		
PU	F	CV	F-B	F	CV	F-B	F	CV	F-B	F	CV	F-B
159	1045	16	848	873	57	667	647	69	426	695	14	496
160	453	19	257	245	19	39	365	72	143	340	23	141
161	641	5	445	1356	21	1150	811	39	590	476	16	277
162	304	18	108	475	30	270	671	63	450	411	28	212
163	206	5	9	222	10	16	259	29	38	201	19	2
164	404	13	208	838	63	632	556	55	335	438	19	239
165	513	21	317	317	36	111	401	39	180	390	10	191
166	538	33	341	359	35	153	555	69	334	325	33	127
167	240	11	43	511	34	306	505	24	284	277	10	79
168	393	14	197	1081	43	875	598	44	377	451	27	253
169	216	17	19	218	14	12	216	6	-5	201	12	2
170	221	6	24	260	12	54	235	13	14	200	10	2
171	239	11	42	287	26	81	380	11	159	248	27	49
172	299	28	102	510	33	304	369	34	147	215	13	16
174	491	9	295	511	54	305	425	31	203	319	11	120
175	208	5	12	201	5	-5	235	20	14	208	7	9
176	191	5	-5	242	15	36	240	9	19	193	6	-6
177	1205	3	1009	1338	18	1132	795	60	574	611	18	413
178	221	6	24	244	12	38	252	5	31	218	5	19
179	224	6	28	432	75	226	317	26	96	231	8	33
180	241	3	44	211	9	5	226	12	5	196	10	-3
181	197	11	0	252	21	46	257	23	36	222	11	23
182	1211	19	1014	2794	12	2588	1044	58	823	853	12	654
183	456	29	259	724	17	519	685	51	464	398	28	199
184	385	29	189	995	17	789	371	24	149	243	9	44
185	636	32	439	1341	20	1135	513	48	292	516	10	317
186	392	26	195	723	47	517	293	38	72	188	0	-10
187	193	4	-4	189	9	-17	270	36	49	200	13	1
188	192	8	-5	196	4	-10	201	20	-20	192	5	-7
189	304	7	107	533	34	328	308	9	87	235	10	36
190	732	20	536	1045	21	839	344	39	123	451	28	252
191	232	18	36	577	75	372	373	47	152	222	9	23
192	231	22	34	294	47	89	232	14	11	203	8	4
193	833	18	637	857	36	651	379	40	158	517	9	318
194	1261	19	1065	1566	24	1360	971	20	750	716	14	517
195	1451	30	1255	1452	12	1246	750	47	529	550	16	352
196	385	8	189	1821	39	1615	549	40	328	370	21	172
197	201	8	5	260	17	54	244	33	23	187	8	-12
198	242	11	46	426	58	220	229	16	8	192	6	-6
199	242	16	46	197	5	-9	257	22	36	207	9	8
200	878	10	682	2667	37	2461	1103	72	882	749	17	551
201	190	8	-7	323	42	117	240	14	19	226	12	28
202	209	4	12	185	5	-21	233	35	12	182	6	-17
203	848	9	652	758	26	552	276	14	55	540	7	341
204	310	5	114	637	73	431	282	10	61	239	5	40
205	251	14	55	438	90	233	193	4	-28	207	4	9
206	673	29	476	926	20	721	403	34	182	418	14	219
207	379	34	183	320	18	114	370	48	149	282	37	83
208	852	18	656	1759	20	1554	605	75	384	671	12	472
209	312	24	116	544	44	338	356	48	135	298	18	99
210	901	24	705	1024	50	818	661	48	440	575	13	376
211	1016	19	819	410	28	205	553	52	332	660	32	462
212	187	2	-9	238	25	33	195	9	-26	184	6	-14
213	246	11	49	337	49	132	275	29	53	225	10	27
214	929	14	733	1189	22	983	783	39	562	521	22	322
215	340	62	143	414	45	208	446	27	225	224	15	25
216	197	5	1	210	6	4	231	24	10	201	7	3
217	754	15	558	1633	42	1428	455	59	234	465	22	266
Mean Background	196			206			221			199		
Mean CV		15			32			28			13	

Table 6.8 *Multiplexing of cellular adhesion. F: integrated mean fluorescence intensities, CV: calculated coefficient of variance, F-B: background corrected mean fluorescence intensities.*

6.3.3 Applications of cell adhesion screening

The preparation of human primary renal tubular epithelial cells and incubation with polymer microarrays were carried out by Sara Campbell in the Renal Group (University of Southampton, School of Medicine).

Macroscopically normal kidney tissue was obtained following nephrectomy for renal cell carcinoma. Cortical tissue (2.0-5.0 g) was taken into chilled DMEM/Ham's F12 media containing penicillin (200 units.mL^{-1}), streptomycin (200 mg.mL^{-1}) and finely chopped using cross blades. The chopped tissue was washed three times with the above media with centrifugation (250 x g) between washes, before being subjected to enzymatic digestion in an orbital incubator (1 hour @ 37 °C) using collagenase type IV (0.10 % w/v, Worthington, Lorne Laboratories) in PBS. The disaggregated cell mixture was centrifuged at 250 x g for 5 min. The resulting cell pellet was resuspended in media and passed sequentially through 70 and 40 μm sieves. After further centrifugation at 250 g for 5 minutes, the cell pellet was resuspended at a density of 10^5 cells.mL^{-1} in a fully defined DMEM/Ham's F12 medium containing glutamine (2.0 mmol), penicillin (100 units.mL^{-1}), streptomycin (100 mg.mL^{-1}), epithelial growth factor (EGF) (10 ng.mL^{-1}), hydrocortisone (36 ng.mL^{-1}), human insulin (5.0 μg.mL^{-1}), prostaglandin-E_1 (PGE_1) (10 ng.mL^{-1}), sodium selanite (5.0 ng.mL^{-1}), iron loaded transferrin (5.0 μg.mL^{-1}) and tri-iodothyronine (T_3) (5.0 pg.mL^{-1}) in 25 cm^2 filtered culture flasks and incubated at 37 °C with 5 % CO_2. Cultures were inspected on a daily basis and the media changed every 48 h until grown to confluence. At confluence the cultures were passaged using trypsin (0.050 % w/v), EDTA (0.20 % w/v) in PBS and, after washing with PBS-containing trypsin inhibitor (0.15 % w/v, Sigma-Aldrich) the cells were resuspended (1.0 x 10^5 cells/slide) in the growth media on the polymer slides. The growth media was changed every 48 h and the cells were incubated onto polymer arrays for a total of 5 days. Following washing in PBS, the cells were fixed in *p*-formaldehyde (3.7 % w/v) for 15 min, permeabilised with Triton-X 100 (0.10 % v/v) for 2 min and washed 3 times in PBS. The slides were blocked with goat serum (5.0 % v/v in PBS) and incubated with CAM5-2 (low molecular weight cytokeratin) monoclonal antibody (Cambridge Bioscience) overnight at 4 °C and visualised using an AlexaFluor® 488 labelled IgG

antibody (Molecular Probes, Invitrogen) for 30 min. The cell nuclei were stained with Hoechst 33342 (0.050 $\mu g.mL^{-1}$, Sigma-Aldrich) for 10 min. The analysis was carried out using the high resolution HCS platform (x20 objective) and the Pathfinder™ software.

PU-	Polyol	Polyol MW (Da)	Dis.	Ext.	x (Polyol)	x (Dis)	x (Ext)	Average number of epithelial cells	Standard deviation
3	PEG	400	HDI	none	0.485	0.515	0.000	0.3	0.5
4	PPG	2000	HDI	none	0.485	0.515	0.000	1.8	1.7
8	PEG	400	BICH	none	0.485	0.515	0.000	0.0	0.0
9	PPG	2000	BICH	none	0.485	0.515	0.000	11.5	2.9
10	PTMG	2000	BICH	none	0.485	0.515	0.000	3.5	2.6
12	PEG	900	TDI	none	0.485	0.515	0.000	19.3	8.3
13	PEG	400	TDI	none	0.485	0.515	0.000	37.0	23.3
14	PPG	2000	TDI	none	0.485	0.515	0.000	23.3	18.5
15	PTMG	2000	TDI	none	0.485	0.515	0.000	29.3	14.2
16	PEG	2000	MDI	none	0.485	0.515	0.000	0.0	0.0
17	PEG	900	MDI	none	0.485	0.515	0.000	16.8	10.8
18	PEG	400	MDI	none	0.485	0.515	0.000	143.5	41.3
19	PPG	2000	MDI	none	0.485	0.515	0.000	63.5	20.0
20	PTMG	2000	MDI	none	0.485	0.515	0.000	64.8	10.9
22	PEG	900	PDI	none	0.485	0.515	0.000	2.3	2.9
23	PEG	400	PDI	none	0.485	0.515	0.000	87.3	19.7
24	PPG	2000	PDI	none	0.485	0.515	0.000	30.0	14.3
25	PTMG	2000	PDI	none	0.485	0.515	0.000	17.8	14.7
28	PEG	400	HMDI	none	0.485	0.515	0.000	2.8	3.6
29	PPG	2000	HMDI	none	0.485	0.515	0.000	1.0	0.8
30	PTMG	2000	HMDI	none	0.485	0.515	0.000	3.5	4.4
31	PEG	2000	HDI	BD	0.250	0.520	0.230	0.0	0.0
33	PEG	900	HDI	BD	0.250	0.520	0.230	0.3	0.5
35	PEG	400	HDI	BD	0.250	0.520	0.230	8.5	3.7
37	PPG	2000	HDI	BD	0.250	0.520	0.230	23.0	6.8
38	PPG	2000	HDI	ED	0.250	0.520	0.230	0.0	0.0
40	PTMG	2000	HDI	ED	0.250	0.520	0.230	0.0	0.0
41	PEG	2000	BICH	BD	0.250	0.520	0.230	0.0	0.0
43	PEG	900	BICH	BD	0.250	0.520	0.230	0.0	0.0
45	PEG	400	BICH	BD	0.250	0.520	0.230	0.8	1.5
46	PEG	400	BICH	ED	0.250	0.520	0.230	12.5	3.7
47	PPG	2000	BICH	BD	0.250	0.520	0.230	16.5	12.6
48	PPG	2000	BICH	ED	0.250	0.520	0.230	6.5	6.2
49	PTMG	2000	BICH	BD	0.250	0.520	0.230	41.3	30.5
50	PTMG	2000	BICH	ED	0.250	0.520	0.230	48.0	55.6
53	PEG	900	TDI	BD	0.250	0.520	0.230	0.3	0.5
55	PEG	400	TDI	BD	0.250	0.520	0.230	54.5	21.0
57	PPG	2000	TDI	BD	0.250	0.520	0.230	101.8	32.1
59	PTMG	2000	TDI	BD	0.250	0.520	0.230	121.8	45.3
61	PEG	2000	MDI	BD	0.250	0.520	0.230	5.0	3.2
63	PEG	900	MDI	BD	0.250	0.520	0.230	23.0	12.6
65	PEG	400	MDI	BD	0.250	0.520	0.230	79.0	23.2
67	PPG	2000	MDI	BD	0.250	0.520	0.230	83.5	22.9
69	PTMG	2000	MDI	BD	0.250	0.520	0.230	61.5	20.0
71	PEG	2000	PDI	BD	0.250	0.520	0.230	0.0	0.0
73	PEG	900	PDI	BD	0.250	0.520	0.230	0.0	0.0
77	PPG	2000	PDI	BD	0.250	0.520	0.230	64.8	74.8
79	PTMG	2000	PDI	BD	0.250	0.520	0.230	30.5	15.2
81	PEG	2000	HMDI	BD	0.250	0.520	0.230	0.0	0.0
83	PEG	900	HMDI	BD	0.250	0.520	0.230	1.0	2.0
85	PEG	400	HMDI	BD	0.250	0.520	0.230	103.8	29.4
87	PPG	2000	HMDI	BD	0.250	0.520	0.230	11.8	20.2
89	PTMG	2000	HMDI	BD	0.250	0.520	0.230	24.8	20.6
91	PTMG	650	HDI	BD	0.485	0.515	0.000	2.0	3.4
92	PTMG	1000	HDI	BD	0.485	0.515	0.000	41.0	35.4
93	PTMG	650	BICH	BD	0.485	0.515	0.000	5.0	4.2
94	PTMG	1000	BICH	BD	0.485	0.515	0.000	24.8	17.9
95	PTMG	650	MDI	BD	0.485	0.515	0.000	45.5	20.4
96	PTMG	1000	MDI	BD	0.485	0.515	0.000	83.3	18.2

PU-	Polyol	Polyol MW (Da)	Dis.	Ext.	x (Polyol)	x (Dis)	x (Ext)	Average number of epithelial cells	Standard deviation
97	PHNGAD	1800	BICH	DMAPD	0.250	0.520	0.230	18.5	12.1
123	PPG	2000	MDI	DMAPD	0.250	0.520	0.230	2.0	1.2
158	PTMG	250	MDI	OFHD	0.250	0.520	0.230	7.8	9.7
159	PTMG	250	MDI	BD	0.250	0.520	0.230	108.5	27.0
160	PTMG	250	MDI	EG	0.250	0.520	0.230	132.5	18.0
161	PTMG	650	MDI	EG	0.250	0.520	0.230	150.3	21.8
162	PTMG	1000	MDI	EG	0.250	0.520	0.230	83.3	31.8
163	PTMG	2000	MDI	EG	0.250	0.520	0.230	106.3	44.9
164	PTMG	250	MDI	PG	0.250	0.520	0.230	119.5	35.4
165	PTMG	650	MDI	PG	0.250	0.520	0.230	144.3	4.3
166	PTMG	1000	MDI	PG	0.250	0.520	0.230	85.0	32.5
167	PTMG	2000	MDI	PG	0.250	0.520	0.230	74.3	22.1
168	PTMG	250	BICH	none	0.485	0.515	0.000	59.3	50.3
169	PTMG	650	BICH	none	0.485	0.515	0.000	0.8	1.0
170	PTMG	1000	BICH	none	0.485	0.515	0.000	0.0	0.0
171	PTMG	250	HDI	none	0.485	0.515	0.000	81.8	24.8
172	PTMG	650	HDI	none	0.485	0.515	0.000	77.8	48.4
174	PTMG	250	MDI	none	0.485	0.515	0.000	59.8	55.7
175	PTMG	650	MDI	none	0.485	0.515	0.000	106.0	17.8
176	PTMG	1000	MDI	none	0.485	0.515	0.000	94.0	15.8
177	PTMG	250	HDI	NMPD	0.250	0.520	0.230	113.0	8.8
178	PTMG	1000	HDI	NMPD	0.250	0.520	0.230	109.8	14.3
179	PTMG	2000	HDI	NMPD	0.250	0.520	0.230	22.3	16.9
180	PTMG	1000	BICH	NMPD	0.250	0.520	0.230	31.0	24.8
181	PTMG	2000	BICH	NMPD	0.250	0.520	0.230	30.0	19.7
182	PTMG	650	MDI	NMPD	0.250	0.520	0.230	142.3	18.3
183	PTMG	1000	MDI	NMPD	0.250	0.520	0.230	95.3	29.7
184	PTMG	2000	MDI	NMPD	0.250	0.520	0.230	132.3	9.9
185	PHNAD	900	MDI	OFHD	0.170	0.520	0.330	3.0	1.6
186	PTMG	650	BICH	OFHD	0.250	0.520	0.230	29.8	32.7
187	PTMG	1000	BICH	OFHD	0.250	0.520	0.230	80.3	58.4
188	PTMG	2000	BICH	OFHD	0.250	0.520	0.230	5.5	3.1
189	PPG	1000	BICH	OFHD	0.170	0.520	0.330	7.5	8.7
190	PTMG	650	HDI	OFHD	0.250	0.520	0.230	59.0	59.3
191	PTMG	1000	HDI	OFHD	0.250	0.520	0.230	106.5	16.5
192	PTMG	2000	HDI	OFHD	0.250	0.520	0.230	80.8	26.5
193	PPG	1000	MDI	DMAPD	0.170	0.520	0.330	133.5	22.0
194	PTMG	650	MDI	OFHD	0.250	0.520	0.230	55.8	19.7
195	PTMG	1000	MDI	OFHD	0.250	0.520	0.230	141.0	40.1
196	PTMG	2000	MDI	OFHD	0.250	0.520	0.230	117.5	23.6
197	PTMG	650	BICH	DHM	0.250	0.520	0.230	9.3	11.5
198	PTMG	1000	BICH	DHM	0.250	0.520	0.230	19.8	18.1
199	PTMG	2000	BICH	DHM	0.250	0.520	0.230	70.5	9.7
200	PTMG	650	HDI	DHM	0.250	0.520	0.230	135.8	1.3
201	PTMG	1000	HDI	DHM	0.250	0.520	0.230	104.0	17.6
202	PTMG	2000	HDI	DHM	0.250	0.520	0.230	20.3	26.9
203	PTMG	650	MDI	DHM	0.250	0.520	0.230	46.3	32.0
204	PTMG	1000	MDI	DHM	0.250	0.520	0.230	88.3	14.2
205	PTMG	2000	MDI	DHM	0.250	0.520	0.230	69.3	2.6
206	PPG	1000	HDI	OFHD	0.250	0.520	0.230	25.3	33.2
207	PPG	1000	BICH	OFHD	0.250	0.520	0.230	3.8	7.5
208	PPG	1000	MDI	OFHD	0.250	0.520	0.230	42.0	35.2
209	PPG	1000	HDI	PG	0.250	0.520	0.230	64.5	12.7
210	PPG	1000	BICH	PG	0.250	0.520	0.230	9.5	4.8
211	PPG	1000	MDI	PG	0.250	0.520	0.230	79.8	25.7
212	PHNAD	900	HDI	PG	0.250	0.520	0.230	125.8	17.5
213	PHNAD	900	BICH	PG	0.250	0.520	0.230	12.8	21.6
214	PHNAD	900	MDI	PG	0.250	0.520	0.230	93.3	24.7
215	PHNAD	900	HDI	BD	0.250	0.520	0.230	21.5	23.1
216	PHNAD	900	BICH	BD	0.250	0.520	0.230	1.3	1.5
217	PHNAD	900	MDI	BD	0.250	0.520	0.230	153.0	28.5

Table 6.9 *List of screened polymers with monomer composition; average number and standard deviation of the human renal tubular epithelial cell bound to each polymer (average of 4 polymer spots).Dis.: diisocyanate; Ext.: chain extender.*

6.3.4 Immobilisation of non-adherent cells

6.3.4.1 Initial investigation

Non-adherent cell lines (JURKAT, RMA-S and JY, kindly provided by Salim Khakoo, Cancer Research, Southampton, UK) were grown in RPMI 1640 growth medium supplemented with heat inactivated fetal calf serum (10 % v/v), penicillin (100 units.mL^{-1}), streptomycin (100 mg.mL^{-1}) and L-glutamine (4.0 mM) at 37 °C with 5 % CO_2. Cells were stained with CellTracker™ Green according to the manufacturer's protocols. Prior to seeding onto the polymer array, cells were resuspended in growth medium (3.0 x 10^6 cells/slide in 15 mL). The slides were subsequently placed in an incubator (24 h @ 37°C, 5% CO_2). After a controlled washing in PBS (30 mL, 2 min shaking on a microplate shaker at 600 rpm), the cells were fixed in an aqueous solution of *p*-formaldehyde and sucrose (3.7 % w/v and 4.0 % w/v, respectively) for 15 min, rinsed and stored in PBS at 4 °C. Image capture was carried out with a BioAnalyzer 4F/4S white light scanner using the FITC filter.

Slide number	Slide 1			Slide 2		
Slide detail	JY Track G			RMA-S Track G		
Filter used	FITC			FITC		
PU	F	CV	F-B	F	CV	F-B
3	300	2	6	683	17	444
4	314	1	20	676	15	437
8	307	6	13	528	27	289
9	399	17	105	508	17	269
10	320	8	26	746	19	507
12	318	4	24	807	9	568
13	294	3	0	479	17	240
14	291	1	-3	412	6	173
15	328	20	34	806	14	567
16	304	3	10	748	29	509
17	298	6	3	273	17	34
18	299	3	5	301	6	62
19	327	8	33	782	16	543
20	314	4	20	745	9	506
22	303	5	9	483	9	244
23	311	3	17	326	11	87
24	342	27	48	674	26	435
25	284	5	-10	422	24	183
28	280	3	-14	351	15	112
29	781	49	487	326	12	87
30	290	7	-4	466	32	227
31	286	5	-8	399	7	160
33	304	2	9	332	14	93
35	358	24	64	243	3	4
37	534	32	240	479	23	240
38	344	6	50	670	15	432
40	318	4	23	465	14	226
41	310	7	16	453	11	214
43	291	2	-3	469	5	230
45	289	2	-5	315	14	76
46	294	7	0	290	16	51
47	296	1	1	399	12	160
48	315	13	21	783	23	544
49	291	2	-3	704	14	465
50	289	5	-5	495	14	256
53	283	3	-11	352	24	114
55	319	3	25	394	24	155
57	709	20	415	485	20	246
59	290	4	-4	407	6	168
61	321	29	27	231	3	-7
63	291	2	-3	285	15	46
65	320	1	26	286	21	47
67	415	28	121	429	10	190
69	286	3	-9	364	13	125
71	302	1	8	329	10	90
73	298	5	4	262	7	23
77	397	27	103	607	14	368
79	291	4	-3	423	19	184
81	340	4	46	377	21	138
83	317	4	22	247	2	8
85	300	3	5	557	26	318
87	440	36	146	390	8	151
89	338	14	44	571	13	332
91	309	2	15	349	25	110
92	316	3	22	354	9	115
93	324	6	30	413	10	174
94	287	5	-7	604	22	365
95	470	1	176	306	4	67
96	538	50	244	271	4	32
97	355	5	61	546	8	307
123	292	6	-2	414	21	175

Slide number	Slide 1			Slide 2		
Slide detail	JY Track G			RMA-S Track G		
Filter used	FITC			FITC		
PU	F	CV	F-B	F	CV	F-B
159	391	33	97	253	5	14
160	280	4	-15	299	15	61
161	582	32	288	250	9	11
162	281	3	-13	401	23	162
163	274	2	-20	510	25	271
164	295	9	0	260	6	21
165	362	27	68	242	3	3
166	472	28	178	289	10	50
167	435	57	141	511	22	273
168	306	17	12	332	11	93
169	313	8	19	448	25	209
170	291	12	-3	522	19	283
171	414	14	120	300	10	61
172	296	11	2	476	7	237
174	364	15	70	344	22	105
175	293	6	-1	526	11	287
176	302	6	8	404	16	165
177	399	47	104	272	7	33
178	314	5	20	465	14	226
179	324	6	30	439	5	201
180	300	13	6	582	14	343
181	389	34	95	482	6	243
182	409	43	114	255	3	16
183	563	41	269	274	5	35
184	323	19	29	412	24	173
185	439	33	145	436	14	197
186	332	34	38	534	22	295
187	373	18	79	599	28	360
188	332	20	38	404	17	165
189	343	33	49	315	16	76
190	361	18	67	412	29	173
191	276	2	-18	542	19	303
192	280	2	-14	521	13	282
193	553	4	259	359	11	121
194	500	67	205	261	1	22
195	567	52	273	298	6	59
196	355	11	61	360	19	121
197	296	12	2	275	15	36
198	287	2	-8	458	23	219
199	280	2	-14	467	16	228
200	629	52	335	254	3	15
201	573	40	279	375	12	136
202	265	7	-29	442	40	203
203	393	21	99	246	1	7
204	710	44	416	329	10	90
205	275	2	-19	371	15	132
206	414	18	120	274	13	35
207	833	23	539	341	9	102
208	466	52	172	414	17	175
209	376	37	82	311	15	72
210	751	60	457	309	17	70
211	498	31	204	391	20	152
212	288	9	-6	331	5	93
213	302	7	7	365	23	126
214	361	30	67	293	11	54
215	436	36	142	245	11	6
216	285	3	-9	-252	23	252
217	467	33	173	239	3	0
Mean Background	294			239		
Mean CV		16			14	

Table 6.10 *Immobilisation of non-adherent cell lineages. F: integrated mean fluorescence intensities, CV: calculated coefficient of variance, F-B: background corrected mean fluorescence intensities.*

6.3.4.2 Immobilisation of mouse Bone Marrow Dendritic Cells

The preparation of bone marrow dendritic cells, incubation with polymer microarrays and phagocytosis assay and analyses were carried out by Dr. Alexandra Mant in Cancer Research (University of Southampton, School of Medicine). The polymer microarray preparation and analysis, together with the polymer-coated coverslip preparation were carried out by G. Tourniaire in the University of Edinburgh (Department of Chemistry).

Preparation of primary murine bone marrow-derived dendritic cells:

Bone marrow-derived dendritic cells (BMDC) were purified from the femurs of 8-12 weeks old C57BL/6 mice, according to the method of Lutz *et al.*[234] and were used on day 10 of *in vitro* culture.

BMDC polymer microarray adhesion assay:

BMDC were stained with carboxyfluorescein succinimidyl ester (5.0 μM, CFSE, Molecular Probes, Invitrogen) to monitor cell adhesion as follows: an aliquot of cells (4.0×10^6) was centrifuged (5 min @ 20 °C, 300 x *g*) and washed once with PBS before resuspension in PBS (1.0 mL) containing CFSE (5 μM) and incubating for 10 min at room temperature in the dark. After staining, the cells were centrifuged (5 min @ 20 °C, 300 x *g*) and gently resuspended in cell culture medium (1.0 mL), R10: RPMI 1640 (Gibco, Invitrogen) supplemented with penicillin (100 units.mL^{-1}), streptomycin (100 μg.mL^{-1}) and L-glutamine (2.0 mM), 2-mercaptoethanol (50 μM, Sigma-Aldrich) and heat-inactivated and filtered low endotoxin foetal calf serum (10 % v/v, Autogen Bioclear). The cells were gently pipetted onto the surface of a polymer microarray contained in sterile Petri dish. A further 20 mL R10 was carefully added to the dish and was subsequently incubated (2 h @ 37 °C, 5 % CO_2). After gentle washing with R10 and then PBS, the cells were fixed with formaldehyde (4.0 % w/v) in PBS for 15 min at room temperature, then rinsed and stored in PBS at 4 °C. Adhesion was checked using a Zeiss Axiovert 200 fluorescence microscope. For precise quantification of cell adhesion, the fixed cells were further stained with a solution of DAPI (0.50 μg.mL^{-1}) for 15 min at room temperature. Slides were rinsed and stored in PBS at 4 °C. Image capture and

analyses were carried out using the high resolution HCS platform (x10 objective) and the Pathfinder™ software. Cell compatibility with the different polymers was determined by counting of the number of cells present on each spot using both the DAPI and FITC channels (**Table 6.11**).

PU	Average number of immobilised BMDC	PU	Average number of immobilised BMDC	PU	Average number of immobilised BMDC
3	1	63	0	178	1
4	1	65	6	179	1
8	0	67	3	180	1
9	0	69	1	181	6
10	0	71	0	182	8
12	1	73	1	183	0
13	0	77	4	184	1
14	0	79	1	185	0
15	2	81	0	186	2
16	0	83	1	187	3
17	1	85	1	188	2
18	0	87	1	189	2
19	3	89	1	190	5
20	2	91	5	191	6
22	1	92	4	192	0
23	0	93	3	193	5
24	0	94	0	194	7
25	3	95	8	195	6
28	1	96	7	196	5
29	2	97	5	197	3
30	1	123	0	198	0
31	0	158	4	199	0
33	4	159	12	200	4
35	1	160	3	201	6
37	0	161	3	202	0
38	1	162	5	203	1
40	1	163	3	204	2
41	1	164	4	205	0
43	0	165	8	206	0
45	1	166	14	207	0
46	1	167	1	208	2
47	3	168	0	209	1
48	0	169	2	210	1
49	2	170	2	211	0
50	2	171	4	212	2
53	1	172	1	213	2
55	1	174	11	214	2
57	6	175	5	215	2
59	4	176	1	216	0
61	1	177	8	217	3

Table 6.11 *BMDC adhesion assay on polymer microarray*

Polymer coating of coverslips:

Prior to spin coating on a P6708 spin coater (Speedlines Technologies), glass cover slips (22 mm diameter, CB00220RA1, Menzel-Gläser) were cleaned with tetrahydrofuran (THF). 50 µL of the polymer solutions (2.0 % w/v in THF) was placed onto the coverslips and spun for 10 s at 2000 rpm. Coverslips were dried under vacuum (12 h @ 45 °C / 200 mbar) and irradiated with UV light for 20 min before use.

Phagocytosis assay:

Coverslips coated with polymer PU159, PU166 or PU174, or poly-L-lysine solution (0.01 % w/v, Sigma histology grade or Sigma tissue culture grade, Sigma-Aldrich, Dorset, UK), or uncoated (incubated with PBS alone), were sterilised by UV light for 15 min in the bottom of a 6-well polystyrene culture plate (Greiner Bio-One). A drop of R10 containing BMDC (5.0×10^5 cells/coverslip in 0.50 mL) was pipetted into the centre of each coverslip, and the plate incubated (37 °C, 5 % CO_2) for the cells to adhere, taking care not to disturb the meniscus. After 30 min, a further 1.0 mL of R10 was added to each coverslip, containing 5.0 µL of 3.0 µm diameter sulphate latex microspheres (IDC Latex), pre-coated with passively adsorbed foetal calf serum proteins. The microspheres were brought into contact with the adhered cells by centrifuging the plate (3 min @ 20 °C, 200 *g*). The plate was then incubated (30min @ 37 °C, 5 % CO_2). After the incubation, the R10 was removed from the coverslips, which were rinsed briefly and gently with PBS, before being fixed with formaldehyde (4.0 % w/v) in PBS for 7 min at room temperature. The BMDC were permeabilised by incubating with Triton X-100 (0.1 % v/v) in PBS for 7 min at room temperature, then washed 3 times with PBS before being stained with rabbit anti-calnexin antibody (Stressgen) and goat anti-rabbit AlexaFluor® 488 secondary antibody (Molecular Probes, Invitrogen). Nuclei were stained with TO-PRO®-3 (Molecular Probes, Invitrogen).

Quantitation of phagocytosis:

Coverslips were examined using a Leica SP2 laser scanning confocal microscope with a x40 objective. Three independent experiments were carried out, in which each coverslip was represented in duplicate. Phagocytosis was quantified by counting the number of microspheres internalised and the number of cells in a randomly selected field of view. Internalised microspheres were those defined as surrounded by calnexin staining in all three dimensions (**Figure 3.7**). Figures for phagocytosis efficiency were derived from the counts of two to four fields of view per treatment, encompassing a minimum of 73 and a maximum of 556 cells (**Table 3.1**). The degree of adhesion was classified by comparing the number of cells present in four randomly selected fields of view for each treatment and checking that these were typical over the three independent experiments.

6.4 Experimental for Chapter 4

6.4.1 Selective enrichment of multipotent mesenchymal stromal cells (STRO-1+)

The preparation of unselected bone marrow mononuclear cell and STRO-1+ separation, culturing and plating was carried out by Dr. Rahul Tare in the Bone and Joint Research Group (University of Southampton, School of Medicine).

6.4.1.1 Unselected bone marrow mononuclear cells and STRO-1+ cells preparation

STRO-1+ cells were isolated using the magnetically activated cell sorting (MACS) technique described by Stewart and co-workers (1999)[208]. In brief, red blood cells were removed by centrifugation using lymphoprep solution (Robbins scientific). The cells from the buffy coat (bone marrow mononuclear cells) were resuspended in blocking solution (1.0×10^8 cells per 10 mL Hank's buffered saline solution (HBSS): HEPES (10 mM) with fetal calf serum (FCS, 5.0 % v/v), human normal AB serum (10 % v/v), and bovine serum albumin (BSA, 1.0 % w/v)), followed by incubation with the STRO-1 mouse monoclonal antibody (undiluted culture supernatant from the STRO-1 hybridoma, provided by Dr. J. Beresford, University of Bath). Cells were then incubated either with MACS anti-IgM beads (1:5 dilution, Miltenyi Biotech) or with the fluorescein (FITC)-conjugated AffiniPure $F(ab')_2$ fragment Goat anti-mouse IgM, μ chain specific (1:20 dilution, Jackson ImmunoResearch Laboratories Inc.), after washing the excess STRO-1 antibody with MACS buffer (HBSS, HEPES (10 mM) containing BSA (1.0 % w/v)). Cell suspensions incubated with the MACS anti-IgM beads were added to a column within the magnet and the STRO-1 negative fraction was eluted using the MACS buffer. Since the magnetically labelled STRO-1 positive cells were held in the column under the influence of the magnetic field. The column was washed to remove traces of the STRO-1 negative fraction and the STRO-1 positive fraction was then eluted in 1.0 mL MACS buffer in the absence of the magnet.

6.4.1.2 Polymer microarray printing

Polymer microarrays were prepared using the same sample and conditions as described in chapter 6.3.1.

6.4.1.3 Incubation on microarrays

STRO-1+ cells, isolated using MACS, and preparations of unselected bone marrow mononuclear cells containing FITC-labelled STRO-1+ cells were resuspended in α-MEM (1.5 mL / slide with 10 % v/v FCS) at densities of 5.0×10^5 and 1.0×10^7 cells respectively. The cell suspensions were directly plated onto polymer arrays and incubated (19h @ 37 °C, 5 % CO_2). MACS-isolated STRO-1+ cells bound to the polymers on the slide were fluorescently immunolabelled using STRO-1 mouse monoclonal primary antibody, followed by the (FITC)-conjugated AffiniPure $F(ab')_2$ fragment Goat anti-mouse IgM.

6.4.1.4 Coverslips coating

Polymer-coated coverslips were prepared using the same conditions as described in chapter 6.3.4.2 - *Polymer coating of coverslips* with the following samples: PU 16, 17 and 61.

6.4.1.5 Incubation on coverslips

Each polymer-coated coverslip was placed into a well of a 6-well plate and incubated (19h @ 37 °C, 5 % CO_2) with unselected bone marrow mononuclear cells (1.0×10^7 in 1.5 mL α-MEM with 10 % v/v FCS) containing either unlabelled or FITC-labelled STRO-1+ cells.

6.4.1.6 Washing, fixing and storing

Following incubation and thorough washing with PBS, cells were fixed in p-formaldehyde (4.0 % w/v in PBS) for 30 min, rinsed in PBS and nuclei were stained using Hoechst 33342 (0.50 $\mu g.mL^{-1}$ for 15 min, Sigma-Aldrich). Slides were stored in PBS at 4 °C, whereas coverslips were mounted in aqueous mounting medium (Aquatex®, R1329, Agar Scientific) and stored at 4 °C.

		PU 16	PU 17	PU 61
		% STRO-1+	% STRO-1+	% STRO-1+
Patient 1	Field 1	32	12	12
	Field 2	27	11	33
	Field 3	33	12	16
	Field 4	35	17	25
	Field 5	38	9	17
	Mean P1	**33**	**12**	**21**
Patient 2	Field 1	47	32	9
	Field 2	48	29	43
	Field 3	48	58	57
	Field 4	35	37	38
	Field 5	50	35	17
	Mean P2	**46**	**38**	**33**
Patient 3	Field 1	88	51	52
	Field 2	81	48	41
	Field 3	77	46	62
	Field 4	93	22	42
	Field 5	73	47	59
	Mean P3	**82**	**43**	**51**
	Overall Mean	**54**	**31**	**35**
	Standard Deviation	26	16	15
	Standard Error	15	9	9

Table 6.12 *Selective immobilisation of STRO-1+ cell on polymer-coated coverslip.*

6.4.2 Novel substrates for embryonic stem cells culture

6.4.2.1 Oct4-GFP cells culture

The cell line used throughout the study were modified murine embryonic stem cells named Oct4-GFP. This cell line is feeder-independent and was cultivated in the undifferentiated state on gelatine-coated (0.20 % v/v in PBS) tissue culture flasks (75 cm^2, Iwaki, Asahi Techno Glass). Cells were maintained in Glasgow minimum essential medium (GMEM, Sigma-Aldrich) containing minimum essential medium non-essential amino acids (0.1 mM), glutamine (2 mM), sodium pyruvate (1 mM), 2-mercaptoethanol (100 mM) and fetal calf serum (10 % v/v). This medium will be referred to as ESC medium. To maintain the pluripotent undifferentiated state *in vitro*, this medium was supplemented with leukaemia-inhibitory factor (LIF) (100 units.mL^{-1}). The cells were passaged every 48 h.

Initial experiments carried out using the microarray platform were carried out using ESC medium without antibiotics (penicilin and streptomycin). As a result of bacterial contamination issues in absence of antibiotics, the last experiments (on coverslips) were carried out using ESC medium supplemented with penicillin (100 units.mL^{-1}) and streptomycin (100 mg.mL^{-1}).

6.4.2.2 Polymer microarray printing

Polymer microarrays were prepared using the same conditions as described in section 6.3.1. However, with 32 aQu solid pins (K2785, Genetix), resulting in 124 poly(urethanes) printed in quadruplicate within 1 fields of 16 x 32 spots, with one pattern of 4 x 4 spots left empty.

6.4.2.3 Polymer microarray screen

A suspension of Oct4-GFP were plated (1.0 x 105 cells / slide in 15 mL ESC medium containing LIF) on top of the 14 polymer microarrays each in a different Petri dish (10 mm diameter). After 24 h, the medium was changed, half the slides were incubated with the same ESC medium containing LIF whereas the other half were incubated with ESC medium in absence of LIF. Subsequently, both media were changed every 48 h. At each time point, two slides (one cultivated in LIF medium and one without) were rinsed in PBS prior to fixing in *p*-formaldehyde (4.0 % w/v in PBS for 15 min). Analysis of adhesion and cellular phenotype (expression of GFP) was carried out manually using a fluorescent microscope.

PU	A	U	PU	A	U
3	×		160	×	
4	×		161	✓	
8	×		162	✓	
9	×		163	✓	
10	×		164	×	
12	×		165	×	
13	×		166	✓	
14	×		168	×	
15	×		169	×	
16	×		171	×	
17	×		172	✓	
18	×		174	✓	
19	×		175	✓	
20	×		176	×	
22	×		177	✓	
23	×		179	×	
24	×		180	×	
25	×		181	✓	
28	×		182	✓	
29	×		183	✓	
30	×		184	✓	
31	×		185	×	
33	×		186	✓	
35	×		187	×	
38	×		188	✓	
41	×		189	×	
43	✓		190	✓	✓
45	×		191	✓	
46	×		193	✓	
47	×		194	✓	
48	✓		195	✓	
49	×		196	✓	
50	×		197	✓	
53	×		198	×	
55	×		199	✓	
57	×		200	✓	
59	×		201	✓	
61	×		202	✓	
63	×		203	✓	
65	×		204	✓	
67	×		205	✓	
69	×		206	✓	✓
71	×		207	×	
73	×		208	✓	
77	×		209	✓	
79	✓		210	×	
81	×		211	×	
83	×		212	✓	
85	✓		213	×	
87	✓		214	✓	✓
89	×		215	✓	
93	✓		216	×	
94	×		217	✓	
95	×		218	✓	
96	✓		219	✓	
97	×		220	✓	
98	✓		221	✓	✓
99	✓		223	×	
100	✓		224	×	
101	✓		225	✓	
158	×		226	✓	
159	✓		229	×	

Table 6.13 *Immobilisation of Oct4-GFP on poly(urethane) microarrays.*
A: ✓ adhesion observed, × no adhesion observed

U: ✓ undifferentiated phenotype observed in absence of LIF in the growth medium.

6.4.2.4 Polymer coating of coverslips

Polymer-coated coverslips (19 mm diameter, CB00190RA1, Menzel-Gläser) were prepared using the conditions described previously (6.3.4.2 - *Polymer coating of coverslips*).

6.4.2.5 Coverslip screening by microscopy

Two of each polymer coated coverslips were placed in 12 well-plates (Iwaki, Asahi Techno Glass); the remaining two wells were used as controls and were coated with gelatine (0.20 % v/v in PBS). A total of three 12 well-plate was prepared. A suspension of Oct4-GFP was plated (1.0×10^4 cells / well in 2.0 mL ESC medium) in each well. Half the wells were incubated with medium containing LIF whereas the other half did not contain LIF. Both media were changed every 48 h. After 5, 7 and 9 days of incubation, respectively, the media were removed, the cells rinsed with PBS (2.0 mL / well), fixed in *p*-formaldehyde (1.0 mL / well, 4.0 % w/v in PBS for 15 min) and their nuclei stained with Hoechst 33342 (1.0 mL / well for 10 min, 0.5 $\mu g.mL^{-1}$). Each coverslip was mounted onto a microscope slide using Aquatex® (R1329, Agar Scientific) mounting medium. Cells growing on top of each coated coverslip were visualised using both DAPI and FITC channels of the high resolution HCS platform and Pathfinder™ software.

6.4.2.6 Clonal growth experiment

Two of each polymer coated coverslips were placed in 12 wells-plate, the remaining two wells were used as controls and were coated with gelatine (0.20 % v/v in PBS), a total of three 12 well-plate was prepared. A suspension of Oct4-GFP was plated (100 cells / well in 2.0 mL ESC medium) in each well. Half the wells were incubated with medium containing LIF whereas the other half did not contain LIF. Both media were changed every 48 h. After 9 days of culture, each colony was screened for alkaline phosphatase activity according to manufacturer protocol (leukocyte alkaline phosphatase kit, Sigma-Aldrich) and each colony was scored by microscopic examination.

A

	161		190		206		214		221		0.2 % gelatine	
	N	P	N	P	N	P	N	P	N	P	N	P
Plate 1	1	2.00	7	1.71	4	1.00	5	1.80	8	1.38	14	1.43
Plate 2	1	2.00	5	1.20	4	1.50	6	1.17	5	1.40	8	1.75
Plate 3	3	2.33	5	1.20	5	1.40	5	1.80	2	3.00	12	1.58
Total number of colony	5		17		13		16		15		34	
Overall phenotype scoring		**2.11**		**1.37**		**1.30**		**1.59**		**1.93**		**1.59**

B

	161		190		206		214		221		0.2 % gelatine	
	N	P	N	P	N	P	N	P	N	P	N	P
Plate 1	0	NA	0	NA	4	2.75	0	NA	3	2.33	6	3.00
Plate 2	1	3.00	0	NA	2	3.00	1	3.00	1	3.00	4	3.00
Plate 3	0	NA	1	3.00	2	2.50	3	3.00	2	3.00	6	3.00
Total number of colony	1		1		8		4		6		16	
Overall phenotype scoring		**3.00**		**3.00**		**2.75**		**3.00**		**2.78**		**3.00**

Table 6.14 *Clonal growth experiments. (A) In presence of LIF, (B) in absence of LIF. N: number of colony scored, P: average phenotype scoring on each coverslip.*

6.5 Experimental for Chapter 5

6.5.1 Choice of coverslips

The printing was carried out according to the parameters previously described (6.3.1). Three identical polymer microarrays were prepared by printing 15 poly(urethanes) solutions (**Table 5.1**) each as 24 identical spots at different positions on the gold-coated microscope slides (3 sub-arrays of 4 x 2 spots per sample).

Following drying, the arrays were incubated with 300 µL of AlexaFluor® 647 labelled fibrinogen (25 $\mu g.mL^{-1}$ in PBS, 3 h @ 37 °C). Three different types of coverslips were investigated to generate a thin film of protein solution on top of the printed arrays: standard glass coverslip (22 x 50 mm, BB022050A1, Menzel-Gläser), HybriSlips™ (60 mm x 22 mm, H18202, Invitrogen) and GeneFrame® (60 mm x 21 mm, AB-1130, ABgene).

Following washing and drying, the slides were scanned using the low resolution scanner and the fluorescence intensity arising from protein binding to each polymer spots integrated. The standard deviation and coefficient of variance (CV = % standard deviation / mean) were calculated from the integrated intensity resulting from the 24 identical spots for each of the 15 polymers.

6.5.2 Washing techniques

Following incubation of the protein solution onto the polymer microarray, superfluous protein solution had to be washed away. Initial experiments were carried out using a stream of de-ionised water, however, this methodology was difficult to reproduce due to several parameters such as pressure, time and angle of incidence of the stream. In order to obtain reproducible results, the washing method was standardised. It comprised of three 50 mL tubes (sterile polypropylene centrifuge tube, FB55956, Fisher Scientific) containing water, PBS and water. Following dipping of the slide, each tube was sealed and subsequently inverted 10 times (2 seconds per stroke). After the last washing, the slide was dried using a stream of N_2 and was then ready for scanning.

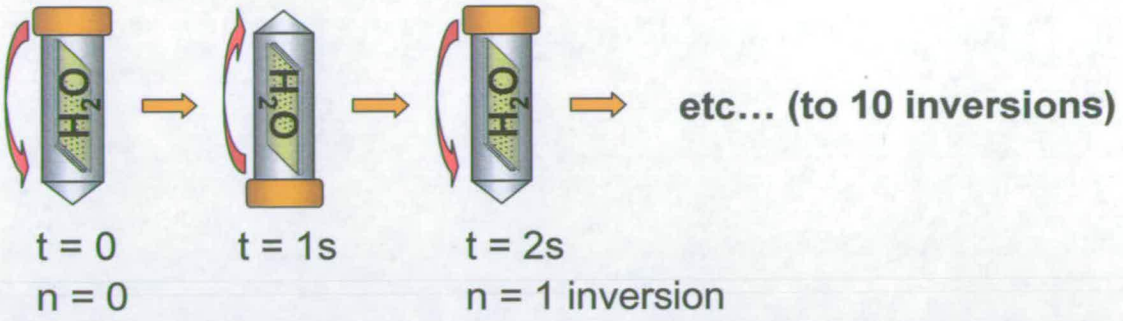

Figure 6.1 *Illustration of the standardised washing technique.*

6.5.3 Determination of protein concentrations

Five identical polymer microarrays were prepared by printing 32 poly(urethanes) solutions each as 8 identical spots within one field of 16 x 16 using the previously described conditions (6.3.1).

Following drying, each array was incubated with a different concentration of AlexaFluor® 647 labelled fibrinogen solution: [Fg] = 5.0, 12.5, 25, 50 and 100 $\mu g.mL^{-1}$ in PBS (300 µL / slide, 2 h @ 37 °C using GeneFrame® coverslips).

Following washing and drying, the polymer microarrays were scanned using the low resolution scanner with a Cy5 filter. The average fluorescent intensities arising from each set of 8 identical polymer spots were calculated on each slide (**Table 6.15**). These average fluorescent intensities were plotted against the concentrations of the fibrinogen solution used.

	Fibrinogen concentration in µg.mL-1				
PU	5.0	12.5	25	50	100
7	14566	17909	21182	20705	30677
8	29493	32334	251211	236368	426209
12	18327	24240	50708	104587	115581
16	15160	16523	45413	16816	25425
23	20545	21725	102097	197702	104186
25	14121	16300	48124	19164	62881
28	20485	20642	61896	113197	225429
37	13902	15388	33816	19836	54498
63	14697	14329	26685	32352	67878
65	27237	43957	366497	840137	1286399
73	14331	13661	19077	14144	21443
77	14266	19939	46634	164827	173723
79	154159	281474	581207	813478	955215
91	21398	42510	85825	220910	291750
92	14340	14223	102758	32653	188236
101	17387	19992	133028	153476	405982
102	16811	20122	39104	54494	129589
107	15921	21986	126788	177183	250789
154	15063	14182	38952	40946	46146
155	16244	16137	29683	46302	100856
156	60716	168124	258795	523776	714584
157	187057	532127	817099	1144489	1672833
159	214878	601370	1044517	1979599	1484462
160	247707	493511	1207369	1289407	1550765
163	22522	110592	162516	363398	437046
166	17649	84224	292008	401972	481574
171	14165	63507	93197	154722	144301
173	15998	18241	43311	57727	77955
191	21355	198674	488932	864142	1381533
233	14541	12698	18064	19163	23383
253	27474	17919	25698	34108	24416
255	16641	13285	23582	25423	24416

Table 6.15 *Average fluorescent intensities (a.u.) for the 8 identical polymer spots arising from the adsorption of labelled fibrinogen at different concentrations on a library of 32 poly(urethanes).*

6.5.4 Reproducibility of the method

Two identical polymer microarrays were prepared by printing 119 poly(urethanes) solutions each as 4 identical spots within two fields of 16 x 16 using the conditions described (6.3.1).

Following drying, each array was incubated with the same solution of FITC labelled glycoprotein X (confidential) (300 µL / slide, 2.50 $\mu g.mL^{-1}$ in 0.5 % w/v human serum albumin (HSA) in PBS, 2 h @ 37 °C using GeneFrame® coverslips).

Following washing and drying, each polymer microarray was scanned using the low resolution scanner with FITC filter and the fluorescence intensities arising from glycoprotein X adsorption to each polymer spots integrated (**Table 6.16**).

	Slide 1		Slide 2			Slide 1		Slide 2	
PU	F	CV	F	CV	PU	F	CV	F	CV
150	47889	2	45956	6	209	32955	8	32563	5
151	25658	3	24741	2	210	33840	19	48646	3
152	35551	9	32872	3	211	84591	2	79295	4
153	55673	4	48429	6	212	61889	15	53667	3
154	45081	16	38120	3	213	76176	6	81094	8
155	32128	3	31509	3	214	120014	3	119779	3
156	41876	5	38150	8	215	43191	2	47421	13
157	64223	6	55492	5	216	60862	7	85244	66
158	44876	9	40129	11	217	144319	6	143507	5
159	37203	22	61912	6	218	348500	17	335476	14
160	36973	5	30835	5	219	117169	5	101550	5
161	93259	4	91254	4	220	167456	2	160277	6
162	84576	5	84529	3	221	36734	3	36809	5
163	76070	3	72008	5	222	46436	5	41837	1
164	35869	6	30689	4	223	177949	5	166529	2
165	76939	2	76173	5	224	46308	3	43426	2
166	98604	2	102716	5	225	53433	12	52806	10
167	51625	4	52043	5	226	149765	5	162170	5
168	45875	7	38098	4	228	16030	8	18260	7
169	45748	5	46115	5	229	87997	14	85156	6
170	40471	5	39721	3	230	23189	14	36964	7
171	55668	19	41211	4	232	44217	14	40657	9
172	35431	4	31951	5	233	19721	12	23828	5
173	35288	3	37383	10	234	17295	11	28120	14
174	63887	4	69226	6	235	42886	8	46446	3
175	65497	1	71427	5	238	37163	4	32849	4
176	97908	9	92183	8	241	102341	4	101255	4
177	64342	4	58403	4	244	92538	24	68682	6
178	41010	10	50903	49	245	60077	3	62674	6
179	36973	23	35126	6	246	65175	5	57619	11
180	50558	5	42743	6	247	54228	6	49646	5
181	54576	8	47786	1	248	76535	8	79184	17
182	93338	7	104584	7	249	46042	3	45827	7
183	77227	4	82878	5	250	53974	10	57209	9
184	107540	6	109348	2	251	51586	13	58382	30
185	65268	2	65461	5	252	58736	38	46457	5
186	57303	10	52115	4	253	123261	6	109460	4
187	78007	64	63082	5	254	73767	2	68634	4
188	50013	7	48313	13	255	65612	31	74802	32
189	21660	21	35909	6	256	188307	4	178045	5
190	61035	4	61273	3	257	180184	21	170769	8
191	42746	6	42374	5	258	546857	20	381081	24
192	69183	4	78344	3	259	799581	15	460929	37
193	64599	5	61382	3	260	67487	3	60821	6
194	122684	8	167796	7	262	84561	11	58920	5
195	105648	3	116603	4	263	42033	10	37834	6
196	155647	6	207234	4	264	1277122	15	1541015	17
197	48991	4	46422	2	266	16805	6	22398	27
198	75222	6	78792	13	267	23143	7	27927	7
199	47181	3	42714	5	268	308270	4	287010	4
200	125748	5	161140	3	269	39712	7	40038	2
201	33245	5	31951	3	270	118709	2	132048	7
202	53523	14	52853	10	271	2080968	16	2509736	13
203	92243	3	94544	6	272	66780	19	77929	4
204	350394	7	413239	5	273	59024	5	54549	3
205	81243	1	77447	5	274	60199	16	62730	13
206	20944	11	29402	5	275	208282	3	242815	3
207	26408	15	34163	21	276	71034	5	68118	7
208	79607	16	78250	2	277	71277	5	110711	32
					278	49138	10	48693	7

Table 6.16 *Reproducibility study. Average fluorescent intensities (a.u.) and corresponding coefficient of variance (CV) for the 4 identical polymer spots arising from the adsorption of labelled glycoprotein X on 2 identical poly(urethanes) microarrays.*

6.5.5 Investigation of assay duplexing

The investigation of the assay duplexing was run with two sets of three polymer microarrays prepared with from 2 different polymer libraries. Both libraries were printed using the previously described conditions (6.3.1).

Library PA1: contained 176 poly(acrylates) each printed as 4 identical spots within three fields (two fields of 16 x 16 and one field of 12 x 16) (**Table 6.17**).

Library PA2: contained 83 poly(acrylates) and 56 grafted poly(allylamines) each printed as 4 identical spots within three fields (two fields of 16 x 16 and one field of 3 x 16) (**Table 6.18**).

A solution of Glycophorin A (G7903, Sigma-Aldrich) was labelled as described according to manufacturer protocol (6.2.1) with AlexaFluor® 546.

For this experiment three labelled protein stock solutions were prepared in 1.0 % v/v whole Human Serum (HS) (55979, MP Biomedicals, Stretton Scientific) in PBS.

600 µL of AlexaFluor® 546 labelled Glycophorin A @ 25.0 $\mu g.mL^{-1}$
300 µL of FITC labelled Glycoprotein X (confidential) @ 5.0 $\mu g.mL^{-1}$
300 µL of FITC labelled Glycoprotein Y (confidential) @ 50.0 $\mu g.mL^{-1}$

The solutions containing two labelled proteins were prepared by mixing 150 µL of each stock solution. The single probe solutions were prepared by diluting the stock solutions (150 µL) by a factor of two using 1.0 % v/v HS in PBS.
Each array was incubated with different protein solution (300 µL / slide, 2 h @ 37 °C using GeneFrame® coverslips):

System 1:

Slide 1: FITC labelled Glycoprotein X (2.50 $\mu g.mL^{-1}$) + AlexaFluor® 546 labelled Glycophorin A (12.5 $\mu g.mL^{-1}$) in 1.0 % v/v HS in PBS.

Slide 2: FITC labelled Glycoprotein X (2.50 $\mu g.mL^{-1}$) in 1.0 % v/v HS in PBS.

Slide 3: AlexaFluor® 546 labelled Glycophorin A (12.5 $\mu g.mL^{-1}$) in 1.0 % v/v HS in PBS.

System 2:

Slide 4: FITC labelled Glycoprotein Y (25.0 $\mu g.mL^{-1}$) + AlexaFluor® 546 labelled Glycophorin A (12.5 $\mu g.mL^{-1}$) in 1.0 % v/v HS in PBS.

Slide 5: FITC labelled Glycoprotein Y (25.0 $\mu g.mL^{-1}$) in 1.0 % v/v HS in PBS.

Slide 6: AlexaFluor® 546 labelled Glycoprotein A (25.0 $\mu g.mL^{-1}$) in 1.0 % v/v HS in PBS.

Following washing and drying, each polymer microarray was scanned using the low resolution scanner with:

Slide 1: FITC and Cy3 filters
Slide 2: FITC filter only.
Slide 3: Cy3 filter only.
Slide 4: FITC and Cy3 filters.
Slide 5: FITC filter only.
Slide 6: Cy3 filter only.

For each scan, the fluorescence intensities arising from protein binding to each polymer spots were integrated (**Table 6.17 and 6.18**).

	Slide 1				Slide 2		Slide 3	
Filter	FITC		Cy3		FITC		Cy3	
PA	F	CV	F	CV	F	CV	F	CV
1a5	125156	4	78695	15	27400	7	37019	17
1a7	202573	6	161189	13	119741	16	275257	28
1a9	369002	4	478378	13	226331	13	178498	2
1b7	32773	6	185933	6	25485	1	112173	10
1c7	46609	7	374893	9	19411	6	42619	16
1c9	218493	6	1191781	17	53068	20	115905	10
2a5	32304	3	214914	12	44697	10	132240	77
2a7	23847	6	55274	38	33661	3	50143	6
2a9	33562	7	84392	17	32048	8	204598	23
2b7	55545	13	589223	5	28618	6	90010	9
2b9	59391	3	563384	8	32760	9	330162	7
2BA7	21540	6	27768	4	18579	12	25056	19
2BA9	24237	5	140687	9	65614	6	225709	18
2BB7	23335	9	91987	17	26134	5	64295	13
2BB9	29795	7	628863	10	45387	2	543289	30
2BC9	27080	8	312720	25	65086	9	323359	11
2BE7	64902	4	577994	12	91359	5	185210	7
2BE9	144186	9	1821842	10	53396	16	149049	9
2BG5	18664	11	24900	8	16232	8	16377	3
2BG7	18157	2	24599	9	16204	5	86344	32
2BG9	49890	5	2914715	9	33953	8	57839	11
2c5	26165	4	131944	13	25398	6	45650	12
2c7	40496	4	117741	7	37462	5	36095	10
2c9	36961	7	205905	29	52368	2	364935	11
2e7	33152	3	111933	27	48117	3	194574	41
2e9	28713	5	83892	6	22704	19	119788	18
2f5	26439	23	135734	57	923664	8	3696663	6
2f7	252034	10	585027	10	784435	5	1361849	17
2g5	194209	9	1395650	21	260539	3	1387544	8
2g7	190158	30	969493	16	264316	5	118656	37
2g9	113269	13	687629	20	72370	25	428036	8
2h5	32788	19	253755	6	40410	11	62668	42
2h7	225301	7	783984	9	1005665	20	3002474	21
2h9	76693	6	849606	4	427205	11	2931275	11
3a5	24693	5	47208	6	26593	7	40047	25
3a7	33022	7	285946	12	63893	11	47836	4
3a9	34777	4	233767	15	26126	3	65149	11
3AA5	84422	18	319474	15	30457	5	198039	24
3AA7	51110	15	167802	35	150375	15	115171	12
3AA9	75791	28	312469	22	130007	13	529048	36
3AB 5	49485	17	124620	27	342252	17	161430	13
3AB 7	73580	18	224642	20	122175	15	539158	15
3AB 9	32163	10	153570	12	190360	11	127072	36
3AC 5	95720	10	310735	36	93115	2	295100	25
3AC 7	31875	16	213081	12	239011	9	156066	17
3AC 9	27693	7	158827	13	19276	2	49599	8
3AE 5	48601	48	383069	8	253349	24	214582	12
3AE 7	28263	9	254599	6	20891	4	75588	19
3AE 9	38966	40	127812	8	95987	7	163477	25
3b7	30176	6	34082	9	20548	5	23242	9
3b9	38097	16	157316	10	31805	13	29681	7
3BA5	18025	3	25343	5	16559	19	18978	3
3BA7	19250	4	32942	16	21477	3	56886	5
3BA9	21702	5	46134	9	27884	4	30594	18
3BB5	18879	3	30082	7	15478	3	21204	3
3BB7	19226	4	26418	10	19245	3	24869	22
3BB9	23560	2	69262	25	21918	21	23535	10
3BC5	18709	2	25114	9	21372	4	19536	11
3BC7	18646	5	31187	6	16343	11	20858	12

	Slide 1				Slide 2		Slide 3	
Filter	FITC		Cy3		FITC		Cy3	
PA	F	CV	F	CV	F	CV	F	CV
3BC9	18178	3	25337	11	14791	2	18837	13
3BE5	18840	4	23226	3	16487	2	21002	19
3BE7	19392	4	23204	6	16029	4	16360	4
3BE9	24270	4	69287	12	31390	7	23252	4
3BG5	19114	2	22692	3	16448	9	17129	9
3BG7	20377	8	24551	6	15810	1	17180	4
3BG9	20563	9	26759	15	47072	6	28906	40
3c5	28896	9	76246	14	35154	12	29565	12
3c7	30707	16	335428	10	57371	17	43641	23
3c9	36060	3	137184	25	112585	6	44236	9
3e5	155516	3	1761482	2	49693	16	146389	41
3e7	105150	12	1224817	10	171746	24	1833371	12
3e9	35475	17	122849	7	238229	5	298992	21
3f5	21950	9	89553	15	48717	14	160112	8
3f7	61728	18	603636	6	80758	64	1828614	14
3f9	42724	10	191813	19	61393	9	215413	30
3g5	32421	28	846902	35	20340	13	55391	8
3g7	120588	5	2009447	3	383283	14	1630572	14
3g9	157775	13	1872513	5	374827	7	1648771	7
3h7	81961	11	2813254	5	502404	2	3186196	3
3h9	42224	14	323173	23	136994	8	900748	22
3i5	77976	58	571344	6	154580	41	1401596	45
3i7	68020	10	1874053	6	87184	20	678711	26
3i9	31668	9	293171	21	48655	8	456779	52
3j5	21809	8	44156	12	34970	26	29890	10
3j7	20094	4	63104	48	23204	25	83403	29
3j9	64284	8	876097	50	41221	12	521738	39
3l9	1544500	18	2616138	16	1305891	15	2187336	5
3m5	151860	29	705611	22	168699	40	301843	54
3m7	106279	7	308669	10	57909	29	371376	73
3m9	35075	34	125534	15	170422	11	167121	18
3n5	39226	37	85394	63	73965	19	32699	22
3n7	20889	4	39380	4	56576	6	42008	13
3n9	125799	40	672074	28	78083	3	1105022	7
3v5	22868	13	31637	9	33151	24	21451	6
3v7	25907	8	50257	35	20136	2	24950	18
3v9	50333	20	331203	96	160799	18	126720	17
3x5	96239	11	194282	16	138928	5	354342	46
3x7	104750	10	169658	33	416222	7	352941	32
3x9	104778	19	334738	28	126686	27	167832	33
3z5	42015	3	83942	22	414272	14	51374	8
3z7	29430	12	78480	35	23205	39	41575	57
3z9	23623	5	69067	26	82077	14	32393	17
4a7	23568	7	28056	6	25022	7	30226	20
4a9	24544	2	28931	4	19229	1	23096	16
4b9	19787	4	25244	4	17292	4	22376	14
4c5	20586	7	25384	3	16985	13	20211	3
4c7	21699	1	26790	4	18301	2	20349	13
4c9	21015	5	34485	25	22798	16	21121	7
5a7	19587	3	41782	9	18260	6	25669	10
5a9	20522	3	72669	12	16809	1	38027	37
5AA5	201496	37	660551	19	356008	19	379231	15
5AA7	58900	2	778850	7	72187	11	175750	5
5AA9	40259	2	306823	11	44023	9	75107	3
5AB5	49163	8	475700	5	51720	10	103606	12
5AB7	63513	6	1055966	9	61441	6	89965	9
5AB9	40381	7	177816	23	73835	28	173512	98
5AC5	20881	4	51208	5	34405	10	52599	15
5AC7	25220	7	88488	23	21498	12	22816	9

	Slide 1				Slide 2		Slide 3	
Filter	FITC		Cy3		FITC		Cy3	
PA	F	CV	F	CV	F	CV	F	CV
5AC9	26144	22	94524	33	67232	30	63798	3
5AE5	35061	10	497507	21	37198	4	178041	11
5AE7	45810	8	2277434	24	37298	9	358239	30
5AE9	29220	12	1218309	17	19448	2	34527	14
5b7	19541	3	25951	2	16740	6	22369	11
5b9	19479	4	44823	16	15858	2	22489	16
5c5	22258	3	42918	5	18675	6	27308	16
5c7	35559	9	61621	18	73963	11	103795	6
5c9	23263	7	61827	6	35525	12	42736	19
5e5	26868	7	55593	9	16556	13	16068	1
5e7	24331	13	60184	15	21641	11	70908	20
5f9	75668	7	124295	20	60034	16	59667	25
5h7	25921	16	114458	7	27077	8	271132	20
5h9	57675	17	251733	13	172308	33	321784	15
5i5	139038	18	3180076	11	802488	4	601745	36
5i7	61358	18	1678612	4	44350	19	66757	19
5i9	55109	8	365620	6	40622	10	61043	45
5j5	22403	3	44467	8	20729	7	40107	24
5j9	47296	12	171298	13	22228	6	73813	4
5l5	27458	31	101471	23	17993	2	156587	10
5l7	22424	6	54382	7	22047	9	124108	13
5l9	21650	4	30251	11	44217	11	223625	41
5m7	18875	3	31561	16	22148	31	33235	47
5m9	37086	8	281584	9	102794	9	326233	19
5n5	19496	7	33381	6	93947	16	76540	19
5n7	22945	6	41000	8	179507	20	36808	23
5v7	18662	4	24837	4	15686	1	17086	3
5v9	27833	17	70147	13	19895	13	19430	7
5x5	423184	5	227588	9	132326	10	89452	3
5x7	128337	12	271878	6	224726	14	236848	86
5x9	34443	13	171493	7	32004	6	139680	20
5z5	30456	2	41505	3	24211	13	29525	18
5z7	21362	12	53657	15	19834	5	38225	14
5z9	19905	3	75058	11	17740	3	23112	11
6a5	25254	14	87023	20	38359	4	78238	26
6a9	35481	7	1278447	7	47797	18	290707	47
6b7	19117	3	39810	5	18644	8	28084	27
6b9	23427	10	91600	11	51042	9	165866	27
6c5	59369	7	604660	5	98921	9	82256	27
6c7	32095	8	327903	15	171863	30	80156	16
6c9	26783	1	547677	11	72808	16	186419	23
6e9	175002	11	2583056	8	465923	14	483575	16
6f9	103661	10	816073	11	225580	14	367970	15
6g9	18332	7	25426	12	83762	26	122280	35
6h9	59238	9	893946	20	188409	23	181631	68
7a5	41114	13	191148	13	260855	16	150451	15
7a7	40598	9	731752	17	93793	33	205483	12
7a9	49988	6	800337	6	53215	10	104965	24
7b5	36636	13	161473	23	58108	31	71286	8
7b7	63593	17	930704	7	53797	5	39261	13
7b9	52597	8	812979	12	123067	18	95776	23
7c5	49254	8	268205	5	68425	36	64602	23
7c7	50967	13	405038	29	52499	9	50051	28
7c9	57760	21	867921	21	43762	4	57525	5
7e5	18113	3	26485	13	419837	42	442890	71
7e7	148525	8	1110805	5	493444	16	449552	89
7e9	68003	9	814973	6	597614	9	803522	16
7f9	59891	16	717471	15	351497	7	243786	7

Table 6.17 *Results for system 1 on PA1. F: mean fluorescence intensities, CV: coefficient of variance.*

	Slide 4				Slide 5		Slide 6	
	Cy3		FITC		FITC		Cy3	
PA 2	F	CV	F	CV	F	CV	F	CV
2BAe7-1.0	346782	11	146952	8	125195	2	219221	7
2BAe7-1.5	143567	6	100768	26	83372	9	95739	13
2BAe7-2.0	53727	9	69619	6	96113	7	62732	4
2BAg7-1.0	111462	11	110961	12	150573	16	128445	6
2BAg7-1.5	74781	4	83153	5	108903	4	81851	19
2BAg7-2.0	78337	6	202876	6	226096	5	62332	9
2BCe7-1.0	136815	15	69215	3	94274	6	243898	36
2BCe7-1.5	489923	5	89272	8	103814	9	169663	11
2BCg7-1.0	338278	10	225087	5	436230	9	1088043	11
2GA11-5	540025	34	88335	6	75300	4	122481	14
2GA11-7	947672	42	79553	21	148582	39	820312	57
2GA11-9	367744	8	90159	66	63227	9	354299	7
2GA12-5	2785591	9	1391442	10	3270710	13	2598594	5
2GA12-7	4234238	10	3942639	10	3896981	6	3729871	8
2GA12-9	239801	8	107542	2	142360	13	315980	5
2GA13-9	1313875	7	367682	5	419514	6	477844	9
2GA14-7	3358779	7	2812605	5	2975763	5	3104752	6
2GA14-9	225475	9	162521	7	201299	16	292661	9
2GA15-7	3366777	1	3112681	2	3314517	2	3059708	3
2GA15-9	1588449	11	92223	16	279316	6	2252663	0
2GA1-7	146826	29	55460	47	38433	15	193263	17
2GA1-9	616694	7	307691	5	356006	10	774093	11
2GA2-7	24172	3	20021	13	15855	2	28540	22
2GA2-9	68280	10	37334	15	51556	6	69479	9
2GA3-7	176785	36	59011	15	76196	18	148629	13
2GA3-9	806717	25	255286	16	222689	7	835104	18
2GA4-5	1016542	57	374646	5	752239	8	982839	11
2GA4-7	357944	9	281389	8	328031	5	536858	25
2GA4-9	420675	15	45885	5	167328	23	470723	16
2GA5-5	30834	7	21558	3	17682	2	24438	9
2GA5-7	97688	5	37750	5	41543	12	122845	5
2GA5-9	501214	11	85368	6	74631	13	707751	11
2GA6-5	414680	3	154145	10	214493	7	696065	6
2GA6-7	544416	21	165023	5	170438	5	805813	7
2GA6-9	666118	15	207788	13	375161	16	768565	12
2GA7-5	365359	15	83941	3	90642	5	616074	11
2GA7-7	626889	24	90119	4	184421	13	690169	14
2GA7-9	381803	9	70293	5	72428	3	521847	13
2GA8-5	2433257	4	3117033	5	3734986	9	2321653	2
2GA8-9	260689	13	162277	6	180401	11	352841	12
2GA9-5	460764	10	156857	7	193078	9	689513	3
2GA9-7	418446	2	212517	1	243814	6	678696	10
2GA9-9	859105	17	395418	5	461216	6	1147646	12
3BAe7-1.0	1285339	13	314460	4	362487	9	759162	14
3BCe7-1.0	412799	13	130207	12	155709	7	452912	13
3BCg7-1.0	294077	7	211085	11	281677	14	423956	2
3e7	1706236	8	398411	9	188526	8	981099	10
3e9	372291	70	190988	17	152445	12	258394	19
3GA11-9	149781	8	51901	2	61559	16	229047	15
3GA13-9	3709346	7	1030671	13	1239605	7	3282161	4
3GA14-5	3163126	5	300145	14	2805861	5	3335961	4
3GA1-9	360317	4	107768	2	113244	11	373040	12
3GA2-9	455185	8	160664	6	136872	10	477322	13
3GA4-9	1432490	21	108173	6	427125	4	1133113	41
3GA5-9	1985547	6	329099	5	216522	7	1576388	28
3GA7-9	140962	14	106427	26	81056	6	155467	9
3GA9-5	429411	7	776207	3	698258	6	410022	14
3GA9-7	972947	8	178151	4	247112	16	964786	6
3GA9-9	168221	4	85208	6	85434	4	238601	16
7f7	658059	18	112067	15	163335	6	471366	22
7g7	460858	12	139374	20	143094	8	747188	6
7g9	517271	16	177700	7	214197	7	437670	4
7h7	1052885	17	332460	9	366027	18	2457193	7
7h9	351477	14	191362	21	296271	18	1428897	4
8e5	56057	4	30965	10	36270	13	105122	11
8e9	175288	9	36891	6	25412	8	58619	8
8f5	1378618	17	235823	20	297268	15	1029651	7
8f7	322197	6	107717	5	178725	4	545011	34
8f9	104510	8	44820	9	35273	6	116939	3
8g5	46893	6	25073	4	33037	10	59001	8

	Slide 4				Slide 5		Slide 6	
	Cy3		FITC		FITC		Cy3	
PA 2	F	CV	F	CV	F	CV	F	CV
8g7	105148	15	60256	21	77343	8	130645	5
8g9	159010	15	54174	4	75783	16	152523	10
8h5	2684290	5	179100	13	293911	13	2992967	10
8h7	1501543	7	134232	12	160682	4	3122594	7
8h9	225996	11	68792	3	107284	7	1537994	8
9e9	33779	12	27084	18	22462	13	41570	20
9f5	32952	13	29129	14	29485	15	26840	4
9f9	27759	6	21633	3	20624	10	27408	10
9g5	301057	17	60384	13	87981	19	624945	16
9g9	64711	14	51080	14	52168	27	89228	55
9h5	3459030	21	149361	11	187091	14	4393649	10
9h7	693057	6	230586	14	270778	5	3693064	9
9h9	779424	1	310474	1	381859	8	2645425	12
1/5a	402888	11	50829	7	47893	0	379799	6
1/6b	831193	18	1916392	11	2183045	2	1087168	29
1/7c	365501	9	51699	2	69145	19	327331	22
2/3a	418327	17	93666	18	249580	5	409946	13
1/4c	711402	5	99249	10	110893	18	848113	8
1/6a	136165	5	337915	3	612494	16	170726	5
1/7b	433402	6	110703	12	148128	13	493486	4
1/8c	507546	6	63878	5	73007	7	480405	24
1/4b	501495	12	114290	7	113201	2	657594	3
1/5c	526149	17	80898	9	83727	8	1087469	41
1/7a	700229	4	590746	5	740226	11	916320	11
1/8b	531673	3	95415	9	110288	15	697751	7
1/4a	497165	9	148075	2	148446	3	699665	10
1/5b	444725	14	86293	5	94927	7	682255	19
1/6c	152785	4	594903	1	972501	6	196173	7
1/8a	390415	28	60552	16	59875	10	493381	12
2/5a	315184	6	39877	20	53307	20	390270	10
2/7b	346640	7	129295	42	648336	73	264791	12
2/8c	412033	8	59141	4	152057	62	427293	16
3/4c	102157	20	44254	18	37084	17	77039	14
2/4c	124827	7	105618	8	211553	14	117692	16
2/7a	131469	8	401591	11	812906	9	163312	10
2/8b	358553	4	156161	13	221606	18	424032	8
2/9c	394556	4	332930	7	300893	23	523063	8
2/4b	100354	4	217644	4	307153	11	127878	16
2/5c	260050	24	77500	26	73984	16	454018	8
2/8a	344274	11	121971	19	126785	21	372114	4
2/9b	382766	7	252335	10	289393	5	468410	23
2/3b	522154	13	118114	28	141594	3	613769	9
2/5b	281253	20	49768	50	46722	27	248933	26
2/7c	381445	6	110448	18	98779	13	382093	4
2/9a	470241	8	443449	8	502413	6	523413	5
3/8b	784744	14	108108	6	157069	30	753108	6
5/6b	400376	4	70882	13	67319	17	405772	3
5/7c	402987	10	129782	19	112342	15	493683	3
6/7a	373340	13	196337	8	225604	7	454240	25
3/8a	402042	13	68160	6	84025	12	413535	11
5/6a	52492	5	211430	6	542832	33	112811	2
5/7b	345315	13	154326	21	146912	11	475387	6
5/8c	276129	2	89123	29	93505	13	313792	6
3/5b	410223	7	168213	7	118201	3	544793	9
4/7a	231452	2	132225	8	123671	11	352792	8
5/7a	243100	6	252806	10	168637	28	452840	10
5/8b	145806	16	53350	7	55541	31	344804	11
3/5a	392418	13	65103	27	71705	15	522144	10
3/8c	437745	3	82320	7	104264	13	524715	5
5/6c	351134	9	58046	4	56885	12	447147	5
5/8a	362869	6	122683	9	133335	11	420426	7
6/9a	154164	24	46332	13	39911	9	202634	13
8/9b	483127	16	398228	4	439360	7	603354	7
6/8b	143085	11	561572	14	1173930	16	215878	7
7/8c	342864	16	120785	7	181872	4	349699	7
6/8a	393982	9	173114	20	155013	8	384493	3
7/8b	324796	8	193533	23	165854	17	372752	6
6/7b	657657	7	2682738	7	3676963	12	1260654	28
7/8a	280979	5	155253	8	242466	10	321296	16

Table 6.18 *Results for system 2 on PA2. F: mean fluorescence intensities, CV: coefficient of variance.*

6.5.6 Potential diagnostic application

Three identical polymer microarrays were prepared by printing 147 poly(acrylates) solutions (Table 6.20) each as 4 identical spots within three fields (two fields of 16 x 16 and one field of 8 x 16) using the conditions previously described (6.3.1).

Each printed polymer microarray was incubated for 5 minutes at room temperature with one of the following three protein solutions prepared in 1.0 % v/v whole Human Serum (HS) in PBS:

300 µL of FITC labelled Glycoprotein Y (confidential) @ 25.0 $\mu g.mL^{-1}$

300 µL of AlexaFluor® 546 labelled Glycophorin A @ 12.5 $\mu g.mL^{-1}$

300 µL of AlexaFluor® 647 labelled Fibrinogen @ 25.0 $\mu g.mL^{-1}$

Following washing and drying, each polymer microarray was scanned using the low resolution scanner with the filter relevant to the fluorescent label used. For each scan, the fluorescence intensities arising from protein binding to each polymer spots were integrated and the mean fluorescence intensities calculated (**Table 6.19**).

	Glycoprotein Y		Glycophorin A		Fibrinogen	
Filter	FITC		Cy3		Cy5	
PA	F	F / B	F	F / B	F	F / B
1a5	126354	8	96458	5	21540	2
1a7	245773	16	184940	10	23250	2
1a9	344150	22	243954	13	914862	66
1b7	79714	5	136951	7	1774646	128
1c7	78623	5	153513	8	1405470	101
1c9	117582	8	151011	8	1011447	73
2a5	35490	2	41739	2	63299	5
2a7	34676	2	33652	2	140505	10
2a9	48771	3	61294	3	588495	42
2b7	51903	3	57185	3	14707	1
2b9	43753	3	86336	5	727384	52
2BA7	17414	1	24228	1	18902	1
2BA9	105360	7	392548	21	1454879	105
2BB7	26445	2	65418	3	24623	2
2BB9	84827	6	534959	28	1139349	82
2BC9	72338	5	265040	14	1654332	119
2BE7	57381	4	119551	6	101119	7
2BE9	153453	10	722393	38	1036523	75
2BG9	963146	63	2163131	115	319236	23
2c5	25993	2	39351	2	17153	1
2c7	39982	3	34028	2	20840	1
2c9	50640	3	62578	3	492442	35
2e9	124478	8	269007	14	2543579	183
2f5	160403	10	1081877	57	356164	26
2f7	131956	9	209871	11	892169	64
2f9	46474	3	98041	5	1262800	91
2g7	252973	17	2203012	117	952157	69
2g9	124416	8	1947104	103	1321245	95
2GA1-7	141182	9	23322	1	557527	40
2GA1-9	192753	13	1638090	87	1058035	76
2GA2-9	71951	5	91220	5	554870	40
2h7	287968	19	1988650	106	1195384	86
2h9	165196	11	2314007	123	516587	37
3a5	38087	2	47656	3	29506	2
3a7	42701	3	47449	3	19105	1
3a9	42694	3	59866	3	26316	2
3AB5	212083	14	133087	7	149572	11
3AB7	95485	6	95366	5	780567	56
3AB9	241229	16	96660	5	30788	2
3AC5	67012	4	165565	9	556647	40
3AC7	135703	9	114055	6	23612	2
3AC9	49564	3	261742	14	37234	3
3AE5	245149	16	124968	7	1305999	94
3AE7	77680	5	106106	6	1117756	80
3AE9	97866	6	65671	3	61248	4
3b7	30434	2	45077	2	15733	1
3b9	41641	3	56329	3	16258	1
3BA5	15907	1	18854	1	14071	1
3BA7	54818	4	38282	2	29757	2
3BB5	15335	1	20188	1	13901	1
3BB9	50457	3	24099	1	27855	2
3BE7	16885	1	33668	2	17527	1
3BE9	76822	5	72464	4	14433	1
3c5	42186	3	48420	3	15428	1
3c7	46614	3	86768	5	26064	2
3c9	61547	4	1223560	65	1134527	82
3e7	357291	23	2467484	131	2012793	145
3e9	54186	4	291451	15	77635	6
3f7	245302	16	2032214	108	1611395	116
3f9	128379	8	40699	2	81990	6
3g5	324941	21	2608568	138	1442475	104
3g7	304357	20	2970892	158	846144	61
3g9	85188	6	88026	5	27902	2
3h7	173415	11	2946051	156	1041977	75
3h9	164358	11	57718	3	41707	3
3i5	119194	8	55559	3	619472	45
3i7	82489	5	205062	11	378107	27
3i9	153198	10	94016	5	441693	32
3j5	30449	2	96519	5	22546	2
3j7	49301	3	747023	40	35480	3
3j9	140835	9	2247174	119	659245	47
3l9	233860	15	1434224	76	727447	52
3m5	497219	32	1614549	86	983364	71
3m7	325896	21	142873	8	858547	62

	Glycoprotein Y		Glycophorin A		Fibrinogen	
Filter	FITC		Cy3		Cy5	
PA	F	F / B	F	F / B	F	F / B
3m9	120479	8	200426	11	170805	12
3n9	97927	6	520977	28	799250	58
3v7	23937	2	27801	1	23892	2
3x5	186714	12	149399	8	221763	16
3z5	53127	3	62151	3	62315	4
5a7	34676	2	33569	2	20457	1
5a9	27721	2	25967	1	17454	1
5AA5	144659	9	738635	39	303573	22
5AA7	61294	4	202461	11	45433	3
5AA9	34668	2	42764	2	169248	12
5AB5	57439	4	84069	4	93602	7
5AB7	45847	3	62756	3	295001	21
5AB9	38364	3	41208	2	183593	13
5AC5	18005	1	25865	1	51160	4
5AC7	21730	1	40962	2	48838	4
5AC9	18075	1	25398	1	14462	1
5AE5	85820	6	70240	4	800458	58
5AE7	38232	2	65505	3	29576	2
5AE9	30523	2	64910	3	32596	2
5b9	22065	1	21974	1	20479	1
5c5	22892	1	24681	1	16484	1
5c7	23564	2	25098	1	17147	1
5c9	19773	1	23950	1	16969	1
5e5	31782	2	124511	7	24666	2
5e7	39487	3	232918	12	36841	3
5f9	20108	1	92914	5	22985	2
5h7	60128	4	293588	16	39437	3
5h9	67536	4	850491	45	377333	27
5i5	184725	12	73399	4	42779	3
5i7	111377	7	761276	40	363808	26
5j5	22646	1	61116	3	19459	1
5j9	21554	1	134926	7	52898	4
5l5	17516	1	55399	3	22490	2
5l7	20744	1	21936	1	16908	1
5m7	23121	2	46419	2	40362	3
5m9	278210	18	438389	23	191251	14
5n5	66433	4	314106	17	50175	4
5n7	51577	3	23344	1	16476	1
5x5	122712	8	77139	4	317822	23
5x7	133859	9	65281	3	246302	18
5z9	17327	1	22811	1	14810	1
6a5	69883	5	59153	3	20171	1
6a9	42145	3	58677	3	21117	2
6b7	18153	1	21786	1	15950	1
6b9	27743	2	25416	1	20221	1
6c7	47434	3	45702	2	20511	1
6c9	41249	3	45743	2	21256	2
6e9	235506	15	487561	26	532143	38
6f9	208927	14	518690	28	567691	41
6g9	48912	3	116391	6	34051	2
6h9	232759	15	2661962	141	425258	31
7a5	88409	6	185501	10	52227	4
7a7	133447	9	178430	9	269732	19
7a9	296223	19	302695	16	1082503	78
7b5	27156	2	31150	2	17274	1
7b7	59370	4	73164	4	101618	7
7b9	90667	6	70344	4	151900	11
7e9	68866	4	247548	13	1141247	82
7h7	359944	24	2972705	158	1034611	74
7h9	136372	9	346037	18	1175185	85
8e9	245311	16	164091	9	1715256	123
8f5	312891	20	1995489	106	1623185	117
8f7	76689	5	83181	4	981164	71
8f9	85922	6	138259	7	704368	51
8g5	200372	13	78759	4	720958	52
8g7	199359	13	2182318	116	1288517	93
8g9	90989	6	73246	4	656695	47
8h5	384833	25	3610024	192	1550943	112
8h7	410778	27	2874676	153	852428	61
8h9	138129	9	1757148	93	671462	48
9h5	378303	25	3334026	177	1172237	84
9h7	404476	26	2192636	116	843499	61
9h9	214251	14	454080	24	383308	28
Background	15316		18848		13899	

Table 6.19 *Protein fingerprint F: mean fluorescence intensities, F/B: mean intensities divided by background.*

Reference List

(1) Schena, M.; Shalon, D.; Davis, R. W.; Brown, P. O. *Science* **1995**, *270*, 467-470.

(2) Martel, R. R.; Rounseville, M. P.; Botros, I. W.; Seligmann, B. E. in: *Microarray technology and its applications*, Müller, U. R. and Nicolau, D. V.(eds), Chapter 1, pp 3-22. Berlin: Springer, **2005**.

(3) Hanson, K. L.; Filipponi, L.; Nicolau, D. V. in: *Microarray technology and its applications*, Müller, U. R. and Nicolau, D.(eds), Chapter 2, pp 23-44. Berlin: Springer, **2005**.

(4) Zammatteo, N.; Jeanmart, L.; Hamels, S.; Courtois, S.; Louette, P.; Hevesi, L.; Remacle, J. *Anal.Biochem.* **2000**, *280*, 143-150.

(5) Blencowe, A.; Hayes, W. *Soft Matter* **2005**, *1*, 178-205.

(6) Caelen, I.; Gao, H.; Sigrist, H. *Langmuir* **2002**, *18*, 2463-2467.

(7) Kanoh, N.; Asami, A.; Kawatani, M.; Honda, K.; Kumashiro, S.; Takayama, H.; Simizu, S.; Amemiya, T.; Kondoh, Y.; Hatakeyama, S.; Tsuganezawa, K.; Utata, R.; Tanaka, A.; Yokoyama, S.; Tashiro, H.; Osada, H. *Chemistry-An Asian Journal* **2006**, *1*, 789-797.

(8) Martel, R. R.; Botros, I. W.; Rounseville, M. P.; Hinton, J. P.; Staples, R. R.; Morales, D. A.; Farmer, J. B.; Seligmann, B. E. *Assay and Drug Development Technologies* **2002**, *1*, 61-71.

(9) Beier, M.; Hoheisel, J. D. *Nucleic Acids Res.* **1999**, *27*, 1970-1977.

(10) Schaeferling, M.; Schiller, S.; Paul, H.; Kruschina, M.; Pavlickova, P.; Meerkamp, M.; Giammasi, C.; Kambhampati, D. *Electrophoresis* **2002**, *23*, 3097-3105.

(11) Orner, B. P.; Derda, R.; Lewis, R. L.; Thomson, J. A.; Kiessling, L. L. *J.Am.Chem.Soc.* **2004**, *126*, 10808-10809.

(12) Afanassiev, V.; Hanemann, V.; Wolfl, S. *Nucleic Acids Res.* **2000**, *28*, E66.

(13) Müller, U. R.; Papen, R. in: *Microarray technology and its applications*, Müller, U. R. and Nicolau, D. V.(eds), Chapter 5, pp 73-88. Berlin: Springer, **2005**.

(14) TeleChem-Stealth Pins, http://www.arrayit.com/Products/Printing/Stealth/stealth.html, Accessed the 14th Nov. 2006.

(15) McQuain, M. K.; Seale, K.; Peek, J.; Levy, S.; Haselton, F. R. *Anal.Biochem.* **2003**, *320*, 281-291.

(16) Schwenk, J. M.; Stoll, D.; Templin, M. F.; Joos, T. O. *Biotechniques* **2002**, *Suppl*, 54-61.

(17) Hitachi- X-cut pin, http://www.miraibio.com/component/option,com_docman/task,doc_download/gid,21/Itemid,214/, Accessed the 14th Nov. 2006.

(18) Lee, K. B.; Park, S. J.; Mirkin, C. A.; Smith, J. C.; Mrksich, M. *Science* **2002**, *295*, 1702-1705.

(19) Doktycz, M. J. in: *Microarray technology and its applications*, Müller, U. R. and Nicolau, D. V.(eds), Chapter 4, pp 63-72. Berlin: Springer, **2005**.

(20) Roth, E. A.; Xu, T.; Das, M.; Gregory, C.; Hickman, J. J.; Boland, T. *Biomaterials* **2004**, *25*, 3707-3715.

(21) Microdrop-Dispenser Heads, http://www.microdrop.de/wDeutsch/products/14_04-2006-e%20MD-Heads.pdf, Accessed the 14th Nov. 2006.

(22) Calvert, P. *Chem.Mat.* **2001**, *13*, 3299-3305.

(23) Storhoff, J. J.; Marla, S.; Garimella, V.; Mirkin, C. A. in: *Microarray technology and its applications*, Müller, U. R. and Nicolau, D. V.(eds), Chapter 8, pp 147-180. Berlin: Springer, **2005**.

(24) Lindroos, K.; Sigurdsson, S.; Johansson, K.; Ronnblom, L.; Syvanen, A. C. *Nucleic Acids Res.* **2002**, *30*, e70.

(25) Stears, R. L.; Getts, R. C.; Gullans, S. R. *Physiol Genomics* **2000**, *3*, 93-99.

(26) Bruchez, M., Jr.; Moronne, M.; Gin, P.; Weiss, S.; Alivisatos, A. P. *Science* **1998**, *281*, 2013-2016.

(27) Chan, W. C.; Nie, S. *Science* **1998**, *281*, 2016-2018.

(28) Baeyens, W. R.; Schulman, S. G.; Calokerinos, A. C.; Zhao, Y.; Garcia Campana, A. M.; Nakashima, K.; De, K. D. *J.Pharm.Biomed.Anal.* **1998**, *17*, 941-953.

(29) Huang, R. P. *J.Immunol.Methods* **2001**, *255*, 1-13.

(30) Whitney, L. W.; Becker, K. G. *J.Neurosci.Methods* **2001**, *106*, 9-13.

(31) Ge, H. *Nucleic Acids Res.* **2000**, *28*, e3.

(32) Wegner, G. J.; Lee, H. J.; Corn, R. M. *Anal.Chem.* **2002**, *74*, 5161-5168.

(33) Marvin, L. F.; Roberts, M. A.; Fay, L. B. *Clin.Chim.Acta* **2003**, *337*, 11-21.

(34) Villanueva, J.; Philip, J.; Entenberg, D.; Chaparro, C. A.; Tanwar, M. K.; Holland, E. C.; Tempst, P. *Anal.Chem.* **2004**, *76*, 1560-1570.

(35) Bons, J. A.; Wodzig, W. K.; van Dieijen-Visser, M. P. *Clin.Chem.Lab Med.* **2005**, *43*, 1281-1290.

(36) Combaret, V.; Bergeron, C.; Brejon, S.; Iacono, I.; Perol, D.; Negrier, S.; Puisieux, A. *Cancer Lett.* **2005**, *228*, 91-96.

(37) Arlinghaus, H. F.; Schroder, M.; Feldner, J. C.; Brandt, O.; Hoheisel, J. D.; Lipinsky, D. *Appl.Surf.Sci.* **2004**, *231-2*, 392-396.

(38) Pease, A. C.; Solas, D.; Sullivan, E. J.; Cronin, M. T.; Holmes, C. P.; Fodor, S. P. *Proc.Natl.Acad.Sci.U.S.A* **1994**, *91*, 5022-5026.

(39) Miki, R.; Kadota, K.; Bono, H.; Mizuno, Y.; Tomaru, Y.; Carninci, P.; Itoh, M.; Shibata, K.; Kawai, J.; Konno, H.; Watanabe, S.; Sato, K.; Tokusumi, Y.; Kikuchi, N.; Ishii, Y.; Hamaguchi, Y.; Nishizuka, I.; Goto, H.; Nitanda, H.; Satomi, S.; Yoshiki, A.; Kusakabe, M.; DeRisi, J. L.; Eisen, M. B.; Iyer, V. R.; Brown, P. O.; Muramatsu, M.; Shimada, H.; Okazaki, Y.; Hayashizaki, Y. *Proc.Natl.Acad.Sci.U.S.A* **2001**, *98*, 2199-2204.

(40) Schena, M.; Shalon, D.; Heller, R.; Chai, A.; Brown, P. O.; Davis, R. W. *Proc.Natl.Acad.Sci.U.S.A* **1996**, *93*, 10614-10619.

(41) Chaudhary, J.; Schmidt, M. *Chromosome Res.* **2006**, *14*, 567-586.

(42) Wang, D. G.; Fan, J. B.; Siao, C. J.; Berno, A.; Young, P.; Sapolsky, R.; Ghandour, G.; Perkins, N.; Winchester, E.; Spencer, J.; Kruglyak, L.; Stein, L.; Hsie, L.; Topaloglou, T.; Hubbell, E.; Robinson, E.; Mittmann, M.; Morris, M. S.; Shen, N.; Kilburn, D.; Rioux, J.; Nusbaum, C.; Rozen, S.; Hudson, T. J.; Lipshutz, R.; Chee, M.; Lander, E. S. *Science* **1998**, *280*, 1077-1082.

(43) Hacia, J. G. *Nat.Genet.* **1999**, *21*, 42-47.

(44) Mirnics, K.; Middleton, F. A.; Marquez, A.; Lewis, D. A.; Levitt, P. *Neuron* **2000**, *28*, 53-67.

(45) Whitney, L. W.; Becker, K. G.; Tresser, N. J.; Caballero-Ramos, C. I.; Munson, P. J.; Prabhu, V. V.; Trent, J. M.; McFarland, H. F.; Biddison, W. E. *Ann.Neurol.* **1999**, *46*, 425-428.

(46) Spellman, P. T.; Sherlock, G.; Zhang, M. Q.; Iyer, V. R.; Anders, K.; Eisen, M. B.; Brown, P. O.; Botstein, D.; Futcher, B. *Mol.Biol.Cell* **1998**, *9*, 3273-3297.

(47) Wilson, M.; DeRisi, J.; Kristensen, H. H.; Imboden, P.; Rane, S.; Brown, P. O.; Schoolnik, G. K. *Proc.Natl.Acad.Sci.U.S.A* **1999**, *96*, 12833-12838.

(48) Petrik, J. *Transfus.Med.* **2006**, *16*, 233-247.

(49) Wadlow, R.; Ramaswamy, S. *Curr.Mol.Med.* **2005**, *5*, 111-120.

(50) de Longueville, F.; Surry, D.; Meneses-Lorente, G.; Bertholet, V.; Talbot, V.; Evrard, S.; Chandelier, N.; Pike, A.; Worboys, P.; Rasson, J. P.; Le, B. B.; Remacle, J. *Biochem. Pharmacol.* **2002**, *64*, 137-149.

(51) Cahill, D. P.; Kinzler, K. W.; Vogelstein, B.; Lengauer, C. *Trends Biochem.Sci.* **1999**, *24*, M57-M60.

(52) Pollack, J. R.; Perou, C. M.; Alizadeh, A. A.; Eisen, M. B.; Pergamenschikov, A.; Williams, C. F.; Jeffrey, S. S.; Botstein, D.; Brown, P. O. *Nat.Genet.* **1999**, *23*, 41-46.

(53) Chiang, A. P.; Beck, J. S.; Yen, H. J.; Tayeh, M. K.; Scheetz, T. E.; Swiderski, R. E.; Nishimura, D. Y.; Braun, T. A.; Kim, K. Y.; Huang, J.; Elbedour, K.; Carmi, R.; Slusarski, D. C.; Casavant, T. L.; Stone, E. M.; Sheffield, V. C. *Proc.Natl.Acad.Sci.U.S.A* **2006**, *103*, 6287-6292.

(54) Takabatake, N.; Shibata, Y.; Abe, S.; Wada, T.; Machiya, J.; Igarashi, A.; Tokairin, Y.; Ji, G.; Sato, H.; Sata, M.; Takeishi, Y.; Emi, M.; Muramatsu, M.; Kubota, I. *Am. J. Respir. Crit. Care Med.* **2006**, *174*, 875-885.

(55) Hain, T.; Steinweg, C.; Chakraborty, T. *J.Biotechnol.* **2006**, *126*, 37-51.

(56) Sergeev, N.; Distler, M.; Courtney, S.; Al-Khaldi, S. F.; Volokhov, D.; Chizhikov, V.; Rasooly, A. *Biosens.Bioelectron.* **2004**, *20*, 684-698.

(57) Abdullah-Sayani, A.; Bueno-de-Mesquita, J. M.; van de Vijver, M.J., V *Nat. Clin. Pract. Oncol.* **2006**, *3*, 501-516.

(58) Huang, Y. F.; Huang, C. C.; Hu, C. C.; Chang, H. T. *Electrophoresis* **2006**, *27*, 3503-3522.

(59) Tomizaki, K. Y.; Usui, K.; Mihara, H. *Chembiochem.* **2005**, *6*, 782-799.

(60) Angenendt, P. *Drug Discovery Today* **2005**, *10*, 503-511.

(61) Miller, J. C.; Zhou, H.; Kwekel, J.; Cavallo, R.; Burke, J.; Butler, E. B.; Teh, B. S.; Haab, B. B. *Proteomics* **2003**, *3*, 56-63.

(62) Robinson, W. H.; DiGennaro, C.; Hueber, W.; Haab, B. B.; Kamachi, M.; Dean, E. J.; Fournel, S.; Fong, D.; Genovese, M. C.; de Vegvar, H. E.; Skriner, K.; Hirschberg, D. L.; Morris, R. I.; Muller, S.; Pruijn, G. J.; van Venrooij, W. J.; Smolen, J. S.; Brown, P. O.; Steinman, L.; Utz, P. J. *Nat.Med.* **2002**, *8*, 295-301.

(63) Sreekumar, A.; Nyati, M. K.; Varambally, S.; Barrette, T. R.; Ghosh, D.; Lawrence, T. S.; Chinnaiyan, A. M. *Cancer Res.* **2001**, *61*, 7585-7593.

(64) Rowe, C. A.; Tender, L. M.; Feldstein, M. J.; Golden, J. P.; Scruggs, S. B.; MacCraith, B. D.; Cras, J. J.; Ligler, F. S. *Anal.Chem.* **1999**, *71*, 3846-3852.

(65) Lesaicherre, M. L.; Lue, R. Y.; Chen, G. Y.; Zhu, Q.; Yao, S. Q. *J.Am.Chem.Soc.* **2002**, *124*, 8768-8769.

(66) Zhu, H.; Klemic, J. F.; Chang, S.; Bertone, P.; Casamayor, A.; Klemic, K. G.; Smith, D.; Gerstein, M.; Reed, M. A.; Snyder, M. *Nat.Genet.* **2000**, *26*, 283-289.

(67) Zhu, H.; Bilgin, M.; Bangham, R.; Hall, D.; Casamayor, A.; Bertone, P.; Lan, N.; Jansen, R.; Bidlingmaier, S.; Houfek, T.; Mitchell, T.; Miller, P.; Dean, R. A.; Gerstein, M.; Snyder, M. *Science* **2001**, *293*, 2101-2105.

(68) Uttamchandani, M.; Walsh, D. P.; Yao, S. Q.; Chang, Y. T. *Curr.Opin.Chem.Biol.* **2005**, *9*, 4-13.

(69) Shin, I.; Park, S.; Lee, M. R. *Chem.Eur.J.* **2005**, *11*, 2894-2901.

(70) Wang, D.; Liu, S.; Trummer, B. J.; Deng, C.; Wang, A. *Nat.Biotechnol.* **2002**, *20*, 275-281.

(71) Bock, C.; Coleman, M.; Collins, B.; Davis, J.; Foulds, G.; Gold, L.; Greef, C.; Heil, J.; Heilig, J. S.; Hicke, B.; Hurst, M. N.; Husar, G. M.; Miller, D.; Ostroff, R.; Petach, H.; Schneider, D.; Vant-Hull, B.; Waugh, S.; Weiss, A.; Wilcox, S. K.; Zichi, D. *Proteomics* **2004**, *4*, 609-618.

(72) Shi, H.; Tsai, W. B.; Garrison, M. D.; Ferrari, S.; Ratner, B. D. *Nature* **1999**, *398*, 593-597.

(73) Feilner, T.; Hultschig, C.; Lee, J.; Meyer, S.; Immink, R. G.; Koenig, A.; Possling, A.; Seitz, H.; Beveridge, A.; Scheel, D.; Cahill, D. J.; Lehrach, H.; Kreutzberger, J.; Kersten, B. *Mol.Cell Proteomics* **2005**, *4*, 1558-1568.

(74) Salisbury, C. M.; Maly, D. J.; Ellman, J. A. *J.Am.Chem.Soc.* **2002**, *124*, 14868-14870.

(75) Gosalia, D. N.; Salisbury, C. M.; Maly, D. J.; Ellman, J. A.; Diamond, S. L. *Proteomics* **2005**, *5*, 1292-1298.

(76) Collins, M. O.; Yu, L.; Coba, M. P.; Husi, H.; Campuzano, I.; Blackstock, W. P.; Choudhary, J. S.; Grant, S. G. *J.Biol.Chem.* **2005**, *280*, 5972-5982.

(77) Min, D. H.; Su, J.; Mrksich, M. *Angew.Chem., Int.Ed.Engl.* **2004**, *43*, 5973-5977.

(78) Funeriu, D. P.; Eppinger, J.; Denizot, L.; Miyake, M.; Miyake, J. *Nat.Biotechnol.* **2005**, *23*, 622-627.

(79) Diaz-Mochon, J. J.; Bialy, L.; Bradley, M. *Chem.Commun.* **2006**, 3984-3986.

(80) Diaz-Mochon, J. J.; Bialy, L.; Keinicke, L.; Bradley, M. *Chem.Commun.* **2005**, 1384-1386.

(81) Ruiz-Ballesteros, E.; Mollejo, M.; Rodriguez, A.; Camacho, F. I.; Algara, P.; Martinez, N.; Pollan, M.; Sanchez-Aguilera, A.; Menarguez, J.; Campo, E.; Martinez, P.; Mateo, M.; Piris, M. A. *Blood* **2005**, *106*, 1831-1838.

(82) Kozarova, A.; Petrinac, S.; Ali, A.; Hudson, J. W. *J.Proteome Res.* **2006**, *5*, 1051-1059.

(83) Vidal, M. *Cell* **2001**, *104*, 333-339.

(84) Townsend, M. B.; Dawson, E. D.; Mehlmann, M.; Smagala, J. A.; Dankbar, D. M.; Moore, C. L.; Smith, C. B.; Cox, N. J.; Kuchta, R. D.; Rowlen, K. L. *J.Clin.Microbiol.* **2006**, *44*, 2863-2871.

(85) de, L. J.; Susce, M. T.; Pan, R. M.; Fairchild, M.; Koch, W. H.; Wedlund, P. J. *J.Clin.Psychiatry* **2005**, *66*, 15-27.

(86) Slater, K. *Curr.Opin.Biotechnol.* **2001**, *12*, 70-74.

(87) Harrison, R. *J.Exp.Zool.* **1914**, *17*, 521-544.

(88) Ranaldi, G.; Marigliano, I.; Vespignani, I.; Perozzi, G.; Sambuy, Y. *J.Nutr.Biochem.* **2002**, *13*, 157-167.

(89) Allen, L. T.; Tosetto, M.; Miller, I. S.; O'Connor, D. P.; Penney, S. C.; Lynch, I.; Keenan, A. K.; Pennington, S. R.; Dawson, K. A.; Gallagher, W. M. *Biomaterials* **2006**, *27*, 3096-3108.

(90) Liu, A. Y. *Cancer Res.* **2000**, *60*, 3429-3434.

(91) Kuschel, C.; Steuer, H.; Maurer, A. N.; Kanzok, B.; Stoop, R.; Angres, B. *Biotechniques* **2006**, *40*, 523-531.

(92) Flaim, C. J.; Chien, S.; Bhatia, S. N. *Nat.Methods* **2005**, *2*, 119-125.

(93) Ziauddin, J.; Sabatini, D. M. *Nature* **2001**, *411*, 107-110.

(94) Tourniaire, G.; Collins, J.; Campbell, S.; Mizomoto, H.; Ogawa, S.; Thaburet, J. F.; Bradley, M. *Chem.Commun.* **2006**, 2118-2120.

(95) Ko, I. K.; Kato, K.; Iwata, H. *Biomaterials* **2005**, *26*, 687-696.

(96) Chen, C. S.; Mrksich, M.; Huang, S.; Whitesides, G. M.; Ingber, D. E. *Science* **1997**, *276*, 1425-1428.

(97) Yamauchi, F.; Kato, K.; Iwata, H. *Biochim.Biophys.Acta* **2004**, *1672*, 138-147.

(98) Yamazoe, H.; Iwata, H. *J.Biosci.Bioeng.* **2005**, *100*, 292-296.

(99) Stephan, J. P.; Schanz, S.; Wong, A.; Schow, P.; Wong, W. L. *Am.J.Pathol.* **2002**, *161*, 787-797.

(100) Takita, M.; Furuya, T.; Sugita, T.; Kawauchi, S.; Oga, A.; Hirano, T.; Tsunoda, S.; Sasaki, K. *Cytometry A* **2003**, *55*, 24-29.

(101) Oode, K.; Furuya, T.; Harada, K.; Kawauchi, S.; Yamamoto, K.; Hirano, T.; Sasaki, K. *Am.J.Pathol.* **2000**, *157*, 723-728.

(102) Wilson, W. C., Jr.; Boland, T. *Anat.Rec.A Discov.Mol.Cell Evol.Biol.* **2003**, *272*, 491-496.

(103) Nakamura, M.; Kobayashi, A.; Takagi, F.; Watanabe, A.; Hiruma, Y.; Ohuchi, K.; Iwasaki, Y.; Horie, M.; Morita, I.; Takatani, S. *Tissue Eng.* **2005**, *11*, 1658-1666.

(104) Xu, T.; Jin, J.; Gregory, C.; Hickman, J. J.; Boland, T. *Biomaterials* **2005**, *26*, 93-99.

(105) LaVision BioTec-FIPS, http://www.lavisionbiotec.de/start_product_index.html, Accessed the 14th Nov. 2006.

(106) CellProfiler, http://jura.wi.mit.edu/cellprofiler/, Accessed the 14th Nov. 2006.

(107) Definiens Cellenger, http://www.definiens.com/products/cellenger.php, Accessed the 14th Nov. 2006.

(108) Imstar-HCS Pathfinder, http://www.imstar.fr/products/cytology/, Accessed the 14th Nov. 2006.

(109) How, S. E.; Yingyongnarongkul, B.; Fara, M. A.; Diaz-Mochon, J. J.; Mittoo, S.; Bradley, M. *Comb.Chem.High Throughput Screen.* **2004**, *7*, 423-430.

(110) Moffat, J.; Sabatini, D. M. *Nat.Rev.Mol.Cell Biol.* **2006**, *7*, 177-187.

(111) Yamauchi, F.; Kato, K.; Iwata, H. *Nucleic Acids Res.* **2004**, *32*, e187.

(112) Bailey, S. N.; Ali, S. M.; Carpenter, A. E.; Higgins, C. O.; Sabatini, D. M. *Nat.Methods* **2006**, *3*, 117-122.

(113) Kato, K.; Umezawa, K.; Funeriu, D. P.; Miyake, M.; Miyake, J.; Nagamune, T. *Biotechniques* **2003**, *35*, 1014-1021.

(114) Kato, K.; Umezawa, K.; Miyake, M.; Miyake, J.; Nagamune, T. *Biotechniques* **2004**, *37*, 444-452.

(115) Chang, T. W. *J.Immunol.Methods* **1983**, *65*, 217-223.

(116) Hoff, A.; Andre, T.; Schaffer, T. E.; Jung, G.; Wiesmuller, K. H.; Brock, R. *Chembiochem.* **2002**, *3*, 1183-1191.

(117) Campbell, C. J.; O'Looney, N.; Chong, K. M.; Robb, J. S.; Ross, A. J.; Beattie, J. S.; Petrik, J.; Ghazal, P. *Anal.Chem.* **2006**, *78*, 1930-1938.

(118) Drickamer, K. *Curr.Opin.Struct.Biol.* **1999**, *9*, 585-590.

(119) Soen, Y.; Chen, D. S.; Kraft, D. L.; Davis, M. M.; Brown, P. O. *PLoS.Biol.* **2003**, *1*, E65.

(120) Yamazaki, V.; Sirenko, O.; Schafer, R. J.; Nguyen, L.; Gutsmann, T.; Brade, L.; Groves, J. T. *BMC.Biotechnol.* **2005**, *5*, 18.

(121) Anderson, D. G.; Levenberg, S.; Langer, R. *Nat.Biotechnol.* **2004**, *22*, 863-866.

(122) Bailey, S. N.; Sabatini, D. M.; Stockwell, B. R. *Proc.Natl.Acad.Sci.U.S.A* **2004**, *101*, 16144-16149.

(123) Lee, M. Y.; Park, C. B.; Dordick, J. S.; Clark, D. S. *Proc.Natl.Acad.Sci.U.S.A* **2005**, *102*, 983-987.

(124) Balagadde, F. K.; You, L.; Hansen, C. L.; Arnold, F. H.; Quake, S. R. *Science* **2005**, *309*, 137-140.

(125) Whitesides, G. M. *Nature* **2006**, *442*, 368-373.

(126) El-Ali, J.; Sorger, P. K.; Jensen, K. F. *Nature* **2006**, *442*, 403-411.

(127) Huang, Y.; Joo, S.; Duhon, M.; Heller, M.; Wallace, B.; Xu, X. *Anal.Chem.* **2002**, *74*, 3362-3371.

(128) Fuchs, A. B.; Romani, A.; Freida, D.; Medoro, G.; Abonnenc, M.; Altomare, L.; Chartier, I.; Guergour, D.; Villiers, C.; Marche, P. N.; Tartagni, M.; Guerrieri, R.; Chatelain, F.; Manaresi, N. *Lab Chip* **2006**, *6*, 121-126.

(129) Albrecht, D. R.; Tsang, V. L.; Sah, R. L.; Bhatia, S. N. *Lab Chip* **2005**, *5*, 111-118.

(130) Williams, D. F. *Definitions in Biomaterials - Proceedings of a Consensus Conference of the European Society for Biomaterials*; Elsevier: New York, 1987.

(131) Langer, R.; Tirrell, D. A. *Nature* **2004**, *428*, 487-492.

(132) Williams, D. F. *Med.Device Technol.* **2003**, *14*, 10-13.

(133) Elwing, H.; Askendal, A.; Lundstrom, I. *J.Biomed.Mater.Res.* **1987**, *21*, 1023-1028.

(134) Courtney, J. M.; Forbes, C. D. *Br.Med.Bull.* **1994**, *50*, 966-981.

(135) Elwing, H. *Biomaterials* **1998**, *19*, 397-406.

(136) Remes, A.; Williams, D. F. *Biomaterials* **1992**, *13*, 731-743.

(137) Colman, R. W. *J.Clin.Invest* **1984**, *73*, 1249-1253.

(138) Hirsh, J. *Annu.Rev.Med.* **1987**, *38*, 91-105.

(139) Gristina, A. G. *Science* **1987**, *237*, 1588-1595.

(140) Brem, H.; Kirsner, R. S.; Falanga, V. *Am.J.Surg.* **2004**, *188*, 1-8.

(141) Labarre, D. *Trends Biomater.Artif.Organs* **2001**, *15*, 1-3.

(142) Uchida, E.; Uyama, Y.; Ikada, Y. *Langmuir* **1994**, *10*, 481-485.

(143) Lopez, G. P.; Albers, M. W.; Schreiber, S. L.; Carroll, R.; Peralta, E.; Whitesides, G. M. *J.Am.Chem.Soc.* **1993**, *115*, 5877-5878.

(144) Kiaei, D.; Hoffman, A. S.; Horbett, T. A. *J.Biomater.Sci.Polym.Ed.* **1992**, *4*, 35-44.

(145) Kiaei, D.; Hoffman, A. S.; Horbett, T. A.; Lew, K. R. *J.Biomed.Mater.Res.* **1995**, *29*, 729-739.

(146) Langer, R.; Peppas, N. A. *AIChE J.* **2003**, *49*, 2990-3006.

(147) Ratner, B. D.; Bryant, S. J. *Annu.Rev.Biomed.Eng* **2004**, *6*, 41-75.

(148) Sawhney, A. S.; Pathak, C. P.; Hubbell, J. A. *Macromolecules* **1993**, *26*, 581-587.

(149) Peter, S. J.; Suggs, L. J.; Yaszemski, M. J.; Engel, P. S.; Mikos, A. G. *J.Biomater.Sci.Polym.Ed.* **1999**, *10*, 363-373.

(150) Uchida, K.; Yamato, M.; Ito, E.; Kwon, O. H.; Kikuchi, A.; Sakai, K.; Okano, T. *J.Biomed.Mater.Res.* **2000**, *50*, 585-590.

(151) Ito, E.; Suzuki, K.; Yamato, M.; Yokoyama, M.; Sakurai, Y.; Okano, T. *J.Biomed.Mater.Res.* **1998**, *42*, 148-155.

(152) Gray, J. E.; Norton, P. R.; Griffiths, K. *Appl.Surf.Sci.* **2003**, *217*, 210-222.

(153) Elbert, D. L.; Hubbell, J. A. *Annu.Rev.Mat.Sci.* **1996**, *26*, 365-394.

(154) Nomizu, M.; Weeks, B. S.; Weston, C. A.; Kim, W. H.; Kleinman, H. K.; Yamada, Y. *FEBS Lett.* **1995**, *365*, 227-231.

(155) Varki, A. *Proc.Natl.Acad.Sci.U.S.A* **1994**, *91*, 7390-7397.

(156) Lopina, S. T.; Wu, G.; Merrill, E. W.; Griffith-Cima, L. *Biomaterials* **1996**, *17*, 559-569.

(157) Michanetzis, G. P.; Katsala, N.; Missirlis, Y. F. *Biomaterials* **2003**, *24*, 677-688.

(158) Nguyen, K. T.; Su, S. H.; Sheng, A.; Wawro, D.; Schwade, N. D.; Brouse, C. F.; Greilich, P. E.; Tang, L.; Eberhart, R. C. *Biomaterials* **2003**, *24*, 5191-5201.

(159) Anderson, D. G.; Burdick, J. A.; Langer, R. *Science* **2004**, *305*, 1923-1924.

(160) Murthy, N.; Campbell, J.; Fausto, N.; Hoffman, A. S.; Stayton, P. S. *Bioconjug.Chem.* **2003**, *14*, 412-419.

(161) von Recum, H. A.; Kim, S. W.; Kikuchi, A.; Okuhara, M.; Sakurai, Y.; Okano, T. *J.Biomed.Mater.Res.* **1998**, *40*, 631-639.

(162) Schmatloch, S.; Schubert, U. S. *Macromol.Rapid Commun.* **2004**, *25*, 69-76.

(163) Washburn, N. R.; Yamada, K. M.; Simon, C. G., Jr.; Kennedy, S. B.; Amis, E. J. *Biomaterials* **2004**, *25*, 1215-1224.

(164) Meredith, J. C.; Smith, A. P.; Karim, A.; Amis, E. J. *Macromolecules* **2000**, *33*, 9747-9756.

(165) Danielson, E.; Golden, J. H.; McFarland, E. W.; Reaves, C. M.; Weinberg, W. H.; Wu, X. D. *Nature* **1997**, *389*, 944-948.

(166) Mei, Y.; Kumar, A.; Gao, W.; Gross, R.; Kennedy, S. B.; Washburn, N. R.; Amis, E. J.; Elliott, J. T. *Biomaterials* **2004**, *25*, 4195-4201.

(167) 10X Blocking buffer product information, http://www.sigmaaldrich.com/sigma/datasheet/B6429dat.pdf, Accessed the 14th Nov. 2006.

(168) Forster, T. *Annalen der Physik* **1948**, *2*, 55-75.

(169) Gersten, J.; Nitzan, A. *J.Chem.Phys.* **1981**, *75*, 1139-1152.

(170) Ishida, A.; Majima, T. *Analyst* **2000**, *125*, 535-540.

(171) Liebermann, T.; Knoll, W. *Colloids Surf., A* **2000**, *171*, 115-130.

(172) Dulkeith, E.; Morteani, A. C.; Niedereichholz, T.; Klar, T. A.; Feldmann, J.; Levi, S. A.; van Veggel, F. C. J. M.; Reinhoudt, D. N.; Moller, M.; Gittins, D. I. *Phys.Rev.Lett.* **2002**, *89*.

(173) Folkman, J.; Moscona, A. *Nature* **1978**, *273*, 345-349.

(174) Folch, A.; Toner, M. *Annu.Rev.Biomed.Eng.* **2000**, *2*, 227-256.

(175) Deegan, R. D.; Bakajin, O.; Dupont, T. F.; Huber, G.; Nagel, S. R.; Witten, T. A. *Nature* **1997**, *389*, 827-829.

(176) Johann, R. M. *Anal.Bioanal.Chem.* **2006**, *385*, 408-412.

(177) Leifer, D.; Lipton, S. A.; Barnstable, C. J.; Masland, R. H. *Science* **1984**, *224*, 303-306.

(178) De Silva, M. N.; Paulsen, J.; Renn, M. J.; Odde, D. J. *Biotechnol.Bioeng.* **2006**, *93*, 919-927.

(179) Weiss, A.; Wiskocil, R. L.; Stobo, J. D. *J.Immunol.* **1984**, *133*, 123-128.

(180) Engelhard, V. H.; Strominger, J. L.; Mescher, M.; Burakoff, S. *Proc.Natl.Acad.Sci.U.S.A* **1978**, *75*, 5688-5691.

(181) Ljunggren, H. G.; Karre, K. *J.Exp.Med.* **1985**, *162*, 1745-1759.

(182) Ljunggren, H. G.; Paabo, S.; Cochet, M.; Kling, G.; Kourilsky, P.; Karre, K. *J.Immunol.* **1989**, *142*, 2911-2917.

(183) Rossi, M.; Young, J. W. *J.Immunol.* **2005**, *175*, 1373-1381.

(184) Rock, K. L.; Shen, L. *Immunol.Rev.* **2005**, *207*, 166-183.

(185) Pierre, P.; Turley, S. J.; Gatti, E.; Hull, M.; Meltzer, J.; Mirza, A.; Inaba, K.; Steinman, R. M.; Mellman, I. *Nature* **1997**, *388*, 787-792.

(186) Cougoule, C.; Wiedemann, A.; Lim, J.; Caron, E. *Semin.Cell Dev.Biol.* **2004**, *15*, 679-689.

(187) DeMali, K. A.; Burridge, K. *J.Cell Sci.* **2003**, *116*, 2389-2397.

(188) Alison, M. R.; Poulsom, R.; Forbes, S.; Wright, N. A. *J.Pathol.* **2002**, *197*, 419-423.

(189) Eckfeldt, C. E.; Mendenhall, E. M.; Verfaillie, C. M. *Nat.Rev.Mol.Cell Biol.* **2005**, *6*, 726-737.

(190) Edwards, R. G. *Reprod.Biomed.Online* **2004**, *9*, 541-583.

(191) de Wynter, E. A.; Emmerson, A. J.; Testa, N. G. *Baillieres Best Pract.Res.Clin.Haematol.* **1999**, *12*, 1-17.

(192) Burkert, J.; Wright, N. A.; Alison, M. R. *J.Pathol.* **2006**, *209*, 287-297.

(193) Guo, W.; Lasky, J. L., III; Wu, H. *Pediatr.Res.* **2006**, *59*, 59R-64R.

(194) Dupont, B. *Immunol.Rev.* **1997**, *157*, 5-12.

(195) Srivastava, D.; Ivey, K. N. *Nature* **2006**, *441*, 1097-1099.

(196) Lindvall, O.; Kokaia, Z. *Nature* **2006**, *441*, 1094-1096.

(197) Rando, T. A. *Nature* **2006**, *441*, 1080-1086.

(198) Davila, J. C.; Cezar, G. G.; Thiede, M.; Strom, S.; Miki, T.; Trosko, J. *Toxicol.Sci.* **2004**, *79*, 214-223.

(199) Pouton, C. W.; Haynes, J. M. *Adv.Drug Deliv.Rev.* **2005**, *57*, 1918-1934.

(200) McNeish, J. *Nat.Rev.Drug Discov.* **2004**, *3*, 70-80.

(201) Thomson, J. A.; Itskovitz-Eldor, J.; Shapiro, S. S.; Waknitz, M. A.; Swiergiel, J. J.; Marshall, V. S.; Jones, J. M. *Science* **1998**, *282*, 1145-1147.

(202) Compston, J. E. *J.Endocrinol.* **2002**, *173*, 387-394.

(203) Owen, M. *J.Cell Sci.Suppl* **1988**, *10*, 63-76.

(204) Pittenger, M. F.; Mackay, A. M.; Beck, S. C.; Jaiswal, R. K.; Douglas, R.; Mosca, J. D.; Moorman, M. A.; Simonetti, D. W.; Craig, S.; Marshak, D. R. *Science* **1999**, *284*, 143-147.

(205) Horwitz, E. M.; Le, B. K.; Dominici, M.; Mueller, I.; Slaper-Cortenbach, I.; Marini, F. C.; Deans, R. J.; Krause, D. S.; Keating, A. *Cytotherapy.* **2005**, *7*, 393-395.

(206) Howard, D.; Partridge, K.; Yang, X.; Clarke, N. M.; Okubo, Y.; Bessho, K.; Howdle, S. M.; Shakesheff, K. M.; Oreffo, R. O. *Biochem.Biophys.Res.Commun.* **2002**, *299*, 208-215.

(207) Simmons, P. J.; Torok-Storb, B. *Blood* **1991**, *78*, 55-62.

(208) Stewart, K.; Walsh, S.; Screen, J.; Jefferiss, C. M.; Chainey, J.; Jordan, G. R.; Beresford, J. N. *J.Bone Miner.Res.* **1999**, *14*, 1345-1356.

(209) Pease, S.; Braghetta, P.; Gearing, D.; Grail, D.; Williams, R. L. *Dev.Biol.* **1990**, *141*, 344-352.

(210) Xu, C.; Inokuma, M. S.; Denham, J.; Golds, K.; Kundu, P.; Gold, J. D.; Carpenter, M. K. *Nat.Biotechnol.* **2001**, *19*, 971-974.

(211) Smith, A. G.; Heath, J. K.; Donaldson, D. D.; Wong, G. G.; Moreau, J.; Stahl, M.; Rogers, D. *Nature* **1988**, *336*, 688-690.

(212) Williams, R. L.; Hilton, D. J.; Pease, S.; Willson, T. A.; Stewart, C. L.; Gearing, D. P.; Wagner, E. F.; Metcalf, D.; Nicola, N. A.; Gough, N. M. *Nature* **1988**, *336*, 684-687.

(213) Rosner, M. H.; Vigano, M. A.; Ozato, K.; Timmons, P. M.; Poirier, F.; Rigby, P. W.; Staudt, L. M. *Nature* **1990**, *345*, 686-692.

(214) Pesce, M.; Scholer, H. R. *Stem Cells* **2001**, *19*, 271-278.

(215) Herr, W.; Sturm, R. A.; Clerc, R. G.; Corcoran, L. M.; Baltimore, D.; Sharp, P. A.; Ingraham, H. A.; Rosenfeld, M. G.; Finney, M.; Ruvkun, G. *Genes Dev.* **1988**, *2*, 1513-1516.

(216) Nichols, J.; Zevnik, B.; Anastassiadis, K.; Niwa, H.; Klewe-Nebenius, D.; Chambers, I.; Scholer, H.; Smith, A. *Cell* **1998**, *95*, 379-391.

(217) Niwa, H. *Cell Struct.Funct.* **2001**, *26*, 137-148.

(218) Chalfie, M.; Tu, Y.; Euskirchen, G.; Ward, W. W.; Prasher, D. C. *Science* **1994**, *263*, 802-805.

(219) Prasher, D. C. *Trends Genet.* **1995**, *11*, 320-323.

(220) Yoshimizu, T.; Sugiyama, N.; De, F. M.; Yeom, Y. I.; Ohbo, K.; Masuko, K.; Obinata, M.; Abe, K.; Scholer, H. R.; Matsui, Y. *Dev.Growth Differ.* **1999**, *41*, 675-684.

(221) Gendall, A. R.; Dunn, A. R.; Ernst, M. *Int.J.Biochem.Cell Biol.* **1997**, *29*, 829-840.

(222) Zandstra, P. W.; Le, H. V.; Daley, G. Q.; Griffith, L. G.; Lauffenburger, D. A. *Biotechnol.Bioeng.* **2000**, *69*, 607-617.

(223) Rathjen, P. D.; Toth, S.; Willis, A.; Heath, J. K.; Smith, A. G. *Cell* **1990**, *62*, 1105-1114.

(224) Perez-Iratxeta, C.; Palidwor, G.; Porter, C. J.; Sanche, N. A.; Huska, M. R.; Suomela, B. P.; Muro, E. M.; Krzyzanowski, P. M.; Hughes, E.; Campbell, P. A.; Rudnicki, M. A.; Andrade, M. A. *FEBS Lett.* **2005**, *579*, 1795-1801.

(225) Li, L.; Akashi, K. *Biotechniques* **2003**, *35*, 1233-1239.

(226) Yoshikawa, T.; Uchimura, E.; Kishi, M.; Funeriu, D. P.; Miyake, M.; Miyake, J. *J. Controlled Release* **2004**, *96*, 227-232.

(227) Olivier, V.; Faucheux, N.; Hardouin, P. *Drug Discov.Today* **2004**, *9*, 803-811.

(228) Reddy, M. M.; Kodadek, T. *Proc.Natl.Acad.Sci.U.S.A* **2005**, *102*, 12672-12677.

(229) Thaburet, J. F. O.; Mizomoto, H.; Bradley, M. *Macromol. Rapid Commun.* **2004**, *25*, 366-370.

(230) Mizomoto, H. *The synthesis and screening of polymer libraries using a high throughput approach.* **2004**, PhD thesis, University of Southampton, Southampton, UK.

(231) Jose, A. J. *Synthesis and screening of biocompatible polymers using a multiparallel approach.* **2005**, PhD thesis, University of Southampton, Southampton, UK.

(232) Fibrinogen from human plasma product information, http://www.sigmaaldrich.com/sigma/product%20information%20sheet/f3879pis.pdf, Accessed the 14th Nov. 2006.

(233) AlexaFluor 647 protein labelling kit, http://probes.invitrogen.com/media/pis/mp20173.pdf, Accessed the 14th Nov. 2006.

(234) Lutz, M. B.; Kukutsch, N.; Ogilvie, A. L.; Rossner, S.; Koch, F.; Romani, N.; Schuler, G. *J.Immunol.Methods* **1999**, *223*, 77-92.

Appendix I: poly(urethane) library[229]

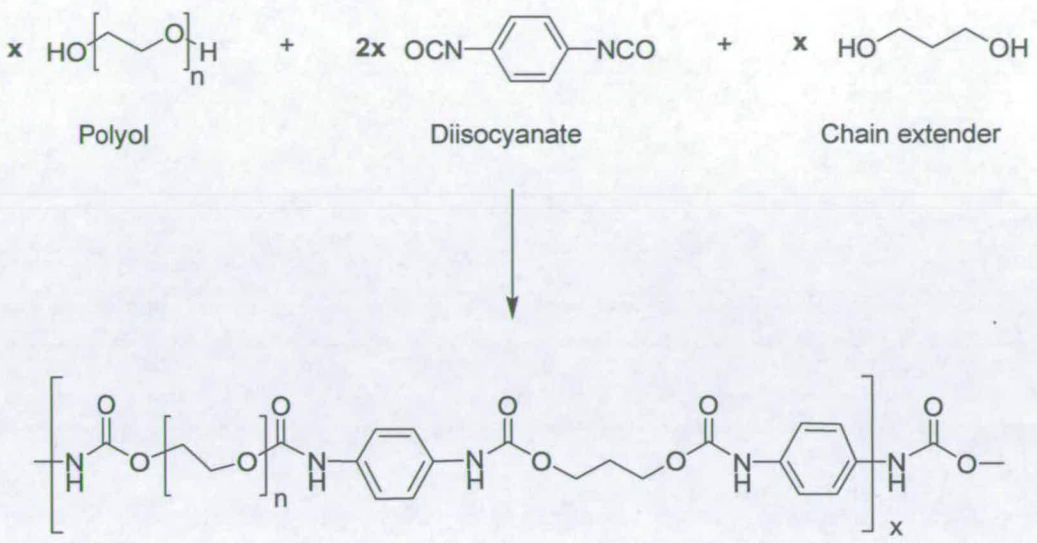

Synthesis of the poly(urethanes)

Polyol	Diisocyanate	Chain Extender
PEG	BICH	ED
PPG	MDI	EG
PTMG	HDI	PG
PHNAD	HMDI	BD
PHNGAD	PDI	DMAPD
	TDI	DEAPD
		DHM
		NMPD
		OFHD

PHNAD: R= $-CH_2(CH_2)_4CH_2-$, $-CH_2C(CH_3)_2CH_2-$

PHNGAD: R= $-CH_2(CH_2)_4CH_2-$, $-CH_2C(CH_3)_2CH_2-$, $-CH_2CH_2OCH_2CH_2-$

List of monomers used in the synthesis of the poly(urethanes).

Monomer abbreviations:

Polyol:

PEG:	poly(ethylene glycol)
PPG:	poly(propylene glycol)
PTMG:	poly(tetramethylene glycol)
PHNAD:	poly[1,6-hexanediol/neopentyl glycol-*alt*-(adiptic acid)]diol
PHNGAD:	poly[1,6-hexanediol/neopentyl glycol/diethylene glycol-*alt*-(adiptic acid)]diol

Diisocyanate (Dis.):

BICH:	1,3-bis(isocyananatomethyl)cyclohexane
MDI:	4,4'-methylenebis(phenylisocyanate)
HDI:	1,6-diisocyanohexane
HMDI:	4,4'-methylenebis(cyclohexylisocyanate)
PDI:	1,4-diisocyanobenzene
TDI:	4-methyl-1,3-phenylene diisocyanate

Chain Extender (Ext.):

ED:	ethylene diamine
BD:	1,4-butanediol
EG:	ethylene glycol
PG:	propylene glycol
DMAPD:	3-dimethylamino-1,2-propanediol
DEAPD:	3-diethylamino-1,2-propanediol
DHM:	diethyl bis(hydroxymethyl)malonate
NMPD:	2-nitro-2-methyl-1,3-propanediol
OFHD:	2,2,3,3,4,4,5,5-octafluoro-1,6-hexanediol

Polymer reference	Polyol		Diisocyanate	Chain Extender	Ratio (% mol.)			Molecular weight		
	Nature	MW (Da)			M (Polyol)	M (Diisocyanate)	M (Extender)	Mw	Mn	D
1	PEG	2000	HDI	none	48.5	51.5	0.0	58000	24000	2.4
2	PEG	900	HDI	none	48.5	51.5	0.0	430000	92000	4.5
3	PEG	400	HDI	none	48.5	51.5	0.0	163000	62000	2.6
4	PPG	2000	HDI	none	48.5	51.5	0.0	65000	32000	2.0
5	PTMG	2000	HDI	none	48.5	51.5	0.0	40000	24000	1.7
6	PEG	2000	BICH	none	48.5	51.5	0.0	59000	29000	2.0
7	PEG	900	BICH	none	48.5	51.5	0.0	228000	98000	2.3
8	PEG	400	BICH	none	48.5	51.5	0.0	200000	80000	2.2
9	PPG	2000	BICH	none	48.5	51.5	0.0	43000	21000	1.9
10	PTMG	2000	BICH	none	48.5	51.5	0.0	94000	44000	2.1
12	PEG	900	TDI	none	48.5	51.5	0.0	138000	32000	4.4
13	PEG	400	TDI	none	48.5	51.5	0.0	38000	21000	1.8
14	PPG	2000	TDI	none	48.5	51.5	0.0	77000	36000	2.1
15	PTMG	2000	TDI	none	48.5	51.5	0.0	53000	28000	1.9
16	PEG	2000	MDI	none	48.5	51.5	0.0	90000	45000	2.0
17	PEG	900	MDI	none	48.5	51.5	0.0	151000	57000	2.7
18	PEG	400	MDI	none	48.5	51.5	0.0	61000	26000	2.4
19	PPG	2000	MDI	none	48.5	51.5	0.0	53000	27000	1.9
20	PTMG	2000	MDI	none	48.5	51.5	0.0	87000	48000	1.8
21	PEG	2000	PDI	none	48.5	51.5	0.0	73000	37000	2.0
22	PEG	900	PDI	none	48.5	51.5	0.0	242000	81000	3.0
23	PEG	400	PDI	none	48.5	51.5	0.0	162000	43000	3.8
24	PPG	2000	PDI	none	48.5	51.5	0.0	73000	41000	1.8
25	PTMG	2000	PDI	none	48.5	51.5	0.0	103000	44000	2.2
26	PEG	2000	HMDI	none	48.5	51.5	0.0	41000	21000	1.9
27	PEG	900	HMDI	none	48.5	51.5	0.0	32000	18000	1.8
28	PEG	400	HMDI	none	48.5	51.5	0.0	101000	55000	1.8
29	PPG	2000	HMDI	none	48.5	51.5	0.0	44000	30000	1.5
30	PTMG	2000	HMDI	none	48.5	51.5	0.0	81000	48000	1.7
31	PEG	2000	HDI	BD	25.0	52.0	23.0	71000	25000	2.8
33	PEG	900	HDI	BD	25.0	52.0	23.0	45000	22000	2.0
35	PEG	400	HDI	BD	25.0	52.0	23.0	196000	69000	2.8
37	PPG	2000	HDI	BD	25.0	52.0	23.0	75000	36000	2.1
38	PPG	2000	HDI	ED	25.0	52.0	23.0	156000	75000	2.1
39	PTMG	2000	HDI	BD	25.0	52.0	23.0	99000	58000	1.7
40	PTMG	2000	HDI	ED	25.0	52.0	23.0	20000	11000	1.9
41	PEG	2000	BICH	BD	25.0	52.0	23.0	45000	25000	1.8
43	PEG	900	BICH	BD	25.0	52.0	23.0	46000	25000	1.8
44	PEG	900	BICH	ED	25.0	52.0	23.0	450000	123000	3.6
45	PEG	400	BICH	BD	25.0	52.0	23.0	70000	39000	1.8
46	PEG	400	BICH	ED	25.0	52.0	23.0	130000	15000	8.5
47	PPG	2000	BICH	BD	25.0	52.0	23.0	70000	31000	2.2
48	PPG	2000	BICH	ED	25.0	52.0	23.0	583000	90000	6.5
49	PTMG	2000	BICH	BD	25.0	52.0	23.0	95000	45000	2.1
50	PTMG	2000	BICH	ED	25.0	52.0	23.0	163000	29000	5.5
51	PEG	2000	TDI	BD	25.0	52.0	23.0	74000	36000	2.1
53	PEG	900	TDI	BD	25.0	52.0	23.0	120000	37000	3.2
55	PEG	400	TDI	BD	25.0	52.0	23.0	71000	26000	2.8
57	PPG	2000	TDI	BD	25.0	52.0	23.0	95000	37000	2.6
59	PTMG	2000	TDI	BD	25.0	52.0	23.0	77000	45000	1.7
61	PEG	2000	MDI	BD	25.0	52.0	23.0	156000	56000	2.8
63	PEG	900	MDI	BD	25.0	52.0	23.0	47000	23000	2.0
65	PEG	400	MDI	BD	25.0	52.0	23.0	76000	38000	2.0
67	PPG	2000	MDI	BD	25.0	52.0	23.0	99000	44000	2.3
69	PTMG	2000	MDI	BD	25.0	52.0	23.0	113000	53000	2.1
71	PEG	2000	PDI	BD	25.0	52.0	23.0	93000	35000	2.7
73	PEG	900	PDI	BD	25.0	52.0	23.0	50000	26000	1.9
77	PPG	2000	PDI	BD	25.0	52.0	23.0	70000	32000	2.2
79	PTMG	2000	PDI	BD	25.0	52.0	23.0	81000	30000	2.7
81	PEG	2000	HMDI	BD	25.0	52.0	23.0	81000	39000	2.1
83	PEG	900	HMDI	BD	25.0	52.0	23.0	145000	46000	3.1
85	PEG	400	HMDI	BD	25.0	52.0	23.0	123000	57000	2.1
87	PPG	2000	HMDI	BD	25.0	52.0	23.0	48000	25000	1.9
89	PTMG	2000	HMDI	BD	25.0	52.0	23.0	54000	32000	1.7
39DE	PTMG	2000	HDI	DEAPD	25.0	52.0	23.0	68000	36000	1.8
39DM	PTMG	2000	HDI	DMAPD	25.0	52.0	23.0	72000	29000	2.5
49DM	PTMG	2000	BICH	DMAPD	25.0	52.0	23.0	70000	39000	1.8
49DE	PTMG	2000	BICH	DEAPD	25.0	52.0	23.0	51000	26000	2.0
91	PTMG	650	HDI	BD	48.5	51.5	0.0	179000	95000	1.9
92	PTMG	1000	HDI	BD	48.5	51.5	0.0	146000	78000	1.9

Polymer reference	Polyol		Diisocyanate	Chain Extender	Ratio (% mol.)			Molecular weight		
	Nature	MW (Da)			M (Polyol)	M (Diisocyanate)	M (Extender)	Mw	Mn	D
93	PTMG	650	BICH	BD	48.5	51.5	0.0	109000	49000	2.2
94	PTMG	1000	BICH	BD	48.5	51.5	0.0	170000	90000	1.9
95	PTMG	650	MDI	BD	48.5	51.5	0.0	52000	26000	2.0
96	PTMG	1000	MDI	BD	48.5	51.5	0.0	66000	34000	1.9
97	PHNGAD	1800	BICH	DMAPD	25.0	52.0	23.0	121000	55000	2.2
98	PHNGAD	1800	BICH	DEAPD	25.0	52.0	23.0	150000	60000	2.6
99	PTMG	650	HDI	DMAPD	25.0	52.0	23.0	125000	62000	2.0
100	PTMG	1000	HDI	DMAPD	25.0	52.0	23.0	81000	41000	2.0
101	PTMG	650	BICH	DMAPD	25.0	52.0	23.0	63000	34000	1.9
102	PTMG	1000	BICH	DMAPD	25.0	52.0	23.0	121000	58000	2.0
103	PHNGAD	1800	MDI	DMAPD	25.0	52.0	23.0	55000	25000	2.2
104	PHNGAD	1800	MDI	DEAPD	25.0	52.0	23.0	38000	17000	2.1
105	PHNGAD	1800	HDI	DMAPD	25.0	52.0	23.0	78000	27000	2.9
106	PHNGAD	1800	HDI	DEAPD	25.0	52.0	23.0	52000	24000	2.2
107	PTMG	650	HDI	DEAPD	25.0	52.0	23.0	233000	95000	2.5
109	PTMG	650	BICH	DEAPD	25.0	52.0	23.0	80000	41000	2.0
110	PTMG	1000	BICH	DEAPD	25.0	52.0	23.0	147000	52000	1.7
111	PTMG	650	MDI	DEAPD	25.0	52.0	23.0	84000	36000	2.2
112	PTMG	1000	MDI	DEAPD	25.0	52.0	23.0	52000	27000	1.9
113	PTMG	2000	MDI	DEAPD	25.0	52.0	23.0	76000	36000	2.1
114	PPG	425	HDI	BD	48.5	51.5	0.0	64000	30000	2.1
115	PPG	1000	HDI	BD	48.5	51.5	0.0	91000	37000	2.3
116	PPG	425	BICH	BD	48.5	51.5	0.0	63000	40000	1.6
117	PPG	1000	BICH	BD	48.5	51.5	0.0	138000	68000	2.0
118	PPG	425	MDI	DMAPD	25.0	52.0	23.0	72000	25000	2.9
119	PPG	1000	MDI	DMAPD	25.0	52.0	23.0	63000	30000	2.2
120	PPG	425	BICH	DEAPD	25.0	52.0	23.0	46000	26000	1.8
121	PPG	1000	BICH	DEAPD	25.0	52.0	23.0	172000	63000	2.7
122	PPG	2000	BICH	DEAPD	25.0	52.0	23.0	106000	51000	2.1
123	PPG	2000	MDI	DMAPD	25.0	52.0	23.0	58000	30000	1.9
124	PPG	2000	TDI	DMAPD	25.0	52.0	23.0	60000	34000	1.8
125	PPG	1000	TDI	DMAPD	25.0	52.0	23.0	110000	32000	3.5
126	PPG	425	TDI	DMAPD	25.0	52.0	23.0	64000	21000	3.1
127	PPG	1000	BICH	DMAPD	25.0	52.0	23.0	165000	79000	2.2
128	PPG	2000	BICH	DMAPD	25.0	52.0	23.0	N.D.	N.D.	N.D.
129	PPG	425	BICH	DMAPD	25.0	52.0	23.0	104000	45000	2.3
130	PTMG	650	TDI	DMAPD	25.0	52.0	23.0	66000	34000	1.9
131	PTMG	1000	TDI	DMAPD	25.0	52.0	23.0	82000	32000	2.5
132	PHNGAD	1800	BICH	BD	25.0	52.0	23.0	76000	32000	2.1
133	PHNGAD	1800	HDI	BD	25.0	52.0	23.0	70000	30000	2.3
134	PHNGAD	1800	MDI	BD	25.0	52.0	23.0	64000	25000	2.5
135	PTMG	250	BICH	DMAPD	25.0	52.0	23.0	36000	19500	1.9
136	PTMG	250	BICH	DEAPD	25.0	52.0	23.0	121000	47000	2.6
137	PTMG	250	BICH	BD	25.0	52.0	23.0	34000	20000	1.7
138	PTMG	250	BICH	EG	25.0	52.0	23.0	47000	28000	1.7
139	PTMG	650	BICH	EG	25.0	52.0	23.0	75000	44000	1.7
140	PTMG	1000	BICH	EG	25.0	52.0	23.0	76000	44000	1.7
141	PTMG	2000	BICH	EG	25.0	52.0	23.0	54000	32000	1.7
142	PTMG	250	BICH	PG	25.0	52.0	23.0	75000	36000	2.1
143	PTMG	650	BICH	PG	25.0	52.0	23.0	73000	36000	2.0
144	PTMG	1000	BICH	PG	25.0	52.0	23.0	51000	31000	1.7
145	PTMG	2000	BICH	PG	25.0	52.0	23.0	98000	56000	1.7
146	PTMG	250	HDI	DMAPD	25.0	52.0	23.0	69000	36000	1.8
147	PTMG	250	HDI	DEAPD	25.0	52.0	23.0	58000	27000	2.1
148	PTMG	250	HDI	BD	25.0	52.0	23.0	80000	42000	1.9
149	PTMG	250	HDI	EG	25.0	52.0	23.0	43000	24000	1.8
150	PTMG	650	HDI	EG	25.0	52.0	23.0	155000	71000	2.2
151	PTMG	1000	HDI	EG	25.0	52.0	23.0	58000	35000	1.7
152	PTMG	2000	HDI	EG	25.0	52.0	23.0	90000	54000	1.7
153	PTMG	250	HDI	PG	25.0	52.0	23.0	310000	102000	3.0
154	PTMG	650	HDI	PG	25.0	52.0	23.0	208000	105000	2.0
155	PTMG	1000	HDI	PG	25.0	52.0	23.0	85000	51000	1.7
156	PTMG	2000	HDI	PG	25.0	52.0	23.0	101000	50000	2.0
157	PTMG	250	MDI	DMAPD	25.0	52.0	23.0	41000	21000	1.9
158	PTMG	250	MDI	OFHD	25.0	52.0	23.0	49000	22000	2.2
159	PTMG	250	MDI	BD	25.0	52.0	23.0	55000	25000	2.2

Polymer reference	Polyol		Diisocyanate	Chain Extender	Ratio (% mol.)			Molecular weight		
	Nature	MW (Da)			M (Polyol)	M (Diisocyanate)	M (Extender)	Mw	Mn	D
160	PTMG	250	MDI	EG	25.0	52.0	23.0	91000	36000	2.5
161	PTMG	650	MDI	EG	25.0	52.0	23.0	188000	86000	2.2
162	PTMG	1000	MDI	EG	25.0	52.0	23.0	160000	74000	2.2
163	PTMG	2000	MDI	EG	25.0	52.0	23.0	203000	79000	2.6
164	PTMG	250	MDI	PG	25.0	52.0	23.0	55000	28000	1.9
165	PTMG	650	MDI	PG	25.0	52.0	23.0	78000	41000	2.0
166	PTMG	1000	MDI	PG	25.0	52.0	23.0	90000	50000	1.8
167	PTMG	2000	MDI	PG	25.0	52.0	23.0	78000	39000	2.0
168	PTMG	250	BICH	none	48.5	51.5	0.0	80000	41000	2.0
169	PTMG	650	BICH	none	48.5	51.5	0.0	90000	30000	3.0
170	PTMG	1000	BICH	none	48.5	51.5	0.0	190000	101000	1.9
171	PTMG	250	HDI	none	48.5	51.5	0.0	128000	69000	1.8
172	PTMG	650	HDI	none	48.5	51.5	0.0	128000	69000	1.8
173	PTMG	1000	HDI	none	48.5	51.5	0.0	190000	114000	1.7
174	PTMG	250	MDI	none	48.5	51.5	0.0	196000	88000	2.2
175	PTMG	650	MDI	none	48.5	51.5	0.0	107000	55000	2.0
176	PTMG	1000	MDI	none	48.5	51.5	0.0	152000	75000	2.0
177	PTMG	250	HDI	NMPD	25.0	52.0	23.0	50000	29000	1.7
178	PTMG	1000	HDI	NMPD	25.0	52.0	23.0	61000	31000	2.0
179	PTMG	2000	HDI	NMPD	25.0	52.0	23.0	58000	33000	1.7
180	PTMG	1000	BICH	NMPD	25.0	52.0	23.0	46000	26000	1.8
181	PTMG	2000	BICH	NMPD	25.0	52.0	23.0	48000	28000	1.7
182	PTMG	650	MDI	NMPD	25.0	52.0	23.0	203000	59000	3.4
183	PTMG	1000	MDI	NMPD	25.0	52.0	23.0	84000	33000	2.5
184	PTMG	2000	MDI	NMPD	25.0	52.0	23.0	104000	45000	2.3
185	PHNAD	900	MDI	OFHD	17.0	52.0	33.0	65000	34000	1.9
186	PTMG	650	BICH	OFHD	25.0	52.0	23.0	59000	34000	1.8
187	PTMG	1000	BICH	OFHD	25.0	52.0	23.0	46000	27000	1.7
188	PTMG	2000	BICH	OFHD	25.0	52.0	23.0	63000	38000	1.7
189	PPG	1000	BICH	OFHD	17.0	52.0	33.0	40000	26000	1.5
190	PTMG	650	HDI	OFHD	25.0	52.0	23.0	63000	38000	1.8
191	PTMG	1000	HDI	OFHD	25.0	52.0	23.0	55000	36000	1.5
192	PTMG	2000	HDI	OFHD	25.0	52.0	23.0	50000	28000	1.8
193	PPG	1000	MDI	DMAPD	17.0	52.0	33.0	37000	19000	1.9
194	PTMG	650	MDI	OFHD	25.0	52.0	23.0	52000	27000	1.9
195	PTMG	1000	MDI	OFHD	25.0	52.0	23.0	81000	38000	2.1
196	PTMG	2000	MDI	OFHD	25.0	52.0	23.0	51000	29000	1.8
197	PTMG	650	BICH	DHM	25.0	52.0	23.0	44000	25000	1.8
198	PTMG	1000	BICH	DHM	25.0	52.0	23.0	41000	25000	1.6
199	PTMG	2000	BICH	DHM	25.0	52.0	23.0	76000	36000	2.1
200	PTMG	650	HDI	DHM	25.0	52.0	23.0	57000	27000	2.1
201	PTMG	1000	HDI	DHM	25.0	52.0	23.0	60000	33000	1.8
202	PTMG	2000	HDI	DHM	25.0	52.0	23.0	65000	38000	1.7
203	PTMG	650	MDI	DHM	25.0	52.0	23.0	81000	34000	2.4
204	PTMG	1000	MDI	DHM	25.0	52.0	23.0	69000	30000	2.2
205	PTMG	2000	MDI	DHM	25.0	52.0	23.0	104000	42000	2.5
206	PPG	1000	HDI	OFHD	25.0	52.0	23.0	60000	28000	2.1
207	PPG	1000	BICH	OFHD	25.0	52.0	23.0	45000	28000	1.6
208	PPG	1000	MDI	OFHD	25.0	52.0	23.0	27000	15000	1.8
209	PPG	1000	HDI	PG	25.0	52.0	23.0	68000	35000	1.9
210	PPG	1000	BICH	PG	25.0	52.0	23.0	54000	31000	1.8
211	PPG	1000	MDI	PG	25.0	52.0	23.0	35000	18000	2.0
212	PHNAD	900	HDI	PG	25.0	52.0	23.0	66000	30000	2.2
213	PHNAD	900	BICH	PG	25.0	52.0	23.0	46000	30000	1.7
214	PHNAD	900	MDI	PG	25.0	52.0	23.0	92000	53000	1.7
215	PHNAD	900	HDI	BD	25.0	52.0	23.0	69000	34000	2.0
216	PHNAD	900	BICH	BD	25.0	52.0	23.0	54000	32000	1.7
217	PHNAD	900	MDI	BD	25.0	52.0	23.0	49000	23000	1.7
218	PHNAD	900	HDI	DMAPD	25.0	52.0	23.0	83000	38000	2.2
219	PHNAD	900	BICH	DMAPD	25.0	52.0	23.0	164000	71000	2.3
220	PHNAD	900	MDI	DMAPD	25.0	52.0	23.0	50000	25000	2.0
221	PHNAD	900	HDI	OFHD	25.0	52.0	23.0	77000	40000	1.9
222	PHNAD	900	BICH	OFHD	25.0	52.0	23.0	44000	22000	1.6
223	PHNAD	900	MDI	OFHD	25.0	52.0	23.0	73000	34000	2.1
224	PHNAD	900	HDI	none	48.5	51.5	0.0	119000	61000	2.0
225	PHNAD	900	BICH	none	48.5	51.5	0.0	135000	69000	1.9
226	PHNAD	900	MDI	none	48.5	51.5	0.0	178000	77000	2.3
228	PPG-PEG	1900	BICH	none	48.5	51.5	0.0	167000	96000	1.7

Polymer reference	Polyol		Diisocyanate	Chain Extender	Ratio (% mol.)			Molecular weight		
	Nature	MW (Da)			M (Polyol)	M (Diisocyanate)	M (Extender)	Mw	Mn	D
229	PPG-PEG	1900	MDI	none	48.5	51.5	0.0	62000	38000	1.6
230	PPG-PEG	1900	HDI	BD	25.0	52.0	23.0	99000	59000	1.7
232	PPG-PEG	1900	MDI	BD	25.0	52.0	23.0	47000	24000	1.9
233	PPG-PEG	1900	HDI	OFHD	25.0	52.0	23.0	91000	59000	1.6
234	PPG-PEG	1900	BICH	OFHD	25.0	52.0	23.0	56000	38000	1.5
235	PPG-PEG	1900	MDI	OFHD	25.0	52.0	23.0	55000	28000	1.9
238	PPG-PEG	1900	MDI	PG	25.0	52.0	23.0	62000	30000	2.1
241	PPG-PEG	1900	MDI	DMAPD	25.0	52.0	23.0	93000	40000	2.3
244	PPG-PEG	1900	MDI	EG	25.0	52.0	23.0	58000	26000	2.2
245	PHNGAD	1800	HDI	OFHD	25.0	52.0	23.0	146000	46000	3.2
246	PHNGAD	1800	BICH	OFHD	25.0	52.0	23.0	91000	38000	2.4
247	PHNGAD	1800	MDI	OFHD	25.0	52.0	23.0	46000	22000	2.1
248	PHNGAD	1800	BICH	DMAPD	25.0	52.0	23.0	94000	42000	2.2
249	PHNGAD	1800	HDI	none	48.5	51.5	0.0	79000	36000	2.2
250	PHNGAD	1800	BICH	none	48.5	51.5	0.0	75000	38000	2.0
251	PHNGAD	1800	MDI	none	48.5	51.5	0.0	65000	26000	2.5
252	PHNGAD	1800	HDI	DHM	25.0	52.0	33.0	32000	19000	1.7
253	PPG-PEG	1900	MDI	DMAPD	17.0	52.0	33.0	108000	51000	2.1
254	PHNGAD	1800	BICH	BD	17.0	52.0	33.0	41000	21000	1.9
255	PPG-PEG	1900	MDI	BD	17.0	52.0	33.0	53000	29000	2.2
256	PPG	425	MDI	none	48.5	51.5	0.0	123000	39000	3.2
257	PTMG	1000	BICH	DMAPD	17.0	52.0	33.0	39000	21000	1.8
258	PTMG	1000	BICH	OFHD	17.0	52.0	33.0	40000	23000	1.7
259	PTMG	2000	BICH	DMAPD	17.0	52.0	33.0	35000	20000	1.8
260	PTMG	2000	BICH	OFHD	17.0	52.0	33.0	39000	24000	1.6
262	PTMG	2000	BICH	BD	17.0	52.0	33.0	40000	23000	1.8
263	PTMG	1000	HDI	OFHD	17.0	52.0	33.0	61000	37000	1.7
264	PTMG	1000	HDI	DMAPD	17.0	52.0	33.0	42000	23000	1.8
266	PPG-PEG	1900	BICH	DMAPD	17.0	52.0	33.0	75000	47000	1.6
267	PPG-PEG	1900	BICH	BD	17.0	52.0	33.0	35000	23000	1.5
268	PTMG	1000	MDI	DMAPD	25.0	52.0	23.0	63000	33000	1.9
269	PPG	2000	MDI	DEAPD	25.0	52.0	23.0	47000	24000	1.9
270	PTMG	2000	MDI	DMAPD	25.0	52.0	23.0	95000	45000	2.1
271	PEG	400	MDI	DMAPD	25.0	52.0	23.0	21000	10000	2.1
272	PEG	400	MDI	none	58.0	42.0	0.0	9000	6500	1.4
273	PPG	425	MDI	DMAPD	25.0	52.0	23.0	23000	12000	1.9
274	PPG	425	MDI	none	48.5	51.5	0.0	15000	9000	1.6
275	PEG	400	MDI	none	48.5	51.5	0.0	18000	10500	1.7
276	PTMG	1000	MDI	OFHD	17.0	52.0	33.0	58000	30000	1.9
277	PTMG	2000	MDI	OFHD	17.0	52.0	33.0	60000	31000	2.0
278	PPG-PEG	1900	MDI	OFHD	17.0	52.0	33.0	54000	27000	2.0

List of (polyurethanes) used in the thesis with their corresponding monomers, polyol molecular weights and monomers molecular ratio used in the synthesis.

Appendix II: poly(acrylate) libraries[230]

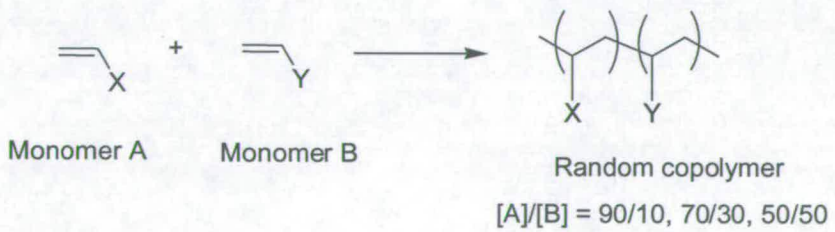

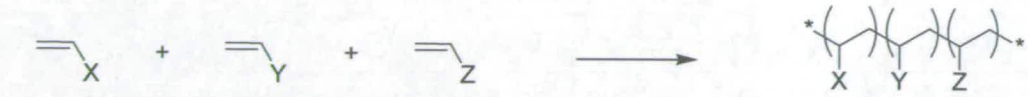

Monomer A Monomer B Monomer C

Random terpolymer

[A]/[B]/[C] = 70/20/10, 70/15/15, 70/10/20

Synthesis of the poly(acrylates).

St

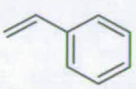

MMA

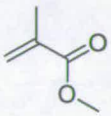

MEMA

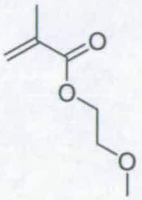

MEA

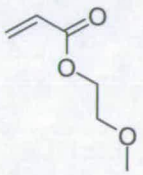

HEMA

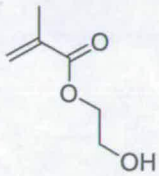

HPMA

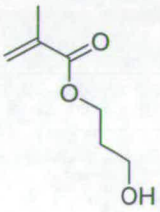

HBMA

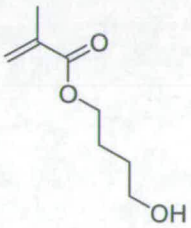

EMA

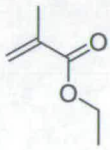

BMA

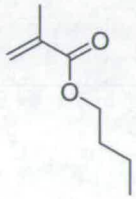

List of monomer A used.

DEAEMA

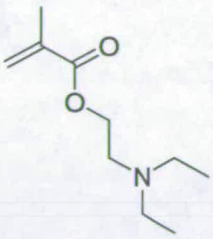

DEAEA

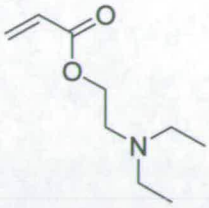

List of monomer C used.

DMAAm

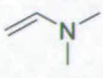

DEAAm

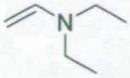

NIPAAm

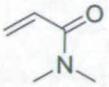

A-H

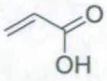

MA-H

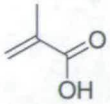

VAA

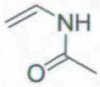

VP-4

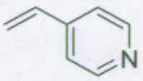

VP-2

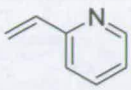

DMVBA

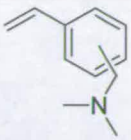

VI

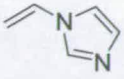

VPNO

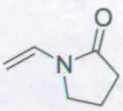

DMAEMA

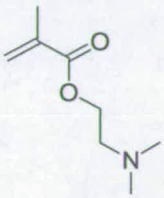

DMAEA

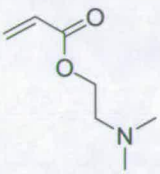

DEAEMA

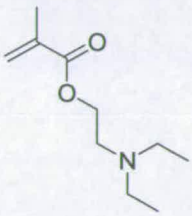

DEAEA

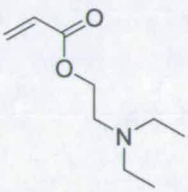

DMAPMAAm

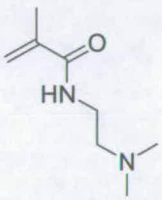

MTEMA

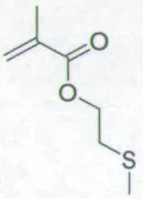

BACOEA

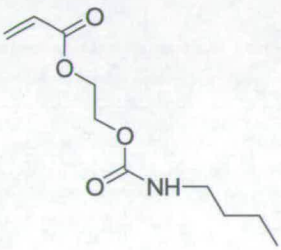

MNPMA

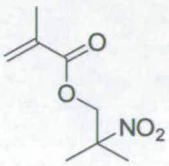

BAEMA

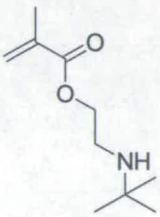

DAAAm

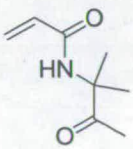

AES-H

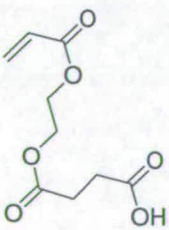

AAG-H

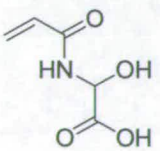

EGMP-H

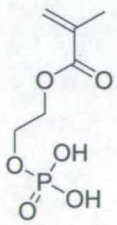

GMA

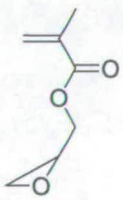

List of monomer B used.

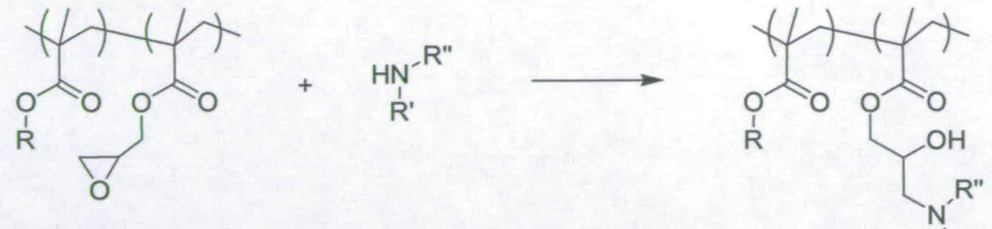

p(MEMA-co-GMA) : R = $-C_2H_4-O-CH_3$

p(MMA-co-GMA) : R = $-CH_3$

Functionalisation scheme for the copolymer of GMA.

TMEDA

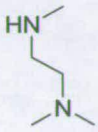

DEMEDA

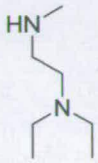

TMPDA

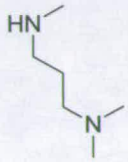

MnHA

DnBA

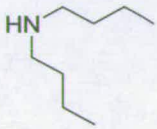

DnHA

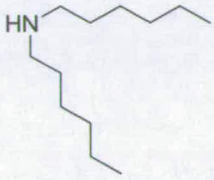

TEDETA

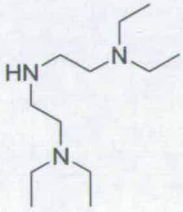

MAn

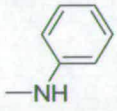

Pyrrole

DBnA

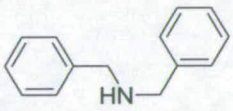

BnMA

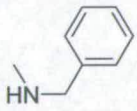

DcHA

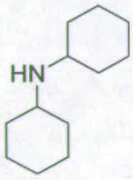

cHMA

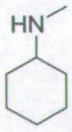

Mpi

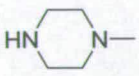

List of amines used to functionalise GMA polymers

Monomers abbreviations:

Monomers A:

St: styrene
MMA: methyl methacrylate
EMA: ethyl methacrylate
BMA: butyl methacrylate
MEMA: 2-methoxyethylmethacrylate
MEA: 2-methoxyethylacrylate
HEMA: 2-hydroxyethylmethacrylate
HPMA: hydroxypropylmethacrylate
HBMA: hydroxybutylmethacrylate

Monomers B:

DEAAm: diethylacrylamide
DMAAm: dimethylacrylamide
NIPAAm: *N*-isopropylacrylamide
DAAAm: diacetone acrylamide(*N*-(1,1-dimethyl-3-oxobutyl)-acrylamide)
DMAPMAAm: *N*-[3-(dimethylamino)propyl]acrylamide
DEAEMA: 2-(diethylamino)ethyl methacrylate
DMAEMA: 2-(diethylamino)ethyl methacrylate
DEAEA: 2-(diethylamino)ethyl acrylate
DMAEA: 2-(diethylamino)ethyl acrylate
MTEMA: 2-(methylthio)ethyl methacrylate
BAEMA: 2-(tert-butylamino)ethyl methacrylate
BACOEA: 2-[[(butylamino)carbonyl]oxy]ethyl acrylate
MNPMA: 2-methyl-2-nitropropyl methacrylate
DMVBA: *N,N*-dimethylvinylbenzylamine
VAA: *N*-vinylacetamide
VI: 1-vinylimidazole
VPNO: 1-vinyl-2-prrolidinone
VP-4: 4-vinylpyridine

VP-2:	2-vinylpyridine
A-H:	acrylic acid
AES-H:	mono-2-(acryloyoxy)ethyl succinate
MA-H:	methacrylic acid
AAG-H:	2-acrylamidoglycolic acid
EGMP-H:	ethylene glycol methacrylate phosphate

Monomers C:

DEAEMA:	2-(diethylamino)ethyl methacrylate
DEAEA:	2-(diethylamino)ethyl acrylate

Amines used to functionalise GMA based co-polymers:

GMA	glycidyl methacrylate
DnBA	di-*N*-Butylamine
DnHA	di-*N*-hexylamine
DcHA	dicyclohexylamine
DBnA	dibenzylamine
MnHA	*N*-methylhexylamine
cHMA	cycloheanemethylamine
BnMA	*N* benzylmethylaimne
MAEPy	2-(2-methylaminoethyl)pyridine
Pyrrole	pyrrole
MAn	*N*-methylaniline
TMEDA	*N,N,N*-trimethylethylenediamine
DEMEDA	*N,N*-diethyl-*N'*-methylethylenediamine
TMPDA	*N,N,N'*-trimethyl-1,3-propanediamine
Mpi	1-methylpiperazine
TEDETA	*N,N,N',N'*-tetraethyldiethylenetriamine

Polymer reference	Monomer (1)	Monomer (2)	Monomer (3)	Ratio (% mol.)			Molecluler weight		
				M (1)	M (2)	M (3)	Mw	Mn	PDI
1a9	St	DEAAm	-	90	10	-	137000	63600	2.2
1a7	St	DEAAm	-	70	30	-	138000	76700	1.8
1a5	St	DEAAm	-	50	50	-	114000	56000	2.0
1b7	St	DMAAm	-	70	30	-	124000	62500	2.0
1c9	St	NIPAAm	-	90	10	-	143000	81700	1.8
1c7	St	NIPAAm	-	70	30	-	137000	67500	2.0
2a9	MMA	DEAAm	-	90	10	-	269000	98900	2.7
2a7	MMA	DEAAm	-	70	30	-	291000	135000	2.2
2a5	MMA	DEAAm	-	50	50	-	278000	116000	2.4
2b9	MMA	DMAAm	-	90	10	-	273000	114000	2.4
2b7	MMA	DMAAm	-	70	30	-	308000	117000	2.6
2c9	MMA	NIPAAm	-	90	10	-	247000	106000	2.3
2c7	MMA	NIPAAm	-	70	30	-	1926400	172000	11.2
2c5	MMA	NIPAAm	-	50	50	-	1004400	108000	9.3
3a9	MEMA	DEAAm	-	90	10	-	218500	73200	3.0
3a7	MEMA	DEAAm	-	70	30	-	215200	62200	3.5
3a5	MEMA	DEAAm	-	50	50	-	194000	62400	3.1
3b9	MEMA	DMAAm	-	90	10	-	198000	67100	3.0
3b7	MEMA	DMAAm	-	70	30	-	213000	70300	3.0
3c9	MEMA	NIPAAm	-	90	10	-	218000	70500	3.1
3c7	MEMA	NIPAAm	-	70	30	-	634000	82500	7.7
3c5	MEMA	NIPAAm	-	50	50	-	417000	70600	5.9
4a9	MEA	DEAAm	-	90	10	-	173000	39700	4.4
4a7	MEA	DEAAm	-	70	30	-	161000	47400	3.4
4b9	MEA	DEAAm	-	90	10	-	213000	56800	3.8
4c9	MEA	NIPAAm	-	90	10	-	547560	46800	11.7
4c7	MEA	NIPAAm	-	70	30	-	1736610	54100	32.1
4c5	MEA	DEAAm	-	50	50	-	3403080	82800	41.1
5a9	HEMA	DEAAm	-	90	10	-	426000	59300	7.2
5a7	HEMA	DEAAm	-	70	30	-	192000	29000	6.6
5b9	HEMA	DMAAm	-	90	10	-	515000	68300	7.5
5b7	HEMA	DMAAm	-	70	30	-	258000	41500	6.2
5c9	HEMA	NIPAAm	-	90	10	-	266000	39500	6.7
5c7	HEMA	DEAAm	-	70	30	-	150000	20600	7.3
5c5	HEMA	DEAAm	-	50	50	-	101000	12700	8.0
6a9	HPMA	DEAAm	-	90	10	-	157000	32500	4.8
6a5	HPMA	DMAAm	-	50	50	-	101000	15300	6.6
6b9	HPMA	DMAAm	-	90	10	-	331000	50500	6.6
6b7	HPMA	DMAA	-	70	30	-	204000	40500	5.0
6c9	HPMA	NIPAAm	-	90	10	-	81300	26800	3.0
6c7	HPMA	NIPAAm	-	70	30	-	67100	16200	4.1
6c5	HPMA	DEAAm	-	50	50	-	106600	13700	7.8
7a9	HBMA	DEAAm	-	90	10	-	175000	30500	5.7
7a7	HBMA	DEAAm	-	70	30	-	128000	19900	6.4
7a5	HBMA	DMAAm	-	50	50	-	61500	11600	5.3
7b9	HBMA	DMAAm	-	90	10	-	431000	52500	8.2
7b7	HBMA	DMAA	-	70	30	-	309000	46200	6.7
7b5	HBMA	DMAAm	-	50	50	-	136000	27000	5.0
7c9	HBMA	NIPAAm	-	90	10	-	111000	26200	4.2
7c7	HBMA	NIPAAm	-	70	30	-	72100	17000	4.2
7c5	HBMA	NIPAAm	-	50	50	-	52100	12300	4.2
3e9	MEMA	DEAEMA	-	90	10	-	418000	102000	4.1
3e7	MEMA	DEAEMA	-	70	30	-	315000	71500	4.4
3e5	MEMA	DEAEMA	-	50	50	-	301000	99200	3.0
3f9	MEMA	DMAEMA	-	90	10	-	455000	79100	5.8
3f7	MEMA	DMAEMA	-	70	30	-	372000	87600	4.2
3f5	MEMA	DMAEMA	-	50	50	-	239000	50800	4.7
3g9	MEMA	DEAEA	-	90	10	-	242000	54300	4.5
3g7	MEMA	DEAEA	-	70	30	-	277000	61100	4.5
3g5	MEMA	DEAEA	-	50	50	-	222000	58600	3.8
3h9	MEMA	DMAEA	-	90	10	-	282000	69500	4.1
3h7	MEMA	DMAEA	-	70	30	-	392000	67100	5.8
3i9	MEMA	MTEMA	-	90	10	-	177000	49100	3.6
3i7	MEMA	MTEMA	-	70	30	-	236000	57600	4.1

Polymer reference	Monomer (1)	Monomer (2)	Monomer (3)	Ratio (% mol.)			Molecluler weight		
				M (1)	M (2)	M (3)	Mw	Mn	PDI
3i5	MEMA	MTEMA	-	50	50	-	146000	46800	3.1
3j9	MEMA	BAEMA	-	90	10	-	273000	61800	4.4
3j7	MEMA	BAEMA	-	70	30	-	315000	64100	4.9
3j5	MEMA	BAEMA	-	50	50	-	295000	75200	3.9
3l9	MEMA	DMAPMAA	-	90	10	-	270000	68300	4.0
3m9	MEMA	BACOEA	-	90	10	-	241000	58700	4.1
3m7	MEMA	BACOEA	-	70	30	-	302000	66800	4.5
3m5	MEMA	BACOEA	-	50	50	-	337000	49000	6.9
3n9	MEMA	DMVBA	-	90	10	-	235000	67800	3.5
3n7	MEMA	DMVBA	-	70	30	-	128000	40700	3.1
3n5	MEMA	DMVBA	-	50	50	-	104000	35900	2.9
3v9	MEMA	VAA	-	90	10	-	377000	79900	4.7
3v7	MEMA	VAA	-	70	30	-	355000	94700	3.7
3v5	MEMA	VAA	-	50	50	-	215000	68600	3.1
3x9	MEMA	VI	-	90	10	-	382000	92200	4.0
3x7	MEMA	VI	-	70	30	-	264000	72200	3.7
3x5	MEMA	VI	-	50	50	-	301700	73500	4.1
3z9	MEMA	VPNO	-	90	10	-	218000	58900	3.7
3z7	MEMA	VPNO	-	70	30	-	253000	56300	4.5
3z5	MEMA	VPNO	-	50	50	-	254000	37900	6.7
3AA9	MEMA	VP-4	-	90	10	-	225000	75600	3.0
3AA7	MEMA	VP-4	-	70	30	-	304000	103000	3.0
3AA5	MEMA	VP-4	-	50	50	-	207000	70800	2.9
3AB9	MEMA	VP-2	-	90	10	-	235000	82400	2.9
3AB7	MEMA	VP-2	-	70	30	-	169000	65800	2.6
3AB5	MEMA	VP-2	-	50	50	-	383000	164000	2.3
3AC9	MEMA	DAAA	-	90	10	-	154000	56900	2.7
3AC7	MEMA	DAAA	-	70	30	-	228000	74200	3.1
3AC5	MEMA	DAAA	-	50	50	-	211000	51400	4.1
3AE9	MEMA	MNPMA	-	90	10	-	129000	50600	2.5
3AE7	MEMA	MNPMA	-	70	30	-	289000	98800	2.9
3AE5	MEMA	MNPMA	-	50	50	-	177000	58500	3.0
5e9	HEMA	DEAEMA	-	90	10	-	175000	35500	4.9
5e7	HEMA	DEAEMA	-	70	30	-	158000	32000	4.9
5e5	HEMA	DEAEMA	-	50	50	-	199000	48800	4.1
5f9	HEMA	DMAEMA	-	90	10	-	180000	40500	4.4
5f7	HEMA	DMAEMA	-	70	30	-	201000	47600	4.2
5f5	HEMA	DMAEMA	-	50	50	-	167000	46100	3.6
5g9	HEMA	DEAEA	-	90	10	-	195000	43300	4.5
5g7	HEMA	DEAEA	-	70	30	-	184000	37000	5.0
5g5	HEMA	DEAEA	-	50	50	-	101000	21900	4.6
5h9	HEMA	DMAEA	-	90	10	-	208000	46700	4.5
5h7	HEMA	DMAEA	-	70	30	-	198000	44600	4.4
5h5	HEMA	DMAEA	-	50	50	-	160000	31500	5.1
5i9	HEMA	MTEMA	-	90	10	-	218000	58400	3.7
5i7	HEMA	MTEMA	-	70	30	-	160000	42000	3.8
5i5	HEMA	MTEMA	-	50	50	-	165000	47900	3.4
5j9	HEMA	BAEMA	-	90	10	-	239000	55300	4.3
5j7	HEMA	BAEMA	-	70	30	-	255000	51900	4.9
5j5	HEMA	BAEMA	-	50	50	-	216000	54900	3.9
5l9	HEMA	DMAPMAA	-	90	10	-	299000	74800	4.0
5l7	HEMA	DMAPMAA	-	70	30	-	257000	69000	3.7
5l5	HEMA	DMAPMAA	-	50	50	-	238000	57300	4.2
5m9	HEMA	BACOEA	-	90	10	-	296000	60600	4.9
5m7	HEMA	BACOEA	-	70	30	-	302000	52000	5.8
5m5	HEMA	BACOEA	-	50	50	-	196000	20700	9.5
5n9	HEMA	DMVBA	-	90	10	-	243000	63600	3.8
5n7	HEMA	DMVBA	-	70	30	-	163000	50600	3.2
5n5	HEMA	DMVBA	-	50	50	-	110000	43800	2.5
5v9	HEMA	VAA	-	90	10	-	266000	62600	4.2
5v7	HEMA	VAA	-	70	30	-	211000	40900	5.2
5v5	HEMA	VAA	-	50	50	-	203000	42900	4.7
5x9	HEMA	VI	-	90	10	-	421000	83100	5.1
5x7	HEMA	VI	-	70	30	-	310000	60300	5.1

Polymer reference	Monomer (1)	Monomer (2)	Monomer (3)	Ratio (% mol.)			Molecluler weight		
				M (1)	M (2)	M (3)	Mw	Mn	PDI
5x5	HEMA	VI	-	50	50	-	284000	52500	5.4
5z9	HEMA	VPNO	-	90	10	-	372000	87000	4.3
5z7	HEMA	VPNO	-	70	30	-	322000	73800	4.4
5z5	HEMA	VPNO	-	50	50	-	243000	63000	3.9
5AA9	HEMA	VP-4	-	90	10	-	312000	72300	4.3
5AA7	HEMA	VP-4	-	70	30	-	163000	42300	3.9
5AA5	HEMA	VP-4	-	50	50	-	141000	48000	2.9
5AB9	HEMA	VP-2	-	90	10	-	290000	59800	4.8
5AB7	HEMA	VP-2	-	70	30	-	154000	44800	3.4
5AB5	HEMA	VP-2	-	50	50	-	153000	58000	2.6
5AC9	HEMA	DAAA	-	90	10	-	543000	88300	6.1
5AC7	HEMA	DAAA	-	70	30	-	403000	77000	5.2
5AC5	HEMA	DAAA	-	50	50	-	240000	47600	5.0
5AE9	HEMA	MNPMA	-	90	10	-	636000	110000	5.8
5AE7	HEMA	MNPMA	-	70	30	-	560000	99500	5.6
5AE5	HEMA	MNPMA	-	50	50	-	477000	89800	5.3
2BA9	MMA	A-H	-	90	10	-	27800	12400	2.2
2BA7	MMA	A-H	-	70	30	-	38700	12500	3.1
2BB9	MMA	AES-H	-	90	10	-	39400	16900	2.3
2BB7	MMA	AES-H	-	70	30	-	N.D.	N.D.	N.D.
2BC9	MMA	MA-H	-	90	10	-	24400	11000	2.2
2BE9	MMA	AAG-H	-	90	10	-	25600	11600	2.2
2BE7	MMA	AAG-H	-	70	30	-	28500	13500	2.1
2BG9	MMA	EGMP-H	-	90	10	-	31400	16800	1.9
2BG7	MMA	EGMP-H	-	70	30	-	N.D.	N.D.	N.D.
2BG5	MMA	EGMP-H	-	50	50	-	N.D.	N.D.	N.D.
3BA9	MEMA	A-H	-	90	10	-	28500	12700	2.2
3BA7	MEMA	A-H	-	70	30	-	42800	15300	2.8
3BA5	MEMA	A-H	-	50	50	-	27700	11900	2.3
3BB9	MEMA	AES-H	-	90	10	-	58200	20300	2.9
3BB7	MEMA	AES-H	-	70	30	-	N.D.	N.D.	N.D.
3BB5	MEMA	AES-H	-	50	50	-	N.D.	N.D.	N.D.
3BC9	MEMA	MA-H	-	90	10	-	30900	12700	2.4
3BC7	MEMA	MA-H	-	70	30	-	39800	15200	2.6
3BC5	MEMA	MA-H	-	50	50	-	37100	17500	2.1
3BE9	MEMA	AAG-H	-	90	10	-	50400	18500	2.7
3BE7	MEMA	AAG-H	-	70	30	-	41400	15700	2.6
3BE5	MEMA	AAG-H	-	50	50	-	31100	13100	2.4
3BG9	MEMA	EGMP-H	-	90	10	-	53600	17700	3.0
3BG7	MEMA	EGMP-H	-	70	30	-	N.D.	N.D.	N.D.
3BG5	MEMA	EGMP-H	-	50	50	-	N.D.	N.D.	N.D.
3e8.5	MEMA	DEAEMA	-	85	15	-	216000	55600	3.9
3e8	MEMA	DEAEMA	-	80	20	-	201000	51500	3.9
3e7.5	MEMA	DEAEMA	-	75	25	-	172000	47100	3.7
3e7	MEMA	DEAEMA	-	70	30	-	155000	42200	3.7
3e6.5	MEMA	DEAEMA	-	65	35	-	122000	37600	3.2
3e6	MEMA	DEAEMA	-	60	40	-	158000	44600	3.5
3e5.5	MEMA	DEAEMA	-	55	45	-	141000	40800	3.5
2e9	MMA	DEAEMA	-	90	10	-	207000	66800	3.1
2e7	MMA	DEAEMA	-	70	30	-	183000	53400	3.4
2f9	MMA	DMAEMA	-	90	10	-	200000	75300	2.7
2f7	MMA	DMAEMA	-	70	30	-	199000	64100	3.1
2f5	MMA	DMAEMA	-	50	50	-	200000	65100	3.1
2g9	MMA	DEAEA	-	90	10	-	149000	46800	3.2
2g7	MMA	DEAEA	-	70	30	-	120000	33600	3.6
2g5	MMA	DEAEA	-	50	50	-	43300	20000	2.2
2h9	MMA	DMAEA	-	90	10	-	186000	58500	3.2
2h7	MMA	DMAEA	-	70	30	-	163000	35600	4.6
2h5	MMA	DMAEA	-	50	50	-	143000	26100	5.5
6e9	HPMA	DEAEMA	-	90	10	-	149000	75800	2.0
6f9	HPMA	DMAEMA	-	90	10	-	166000	83200	2.0
6g9	HPMA	DEAEA	-	90	10	-	145000	70700	2.1
6h9	HPMA	DMAEA	-	90	10	-	120000	60400	2.0
7e9	HBMA	DEAEMA	-	90	10	-	161000	78000	2.1
7e7	HBMA	DEAEMA	-	70	30	-	121000	58900	2.1
7e5	HBMA	DEAEMA	-	50	50	-	111000	56200	2.0

Polymer reference	Monomer (1)	Monomer (2)	Monomer (3)	Ratio (% mol.)			Molecluler weight		
				M (1)	M (2)	M (3)	Mw	Mn	PDI
7f9	HBMA	DMAEMA	-	90	10	-	192000	89000	2.2
7f7	HBMA	DMAEMA	-	70	30	-	149000	70700	2.1
7g9	HBMA	DEAEA	-	90	10	-	103000	51400	2.0
7g7	HBMA	DEAEA	-	70	30	-	48200	21200	2.3
7h9	HBMA	DMAEA	-	90	10	-	133000	66000	2.0
7h7	HBMA	DMAEA	-	70	30	-	80900	28900	2.8
8e9	EMA	DEAEMA	-	90	10	-	114000	25500	4.5
8e5	EMA	DEAEMA	-	50	50	-	126000	35700	3.5
8f9	EMA	DMAEMA	-	90	10	-	112000	43200	2.6
8f7	EMA	DMAEMA	-	70	30	-	120000	41900	2.9
8f5	EMA	DMAEMA	-	50	50	-	124000	38200	3.2
8g9	EMA	DEAEA	-	90	10	-	123000	45000	2.7
8g7	EMA	DEAEA	-	70	30	-	90000	35800	2.5
8g5	EMA	DEAEA	-	50	50	-	44000	17800	2.5
8h9	EMA	DMAEA	-	90	10	-	240000	56100	4.3
8h7	EMA	DMAEA	-	70	30	-	369000	42500	8.7
8h5	EMA	DMAEA	-	50	50	-	291000	30700	9.5
9e9	BMA	DEAEMA	-	90	10	-	208000	78400	2.7
9f9	BMA	DMAEMA	-	90	10	-	278000	105000	2.6
9f5	BMA	DMAEMA	-	50	50	-	256000	78300	3.3
9g9	BMA	DEAEA	-	90	10	-	203000	74100	2.7
9g5	BMA	DEAEA	-	50	50	-	49300	22300	2.2
9h9	BMA	DMAEA	-	90	10	-	188000	76700	2.5
9h7	BMA	DMAEA	-	70	30	-	214000	51100	4.2
9h5	BMA	DMAEA	-	50	50	-	206000	30600	6.7
2BAe7-2.0	MMA	A-H	DEAEMA	70	20	10	73200	36900	2.0
2BAe7-1.5	MMA	A-H	DEAEMA	70	15	15	89000	42200	2.1
2BAe7-1.0	MMA	A-H	DEAEMA	70	10	20	106000	44700	2.4
2BAg7-2.0	MMA	A-H	DEAEA	70	20	10	54200	27500	2.0
2BAg7-1.5	MMA	A-H	DEAEA	70	15	15	63600	31600	2.0
2BAg7-1.0	MMA	A-H	DEAEA	70	10	20	62600	28300	2.2
2BCe7-1.5	MMA	MA-H	DEAEMA	70	15	15	60900	31700	1.9
2BCe7-1.0	MMA	MA-H	DEAEMA	70	10	20	83500	42300	2.0
2BCg7-1.0	MMA	MA-H	DEAEA	70	10	20	56800	26100	2.2
3BAe7-1.0	MEMA	A-H	DEAEMA	70	10	20	168000	58100	2.9
3BCe7-1.0	MEMA	MA-H	DEAEMA	70	10	20	141000	54200	2.6
3BCg7-1.0	MEMA	MA-H	DEAEA	70	10	20	105000	38900	2.7
2GA1-9	MMA	GMA	DnBA	90	10	-	> 2,000,000	N.A.	N.A.
2GA1-7	MMA	GMA	DnBA	70	30	-	> 2,000,000	N.A.	N.A.
2GA2-9	MMA	GMA	DnHA	90	10	-	1900000	529000	3.6
2GA2-7	MMA	GMA	DnHA	70	30	-	> 2,000,000	N.A.	N.A.
2GA3-9	MMA	GMA	DcHA	90	10	-	1280000	276000	4.6
2GA3-7	MMA	GMA	DcHA	70	30	-	> 2,000,000	N.A.	N.A.
2GA4-9	MMA	GMA	DBnA	90	10	-	633000	170000	3.7
2GA4-7	MMA	GMA	DBnA	70	30	-	> 2,000,000	N.A.	N.A.
2GA4-5	MMA	GMA	DBnA	50	50	-	> 2,000,000	N.A.	N.A.
2GA5-9	MMA	GMA	MnHA	90	10	-	> 2,000,000	N.A.	N.A.
2GA5-7	MMA	GMA	MnHA	70	30	-	> 2,000,000	N.A.	N.A.
2GA5-5	MMA	GMA	MnHA	50	50	-	> 2,000,000	N.A.	N.A.
2GA6-9	MMA	GMA	cHMA	90	10	-	> 2,000,000	N.A.	N.A.
2GA6-7	MMA	GMA	cHMA	70	30	-	> 2,000,000	N.A.	N.A.
2GA6-5	MMA	GMA	cHMA	50	50	-	> 2,000,000	N.A.	N.A.
2GA7-9	MMA	GMA	BnMA	90	10	-	1030000	224000	4.6
2GA7-7	MMA	GMA	BnMA	70	30	-	> 2,000,000	N.A.	N.A.
2GA7-5	MMA	GMA	BnMA	50	50	-	> 2,000,000	N.A.	N.A.
2GA8-9	MMA	GMA	MAEPy	90	10	-	> 2,000,000	N.A.	N.A.
2GA8-5	MMA	GMA	MAEPy	50	50	-	> 2,000,000	N.A.	N.A.
2GA9-9	MMA	GMA	Pyrrole	90	10	-	471000	124000	3.8
2GA9-7	MMA	GMA	Pyrrole	70	30	-	718000	160000	4.5
2GA9-5	MMA	GMA	Pyrrole	50	50	-	518000	132000	3.9
2GA11-9	MMA	GMA	MAn	90	10	-	> 2,000,000	N.A.	N.A.
2GA11-7	MMA	GMA	MAn	70	30	-	> 2,000,000	N.A.	N.A.
2GA11-5	MMA	GMA	MAn	50	50	-	> 2,000,000	N.A.	N.A.
2GA12-9	MMA	GMA	TMEDA	90	10	-	N.D.	N.D.	N.D.
2GA12-7	MMA	GMA	TMEDA	70	30	-	N.D.	N.D.	N.D.
2GA12-5	MMA	GMA	TMEDA	50	50	-	N.D.	N.D.	N.D.

Polymer reference	Monomer (1)	Monomer (2)	Monomer (3)	Ratio (% mol.)			Molecluler weight		
				M (1)	M (2)	M (3)	Mw	Mn	PDI
2GA13-9	MMA	GMA	DEMEDA	90	10	-	N.D.	N.D.	N.D.
2GA14-9	MMA	GMA	TMPDA	90	10	-	N.D.	N.D.	N.D.
2GA14-7	MMA	GMA	TMPDA	70	30	-	N.D.	N.D.	N.D.
2GA15-9	MMA	GMA	Mpi	90	10	-	N.D.	N.D.	N.D.
2GA15-7	MMA	GMA	Mpi	70	30	-	N.D.	N.D.	N.D.
3GA1-9	MEMA	GMA	DnBA	90	10	-	762000	149000	5.1
3GA2-9	MEMA	GMA	DnHA	90	10	-	942000	134000	7.0
3GA4-9	MEMA	GMA	DBnA	90	10	-	676000	131000	5.2
3GA5-9	MEMA	GMA	MnHA	90	10	-	358000	75600	4.7
3GA7-9	MEMA	GMA	BnMA	90	10	-	1800000	235000	7.7
3GA9-9	MEMA	GMA	Pyrrole	90	10	-	791000	282000	2.8
3GA9-7	MEMA	GMA	Pyrrole	70	30	-	922000	413000	2.2
3GA9-5	MEMA	GMA	Pyrrole	50	50	-	> 2,000,000	N.A.	N.A.
3GA11-9	MEMA	GMA	MAn	90	10	-	723000	292000	2.5
3GA13-9	MEMA	GMA	DEMEDA	90	10	-	N.D.	N.D.	N.D.
3GA14-5	MEMA	GMA	TMPDA	50	50	-	N.D.	N.D.	N.D.

List of poly(acrylates) used in the thesis with their corresponding monomers and monomer molecular ratio used in the synthesis.

Appendix III: grafted poly(allylamine) library)[231]

A

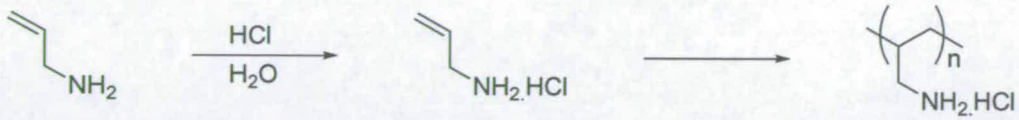

Poly(allylamine hydrochloride)

B

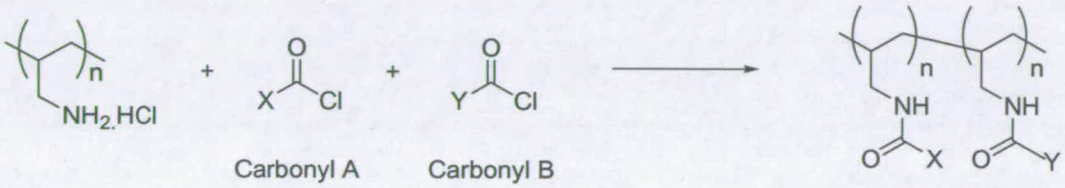

Carbonyl A Carbonyl B

[A]/[B] = 67/33, 50/50, 33/67

Synthesis of the poly(allylamine) derivatives. (A) synthesis of poly(allylamine hydrochloride), (B) grafting with carbonyl chlorides.

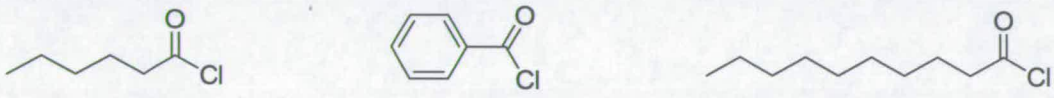

Hexanoyl chloride

Benzoyl chloride

Decanoyl chloride

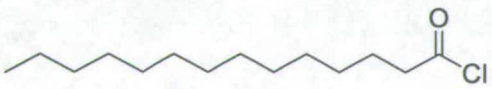

Myristoyl chloride

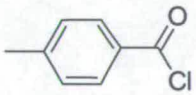

Toluoyl chloride

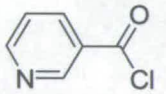

Nicotinoyl chloride

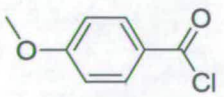

p-Anisoyl chloride

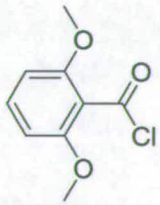

2,6-Dimethoxybenzoyl chloride

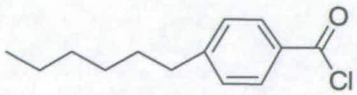

p-Hexylbenzoyl chloride

List of carbonyl chloride (with their respective names) used to graft poly(allylamine hydrochloride).

Polymer reference	Carbonyl chloride		Ratio (% mol.)		Molecular weight		
	Carbonyl (1)	Carbonyl (2)	C(1)	C(2)	Mw	Mn	PDI
1/4a	hexanoyl	myristoyl	33.3	66.7	N.D.	N.D.	N.D.
1/4b	hexanoyl	myristoyl	50.0	50.0	N.D.	N.D.	N.D.
1/4c	hexanoyl	myristoyl	66.7	33.3	N.D.	N.D.	N.D.
1/5a	hexanoyl	toluoyl	33.3	66.7	7210	12300	1.7
1/5b	hexanoyl	toluoyl	50.0	50.0	8720	13900	1.6
1/5c	hexanoyl	toluoyl	66.7	33.3	6860	13800	2.0
1/6a	hexanoyl	p-hexyl benzoyl	33.3	66.7	8970	13500	1.5
1/6b	hexanoyl	p-hexyl benzoyl	50.0	50.0	6780	11400	1.7
1/6c	hexanoyl	p-hexyl benzoyl	66.7	33.3	6770	11700	1.7
1/7a	hexanoyl	2,6-dimethoxybenzoyl	33.3	66.7	8140	12800	1.6
1/7b	hexanoyl	2,6-dimethoxybenzoyl	50.0	50.0	7580	12800	1.7
1/7c	hexanoyl	2,6-dimethoxybenzoyl	66.7	33.3	7800	13700	1.8
1/8a	hexanoyl	p-anisoyl	33.3	66.7	8530	14000	1.6
1/8b	hexanoyl	p-anisoyl	50.0	50.0	8520	14100	1.7
1/8c	hexanoyl	p-anisoyl	66.7	33.3	8320	14100	1.7
2/3a	benzoyl	decanoyl	33.3	66.7	18900	28800	1.5
2/3b	benzoyl	decanoyl	50.0	50.0	9150	14000	1.5
2/4b	benzoyl	myristoyl	50.0	50.0	15500	24200	1.6
2/4c	benzoyl	myristoyl	66.7	33.3	7400	13000	1.8
2/5a	benzoyl	toluoyl	33.3	66.7	7590	12800	1.7
2/5b	benzoyl	toluoyl	50.0	50.0	7470	12300	1.7
2/5c	benzoyl	toluoyl	66.7	33.3	7700	12100	1.6
2/7a	benzoyl	2,6-dimethoxybenzoyl	33.3	66.7	8740	12300	1.4
2/7b	benzoyl	2,6-dimethoxybenzoyl	50.0	50.0	8010	13000	1.6
2/7c	benzoyl	2,6-dimethoxybenzoyl	66.7	33.3	8010	12200	1.5
2/8a	benzoyl	p-anisoyl	33.3	66.7	8350	12800	1.5
2/8b	benzoyl	p-anisoyl	50.0	50.0	9080	14400	1.6
2/8c	benzoyl	p-anisoyl	66.7	33.3	9090	13900	1.5
2/9a	benzoyl	nicotonoyl	33.3	66.7	8530	12900	1.5
2/9b	benzoyl	nicotonoyl	50.0	50.0	28300	82900	2.9
2/9c	benzoyl	nicotonoyl	66.7	33.3	28300	78900	2.7
3/4c	decanoyl	myristoyl	66.7	33.3	N.D.	N.D.	N.D.
3/5a	decanoyl	toluoyl	33.3	66.7	30400	67300	2.2
3/5b	decanoyl	toluoyl	50.0	50.0	26800	76500	2.8
3/8a	decanoyl	p-anisoyl	33.3	66.7	82600	77000	2.7
3/8b	decanoyl	p-anisoyl	50.0	50.0	26800	75700	2.8
3/8c	decanoyl	p-anisoyl	66.7	33.3	24700	71900	2.9
4/7a	myristoyl	2,6-dimethoxybenzoyl	33.3	66.7	14900	39900	2.6
5/6a	toluoyl	p-hexyl benzoyl	33.3	66.7	23100	55300	2.4
5/6b	toluoyl	p-hexyl benzoyl	50.0	50.0	28600	79700	2.7
5/6c	toluoyl	p-hexyl benzoyl	66.7	33.3	29500	88800	3.0
5/7a	toluoyl	2,6-dimethoxybenzoyl	33.3	66.7	24700	42400	1.7
5/7b	toluoyl	2,6-dimethoxybenzoyl	50.0	50.0	27500	77300	2.8
5/7c	toluoyl	2,6-dimethoxybenzoyl	66.7	33.3	24300	73400	3.0
5/8a	toluoyl	p-anisoyl	33.3	66.7	26200	46800	1.8
5/8b	toluoyl	p-anisoyl	50.0	50.0	25400	44200	1.7
5/8c	toluoyl	p-anisoyl	66.7	33.3	25000	43600	1.7
6/7a	p-hexyl benzoyl	2,6-dimethoxybenzoyl	33.3	66.7	N.D.	N.D.	N.D.
6/7b	p-hexyl benzoyl	2,6-dimethoxybenzoyl	50.0	50.0	28600	84400	2.9
6/8a	p-hexyl benzoyl	p-anisoyl	33.3	66.7	34000	89900	2.6
6/8b	p-hexyl benzoyl	p-anisoyl	50.0	50.0	29500	82100	2.8
6/9a	p-hexyl benzoyl	nicotonoyl	33.3	66.7	24300	70700	2.9
7/8a	2,6-dimethoxybenzoyl	p-anisoyl	33.3	66.7	28100	74800	2.6
7/8b	2,6-dimethoxybenzoyl	p-anisoyl	50.0	50.0	28500	85700	2.9
7/8c	2,6-dimethoxybenzoyl	p-anisoyl	66.7	33.3	25000	55300	2.2
8/9b	p-anisoyl	nicotonoyl	50.0	50.0	27700	50500	1.8

List of grafted poly(allylamine) used in the thesis with their corresponding carbonyl chloride used to functionalise them.

Appendix IV: Publications

Polymer microarrays for cellular adhesion†

Guilhem Tourniaire,[a] Jane Collins,[b] Sara Campbell,[b] Hitoshi Mizomoto,[c] Shuichiro Ogawa,[d] Jean-François Thaburet[a] and Mark Bradley*[a]

Received (in Cambridge, UK) 10th February 2006, Accepted 20th March 2006
First published as an Advance Article on the web 30th March 2006
DOI: 10.1039/b602009g

Microarray screening of polymer libraries for cellular adhesion was developed utilising a thin film of agarose to allow unsurpassed localisation of cell binding onto the array substrate and the discovery of cell specific polymers.

The profound impact of arrays in the biological arena cannot be overlooked, taking into consideration the tremendous multiplexing ability an array can offer to a specific application. The most common examples are DNA "arrays" or chips, which are widely used for mRNA profiling, touted for diagnostic applications, used for SNP analysis and potentially have a role to play in DNA sequencing,[1] but the multiplexing power of arrays has been exploited in an increasing number of arenas such as the high-throughput (HT) characterisation of gene function with, for example, cell-based screens developed in a microarray type format.[2]

Polymers are essential in the area of biomaterials and have been used in a myriad of applications.[3] The mechanism of cell attachment onto polymer surfaces in cell culture has been extensively studied[4] and it is broadly accepted that the first steps in this process are the adsorption of extracellular matrix proteins onto the surface of the polymer. Cells then indirectly interact with the polymer through the adsorbed proteins which control a variety of cellular processes such as adhesion, growth and differentiation.[5] As a result of such complex and imperfectly understood interactions, it is still impossible to predict, from the chemical structures of a polymer, how such materials will perform when in contact with cells, blood or body fluids. As a consequence, the use of an HT approach to allow the rapid synthesis of chemically diverse polymers offers an important tool to find correlations between the design and performance of such materials.[6] Traditional methods of synthesis, identification and testing of new polymers are slow and thus over recent years, the field of automated and parallel synthesis of polymers has grown enormously[7] but, as is usually the case in any HT process, the development of high-throughput characterisation and screening methods are often the rate limiting steps. The use of polymer arrays for cellular screening was recently reported[8] where human embryonic stem cells were successfully differentiated following attachment and growth onto a poly(acrylate) array. However, in this case the uncharacterised polymers were prepared using a nanoliter-scale synthetic approach which was complicated by the very rapid evaporation of the "spotted" monomers meaning the exact composition of the final polymer was hard to define.

The poly(urethane)[9] library used in our studies (see Fig. 1 for the monomers used) was prepared by parallel synthesis and all individual members were fully purified and characterised by gel permeation chromatography, differential scanning calorimetry and contact angle measurements prior to use.[9] Before printing in a microarray type format each library member (for details see ESI†) was dissolved in a common solvent and transferred into a 384 well plate prior to contact printing. A number of parameters, such as the nature of solvent and substrate, inking and printing time had to be optimised in this process to ensure uniformity of the polymer spots within the array.

To obtain uniform printing, the polymer library needed to be printed from a common, non-volatile solvent. 1-Methyl-2-pyrrolidinone (NMP) was selected on the basis that the majority (> 95%) of the polymer library was soluble in this solvent and that it allowed uniform spots to be printed. The formation of so called "rings"[10] during solvent evaporation was minimised by a

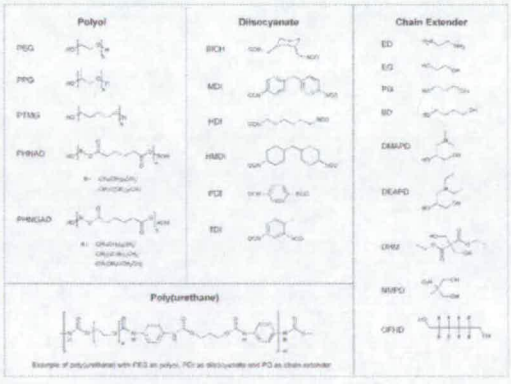

Fig. 1 Structures of the different monomers used in the polymer library synthesis. One example of poly(urethane) structure is given. The monomers, molecular weights, abbreviations and proportions used during the synthesis can be found in the ESI.

[a]*School of Chemistry, University of Edinburgh, Edinburgh, UK EH9 3JJ. E-mail: mark.bradley@ed.ac.uk; Fax: +44 131 650 6453; Tel: +44 131 650 1000*
[b]*The Renal Group, University of Southampton Medical School, Southampton General Hospital, Southampton, UK SO16 6YD. E-mail: J.E.Collins@soton.ac.uk; Tel: +44 2380 79 6447*
[c]*Asahi Kasei Corporation, 1-3-1, Yahoh, Kawasaki-ku, Kawasaki-city, Kanagawa 210-0863, Japan. E-mail: mizomoto.hb@om.asahi-kasei.co.jp*
[d]*Asahi Kasei Corporation, Hibiya-Mitsui Building, 1-2 Yurakucho 1-chome, Chiyoda-ku, Tokyo 100-8440, Japan. E-mail: ogawa.sj@om.asahi-kasei.co.jp; Fax: +81 5456 23039; Tel: +81 545 62 3128*

† Electronic supplementary information (ESI) available: List of monomer abbreviations and molecular weights, experimental details of substrate preparation and cell culture. See DOI: 10.1039/b602009g

 This Journal is © The Royal Society of Chemistry 2006

combination of the high boiling point solvent and successive layering of polymer solutions (5 stamps per spot).

In order to develop a cell compatible assay in a microarray format, the substrate had to comply with the following requirements. Firstly, the substrate had to be unaltered by the contact printing of polymer solution in NMP, which ruled out the use of polymer coatings such as poly(hydroxyethyl methacrylate), p(HEMA)[11] which would be dissolved locally and give rise to polymer mixtures. Secondly, a substrate with low levels of background cell binding had to be developed to facilitate data analysis (the majority of work published to date with cells is the result of dramatic data manipulation to remove data/cells that surround the spots) and thirdly, the substrate had to be stable under UV-irradiation to allow sterilisation prior to the plating of the cells.

A number of substrates were prepared: C18 functionalised Silane-Prep® slides, perfluoroalkylthiol monolayers on gold coated slides and Silane-Prep® slides dip-coated with a layer of agarose gel and the antifouling properties of the different substrates were tested with several mammalian cell lines (HEK293, HeLa, ND7 and B16F10). The C18 functionalised slides, as expected, were highly hydrophobic and were able to reduce non-specific binding, but not all cell lines could be blocked in this manner. The use of perfluoroalkylthiol-modified slides inhibited cellular adhesion, however it was impossible to use UV-irradiation for sterilisation as this degraded the surface. The best results were obtained by dip-coating aminoalkylsilane slides (Silane-Prep®; Sigma) with a thin film of agarose (Fig. 2).[12] Although agarose has been used to amplify loading on DNA arrays[13] and is known to inhibit cellular adhesion in a number of different formats,[14] agarose has not been used as coating material for cell based microarray assays.

The polymer arrays were fabricated by contact printing using polymer solutions in NMP with each polymer printed in quadruplicate. Once printed, the slides were dried overnight under vacuum at 45 °C and sterilised by exposure to UV irradiation for 15 minutes prior to cell plating.

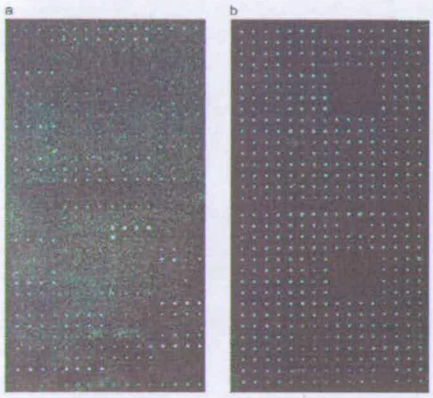

Fig. 2 Non-specific cell binding reduction using an agarose-coated substrate. Non-processed images obtained with Stro-1 + cells stained with CellTracker Green on two arrays with different substrate; (a) unmodified glass slide, (b) agarose-coated slide.

To illustrate the potential of the array, screening was carried out with primary cells using antibody staining as a means of detection. This was undertaken using human renal tubular epithelial cells. The cells were plated at 10^5 cells per slide and incubated for 5 days. Following fixation and permeabilisation, the cells were incubated with CAM5-2 anti-cytokeratin monoclonal antibody and visualised using Alexa Fluor® 488 labelled IgG antibody. Finally Hoechst 33342 was used to stain the nuclei. Analysis was carried out using the HCS platform and the Pathfinder® software (IMSTAR S.A., France). This platform, based on a fluorescent microscope with an X-Y-Z stage, allows the automated capture of single images (0.46 mm^2) for each polymer spot with a resolution of 0.58 μm (Fig. 3).

Cell compatibility was evaluated in terms of the total number of cells immobilised onto each polymer spot which was identified using the DAPI channel and the Pathfinder® software. Several poly(urethanes) were shown to provide significant attachment with an average over the 4 identical polymer spots of up to 153 human renal tubular epithelial cells (for details see ESI†). The 6 poly(urethanes) showing the highest number of bound cells (more than 140 cells per spot) all contained 4,4′-methylenebis(phenylisocyanate) (MDI) (PU-18; 161; 165; 182; 195; 217), while the diol PTMG (650 Da or 1000 Da) was present in four of these top six polymers, thus allowing the rapid and direct correlation of polymer structure with cell binding.

Overall, the microarray platform allows the identification of new polymers for the attachment of various cell types, including primary cells which are of significant interest within the medical community. Using this approach, a whole library of biocompatible polymers presenting a wide range of properties can be screened in a single experiment, in a self-consistent manner allowing the microarray platform to provide a rapid correlation of polymer structure with cell binding ability. Furthermore, since each library member was synthesised on a scale that allowed characterisation prior to array fabrication there is full confidence

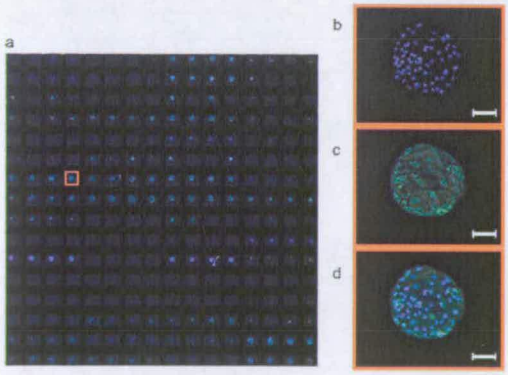

Fig. 3 Primary renal tubular epithelial cells on polymer array. (a) Cells on an array containing 60 polymers each printed as 4 replicate spots; one polymer spot with no background subtraction. (b) Nuclei stained with Hoechst 33342. (c) Cam5-2 antibody staining with Alexa Fluor® 488 secondary antibody. (d) Composite image of (b) and (c) (the bar represents 100 μm). Note: the boundaries of the cells are a function of the polymer spot and are not software processed.

This journal is © The Royal Society of Chemistry 2006

in any structure–activity relationship generated while allowing immediate scale-up following polymer identification. The agarose substrate proved to be very reliable in preventing unwanted cellular adhesion, with the potential to be developed for use with a large variety of cell-specific applications, such as global RNAi cell based phenotypic screens.[15]

We would like to acknowledge the EPSRC (LSI), Dr Rahul Tare and the Wessex Renal and Transplant Research Fund.

Notes and references

1 (*a*) D. N. Howbrook, A. M. van der Valk, M. C. O'Shaughnessy, D. K. Sarker, S. C. Baker and A. W. Lloyd, *Drug Discovery Today*, 2003, **8**, 642 651; (*b*) W. G. Koh, L. J. Itle and M. V. Pishko, *Anal. Chem.*, 2003, **75**, 5783 5789; (*c*) L. Lovmar, M. Fredriksson, U. Liljedahl, S. Sigurdsson and A. C. Syvänen, *Nucleic Acids Res.*, 2003, **31**, e129; (*d*) S. Liu, H. Ren, Q. Gao, D. J. Roach, R. T. Loder, Jr., T. M. Armstrong, Q. Mao, I. Blaga, D. L. Barker and S. B. Jovanovich, *Proc. Natl. Acad. Sci. U. S. A.*, 2000, **97**, 5369 5374.

2 (*a*) J. Ziauddin and D. M. Sabatini, *Nature*, 2001, **411**, 107 110; (*b*) S. E. How, B. Yingyongnarongkul, M. A. Fara, J. J. Diaz-Mochon, S. Mittoo and M. Bradley, *Comb. Chem. High Throughput Screening*, 2004, **7**, 423 430.

3 (*a*) B. D. Ratner, A. S. Hoffman, F. J. Schoen and J. E. Lemons, *Biomaterials Science*, Elsevier, San Diego, 2nd edn., 2004.

4 H. Shin, S. Jo and A. G. Mikos, *Biomaterials*, 2003, **24**, 4353 4364.

5 B. Geiger, A. Bershadsky, R. Pankov and K. M. Yamada, *Nat. Rev. Mol. Cell Biol.*, 2001, **2**, 793 805.

6 J. R. Smith, A. Seyda, N. Weber, D. Knight, S. Abramson and J. Kohn, *Macromol. Rapid Commun.*, 2004, **25**, 127 140.

7 (*a*) R. Hoogenboom, M. A. R. Meier and U. S. Schubert, *Macromol. Rapid Commun.*, 2003, **24**, 15 32; (*b*) A. Akinc, D. M. Lynn, D. G. Anderson and R. Langer, *J. Am. Chem. Soc.*, 2003, **125**, 5316 5323; (*c*) A. J. Jose, S. Ogawa and M. Bradley, *Polymer*, 2005, **46**, 2880 2888.

8 D. G. Anderson, S. Levenberg and R. Langer, *Nat. Biotechnol.*, 2004, **22**, 863 866.

9 J. F. Thaburet, H. Mizomoto and M. Bradley, *Macromol. Rapid Commun.*, 2004, **25**, 366 370.

10 R. D. Deegan, O. Bakajin, T. F. Dupont, G. Huber, S. R. Nagel and T. A. Witten, *Nature*, 1997, **389**, 827 829.

11 J. Folkman and A. Moscona, *Nature*, 1978, **273**, 345 349.

12 Coating with agarose was achieved by dip-coating the slide in a 1% w/v solution of agarose Type I-B (Sigma) at 65 °C followed by removal of the coating on the bottom side. After drying overnight at room temperature, the coated slides could be stored or used immediately for printing.

13 V. Afanassiev, V. Hanemann and S. Wölfl, *Nucleic Acids Res.*, 2000, **28**, e66.

14 (*a*) A. Folch and M. Toner, *Annu. Rev. Biomed. Eng.*, 2000, **2**, 227 256; (*b*) E. A. Roth, T. Xu, M. Das, C. Gregory, J. J. Hickman and T. Boland, *Biomaterials*, 2004, **25**, 3707 3715.

15 D. Vanhecke and M. Janitz, *Drug Discovery Today*, 2005, **10**, 205 212.

This journal is © The Royal Society of Chemistry 2006

Available online at www.sciencedirect.com
SCIENCE DIRECT
Biomaterials 27 (2006) 5299–5306
Biomaterials
www.elsevier.com/locate/biomaterials

Polymer microarrays: Identification of substrates for phagocytosis assays

Alexandra Mant[b], Guilhem Tourniaire[a], Juan J. Diaz-Mochon[a], Tim J. Elliott[b], Anthony P. Williams[b], Mark Bradley[a,*]

[a]School of Chemistry, University of Edinburgh, Joseph Black Buildings, Midlothian EH9 3JJ, UK
[b]School of Medicine, University of Southampton, Mail Point 824, Southampton General Hospital, Southampton, Hants SO16 6YD, UK

Received 31 March 2006; accepted 28 April 2006
Available online 30 June 2006

Abstract

A polymer microarray of 120 polyurethanes was used to identify polymers that promoted the adhesion of bone marrow dendritic cells (BMDC). Identified polymers were coated onto glass cover slips and shown to be efficient substrates for the immobilisation of these primary cells, which underwent efficient phagocytosis while still presumably maintaining their immature state.
© 2006 Elsevier Ltd. All rights reserved.

Keywords: Dendritic cells; Microarrays; Polyurethane; Cell adhesion; Phagocytosis

1. Introduction

Cellular adhesion has been investigated on a large number of substrates including glass, polystyrene, stainless steel, polypropylene and gold [1 3]. These materials are also often coated with various materials to promote cell binding, which include synthetic polymers (e.g. modified-polyethylenimine (PEI)) [2] and a variety of natural polymers ranging from poly L-lysine [3,4], fibronectin [2,5 7] and collagen [2,6] to more exotic materials such as spiders' silk [7]. Other approaches have included the use of monolayers of organic molecules coated onto gold substrates [8], but there are numerous (see for example [9 11]).

Cellular adhesion can be mediated by a variety of interactions, perhaps the most common being based on electrostatic interactions, with a highly positively charged surface leading to cellular immobilisation [2,4]. Such a surface is provided, at physiological pH, by coatings based on poly L-lysine and this has led to a myriad of applications and virtually universal use of poly L-lysine as a substrate for the immobilisation of cell lineages, but other poly-cationic synthetic polymers such as PEI [12] have also been used to immobilise cells. Other materials commonly used, such as polystyrene, are believed to exert/mediate their affects by physiosorption of extracellular matrix proteins, which in turn promote interactions with membrane proteins and hence cell adhesion [2].

Dendritic cells (DC) play a central role in the initiation of immune responses and in the maintenance of tolerance to self [13]. As professional antigen presenting cells, they can engulf particulate matter, such as pathogens, necrotic and apoptotic cells by phagocytosis, process it and present it at the cell surface, bound to MHC class I or MHC class II molecules [14]. This ability means that DC are intensively studied as targets for vaccine design, particularly for vaccines against tumours. DC are a rare constituent of any organ; and one of the most common experimental sources is to purify the immature, highly phagocytic cells from mouse bone marrow dendritic cell (BMDC). However, immature murine BMDC are extremely sensitive to stimuli that cause maturation [15], which affects their ability to capture antigens by phagocytosis, while immobilisation is quite generally complicated by the fact that cellular behaviour may be modified by interactions with the materials used to coat the substrates [16,17].

*Corresponding author. Fax: +44 0 1316506453.
E-mail address: mark.bradley@ed.ac.uk (M. Bradley).

0142-9612/$ - see front matter © 2006 Elsevier Ltd. All rights reserved.
doi:10.1016/j.biomaterials.2006.04.040

However, the immobilisation of DC would be important for several applications, ranging from simple phenotypic studies by microscopy, to the development of innovative cell-based assays. This paper shows how a polymer microarray [18] allowed the rapid and straightforward identification of specific polyurethanes able to act as substrates for cellular attachment of BMDC isolated from mouse. In addition we show that the identified polyurethane polymers compared more than favourably with the traditional adhesion compound, poly L-lysine in terms of cell adhesion and cellular behaviour.

2. Materials and methods

2.1. Synthesis of the polyurethane library [19]

Twelve parallel reactions were carried out in a Stem block on a mM scale by a typical two stage poly addition reaction. In brief, a pre-polymer was prepared by the reaction of 1.0 equivalent of a polyol with 2.0 equivalents of a diisocyanate in dry THF, followed (after titration) by the addition of 1.0 equivalent of a chain extender. The library was tailored by varying the nature of the polyols (250–2000 Da and different compositions); the diisocyanate and the chain extender and the ratio of chain extender/polyol). The monomers' structures used in the synthesis of the polymer library are shown in Fig. 1 together with an example of a representative polyurethane. The monomer used were: Poly(ethylene glycol) (PEG2000, PEG900, PEG400), poly(propylene glycol) (PPG2000, PPG1000, PPG425), poly(tetramethylene glycol) (PTMG2000, PTMG1000, PTMG650, PTMG250), PEG-PPG-PEG (PEG-PPG1900), poly[1,6-hexanediol/neopentyl glycol/diethylene glycol-alt-(adipic acid)] diol (PHNAGD1800), [1,6-hexanediol/neopentyl glycol-alt-(adipic acid)] diol (PHNAD900) were purchased from Aldrich (Fig. 1) and dried in a vacuum oven at 50 °C for 24 h prior to use.

The 120 polymers of the library were all characterised using high-throughput methods such as GPC (column PLgel HTS-D 150 × 7.5 mm ID, Polymer Laboratories, 1-methyl-2-pyrrolidinone (NMP) 1 ml/min), Hyper DSC (Diamond, Perkin Elmer) and FT-IR (Mattson instrument). Polymers were named following a "PUnumber" format (see Supplementary Data for details).

2.2. Preparation of primary murine BMDC

C57BL/6 mice were bred locally and housed in standard facilities in Southampton. Female or male mice were used for bone marrow extraction. BMDC were purified from the femurs of 8–12 weeks old C57BL/6 mice, according to the method of Lutz et al. [20] and were used on day 10 of in vitro culture.

2.3. Polymer microarray preparation

Coating glass slides with agarose was achieved by dip-coating the aminoalkylsilane slide (Sigma-Aldrich) in a 1% w/v solution of agarose Type I-B (Sigma) at 65 °C followed by removal of the coating on the bottom side. After drying overnight at room temperature, the coated slides were stored at room temperature or used immediately for printing [18].

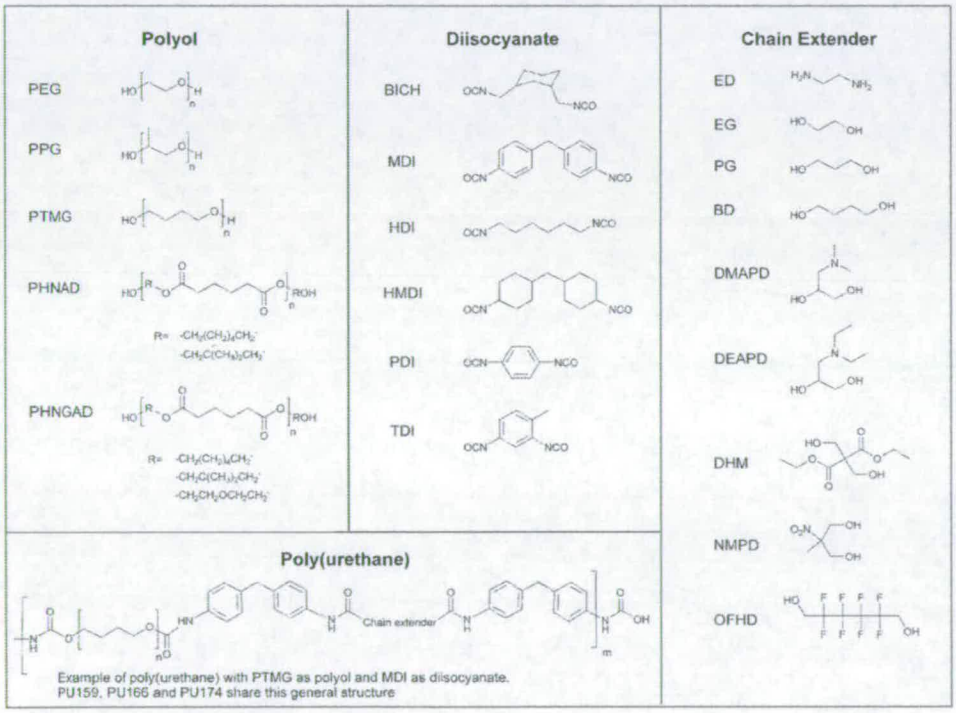

Fig. 1. Components used in the polyurethane library synthesis. A representative structure is shown. See Supplementary Data for details.

The polymer arrays were fabricated by contact printing (Genetix QArray mini; Hampshire, UK) with 16 aQu solid pins (K2785; Genetix; Hampshire, UK) using 1% w/v polymer solutions in NMP placed in polypropylene 384-wells microplates. The following printing conditions were used, 5 stamping per spot, 200 ms inking time and 10 ms stamping time. The typical spot size was 300–320 μm in diameter with spot-to-spot distances of 1120 μm allowing up to 480 polymers to be printed on a standard 25 × 75 mm slide. Polymers were printed in quadruplicate within 2 fields of 16 × 16 spots, while within each field a pattern of 4 × 4 spots was left empty. Once printed, the slides were dried overnight under vacuum at 45 °C and were sterilised by exposure to UV irradiation for 20 min prior to use.

Prior to spin coating on a P6708 spin coater (Speedlines Technologies, IN, USA), 22 mm diameter glass cover slips were cleaned with tetrahydrofuran (THF). Fifty microlitres of the polymer solutions (2% w/v in THF) were placed onto the coverslips and spun for 10 s at 2000 rpm. Coverslips were dried under vacuum for 12 h and irradiated with UV light for 20 min before use.

2.4. Cell-based microarray assays

BMDC were stained with 5 μM carboxyfluorescein succinimidyl ester (CFSE, Molecular Probes, Invitrogen Detection Technologies, Renfrewshire, UK) to monitor cell adhesion as follows: an aliquot of 4×10^6 cells was centrifuged for 5 min at 300*g* at 20 °C and washed once with phosphate-buffered saline (PBS) before resuspension in 1 ml PBS containing 5 μM CFSE and incubating for 10 min at room temperature in the dark. After staining, the cells were centrifuged for 5 min at 300*g* at 20 °C and gently resuspended in 1 ml cell culture medium, R10: RPMI-1640 (Invitrogen, Renfrewshire, UK) supplemented with penicillin, streptomycin and L-glutamine (Invitrogen, 100 U/ml, 100 μg/ml, 2 mM, respectively), 2-mercaptoethanol (50 μM, Sigma) and 10% heat-inactivated and filtered low endotoxin foetal calf serum (Autogen Bioclear, Wiltshire, UK). The cells were gently pipetted onto the surface of a polymer microarray contained in sterile Petri dish. A further 20 ml R10 was carefully added to the dish, which was subsequently incubated at 37 °C with 5% CO_2 for 2 h. After gentle washing with R10 and then PBS, the cells were fixed with 4% w/v formaldehyde in PBS for 15 min at room temperature, then rinsed and stored in PBS at 4 °C. Adhesion was checked using a Zeiss Axiovert 200 fluorescence microscope. For precise quantification of cell adhesion, the fixed cells were further stained with a 0.5 μg/ml solution of DAPI for 15 min at room temperature. Slides were rinsed and stored in PBS at 4 °C. Image capture and analyses were carried out using an IMSTAR high content screening (HCS) device equipped with the Pathfinder™ software (IMSTAR S.A., Paris, France). Cell compatibility with the different polymers was determined by automated counting of the number of cells present on each spot using both the DAPI and FITC channels.

2.5. Analysis of BMDC

BMDC were resuspended in PBS containing 2% v/v HI-FCS and 5 μg/ml phycoerythrin-conjugated hamster anti-CD11c monoclonal antibody (BD Pharmingen Oxfordshire, UK) or a phycoerythrin-conjugated isotype control antibody on ice for 30 min before washing three times with PBS/HI-FCS. Cells were immediately analysed by flow cytometry (FACSCalibur, BD, Oxfordshire, UK). For microscopy, BMDC adhered to coverslips were fixed in 4% v/v formaldehyde in PBS for 7 min at room temperature, permeabilised with 0.1% Triton X-100 for 7 min at room temperature, washed 3 times with PBS and then incubated with anti-CD11c monoclonal antibody for 1 h at room temperature. The coverslips were then washed 3 times with PBS before staining with a Quantum Dot 565 nm-conjugated anti-mouse secondary antibody (Quantum Dot, Cambridge, UK) and the nuclear dye, TO-PRO-3 (Molecular Probes, Invitrogen Detection Technologies, Renfrewshire, UK). Coverslips were mounted and analysed using a Leica SP2 laser scanning confocal microscope and a 100 × objective. Cells stained with secondary antibody alone showed no detectable fluorescence using the same instrument settings.

Phagocytosis assays were carried out with coverslips coated with polymer PU159, PU166 or PU174 (as described above), or 0.01% w/v poly L-lysine solution (Sigma histology grade or Sigma tissue culture grade), or uncoated (incubated with PBS alone), were sterilised by UV light for 15 min in the bottom of a 6-well polystyrene culture plate (Greiner Bio-One, Gloucestershire, UK). A drop of 0.5 ml R10 containing 5×10^5 BMDC was pipetted into the centre of each coverslip, and the plate incubated at 37 °C, 5% CO_2 for the cells to adhere, taking care not to disturb the meniscus. After 30 min, a further 1 ml of R10 was added to each coverslip, containing 5 μl of 3.0 μm diameter sulphate latex microspheres (IDC Latex, OR, USA), pre-coated with passively adsorbed foetal calf serum proteins. The microspheres were brought into contact with the adhered cells by centrifuging the plate for 3 min at 200*g* and 20 °C. The plate was then transferred to 37 °C, 5% CO_2 for a further 30 min.

After the incubation, the R10 was removed from the coverslips, which were rinsed briefly and gently with PBS, before being fixed with 4% formaldehyde in PBS for 7 min at room temperature. The BMDC were permeabilised by incubating with 0.1% v/v Triton X-100 in PBS for 7 min at room temperature, then washed 3 times with PBS before being stained with rabbit anti-calnexin antibody (Stressgen, CA, USA) and goat anti-rabbit AlexaFluor488 secondary antibody (Molecular Probes, Invitrogen Detection Technologies, Renfrewshire, UK). Nuclei were stained with TO-PRO-3.

Phagocytosis quantitation was carried out by examination of the coverslips using a Leica SP2 laser scanning confocal microscope with a 40 × objective. Three independent experiments were carried out, in which each coverslip was represented in duplicate. Phagocytosis was quantified by counting the number of microspheres internalised and the number of cells in a randomly selected field of view. Internalised microspheres were those defined as surrounded by calnexin staining in all three dimensions (Fig. 5). Figures for phagocytosis efficiency were derived from the counts of two to four fields of view per treatment, encompassing a minimum of 73 and a maximum of 556 cells. The degree of adhesion was classified by comparing the number of cells present in four randomly selected fields of view for each treatment and checking that these were typical over the three independent experiments.

3. Results and discussion

The aim of this project was to use a polymer microarray platform in order to discover new substrates for immobilising BMDC. The substrates so identified were used as per traditional coating systems on coverslips both to improve cellular adhesion and to allow different bioassays requiring cellular attachment to a 2D surface (such as phagocytosis and microscopy) to be carried out. The process is summarised in Fig. 2.

In this study 120 well-characterised polyurethanes were used. The advantages of this microarray platform are that it allows a common set of screening conditions for all polymers, requires only very limited amounts of each compound, and limited numbers of cells for each screen.

3.1. Identification of materials for BMDC immobilisation using polymer microarrays

After extraction of BMDC from mice, cells were labelled with CFSE before incubating with the PU polymer microarray. Following fixation, slides were scanned and the number of cells per spot counted to determine which substrates showed good cellular compatibility with BMDC

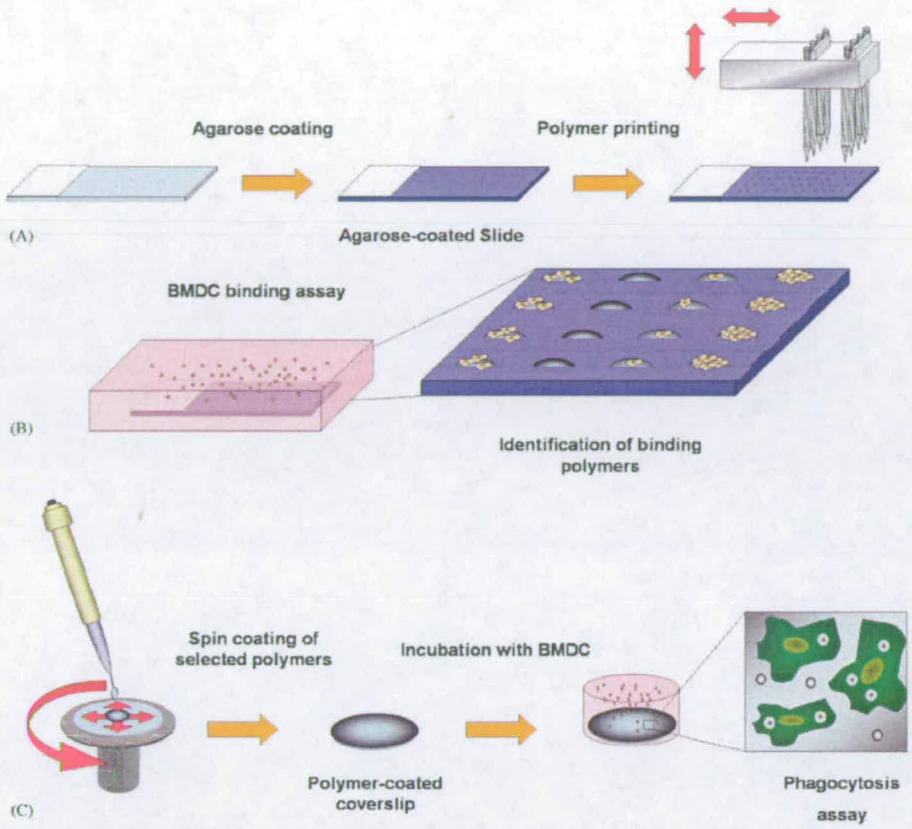

Fig. 2. General protocol for the identification of substrates for phagocytosis studies: (A) polymer microarray preparation; (B) microarray binding assay; (C) phagocytosis onto polymer coated coverslips.

Fig. 3. Quadruplicate spots of a polymer showing good cellular adhesion. Images were taken with the HCS platform from IMSTAR with a 20× objective and DAPI channel.

(Fig. 3). The HCS platform from IMSTAR was used to scan the slides, allowing automated capture of single images for each single polymer spot with 0.58 μm resolution. This analysis also allowed polymers to be discarded which showed autofluorescence, avoiding the identification of false positives.

Three different polyurethanes (PU159, PU166 and PU174) immobilised more than 10 cells per spot (average across 4 identical spots) and were selected and subsequently coated onto coverslips.

Prior to plating on coverslips, the purity of the BMDC preparation was assessed by staining cells with a fluorescent antibody against CD11c, a cell surface marker expressed by BMDC [20]. Stained cells were analysed by flow cytometry, which showed that greater than 90% of the cells were positive for CD11c (Fig. 4A). Cells also stained

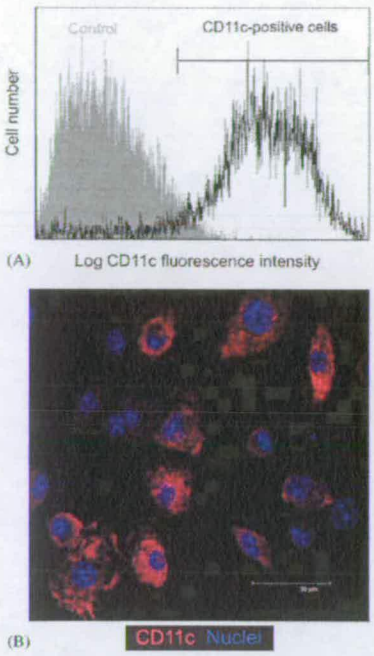

Fig. 4. (A) BMDC were stained with a fluorescently conjugated antibody against a dendritic cell surface marker, CD11c (black line), or with an isotype control antibody (shaded area, control), and analysed by flow cytometry. Cells staining positive for CD11c are indicated by a horizontal bar. (B) The anti-CD11c antibody (red) was used to stain BMDC that had adhered to the polymers (here, PU159), as described in Section 2. Nuclei (blue) were counterstained with TO-PRO-3. The image was obtained using a confocal laser scanning microscope and is a composite of 14, 0.5 μm thick optical sections.

positive for the characteristic costimulatory markers CD80 and CD86 and were brightly stained by antibodies against major histocompatibility complex II (data not shown), all of which taken together indicate that the vast majority of cells in the preparation were BMDC. The CD11c antibody was then used to identify BMDC that had adhered to the polymer-coated coverslips. BMDC adhered rapidly and well to all three polymers, and the vast majority of adhered cells stained positive for CD11c (Fig. 4B). We cannot exclude that a very small number of the cells adhering to the polymers were contaminants, as BMDC preparations are never 100% pure.

3.2. *Phagocytosis*

Although BMDC could adhere well to the three polymers, it was possible that the cells were not able to phagocytose while immobilised. A comparison of phagocytic capacity was made between the three polymers and the traditional cell adhesion compound, poly L-lysine. BMDC were plated and allowed to adhere to coverslips coated with either PU159, PU166, PU174, two grades of commercially available poly L-lysine or coverslips incubated in PBS alone. Cells were then supplied with 3 μm diameter latex microspheres and incubated for 30 min at 37 °C. Post-incubation, the cells were fixed and stained for the endoplasmic reticulum protein, calnexin, which provides a convenient counterstain revealing the presence of internalised microspheres (Fig. 5). Phagocytic capacity was determined by confocal microscopy and counting of the number of microspheres that had been completely internalised (Table 1).

Interestingly, the greatest phagocytic capacity, an average of 4.4 microspheres per cell, was observed for cells that had adhered to coverslips treated with PBS alone (Fig. 5, Control panels). However, the degree of adhesion of cells was very poor, and the cells were liable to be washed away from the coverslip both during the assay and afterwards during staining. Poly L-lysine of both grades greatly improved adhesion, but there was a concomitant decrease in the phagocytic capacity to an average of 1.3 microspheres per cell (Fig. 5, Poly L-lysine panels). Although many microspheres were bound to the cell surface, closer examination of optical sections revealed that most had not been internalised. One possible explanation is that the physical restriction of cell movement caused by adhesion to a substrate inhibits the cytoskeletal rearrangements necessary during phagocytosis. In support of this idea, phagocytosis decreased to zero when the concentration of poly L-lysine was increased tenfold (data not shown). Similar signalling pathways are involved for both cell adhesion to a substrate and adhesion to a particle to be phagocytosed [21]. Whereas cell adhesion can stimulate membrane extension, as for the filopodia and ruffles that engulf a particle, there are also cases where adhesion can inhibit membrane protrusion, such as the inhibition of cell migration in culture caused by cell cell contacts [22], which may provide an alternative explanation for the observed decrease in phagocytosis by cells adhered to poly L-lysine. In addition to reducing the phagocytic capacity, poly L-lysine caused greater background binding of microspheres to the coverslip than was observed for the polymers and PBS control. This is most likely due to charge interactions, since the microspheres carry a net negative charge, and lysine is a positively charged amino acid at physiological pH.

By contrast, phagocytic capacity was much greater for the three polymers, with average values of 3.3 and 3.6 microspheres per cell for PU159 and PU174, respectively, although still less than that observed in the PBS control sample. Adhesion, measured as the number of cells in a field of view, was greater for PU166 than PU159 and PU174, but this was accompanied by a decrease in phagocytic capacity to 2.2 microspheres per cell. Taken together with the results for poly L-lysine, it appears that there is a trade-off between degree of adhesion and phagocytic capacity. Importantly however, adhesion to

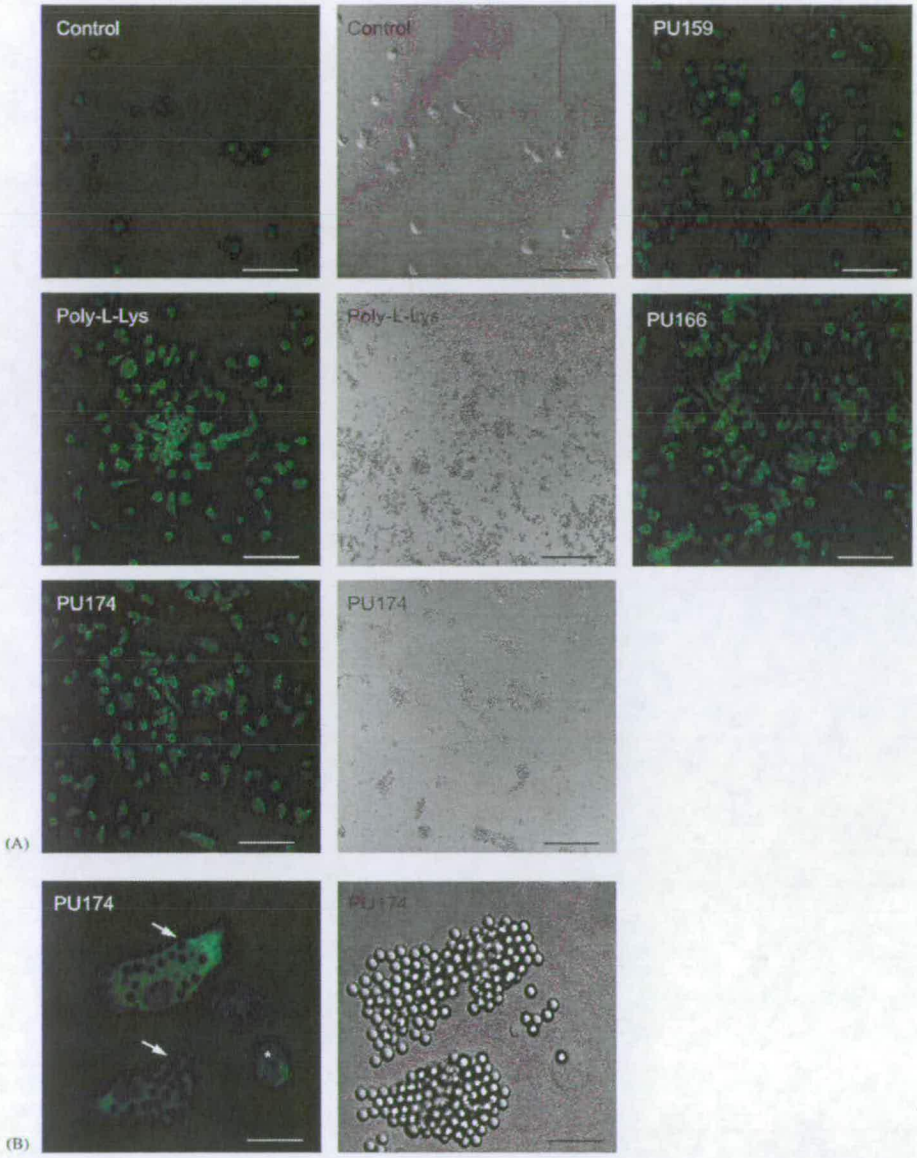

Fig. 5. Confocal laser scanning microscopy, with corresponding phase contrast images of BMDC adhered to coverslips and stained with anti-calnexin antibodies to reveal the presence of internalised microspheres. (A) Images taken with a 40 × objective. Control: coverslips treated with PBS alone; Poly L-Lys: coverslips treated with poly L-lysine; PU174, PU159 and PU166: coverslips coated with polyurethane polymers PU174, PU159 and PU166, respectively. Phase contrast images indicate the number of microspheres bound (but not necessarily internalised) to cells and also reveal the degree on non-specific binding of microspheres to the coverslip. Fluorescence images show optical sections 1.0 μm thick. Horizontal scale bars represent 75 μm. (B) Images taken with a 100 × objective. The fluorescence image shows in more detail the internalised microspheres (typical examples marked by arrows). The asterisk denotes the position of a microsphere that has bound to the cell surface (shown in the corresponding phase contrast image), but has not been internalised. Horizontal scale bars represent 15 μm.

Table 1
Phagocytosis results on different substrates

Treatment	Adhesion	Microspheres/cell	Cells counted	Microspheres counted
Control	Poor	4.4	73	324
Poly L-lysine, histology grade	Good	1.3	312	421
Poly L-lysine, tissue culture grade	Excellent	1.3	529	684
PU-159	Good	3.3	297	969
PU-166	Excellent	2.2	556	1249
PU-174	Good	3.6	301	1073

PU166 was as good as to tissue-culture grade poly L-lysine, but PU166 enabled almost double the phagocytic capacity. Our observations suggest that the PU polymers are superior to poly L-lysine, because they mediate good adhesion, while allowing much greater phagocytic activity.

4. Conclusions

The high multiplexing power of the polymer microarray approach allows the screening of large numbers of different biomaterials under identical conditions in a single experiment, thus enabling the rapid determination of structure - activity relationships. Three polyurethanes were identified using the microarray approach which bound immature DC from murine bone marrows, all of which contained poly(tetramethylene glycol) (PTMG 250 or 1000 Da) as the diol and 4,4′methylene bis(phenylisocyanate) (MDI) as the diisocyanate, with variation found in the chain extender (propyleneglycol, butane-1,4-diol or no chain extender).

This family of polymers will facilitate experimental handling of these cells and aid efforts in elucidating processes underlying antigen uptake, processing, presentation and immune stimulation or tolerisation and for studying intracellular processes such as cell migration and even interactions between cell types.

Acknowledgements

We thank Dr. Fay Chinnery and Dr. Vivien Watson for preparation of dendritic cells, and the Biomedical Imaging Unit at Southampton General Hospital for confocal microscopy facilities and the EPSRC (LSI). AM and APW are supported by a Wellcome Trust Clinical Fellowship to APW.

Appendix A. Supplementary material

Supplementary data associated with this article can be found in the online version at doi:10.1016/j.biomaterials.2006.04.040.

References

[1] Grinnell F, Milam M, Srere PA. Attachment of normal and transformed hamster kidney cells to substrata varying in chemical composition. Biochem Med 1973;7:87–90.

[2] Bledia Y, Domb AJ, Linial M. Culturing neuronal cells on surfaces coated by a novel polyethyleneimine-based polymer. Brain Res Protoc 2000;5:282–9.

[3] Ouyang EC, Wu GY, Wu CH. Biocompatible polymers in liver-targeted gene delivery systems. In: Dumitriu S, editor. Polymeric biomaterials. 2nd ed. New York: Marcel Dekker; 2002. p. 975–81.

[4] Wang GX, Deng XY, Tang CJ, Liu LS, Xiao L, Xiang LH, et al. The adhesive properties of endothelial cells on endovascular stent coated by substrates of poly L-lysine and fibronectin. Artif Cells Blood Substit Immobil Biotechnol 2006;34:11–25.

[5] Steele JG, Dalton BA, Johnson G, Underwood PA. Adsorption of fibronectin and vitronectin onto Primaria and tissue culture polystyrene and relationship to the mechanism of initial attachment of human vein endothelial cells and BHK-21 fibroblasts. Biomaterials 1995;16:1057–67.

[6] Imai K, Sato T, Senoo H. Adhesion between cells and extracellular matrix with special reference to hepatic stellate cell adhesion to three-dimensional collagen fibers. Cell Struct Funct 2000;25:329–36.

[7] Harrison RG. The reaction of embryonic cells to solid structures. J Exp Zool 1914;17:521–44.

[8] Kumar A, Biebuyck HA, Whitesides GM. Patterning self-assembled monolayers: applications in materials science. Langmuir 1994;10:1498–511.

[9] Kato K, Umezawa K, Miyake M, Miyake J, Nagamune T. Transfection microarray of nonadherent cells on an oleyl poly (ethylene glycol) ether-modified glass slide. BioTechniques 2004;37:444–8.

[10] Kato K, Umezawa K, Funeriu DP, Miyake M, Miyake J, Nagamune T. Immobilized culture of nonadherent cells on an oleyl poly (ethylene glycol) ether-modified surface. BioTechniques 2003;35:1014–21.

[11] Chandra RA, Douglas ES, Mathies RA, Bertozzi CR, Francis MB. Programmable cell adhesion encoded by DNA hybridization. Angew Chem Int Ed Engl 2006;45:896–901.

[12] Segura T, Chung PH, Shea LD. DNA delivery from hyaluronic acid-collagen hydrogels via a substrate-mediated approach. Biomaterials 2005;26:1575–84.

[13] Rossi M, Young JW. Human dendritic cells: potent antigen-presenting cells at the crossroads of innate and adaptive immunity. J Immunol 2005;175:1373–81.

[14] Rock KL, Shen L. Cross-presentation: underlying mechanisms and role in immune surveillance. Immunol Rev 2005;207:166–83.

[15] Pierre P, Turley SJ, Gatti E, Hull M, Meltzer J, Mirza A, et al. Developmental regulation of MHC class II transport in mouse dendritic cells. Nature 1997;388:787–92.

[16] Ranaldi G, Marigliano I, Vespignani I, Perozzi G, Sambuy Y. The effect of chitosan and other polycations on tight junction permeability in the human intestinal Caco-2 cell line(1). J Nutr Biochem 2002;13:157–67.

[17] Allen LT, Tosetto M, Miller IS, O'connor DP, Penney SC, Lynch I, et al. Surface-induced changes in protein adsorption and implications for cellular phenotypic responses to surface interaction. Biomaterials 2006;27:3096–108.

[18] Tourniaire G, Collins J, Campbell S, Mizomoto H, Ogawa S, Thaburet JF, et al. Polymer microarrays for cellular adhesion. Chem Commun 2006:2118–20.
[19] Thaburet JF, Mizomoto H, Bradley M. High-throughput evaluation of the wettability of polymer libraries. Macromol Rapid Commun 2004;25:366–70.
[20] Lutz MB, Kukutsch N, Ogilvie ALJ, Rößner S, Koch F, Romani N, et al. An advanced culture method for generating large quantities of highly pure dendritic cells from mouse bone marrow. J Immunol Methods 1999;223:77–92.
[21] Cougoule C, Wiedemann A, Lim J, Caron E. Phagocytosis, an alternative model system for the study of cell adhesion. Semin Cell Dev Biol 2004;15:679–89.
[22] DeMali KA, Burridge K. Coupling membrane protrusion and cell adhesion. J Cell Sci 2003;116:2389–97.

Appendix V: List of Presentations

Oral presentations:

- Asahi Kasei project meeting, 3rd February 2003, Southampton (UK).
- Asahi Kasei project meeting (video conference), 19th March 2003, Southampton (UK).
- Asahi Kasei project meeting, 24th April 2003, Southampton (UK).
- Asahi Kasei project meeting, 09th June 2003, Southampton (UK).
- Asahi Kasei project meeting (video conference), 17th July 2003, Southampton (UK).
- Asahi Kasei project meeting, 08th September 2003, Southampton (UK).
- Asahi Kasei project meeting (video conference), 02nd October 2003, Southampton (UK).
- Asahi Kasei project meeting, 24th November 2003, Southampton (UK).
- Bradley group presentation, 27th November 2003, Southampton (UK).
- Asahi Kasei project meeting (video conference), 19th December 2003, Southampton (UK).
- Asahi Kasei project, closure meeting, 19th February 2004, Southampton (UK).
- Bradley group presentation, 27th May 2004, Southampton (UK).
- Final year presentation, 6th April 2005, Firbush (UK).
- Bradley group presentation, 16th June 2005, Edinburgh (UK).
- Advances in Microarray Technology 2005, 11-13th October 2005, London (UK).
- Screening Europe 2006, 21-22nd February 2006, Prague (CZ).
- Institute of Stem Cell Research (ISCR), 2nd March 2006, Edinburgh (UK).

A Versatile Array of Polymeric Materials

Guilhem A. Tourniaire; Jun Kikuma; Ann J. Jose and Mark Bradley
Department of Chemistry, University of Southampton, SO17 1BJ, UK
E-mail: guilhem@soton.ac.uk

AsahiKASEI

- AIMS OF THE PROJECT -

The aim of this project was to develop **high throughput screening methods** to support the analyses of polymeric materials synthesised using a high throughput approach. This was achieved by developing **arrays of polymeric materials**[1], that could be screened in a high throughput manner.

- PRINTING -

Microarray printing required extensive optimisation to ensure uniform polymer spots and shape. This was achieved by:

Stage 1- Solutions
Polymers were dissolved at 1% w/v in a high viscosity and high boiling point solvent such as N-methyl pyrrolidinone. The solutions were placed into a 384-well polypropylene microplate prior to printing.

Stage 2- Printing
The robot used was the *Qarray mini*® (Genetix Ltd; UK).The solutions were deposited by contact printing using 300 µm solid pins. Each polymer solution was printed as 4 identical spots and each spot was formed by a minimum of 5 contact printings in order to remove the effect of the ring stain formation[2]. The substrates used were gold coated microscope slides which gave the lowest background and most uniform spots. The typical spot diameter was 300 µm (±20 µm) with a volume about 7 nL which is equivalent to about 70 pg of polymer.

Stage 3- Drying
Once printed, the solvent was removed by drying under vacuum at 45°C overnight, to give a microarray with over 750 spots per slide.

- APPARATUS -

Arrayer:
***Qarray mini* (Genetix Ltd, UK)**

Fig. 1. *Qarray mini*

Scanner:
***Bioanalyser 4F/4S scanner* (LaVision BioTech GmbH, D)**
A white light source scanner with CCD camera was used. The advantage over a laser scanner is the large choice of fluorescent filters covering a wider range of wavelength.

Fig. 2. (a) Printed gold coated slide after protein incubation, (b) Scanner; (c) Scan of an array of 512 spots (2 arrays of 16 by 16) using a Cy5 filter (300 ms exposure time), spot integrated over an area of 0.080 mm².

- SCREENING -

Physical characterisation:
As well as being useful for the bio-compatibility evaluation, the array format could be used for various physical characterisations such as composition by TOF-SIMS or functional group characterisation by FT-IR microscopy:

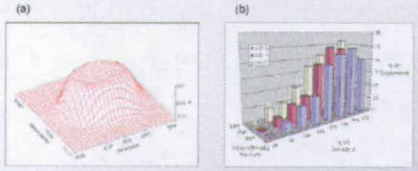

Fig. 5: (a) Mapping by FT-IR of the carbonyl functional group over a typical polymer spot. (b) Monomer composition evaluated by TOF-SIMS of a series of polymer spots; using different initiator to monomers ratio.

Protein binding:
Proteins were labelled using fluorescent dyes such as AlexaFluor® (Molecular Probes, NL). Labelled protein solutions (300µL/slide) were then placed onto the polymer arrays inside a Gene Frame (ABgene, UK) in order to obtain a uniform layer of solution. After a given incubation time, the protein solution was washed away and the slide was scanned to give data such as that shown in Fig. 2c.

Cell compatibility:
HEK293T and HELA cells were transfected with pGFPLuc using Superfect® transfection agent (Qiagen Ltd., UK) in order to obtain green fluorescent cells. Once transfected, the cells were grown on the polymeric array at 37°C under 5% CO_2. After washing, the cells were immobilised with fixing solution (3.7% w/v p-formaldehyde and 4.0% w/v sucrose in H_2O). Both quantitative (using the fluorescent scanner as described for protein binding) and qualitative (using a microscope) analyses were carried out using this format:

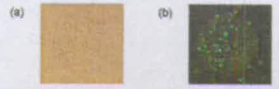

Fig. 3. Images of a polymer spot with attached HELA cell taken using an inverted configuration microscope with both a white light (a), and UV lamp (b), magnification X200.

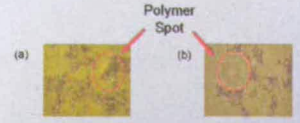

Fig. 4. HEK293T cells growing on an array of polymers. Evidence of cell compatible (a) and cell non-compatible (b) polymers (taken using an inverted configuration microscope, magnification X200)

- CONCLUSION -

It has been shown that polymer arrays are a **versatile format allowing the development of very high throughput methods for the evaluation of cell and protein binding**. Moreover, the quantities of both the analytes and reagent used being minimal, these methods are **particularly attractive on economical and environmental grounds**.

- REFERENCES -

1. G. Tourniaire; M. Bradley; Patent application number 0327283.8.
2. R. D. Deegan, et al., *Nature*, 1997, **389**, 827.

- ACKNOWLEDGEMENTS -

We would like to thank AsahiKASEI for a studentship.

High Throughput Screening of Biocompatible Polymers

Guilhem A. Tourniaire and Mark Bradley
Department of Chemistry, University of Edinburgh, EH9 3JJ, UK
E-mail: G.A.Tourniaire@sms.ed.ac.uk

- AIMS OF THE PROJECT -

The aim of this project was to develop **high throughput screening methods** to support the analyses of polymeric materials synthesised using a parallel approach. This was achieved by developing **arrays of polymeric materials**[1].

- PRINTING -

Microarray printing required extensive optimisation to ensure uniform polymer spot and shape.

Stage 1- Solutions
Polymers were dissolved at 1% w/v in a high viscosity and high boiling point solvent such as N-methyl pyrrolidinone. The solutions were placed into a 384-well polypropylene microplate prior to printing.

Stage 2- Printing
The robot used was the *Qarray mini®* (Genetix Ltd; UK).The solutions were deposited by contact printing using 150 µm solid pins. Each polymer solution was printed as 4 identical spots and each spot was formed by a minimum of 5 contact printings in order to reduce the effect of the ring stain formation[2]. The nature of the substrates were adapted to the different screenings in order to obtain the lowest background and most uniform spots. The typical spot diameter was 300 µm (±20 µm) with a volume about 7 nL which is equivalent to about 70 pg of polymer.

Stage 3- Drying
Once printed, the solvent was removed by drying under vacuum at 45°C overnight, to give a microarray with up to 2048 spots per slide.

- APPARATUS -

Arrayer:
***Qarray mini* (Genetix Ltd, UK)**

Fig. 1. *Qarray mini*

High Throughput Scanner:
***Bioanalyser 4F/4S scanner* (LaVision BioTech GmbH, D)**
White light source scanner with CCD camera allowing the rapid determination of fluorescence intensities.

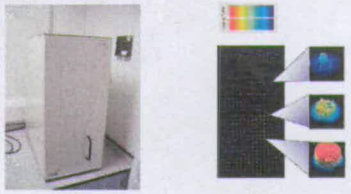

(a) (b)

Fig. 2. (a) High throughput scanner; (b) Scan of an array of 512 spots after incubation with a protein labelled using AlexaFluor® 647. (Cy5 filter; 300 ms exposure time, spot integrated over an area of 0.080 mm²).

High Content Scanner:
Pathfinder™ / OSA Reader™ (IMSTAR S.A., F)
High resolution scanner (up to 0.34 µm) allowing the determination of cell numbers, cellular coverage of the spot, fluorescent intensities…

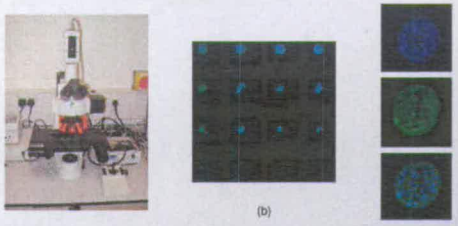

(a) (b) (c)

Fig. 3. (a) High content scanner; (b) Sub-array of 16 spots using composite of FITC and DAPI scan after incubation with human epithelial cells; (c) Example of scan (20X objective) obtained for each polymer spot showing from top to the bottom: the nuclei stained with Hoechst 33342 (DAPI filter), the cytoplasm stained using secondary antibody detection (FITC Filter) and composite images of these filters.

- SCREENING -

Protein binding:
Proteins were labelled using fluorescent dyes such as AlexaFluor® (Molecular Probes, NL). Labelled protein solutions (300µL/slide) were then placed onto the polymer arrays inside a Gene Frame (ABgene, UK) in order to obtain a uniform layer of solution. After a given incubation time, the protein solution was washed away and the slide was scanned to give data such as that shown in Fig. 2b.

Cell compatibility:
Cells were grown on the polymeric array at 37°C under 5% CO_2. After cell staining, the array was washed and the cells immobilised with fixing solution (3.7% w/v p-formaldehyde and 4.0% w/v sucrose in H_2O).

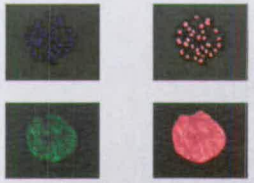

(a) (b) (c)

Fig. 4. (a) Raw scans; (b) Masks generated by the automatic protocols of detection; (c) Results obtained

- CONCLUSION -

It has been shown that polymer arrays are a **versatile format allowing the development of very high throughput methods for the evaluation of cell and protein binding**. Moreover, the quantities of both the analytes and reagent used being minimal, these methods are **particularly attractive on economical and environmental grounds**.

- REFERENCES -

1. G. Tourniaire; M. Bradley; Patent number GB 2408331.
2. R. D. Deegan, et al., *Nature*, 1997, **389**, 827.

- ACKNOWLEDGEMENTS -

We would like to thank AsahiKASEI for a studentship.

High Throughput Screening of Biocompatible Polymers

Guilhem A. Tourniaire; Jérôme Sallette and Mark Bradley
Department of Chemistry, University of Edinburgh, EH9 3JJ, UK
E-mail: G.A.Tourniaire@sms.ed.ac.uk

- AIMS OF THE PROJECT -

The aim of this project was to develop **high throughput screening methods using an IMSTAR Pathfinder™ High-content imaging platform** to support the analyses of polymeric materials synthesised using a parallel approach. This was achieved by developing **arrays of polymeric materials**[1,2].

- PRINTING -

Microarray printing required extensive optimisation to ensure uniform polymer spot and shape.

Stage 1- Solutions

Polymers were dissolved at 1% w/v in a high viscosity and high boiling point solvent such as N-methyl pyrrolidinone. The solutions were placed into a 384-well polypropylene microplate prior to printing.

Stage 2- Printing

The robot used was the *Qarray mini*® (Genetix Ltd; UK).The solutions were deposited by contact printing using 150 μm solid pins. Each polymer solution was printed as 4 identical spots and each spot was formed by a minimum of 5 contact printings in order to reduce the effect of the ring stain formation[3]. The nature of the substrates were adapted to the different screenings in order to obtain the lowest background and most uniform spots. The typical spot diameter was 300 μm (±20 μm) with a volume about 7 nL which is equivalent to about 70 pg of polymer.

Stage 3- Drying

Once printed, the solvent was removed by drying under vacuum at 45°C overnight, to give a microarray with up to 2048 spots per slide.

- APPARATUS -

Arrayer:

***Qarray mini* (Genetix Ltd, UK)**

Fig. 1. *Qarray mini*

High Throughput Scanner:

***Bioanalyser 4F/4S scanner* (LaVision BioTech GmbH, D)**

White light source scanner with CCD camera allowing the rapid determination of fluorescence intensities.

(a) (b)

Fig. 2. (a) High throughput scanner; (b) Scan of an array of 512 spots after incubation with a protein labelled using AlexaFluor® 647. (Cy5 filter; 300 ms exposure time, spot integrated over an area of 0.080 mm²).

High Content screening platform:

Pathfinder™ / OSA Reader™ (IMSTAR S.A., F, www.imstar.fr)

High content, high resolution (0.3 μm) image cytometry platform allowing the determination of cell numbers, cellular coverage in the spot, all individual cell fluorescence intensities, spots fluorescence ratio & morphology characteristics.

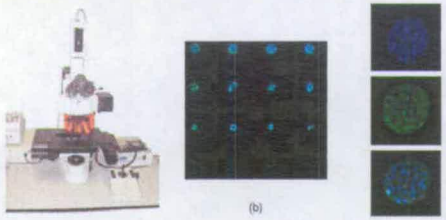

(a) (b) (c)

Fig. 3. (a) High content imaging platform; (b) Sub-array of 16 spots using composite of Fluorescein and DAPI scan after incubation with primary human epithelial tubular cells; (c) Example of scan (20X objective) obtained for each polymer spot showing from top to the bottom: the nuclei stained with Hoechst 33342 (DAPI filter), the cytoplasm stained using secondary antibody detection (Fluorescein Filter) and merged image.

- SCREENING -

Protein binding:

Proteins were labelled using fluorescent dyes such as AlexaFluor® (Molecular Probes, NL). Labelled protein solutions (300μL/slide) were then placed onto the polymer arrays inside a Gene Frame (ABgene, UK) in order to obtain a uniform layer of solution. After a given incubation time, the protein solution was washed away and the slide was scanned to give data such as that shown in Fig. 2b.

Cell compatibility:

Cells were grown on the polymeric array at 37°C under 5% CO_2. After cell staining, the array was washed and the cells fixed (3.7% w/v p-formaldehyde and 4.0% w/v sucrose in H_2O).

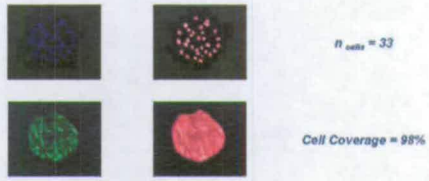

(a) (b) (c)

Fig. 4. (a) Raw images; (b) Masks generated by automatic detection protocols; (c) Results obtained

- CONCLUSION -

It has been shown that polymer arrays are a **versatile format allowing the development of very high throughput methods for the evaluation of cell and protein binding**. Moreover, the quantities of both the analytes and reagent used being minimal, these methods are **particularly attractive on economical and environmental grounds**.

- ACKNOWLEDGMENTS -

We would like to thank Sara Campbell and Jane Collins (University of Southampton) for providing the primary epithelial cells and Charles Homsy (Imstar S.A.) for his expertise and support in image processing.

- REFERENCES -

1. G. Tourniaire; M. Bradley; Patent number GB 2408331.
2. G. Tourniaire et al., Chem. Biol., submitted Nov. 2005.
3. R. D. Deegan, et al., *Nature*, 1997, **389**, 827.
4. E.B. Khomyakova et al., Cell. Mol. Biol. 2004, **50** (3), 217-224.
5. S. Baghdoyan et al, Nucl. Ac. Res. 2004, vol. **32**, N°. 9 e77.